

UNIVERSITE DES SCIENCES ET TECHNOLOGIES DE LILLE

THESE DE DOCTORAT

pour l'obtention du grade de

DOCTEUR EN SCIENCES DE LA VIE ET DE LA SANTE

présentée et soutenue publiquement par

Tobias SCHULZE

**Le rôle du récepteur de S1P, S1P₄, dans le système
immunitaire**

soutenue le 18 Décembre 2007 devant la commission d'examen:

Docteur Isabelle Wolowczuk: Directeur de thèse

Professeur Jean-Claude Michalski: Président

Docteur Sebastian Amigorena: Rapporteur

Docteur Jérôme Estaquier: Rapporteur

Docteur Martin Lipp: Examineur

Docteur Jean Coll: Examineur

This work was done in the laboratory for **Immuno- and Tumorgenetics**

Max-Delbrück-Center for Molecular Medicine

Robert-Rössle-Str. 10

13125 Berlin

Germany

under the supervision of **Dr. Martin Lipp**.

The Max-Delbrück-Center of Molecular Medicine is member of the Hermann von Helmholtz Association of National Research Centers.

A ma Mère

Le rôle du récepteur de S1P, S1P₄, dans le système immunitaire

Résumé

La signalisation par le sphingosine 1-phosphate (S1P) joue un rôle régulateur dans l'homéostasie du système immunitaire ainsi que dans l'induction de la réponse immune. Parmi les récepteurs du S1P, S1P₁ et S1P₄ sont ceux majoritairement exprimés par de nombreux types de cellules immunes. Alors que S1P₁ est connu pour ses fonctions *in vivo*, le rôle fonctionnel de S1P₄ dans le système immunitaire n'a pas encore été élucidé. Nous avons donc caractérisé le système immunitaire des souris déficientes en S1P₄.

Tout d'abord, nous montrons que la composition cellulaire dans les organes lymphoïdes primaires et secondaires ainsi que dans le sang ne montre que de faibles différences. Par contre, les quantités d'IgG₁, d'IgA et d'IgE plasmatiques sont significativement plus élevées chez les souris S1P₄^{-/-}. L'analyse détaillée du compartiment B montre une augmentation significative de 70% des MZ B-lymphocytes dans notre modèle déficient. Une réduction des IgA mucoales suggère une migration perturbée des plasmocytes vers les sites muqueux effecteurs. Comme le profil des immunoglobulines plasmatiques indique une réponse cellulaire orientée T_{H2}, la fonctionnalité a été testée dans des modèles d'asthme, de réaction d'hypersensibilité retardée et d'hypersensibilité de contact, confirmant l'orientation préférentielle de type T_{H2} chez les animaux S1P₄^{-/-}. De plus, nous montrons que S1P₄ joue un rôle dans la migration des lymphocytes T.

Un effet compensatoire de S1P₁ dans le modèle S1P₄^{-/-} ne pouvait être exclu. Afin d'évaluer l'éventuelle redondance des fonctions de S1P₁ et S1P₄, nous avons généré un vecteur lentiviral pour l'inhibition de l'expression de S1P₁ par des petits ARN à interférence (siRNA). Ceci permettra d'obtenir un modèle de souris déficiente pour les deux types de récepteurs sur les cellules hématopoïétiques et donc de mieux discerner les fonctions respectives de S1P₁ et S1P₄ *in vivo*.

Mots clés: sphingosine 1-phosphate, S1P₄, S1P₁, récepteurs couplés aux protéines G, réponse immunitaire, lymphocytes, cellules dendritiques, knock-out, shRNA

The role of S1P₄ in the immune system

Summary

Sphingosine 1-phosphate signalling has a regulatory role in multiple aspects of immune homeostasis as well as during induction of the immune response. S1P₁ and S1P₄ receptors represent the major subclasses of S1P receptors expressed on numerous immune cells. While specific *in vivo* functions have been assigned to the S1P₁, the functional role of S1P₄ expression on immune cells has not been established yet. In order to assess the biological function of the latter receptor, we have characterised the immune phenotype of a mice rendered deficient in S1P₄.

In primary and secondary lymphoid organs as well as in blood, only minor aberrations in the lymphocytes composition could be detected. Nevertheless, plasma IgG1, IgA and IgE levels were significantly elevated in S1P₄^{-/-} animals. A detailed analysis of the B-cell compartment further showed as most significant finding an increase of marginal zone B-cell population in S1P₄^{-/-} mice. A reduced level of mucosal IgA in S1P₄^{-/-} mice suggests a disturbed migration of S1P₄^{-/-} antibody secreting cells to mucosal effector sites. Since the plasma Ig isotype profiling of the S1P₄^{-/-} mice strongly suggests a T_H2 deviation, we used various models of T_H1/T_H2 responses (asthma, delayed type hypersensitivity, contact hypersensitivity) to possibly confirm this hypothesis. Furthermore, we show a role of S1P₄ in the regulation of T-cell migration was shown.

Potential compensatory functions of S1P₁ masking some aspects of the S1P₄ phenotype can not be excluded. In order to address possible overlapping functions of S1P₁ and S1P₄, a lentiviral vector for highly efficient shRNA mediated knock down of S1P₁ was successfully generated. This tool will allow us to generate a mouse model with a S1P₁/S1P₄ double deficient hematopoietic system that will facilitate the precise delineation of S1P₁ and S1P₄ effects in the immune system *in vivo*.

Key words: sphingosine 1-phosphate, S1P₄, S1P₁, G-protein coupled receptors, immune response, lymphocyte, dendritic cells, knock-out, shRNA

RESUME

La sphingosine 1-phosphatase (S1P) induit la majorité de ses effets biologiques en se liant aux récepteurs couplés aux protéines G. Jusqu'à présent, cinq récepteurs de S1P ont été identifiés. Alors que S1P₁₋₃ sont exprimés de manière ubiquitaire, S1P₄ et S1P₅ sont préférentiellement exprimés respectivement par les cellules d'origine hématopoïétiques et par les cellules du système nerveux. S1P joue un rôle essentiel dans le système immunitaire en contrôlant la migration et la prolifération cellulaire ainsi que la sécrétion de cytokines par les cellules immunes. S1P₁ et S1P₄ sont les récepteurs de S1P exprimés au niveau des lymphocytes mais également des autres cellules du système immunitaire. Récemment, de nombreuses fonctions biologiques ont été attribuées à S1P₁. Ce récepteur est essentiel pour l'émigration des lymphocytes T du thymus, ainsi que pour l'émigration des cellules T et B des ganglions lymphatiques et de la plaque de Peyer^{1,2}. De plus, la présence des lymphocytes B de la zone marginale dans la zone marginale dépend de l'expression de S1P₁³. Les cellules sécrétrices d'anticorps dépourvues de S1P₁ présentent une migration réduite hors de la rate aboutissant à une accumulation réduite dans la moelle osseuse⁴. L'inhibition de S1P par son analogue FTY720 a permis de montrer d'autres fonctions de cette molécule dans le système immunitaire, mais les récepteurs de S1P impliqués dans ces processus n'ont pas été identifiés. En particulier, le rôle de S1P₄ *in vivo* restait peu connu. Afin de le préciser, nous avons généré une souris déficiente en S1P₄. L'analyse de son système immunitaire constitue la première partie de ce travail.

S1P₁ et S1P₄ ont une grande affinité pour le même ligand, le S1P. De plus, la transduction intracellulaire du signal implique en partie les mêmes voies de signalisation. Une compensation fonctionnelle de l'absence d'un type de récepteur par un autre a été montrée sur des fibroblastes embryonnaires murins déficients en S1P₂ et S1P₃⁵. De plus, il a été suggéré, dans des études *in vitro*, que S1P₁ et S1P₄ formeraient des complexes, tout au moins dans des lignées cellulaires exprimant ces récepteurs de manière stable⁶. Dans ce contexte, la compensation potentielle par S1P₁ de la déficience en S1P₄ peut rendre difficiles certaines observations faites chez les animaux S1P₄^{-/-}. Afin de mieux discriminer les effets de S1P₄, nous avons décidé de créer un modèle expérimental de double déficience en S1P₁ et S1P₄. Comme la déficience en S1P₁ est létale *in utero*, l'approche du double Knock-out n'a pas été possible. Nous avons donc décidé de réduire l'expression de S1P₁ dans les cellules

hematopoïétiques $S1P_4^{-/-}$ à l'aide d'un vecteur lentiviral shRNA. La génération de ce vecteur lentiviral constitue la deuxième partie de ce travail.

L'analyse par cytométrie en flux (FACS) des organes lymphoïdes primaires et secondaires ainsi que des lymphocytes circulants (PBMC) chez les animaux $S1P_4^{-/-}$ ne montre pas de différences majeures. Cependant, les lymphocytes $CD19^+$ (correspondant aux lymphocytes B immatures) sont en nombre légèrement, mais significativement, réduit dans les ganglions périphériques. Inversement, les lymphocytes T exprimant le marqueur $CD8$ (correspondant aux lymphocytes T cytotoxiques) sont légèrement augmentés dans la moelle osseuse.

Les quantités de IgG1, IgA et IgE plasmatiques sont significativement plus importantes chez les animaux $S1P_4^{-/-}$. Par contre, les IgA muqueuses dans les poumons et l'intestin y sont inférieures. L'analyse des divers stades de développement des lymphocytes B montre par ailleurs un nombre réduit de pré-/pro-B et des lymphocytes B transitionnels de type I. Par contre, le nombre des lymphocytes B de la zone marginale est augmentée dans la rate des souris $S1P_4^{-/-}$. Par contre, la déficience en $S1P_4$ n'affecte pas le nombre des cellules B1 de la cavité péritonéale. L'analyse *in vitro* de la migration lymphocytaire révèle un effet négatif de $S1P_4$ sur le chimiotactisme des $CD4^+$ et $CD8^+$ suivant un gradient de $S1P$. *A contrario*, la migration des cellules B dans les mêmes conditions n'a pas été affectée. D'autres expériences *in vivo* ont confirmé l'implication de $S1P_4$ dans la régulation de la migration. $S1P_4$ ne semble pas impliqué dans la prolifération T et dans la régulation de la production de son propre ligand *i.e.* $S1P$.

L'analyse qualitative des profils d'immunoglobulines des souris $S1P_4^{-/-}$ (*i.e.* plus d'IgG1, IgE et IgA) suggère une orientation de type T_H2 . L'analyse de la sécrétion de cytokines *in vitro* ainsi que les résultats de trois modèles indépendants *in vivo* (hypersensibilité de contact, hypersensibilité retardée et asthme allergique) ont en effet confirmé la polarisation T_H2 de la réponse immunitaire chez les souris $S1P_4^{-/-}$.

En conclusion, l'analyse des animaux déficients en $S1P_4$ nous a permis de montrer des fonctions distinctes du récepteur $S1P_4$. Plusieurs résultats suggèrent une fonction antagoniste de $S1P_4$ sur la signalisation médiée par $S1P_1$. L'observation la plus intéressante est la prédisposition des souris $S1P_4^{-/-}$ à une réponse immunitaire polarisée T_H2 . Les mécanismes à la base de cette observation restent à disséquer. Cependant, les cellules dendritiques qui expriment des taux significatifs de $S1P_4$ chez la souris WT sont des candidats prometteurs en

tant que modulateurs de la réponse vers un profil T_H2 . Leurs propriétés fonctionnelles sont en cours d'étude chez la souris $S1P_4^{-/-}$.

Dans la seconde partie de notre travail de thèse, nous avons développé un vecteur d'expression transitoire de $S1P_1$ couplé à un epitope de l'hémagglutinine afin de tester l'activité suppressive des constructions shRNA spécifiques de $S1P_1$. Quatre plasmides différents contenant des séquences candidates spécifiques et suppressives de $S1P_1$ ont été testés en co-transfection avec le plasmide HA- $S1P_1$. La séquence 3 a montré la plus haute efficacité suppressive pour $S1P_1$. Cette séquence a par la suite été utilisée pour réaliser un vecteur rétroviral afin d'infecter des lignées cellulaires T et des cellules primaires. Cependant ce système n'a pas permis de produire des titres viraux élevés. Nous avons donc généré un vecteur lentiviral contenant l'insert shRNA et le gène reporter GFP. Ce vecteur a permis d'infecter les lignées T TG40 et LBRM avec un très bon rendement et de réduire l'expression endogène de $S1P_1$ de 75-90% par rapport au contrôle. De plus, nous avons démontré que l'expression du gène rapporteur GFP identifie d'une façon fiable les cellules avec un taux d'expression de $S1P_1$ réduite. L'effet suppresseur induit par l'infection par notre vecteur lentiviral est stable dans le temps (minimum 4 semaines). De plus, nous avons vérifié que le shRNA spécifique de $S1P_1$ n'a pas affecté l'expression de $S1P_4$.

En conclusion, nous avons généré un vecteur très efficace pour la suppression de l'expression de $S1P_1$ par la technologie des petits ARN à interférence. Cet outil nous permettra de mieux cerner les implications respectives de $S1P_1$ et $S1P_4$ dans la transduction des effets de S1P dans le système immunitaire.

REMERCIEMENTS

Je remercie chaleureusement:

Monsieur le Professeur Michalski qui m'a fait l'honneur de présider cette thèse et qui m'a accueilli dans son école doctorale,

Isa qui a eu la gentillesse de s'occuper de ma thèse en tant que directeur et qui a su m'encourager dans les moments de doute,

Martin Lipp qui m'a accueilli dans son labo et qui m'a laissé suffisamment de liberté pour réaliser ce travail,

Sebastian Amigorena et Jérôme Estaquier pour avoir accepté de venir de loin pour être mes rapporteurs,

Jean Coll qui s'est joint à mon jury,

Et enfin je remercie Monsieur le Professeur Schlag pour avoir toléré mes caprices non chirurgicaux et pour m'avoir donné l'occasion de m'entraîner aux soins intensifs.

A Frank Wilde et Christian Ried pour les trois questions accordées par jour.

A Sven Golfier pour le travail avec les souris S1P₄^{-/-}.

A Sven Hartmann pour les discussions sur ceci et cela.

A Jenny Grobe et Katrin Räbel qui m'ont appris ce que ça veut dire de travailler en équipe, et pour leur aide.

A Uta Höpcken et à Gerd Müller de m'avoir fait partagé leur expérience.

A Hans-Peter Rahn pour avoir trié mes cellules vertes, rouges et bleues.

A Elena pour être notre maman à tous au labo.

A Kerstin, Dagmar et Andra pour leur soutien et leur tolérance à mon chaos.

A Daniela pour m'avoir épargné plein de paperasses administratives.

A l'illustre collection des habitants et ex-habitants du labo «Immun- und Tumorgenetik» qui ont partagé ma bonne humeur quotidienne.

Aux infirmières des soins intensifs de la Robert-Rössle-Klinik pour avoir veillé sur mon sommeil tranquille pendant les gardes.

A Jean-Yves Cesbron et Catherine Lemaire pour m'avoir rendu professionnellement schizophrène et laissé tiraillé entre la Médecine et la Recherche, l'Allemagne et la France.

Et finalement, à ma petite Sophie qui a supporté mon absence, mais aussi ma présence depuis presque 10 ans, pour tous les projets que l'on envisage encore ensemble.

ABBREVIATIONS

aa	Amino acids
AC	Adenylyl cyclase
ASC	Antibody secreting cells
BAL	Bronchoalveolar lavage
BALF	Bronchoalveolar lavage fluid
BAT	Bronchoalveolar tract
BM	Bone marrow
BMMC	Bone marrow-derived mast cells
BSA	Bovine serum albumin
C1P	Ceramide 1-phosphate
CDase	Ceramidase
CFDA	Carboxyfluorescein diacetat, succinimidyl ester
CHS	Contact hypersensitivity
CIP	Calf Intestine Phosphatase
CoA	Coenzyme A
CRLR	Calcitonin-receptor-like receptor
CTLA4	Cytotoxic T lymphocyted-associated Ag 4
DC	Dendritic cell
dd water	Double distilled water
DOP	4'-deoxypyridoxine
ELISA	Enzyme-linked immunosorbent assay
FCS	Foetal calf serum
FITC	Fluorescein isothiocyanate
FTY720	Fingolimod
GDI	Guanine nucleotide dissociation inhibitor
GEF	Guanine nucleotide exchange factor
GFP	Green fluorescent protein
GFU	Green fluorescing units
GIL	Gastrointestinal lavage
GILF	Gastrointestinal lavage fluid
GIT	Gastrointestinal tract
GM-CSF	Granulocyte/macrophage-colony stimulating factor
GPCR	G protein-coupled receptor
GRK	G-protein coupled receptor kinase
HA tag	Hemagglutinin epitope tag
HRP	Horse radish peroxidase
IEL	Intraepithelial lymphocytes
Ig	Immunoglobulin
IL-12	Interleukin 12
IL-4	Interleukin 4
IL-8	Interleukin 8
INF- γ	Interferon γ
IPTG	Isopropyl-1-thio- β -D-galactoside
LCMV	Lymphocytic choriomeningitis virus
LN	Lymph node
LPA	Lysophosphatidic acid
LPL	Lysophospholipids
LPP	Lipid phosphate phosphatases

LPS	Lipopolysaccharide
lysoPLD	Lysophospholipase D
MAdCAM	Mucosal addressin cell adhesion molecule 1
MAPK	Mitogen-activated protein kinase
MCP-1	Monocyte chemotactic protein 1
MEF	Mouse embryonic fibroblasts
MHC	Major histocompatibility complex
MIP-1 β	Macrophage inflammatory protein 1
mLN	Mesenteric lymph node
MLR	Mixed lymphocyte reaction
MOI	Multiplicity of infection
MZ	Marginal zone
NP-CGG	(4-Hydroxy-3-nitrophenyl)acetyl-conjugated to chicken γ globuline
NP-O-Su	4-hydroxy-3-nitrophenyl acetyl hydroxysuccimide ester
OD	Optical density
ORF	Open reading frame
PA	Phosphaditic acid
PCR	Polymerase chain reaction
PHA	Phytohemagglutinine
PLC	Phospholipase C
PLD	Phospholipase D
pLN	Peripheral lymph node
PP	Peyers patch
PRE	Posttranscriptional regulatory element
PTX	Perussis toxin
RANTES	Regulated upon activation, Normal T-cell Expressed, and Secreted (CCL5)
RGS	Regulators of G protein signalling
Rpm	Rotations per minute
RT	Room temperature
S1P	Sphingosine 1-phosphate
SDF-1 α	Stromal cell derived factor 1 α
SLO	Secondary lymphoid organs
Sph	Sphingosine
SphK	Sphingosine kinase
THI	2-acetyl-4-tetrahydroxybutylimidazol
TMH	Transmembrane helix
TNF- α	Tumor necrosis factor α
VSVG	Vesicular stomatitis virus glycoprotein
Xgal	5-Bromo-4-chloro-3-indolyl- β -D-galactoside

TABLE OF CONTENTS

Titre et Resume (Français)	7
Title and Abstract (English)	9
Resume Substantiel (Français)	10
Remerciements	13
Abbreviations	15
Table of Contents	17
1. Introduction	23
1.1. General introduction.....	23
1.2. Structural characteristics and functional properties of G-protein coupled receptors and their signalling pathways	24
1.2.1. Structural and functional characteristics of GPCRs	25
1.2.2. Regulation of GPCR signalling.....	27
1.2.3. Intracellular signalling of heptahelical receptors	28
1.2.3.1. Signal transduction via G-proteins	28
1.2.3.1.1. Effector molecules of heterotrimeric G-proteins.....	31
1.2.3.1.2. Regulation of signalling by heterotrimeric G-proteins.....	32
1.2.3.2. G-protein-independent signalling by heptahelical receptors.....	33
1.3. Lysophospholipid receptors	34
1.3.1. Brief History.....	34
1.3.2. Nomenclature and classification	35
1.3.3. Sphingosine 1 phosphate receptors	36
1.3.3.2. S1P ₂	37
1.3.3.3. S1P ₃	38
1.3.3.4. S1P ₄	40
1.3.3.4.1. Current knowledge on the role of S1P ₄ in the immune homeostasis	41
1.3.3.5. S1P ₅	42
1.3.4. Lysophosphatidic acid receptors	43
1.3.4.1. LPA ₁	43
1.3.4.2. LPA ₂	44
1.3.4.3. LPA ₃	45
1.3.4.4. LPA ₄ and LPA ₅	45
1.3.5. Other Lysophospholipidreceptors	46
1.4. The ligands: S1P and LPA	46
1.4.1. Sphingolipids.....	46
1.4.1.1. Sphingolipids, a complex network of interconvertible bioactive lipids.....	46
1.4.1.2. Sphingosine metabolism.....	49
1.4.1.2.1. Sphingosine kinase	49
1.4.1.2.2. Biodegradation of S1P.....	50

1.4.1.3.	S1P and its double role as intracellular second messenger and extracellular first messenger.....	50
1.4.1.4.	Sources of extracellular S1P.....	51
1.4.2.	Lysophosphatidic acid.....	51
1.4.2.1.	Extracellular production of LPA.....	52
1.4.2.2.	Intracellular generation of LPA.....	52
1.4.2.3.	LPA degradation.....	53
1.4.2.4.	LPA as intracellular second messenger.....	53
1.5.	Agonist and antagonists of LPL receptors.....	53
1.6.	Lysophospholipidreceptors in the immune system.....	54
1.6.1.	Lymphocytes.....	54
1.6.1.1.	T lymphocytes.....	55
1.6.1.2.	B lymphocytes.....	58
1.6.2.	NK cells.....	59
1.6.3.	Dendritic cells.....	60
1.6.4.	Monocytes/Macrophages.....	62
1.6.5.	Granulocytes.....	63
1.6.5.1.	Neutrophil granulocytes.....	63
1.6.5.2.	Basophil granulocytes.....	64
1.6.5.3.	Eosinophil granulocytes.....	65
1.6.6.	Mast cells.....	65
1.6.7.	Regulatory T-cells.....	67
1.7.	Role of S1P signalling in the immune homeostasis and immune response.....	68
1.7.1.	<i>In vivo</i> roles of S1P signalling in the immune homeostasis.....	69
1.7.1.1.	S1P signalling in T-cell biology <i>in vivo</i>	69
1.7.2.	S1P is implicated in lymphocyte and mast cell trafficking to the gut epithelium and in the development of food allergy.....	70
1.7.3.	Implication of S1P signalling in B-cell biology <i>in vivo</i> and on the humoral immune response.....	71
1.7.4.	S1P impacts on trafficking of peritoneal B-cells.....	72
1.7.5.	Increased tissular S1P levels induce lymphopenia.....	73
2.	Aim of this study.....	74
3.	Materials.....	75
3.1.	Bacterial strains.....	75
3.2.	Plasmids.....	75
3.3.	Cell lines.....	75
3.4.	Mice.....	76
3.5.	Primers.....	76
3.6.	Oligonucleotides.....	77
3.7.	Enzymes.....	77
3.8.	Antibodies and conjugates.....	78

3.9.	Chemicals	78
3.10.	Kits	80
3.11.	Instruments and consumables:.....	80
3.12.	Universal buffers	82
4.	Methods	83
4.1.	Molecular Biology Methods.....	83
4.1.1.	Bacteriological tools.....	83
4.1.1.1.	Liquide Cultures	83
4.1.1.2.	Solide cultures	83
4.1.1.3.	Long term storage.....	84
4.1.1.4.	Preparation and transformation of competent cells.....	84
4.1.1.4.1.	Preparation of competent cells for heat shock transformation	84
4.1.1.4.2.	Preparation of competent cells for electroporation	84
4.1.1.4.3.	Introduction of plasmid DNA by heat shock transformation	85
4.1.1.4.4.	Introduction of plasmid DNA by electroporation	85
4.1.2.	DNA preparation and manipulation	85
4.1.2.1.	Isolation of plasmid DNA from bacterial cultures	85
4.1.2.1.1.	Minipreps of plasmid DNA: alkaline lysis miniprep	85
4.1.2.1.2.	Large scale preparation of plasmid DNA: alkaline lysis protocol followed by anion exchange chromatography.....	86
4.1.2.2.	Preparation and analysis of plasmid DNA	87
4.1.2.2.1.	Clean-up of DNA by phenol extraction	87
4.1.2.2.2.	Ethanol precipitation of DNA	87
4.1.2.2.3.	Determination of nucleic acid concentration.....	88
4.1.2.2.4.	Separation of DNA fragments on agarose gels by electrophoresis.....	88
4.1.2.2.5.	Extraction of DNA fragments from agarose gels.....	88
4.1.2.3.	Enzymatic manipulation of plasmid DNA	89
4.1.2.3.1.	Digestion of DNA with restriction endonucleases	89
4.1.2.3.2.	Dephosphorylation of plasmid DNA with Calf Intestine Phosphatase	89
4.1.2.3.3.	Fill-in of 5'-protruding ends with Klenow Polymerase	89
4.1.2.3.4.	Removal of 3' protruding ends with T4-DNA-polymerase	90
4.1.2.3.5.	Ligation of DNA fragments	90
4.1.2.4.	Isolation and manipulation of genomic DNA	90
4.1.2.5.	DNA sequencing with the chain termination method of Sanger.....	91
4.1.3.	RNA preparation and manipulation	92
4.1.3.1.	Isolation of RNA from primary cells and cell lines	92
4.1.3.1.1.	Isolation of RNA with Trizol	92
4.1.3.1.2.	Isolation of RNA with the RNAeasy Kit.....	93
4.1.3.2.	Quality assessment and quantification of RNA	93
4.1.3.3.	Reverse transcription.....	93
4.1.4.	Polymerase chain reaction.....	94

4.1.5.	Quantitative polymerase chain reaction	95
4.1.6.	siRNA related techniques	96
4.1.6.1.	Selection of appropriate target sequences for shRNA.....	96
4.1.6.2.	Cloning of shRNA oligonucleotides into the shRNA vectors.....	96
4.1.7.	Lentiviral techniques	97
4.1.7.1.	Large scale virus production	97
4.1.7.2.	Concentration of lentiviral particles by ultracentrifugation	98
4.1.7.3.	Determination of lentiviral titers	98
4.1.7.4.	Infection of eukaryotic cells with lentiviral vectors.....	98
4.1.7.4.1.	Infection of adherent cells with lentiviral vectors	98
4.1.7.4.2.	Infection of nonadherent cells with lentiviral vectors	99
4.1.8.	Protein isolation, manipulation and analysis.....	99
4.1.8.1.	Protein isolation from cell lines and primary cells.....	99
4.1.8.2.	Determination of protein concentration using the BCA method.....	99
4.1.8.3.	Protein separation by denaturing discontinuous gel electrophoresis.....	100
4.1.8.4.	Protein transfer to membranes (Western blot) with a tank transfer system	101
4.1.8.5.	Immunodetection of specific proteins	101
4.2.	Cell Biology Methods	102
4.2.1.	Culture of eukaryotic cells	102
4.2.1.1.	Cell culture conditions and media	102
4.2.1.2.	Splitting of adherent cell lines.....	102
4.2.1.3.	Determination of the cell number and viability.....	103
4.2.1.4.	Storage, freezing of eukaryotic cells, thawing and recovery of eukaryotic cells.....	103
4.2.2.	Transfection of eukaryotic cells	103
4.2.2.1.	Calcium phosphate method	103
4.2.2.2.	Cationic lipid-mediated transfection	104
4.2.3.	Isolation of primary lymphocytes from blood and lymphatic organs	104
4.2.3.1.	Isolation of mononuclear cells from lymphatic organs	104
4.2.3.2.	Isolation of mononuclear cells from peripheral blood	105
4.2.3.3.	Ficoll gradient.....	105
4.2.3.4.	Erythrocyte lysis.....	105
4.2.4.	Flow cytometry.....	106
4.2.4.1.	Detection of surface epitopes	106
4.2.4.2.	Detection of intracellular epitopes	106
4.2.5.	Cell separation techniques.....	107
4.2.5.1.	MACS.....	107
4.2.5.2.	Cell sorting by FACS	108
4.2.6.	Enzyme-linked immunosorbent assay.....	108
4.2.6.1.	Isotype determination by sandwich ELISA.....	108
4.2.6.2.	Antibody-sandwich ELISA to detect soluble antigen.....	109

4.2.6.3.	Indirect ELISA for detection of specific antibodies.....	109
4.2.7.	Cytospin.....	110
4.2.8.	In-vitro proliferation assay	110
4.2.9.	In vitro chemotaxis assay	111
4.3.	Animal experimentation	111
4.3.1.	Genotyping of S1P ₄ ^{-/-} animals	111
4.3.2.	Anesthesia and sacrifice	112
4.3.3.	Gastrointestinal lavage	112
4.3.4.	Bronchoalveolar lavage.....	113
4.3.5.	Type IV hypersensitivity assay	113
4.3.6.	Contact hypersensitivity assay	113
4.3.7.	T-cell-depended antibody response to sheep red blood cell antigens	114
4.3.8.	Ovalbumin induced asthma	114
4.3.9.	4'-deoxyipyridoxin induced peripheral lymphopenia	114
4.4.	Determination of S1P content by chromatography	115
4.5.	Statistical analysis	115
5.	Results.....	116
5.1.	Alterations of the homeostasis of the immune system in S1P ₄ -deficient mice and their consequences on immune reactivity.....	116
5.1.1.	S1P ₄ deficiency in mice: immune phenotype.....	116
5.1.1.1.	Phenotypic analysis of primary and secondary lymphoid organs in S1P ₄ ^{-/-} mice by FACS	116
5.1.1.2.	Comparative analysis of cell populations in the bronchoalveolar lavage fluid... 118	
5.1.1.3	Comparative evaluation of Ig levels in plasma and serum of WT and S1P ₄ ^{-/-} mice	119
5.1.1.4.	Determination of mucosal IgA levels.....	121
5.1.1.5.	Quantitative assessment of the B-cell development in S1P ₄ ^{-/-} and WT mice.....	122
5.1.2.	S1P ₄ deficiency in Mice: functional consequences in the immune system.....	126
5.1.2.1.	S1P ₄ deficiency does not impact on the proliferative potential of CD4 ⁺ and CD8 ⁺ T-cells.....	127
5.1.2.2.	S1P ₄ deficiency deviates cytokine secretion <i>in vitro</i>	128
5.1.2.3.	Assessment of plasma and blood cell S1P concentrations	128
5.1.2.4.	Vitamin B6 antagonist DOP induced similar peripheral lymphopenia in WT and S1P ₄ ^{-/-} mice	129
5.1.2.5.	S1P ₄ deficiency affects <i>in vitro</i> migration of CD4 ⁺ and CD8 ⁺ lymphocytes.....	132
5.1.2.7.	S1P ₄ deficiency results in an increased contact hypersensitivity	135
5.1.2.8.	S1P ₄ deficiency results in a reduced classical Type IV hypersensitivity response.....	136
5.1.2.9.	S1P ₄ deficiency results in increased eosinophilic infiltration in a murine asthma model.....	137
5.2.	Knock-down of the S1P ₁ receptor in S1P ₄ ^{-/-} mice.....	141

5.2.1.	Generation of an expression vector for HA-tagged murine S1P ₁	141
5.2.2.1.	Selection of potential siRNA targets within the S1P ₁ ORF	143
5.2.2.2.	Generation of expression plasmids for production of S1P ₁ -specific shRNA.....	145
5.2.2.3.	Assessment of the efficiency of the selected candidate siRNA sequences for S1P ₁ knock down.....	146
5.2.3.	Generation of a retroviral vector for shRNA mediated knock-down of S1P ₁	146
5.2.4.	Generation of a lentiviral vector for shRNA mediated knock-down of S1P ₁	149
6.	Discussion	154
6.1.	Functions of S1P ₄ expression in the immune system.....	154
6.1.1.	S1P ₄ deficiency only marginally affects B and T-cell distribution within lymphatic organs.	154
6.1.2.	Signalling via S1P ₄ impacts on T- but not on B-cell migration	155
6.1.3.	S1P ₄ does not impact on tissular S1P levels.....	157
6.1.4.	Signalling via S1P ₄ does not impact on T-cell proliferation.....	157
6.1.5.	S1P in humoral immune response	158
6.1.5.1.	S1P ₄ ^{-/-} mice show increased IgG1, IgA and IgE levels.....	158
6.1.5.2.	The humoral response to SRBC is normal in S1P ₄ ^{-/-} mice.....	159
6.1.5.3.	S1P ₄ deficiency affects intestinal IgA levels.....	160
6.1.6.	S1P in B-cell lineage development	161
6.1.6.1.	S1P ₄ ^{-/-} deficiency results in reduced number of pre-/pro-B-cells in the bone marrow.....	161
6.2.6.2.	S1P ₄ ^{-/-} deficiency results in reduced number of splenic transitional type II cells but increased numbers of MZ B-cells	163
6.1.6.3.	S1P ₄ ^{-/-} deficiency does not impact on B1 B-cell numbers in the peritoneal cavity	164
6.1.7.	S1P in polarisation of the immune response	165
6.1.7.1.	S1P ₄ deficiency results in an increased intrinsic capacity for secretion of the T _H 2 cytokine IL-5 by CD4 ⁺ T-cells.....	165
6.1.7.2.	S1P ₄ in contact hypersensitivity and type IV hypersensitivity.....	166
6.1.7.3.	Role of S1P ₄ in asthma.....	168
6.2.	Generation of a lentiviral vector system for shRNA-mediated S1P ₁ knock- down	170
7.	Conclusions and perspectives	173
8.	Bibliography.....	175

1. INTRODUCTION

1.1. General introduction

Lysophospholipids represent a quantitatively minor lipid species when compared to their phospholipid counterparts that are the major components of mammalian cell membranes. Initially, they were identified as precursors and metabolites of, respectively, in the *de novo* biosynthesis and the degradation of phospholipids. However, pioneer observations showing that certain members of the lysophospholipid family are implicated in the initiation and regulation of a wide range of cellular processes were already made in the 1960's⁷. Initially considered to mediate their biological effects as intracellular secondary messengers, it took almost 40 years before the first membrane bound receptor for a lysophospholipid was identified⁸. Today, it is generally recognised that lysophospholipids mediate the vast majority of their biological effect *via* membrane receptors. The family of lysophospholipid receptors belongs to the large group of G-protein coupled receptors (GPCRs) characterized by the presence of 7 transmembrane helices. Up to now, 10 lysophospholipid receptors for the major classes of lysophospholipids, lysophosphatidic acid and sphingosine-1-phosphate, have been described. Due to their implication in a wide variety of physiological but also pathological processes they are presently in the centre of intense scientific interest. However, the current knowledge on the implication of specific receptors into cellular signalling pathways and specific biological processes remains more or less patchy, at least for the majority of lysophospholipid receptors. The lysophospholipid receptor S1P₄ has been first described in 1998⁹. Its expression is basically restricted to lymphoid tissue, but the exact function of signalling via S1P₄ in the immune homeostasis has not yet been shown. The characterisation of S1P₄ function defines the general frame of my thesis.

In the following introduction, I will summarise the current knowledge on S1P receptors in general as well as on their biological function in the immune system. In the first instance, I will give a short general overview on the complex biology of GPCRs. Thereafter, the current knowledge on structural and functional properties of lysophospholipid receptors will be introduced, followed by a detailed review of their involvement in various biological processes.

1.2. Structural characteristics and functional properties of G-protein coupled receptors and their signalling pathways

G-protein-coupled receptors (GPCRs) are the largest family of cell surface molecules involved in signal transduction. In vertebrates, this group of receptors comprises 1000 to 2000 members, including more than 1000 receptors binding odorants and pheromones. More than one percent of the human genome and more than 5% of the genome of the nematode *Caenorhabditis elegans* encodes for proteins with a typical structure of GPCRs^{10,11}. The presence of these receptors in plants, yeast, protozoa and the earliest diploblastic metazoa¹²⁻¹⁵ clearly indicates that GPCRs are among the best persevered molecules implicated in signal transduction. The range of their ligands is extremely large and comprises Ca^{2+} , amino acid residues, nucleotides and peptides, peptide and non-peptide neurotransmitters, hormones, growth factors, odorant molecules and even subatomic particles such as photons (**Figure 1**).

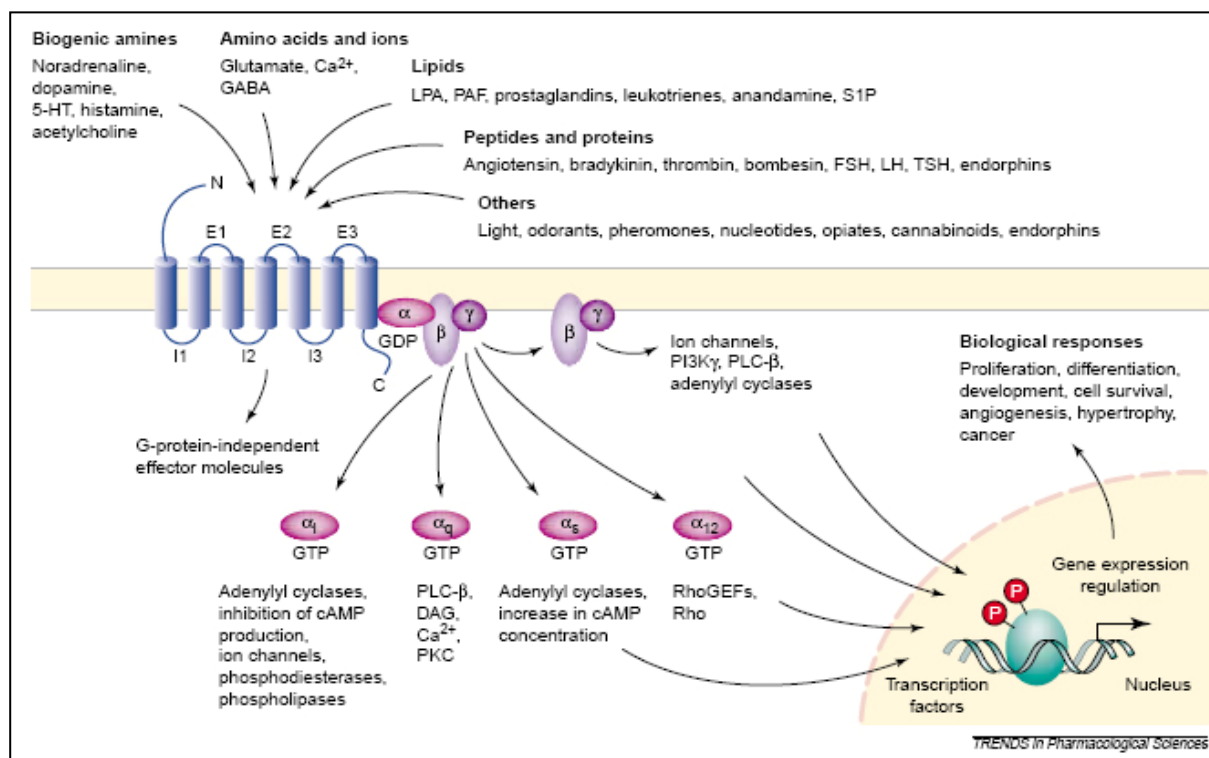


Figure 1: Diversity of GPCR ligands and intracellular signaling pathways

GPCRs are receptors for a broad range of ligands. They couple to 4 classes of G-proteins. Each class of $\text{G}\alpha$ proteins can interact with a specific panel of intracellular signalling pathways. Modified from Marinissen & Gutkind, Trends in Pharmacological Sciences, 2001

Given the implication of these receptors in a multitude of biological processes, it is not surprising that GPCRs are the target of over 50 % of the therapeutic agents currently on the market¹⁰. The common structural hallmark of these receptors is the presence of seven α -helical transmembrane domains. Historically, GPCRs were thought to exclusively transmit their signals *via* the interaction with intracellular heterotrimeric G-proteins, thereby

explaining the name that was given to this group of receptors. However, recent findings indicate that GPCRs may signal *via* alternative, G-protein-independent mechanisms. For this reason, the name “7-transmembrane receptors” may appear to be more appropriate in the future.

1.2.1. Structural and functional characteristics of GPCRs

As mentioned above, GPCRs share a common structural core domain formed by seven hydrophobic transmembrane α -helices (TMH). These are connected by three intra- and three extracellular loops. Two highly conserved cysteine residues are present in the extra-cellular loops I and II of the majority of GPCRs, that are the basis for the formation of a disulfide bridge probably stabilizing a restricted number of conformations of the 7 transmembrane helices. The core domain also possesses an intracellular carboxyl terminus and an extracellular amino terminus. GPCRs share the highest homology within the 7 transmembrane helices. In contrast, the carboxyl terminus, the intracellular loop between α -helix 5 and 6 and the amino terminus present the highest variability. The amino terminus shows the greatest diversity. Based on similarities / differences within the amino-acid sequence, GPCRs were classified in 5 families¹⁶. Sequence homology between these families is very small, while it can reach quite significant values within a family. The structural modifications occurring upon ligand binding to the GPCRs seem to be relatively well conserved. Biochemical and biophysical studies in particular with rhodopsine but also with other GPCRs have shown that a central event in GPCR activation is the rotation of the transmembrane helix VI and separation for transmembrane helix III^{17,18}. These conformational changes usually affect the positioning of the intracellular loops II and III which constitute one of the principal sites of G-protein recognition and activation¹⁹.

Although it appears that the above described conformational changes of the core unit occur in a similar fashion in almost all GPCRs, there is a large diversity of molecular mechanisms insuring the induction of these conformational changes by the natural ligands of the GPCR. The very small ligands of the GPCR subfamily 1a, such as for instance catecholamines, bind in a cavity formed by TMH II and VI. In the case of the light-activated rhodopsin receptor that also belongs to the GPCR subfamily 1a, the target protein of the light photon, retinal, is covalently bound into this pocket and its conformational change induced by the light absorption activates the receptor.

Short peptides are usual ligands for the GPCR subfamily Ib. They interact with the extracellular loops, the superior parts of the TMHs and the amino terminus. The protease-

activated thrombin receptor, which also belongs to the Ib subfamily of GPCRs, is an additional example of a highly sophisticated mechanism of GPCR activation: after cleavage of the amino-terminus of this GPCR by thrombin one product resulting from the cleavage serves as ligand for the receptor.

Members of the group 1c GPCRs interact with glycoprotein hormones and are characterized by a large extracellular amino terminus that binds to the ligands and allows them to interact with extracellular loop I and III.

Another mechanism was identified for the metabotropic glutamate receptor or for the Ca^{2+} sensing receptor both belonging to the GPCR subfamily III. The extracellular domain of the receptor is constituted of two lobes separated by a hinge region. Upon binding of the ligand, these lobes close like a Venus' flytrap and the closed extracellular domain serves as ligand for its core unit.

As illustrated by the examples given above, in spite of a very similar core structure, the development of a wide variety of different molecular mechanisms for ligand recognition endows the GPCRs with a very large spectrum of possible ligands. Further complexity is added to this system by the occurrence of homo- and heterodimerization among GPCRs.

In recent years, increasing numbers of GPCRs have been shown to form hetero- and homodimers²⁰⁻²⁴. In some cases, dimers exist independently of the presence of the ligand²⁰, in other cases, dimerization was positively affected by the ligand²⁴, and finally, as for instance in the case of the δ opioid receptor, increasing concentrations of the ligand decreases receptor dimerization²¹. The mechanisms that mediate dimer formation are also diverse. While some receptors form disulfide bridges, non-covalent interactions may be implicated in the dimerization of others^{20,25}. The localisation of the protein domains implicated in the interaction is not constant in all GPCRs but can involve the amino terminus, the carboxyl terminus, the extracellular domains or even the transmembrane domains^{20,21,25}. The biological consequences of heterodimerization are also diverse. It ranges from changes in receptor trafficking²⁶, agonist-induced internalisation²¹, ligand affinity²⁰ to, most intriguingly, receptor-specificity as shown for the calcitonin-receptor-like receptor (CRLR)²⁷. Indeed, when CRLR associates with RAMP1 (Receptor-Activity Modifying Peptide1), it will generate the calcitonin gene-related peptide receptor, whilst its association with RAMP2 will generate the adrenomedullin receptor²⁷.

1.2.2. Regulation of GPCR signalling

Multiple mechanisms contribute to the regulation of signal transduction at the level of the GPCR itself.

A characteristic feature of GPCR signalling is the short-term or long-term loss of the cellular reactivity to the stimulus, a phenomenon referred to as “desensitisation”. Several biological mechanisms are implicated in this process.

Heterologous desensitisation is a general cellular hyporesponsiveness resulting from phosphorylation of the target GPCR by second messenger-dependent kinases activated *via* GPCRs different from the initial target GPCR. Kinases involved in this process include second messenger-activated protein kinases A and C²⁸.

Homologous or agonist-stimulated desensitisation refers to a process that requires agonist occupation of the involved GPCR. Central players in homologous desensitisation are members of the G-protein-coupled receptor kinase (GRK) family. This kinase family contains seven serine/threonine kinases that preferentially phosphorylate activated GPCRs thereby facilitating arrestin binding to the activated GPCR²⁹. Initially, the binding of arrestin uncouples the receptor from the effector G-protein³⁰. Thereafter, the interaction of receptor bound arrestin with proteins involved in endocytotic processes like clathrin, Adaptor protein 2 (AP-2), N -ethylmaleimide-sensitive fusion protein (NSF) and ADP-ribosylation factor 6 (Arf6) facilitates the endocytosis of the activated GPCR into clathrin-coated vesicles³¹. The post-endocytotic fate of the GPCRs depends on their specific interaction with various scaffolding molecules. Endocytosed receptors may recycle to the cell surface (resensitisation) or can be targeted to the lysosomal compartment for degradation³⁰ (**Figure 2**).

Two proteins centrally involved in this process have recently received considerable interest due to other specific functions that are essential in GPCR biology. Some members of the GRK family (GRK 2 and 3) do not only intervene at the level of the GPCR phosphorylation itself, but can also influence GPCR-mediated signalling at the level of G-proteins, the effector molecules of GPCRs. This regulation occurs by phosphorylation-independent mechanisms involving a RGS motif present in the N-terminal domain of the molecule. This domain enables interaction of GRK 2 with members of the G α_q family of G α proteins leading to an increased rate of GTP hydrolyses and attenuation of the G-protein-mediated signal³² (see also **chapter 1.2.3.1.2.**). Independently of its RGS activity, GRK 2 was shown to efficiently shield interaction between G-proteins and either the corresponding GPCR or its specific effector³³. This adds a further level of complexity to the function of GRKs in the regulation of GPCR signalling. Arrestins do not only promote receptor

internalisation but function also as agonist-regulated adaptor proteins in G-protein independent GPCR signalling processes (see also **chapter 1.2.3.2**)

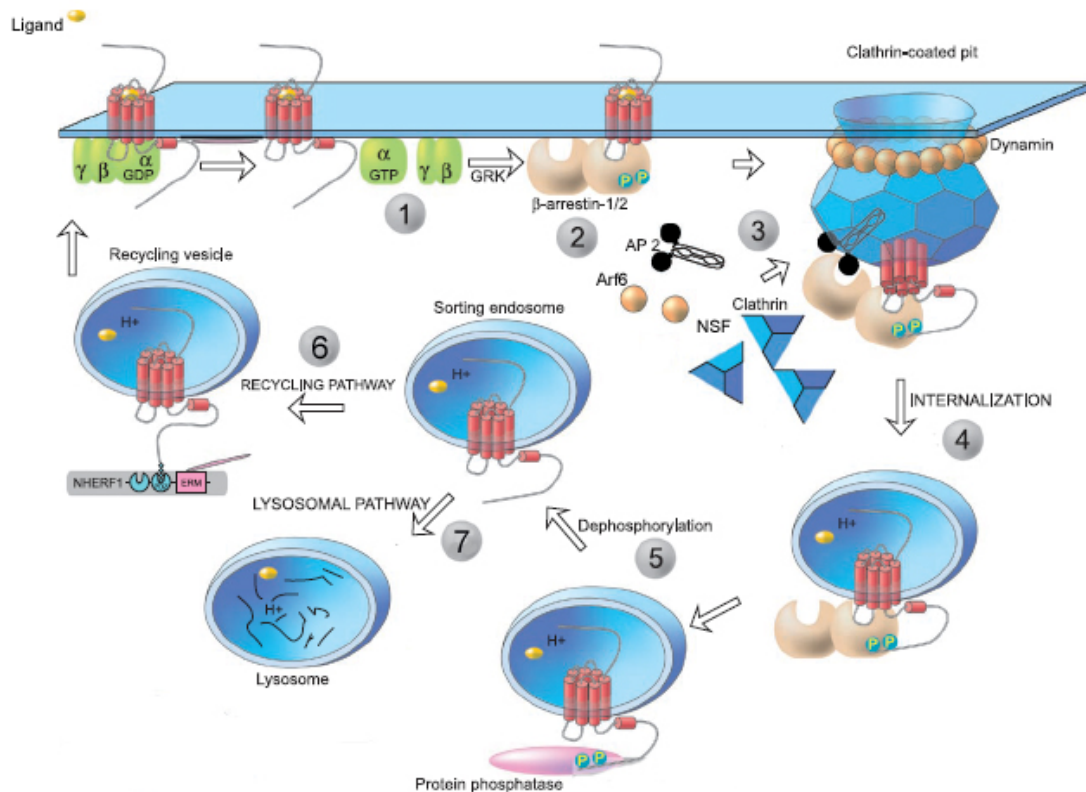


Figure 2: Pathways involved in desensitisation and resensitisation of GPCR signalling. Ligand binding to the GPCR leads not only to activation or inhibition of specific signalling pathways in the cells, but also to activation of GRKs resulting in the phosphorylation of the GPCR (1). GPCR phosphorylation results in an increased affinity for specific arrestins. GPCR bound arrestin prevents sterically further coupling of the receptor to G-proteins leading to short term desensitisation of the receptor (2). β -arrestins binding to phosphorylated GPCR regulate endocytosis. They associate with proteins involved in endocytosis including AP-2, NSF and Arf6(3). This complex formation contributes to formation and budding of clathrin-coated vesicles and internalisation of the GPCR (4). In the endosomes, receptors are dephosphorylated by protein phosphatases (5). Depending on the ability to interact with specific intracellular proteins, dephosphorylated receptor are either recycled back to the plasma membrane (6) or directed to the lysosomes for degradation (7). Adapted from Kristiansen, Pharmacology and Therapeutics, 2004 [Kristiansen, 2004 #670]

1.2.3. Intracellular signalling of heptahelical receptors

1.2.3.1. Signal transduction via G-proteins

As suggested by their name, a central paradigm in the biology of G-protein-coupled receptors is been the intracellular signal transduction *via* G-proteins.

G-proteins belong to the group of regulatory GTPases which are proteins or protein complexes that become activated after GTP binding. Due to an intrinsic GTPase activity, the bound GTP is hydrolysed leading to the inactivation of the regulatory GTPase. The members

of the heterotrimeric G-protein family of GTPases are composed of three subunits: a α -subunit of 39 to 46 kDa, a β -subunit of 37kDa and smaller γ -subunit of 8 kDa. As yet, 23 $G\alpha$ proteins encoded by 16 $G\alpha$ genes, 5 $G\beta$ proteins and 12 different $G\gamma$ proteins have been described³⁴. According to sequence homologies of their α -subunit, G-proteins can be classified into 4 different families: $G\alpha_i$, $G\alpha_q$, $G\alpha_s$ and $G\alpha_{12/13}$ (**Table 1**). Each α unit and the $\beta\gamma$ unit can interact with a specific panel of intracellular signalling pathways (**Figure 1**).

Family	Subtype	Effectors	Expression	Pharmacological modulation
$G_i\alpha$	$G_{iS/\alpha}$	Adenylyl cyclases \uparrow ($G_{iS/OX1,OX2\alpha}$)	$G_i\alpha$: ubiquitous $G_{iO\alpha}$: olfactory neurons, certain CNS ganglia; digestive and urogenital tract	$G_i\alpha$: CTX $G_{iO\alpha}$: CTX
	$G_{i13\alpha}$	Maxi K channel \uparrow ($G_{i13\alpha}$)		
	$G_{iOX1,\alpha}$	Src tyrosine kinases (c-Src, Hck) \uparrow ($G_{i\alpha}$)		
	$G_{iO\alpha}$	GTPase of tubulin \uparrow ($G_{i\alpha}$)		
$G_{i/o}\alpha$	$G_{i/o}\alpha$	Adenylyl cyclase \downarrow ($G_{i/o,2\alpha}$)	$G_{i1-3\alpha}$: neurons, neuroendocrine cells, astroglia, heart $G_{i1-3\alpha}$: neurons and many others $G_{i2\alpha}$: platelets, neurons, adrenal chromaffin cells, neurosecretory cells $G_{i1\alpha}$: rod outer segments, taste buds $G_{i2\alpha}$: cone outer segments $G_{i3\alpha}$: sweet and/or bitter taste buds, chemoreceptor cells in the airways	$G_{i1/2\alpha}$: PTX $G_{i1-3\alpha}$: PTX $G_{i2\alpha}$: ? $G_{i1/2\alpha}$: PTX, CTX $G_{i3\alpha}$: PTX
	$G_{i2\alpha}$	Rap1 GAPII-dependent		
	$G_{i1-3\alpha}$	ERK/MAPkinase activation \uparrow ($G_{i\alpha}$)		
	$G_{i2\alpha}$	Ca^{2+} channels \downarrow ($G_{i/o,2\alpha}$)		
	$G_{i1/2\alpha}$	K^+ channels \uparrow ($G_{i/o,2\alpha}$)		
	$G_{i3\alpha}$	GTPase of tubulin \uparrow ($G_{i\alpha}$)		
	$G_{i3\alpha}$	Src tyrosine kinases (c-Src, Hck) \uparrow ($G_{i\alpha}$) Rap1GAP \uparrow ($G_{i\alpha}$) GRIN1-mediated activation of Cdc42 \uparrow ($G_{i/o,2\alpha}$) cGMP-PDE \uparrow ($G_{i\alpha}$) $G_{i3\alpha}$: ?		
$G_{q/11}\alpha$	$G_{q\alpha}$	Phospholipase C β isoforms \uparrow	$G_{q/11\alpha}$: ubiquitous $G_{13/16\alpha}$: hematopoietic cells	$G_{q/11\alpha}$: YM-254890 $G_{14\alpha}$: ? $G_{15\alpha}$: ? $G_{16\alpha}$: ?
	$G_{11\alpha}$	p63-RhoGEF \uparrow ($G_{q/11\alpha}$)		
	$G_{14\alpha}$	Bruton's tyrosine kinase \uparrow ($G_{q\alpha}$)		
	$G_{15\alpha}$	K^+ channels \uparrow ($G_{q\alpha}$)		
	$G_{16\alpha}$			
$G_{12/13}\alpha$	$G_{12\alpha}$	Phospholipase D \uparrow	Ubiquitous	$G_{12\alpha}$: ? $G_{13\alpha}$: ?
	$G_{13\alpha}$	Phospholipase C ϵ \uparrow		
		NHE-1 \uparrow		
		iNOS \uparrow		
		E-cadherin-mediated cell adhesion: \uparrow		
		p115 RhoGEF \uparrow		
		PDZ-RhoGEF \uparrow		
		Leukaemia-associated RhoGEF (LARG) \uparrow		
		Radixin \uparrow		
		Protein phosphatase 5 (PP5) \uparrow		
		AKAP110-mediated activation of PKA \uparrow		
		HSP90 \uparrow		
		PLC β s \uparrow		
$G\beta/\gamma$	β_{1-5}	Adenylyl cyclase I \downarrow	$\beta_1\gamma_1$: retinal rod cells $\beta_1\gamma_2$: retinal cone cells β_5 : neurons and neuroendocrine organs $\beta_{5(1)}$: retina Most cell types express multiple β and γ subtypes	$G\beta\gamma$: ?
	γ_{1-12}	Adenylyl cyclases II, IV, VII \uparrow PI-3 kinases \uparrow K^+ channels (GIRK1,2,4) \uparrow Ca^{2+} (N-, P/Q-, R-type) channels \downarrow P-Rex1 (guanine nucleotide exchange factor for the small GTPase Rac) \uparrow c-Jun N-terminal kinase (JNK) \uparrow Src kinases \uparrow Tubulin GTPase activity \uparrow G-protein-coupled receptor kinase recruitment to membrane \uparrow Protein kinase D \uparrow Bruton's tyrosine kinase \uparrow p114-RhoGEF \uparrow		

Table 1: The family of mammalian heterotrimeric G proteins subunits

The table shows the different families of α proteins as well as the $\beta\gamma$ proteins with their respective intracellular signalling pathways as well as the tolls for their pharmacological inhibition. PTX: pertussis toxin; CTX: cholera toxin; \uparrow stimulation, \downarrow inhibition

Modified from Milligan and Costens, British Journal of Pharmacology, 2006

The GDP/GTP cycle governing the activation of G-proteins is depicted in **Figure 3**. GDP-bound $G\alpha$ proteins manifest a high affinity for the obligate heterodimer of $G\beta\gamma$. The association with $G\beta\gamma$ proteins supports the membrane localisation of the $G\alpha$ protein and thereby facilitates the interaction with GPCRs. Furthermore, $G\beta\gamma$ binding to the $G\alpha$ unit slows

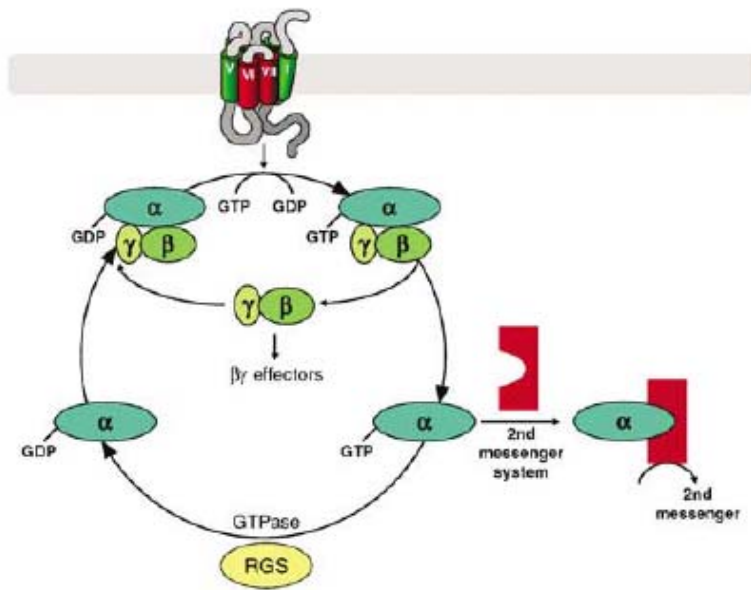


Figure 3: Modell of the GDP/GTP cycle governing the activation of heterotrimeric G proteins

From Milligan and Costensis, British Journal of Pharmacology, 2006

down the spontaneous rate of GTP release, thus acting as a Guanine nucleotide Dissociation Inhibitor (GDI). The interaction of the α -subunit with the intracellular loops II and III of the GPCRs defines the strength (intracellular loop II) and the specificity (intracellular loop III) of the GPCR-heterotrimeric G-protein interaction. Binding of the ligand to the GPCR leads to a conformational change between its intracellular loops II and III, resulting in the release of GDP from the $G\alpha$ protein. Thus, GPCRs act as Guanine nucleotide Exchange Factor (GEF). Nucleotide-free $G\alpha$ protein binds then to GTP that is present in a significant molecular excess over GDP in the cells. The binding of GTP has two consequences: first, the $\beta\gamma$ -complex dissociates from the α -subunit and second, the α -subunit dissociates from the activated GPCR. As long as the GPCR is activated by the bound ligand, it can activate further heterotrimeric G-proteins, leading to an amplification of the initial signal. The free GTP-bound α -subunit can now activate various effector molecules. The activation of the $G\alpha$ -protein is terminated by the hydrolysis of the GTP to GDP through the intrinsic GTPase activity of the α -subunit. This intrinsic GTPase activity that thus determines the length of activation of the α -subunit can be regulated by various mechanisms (see below). Initially, the $\beta\gamma$ -complex was thought to have a purely passive role. However, it has now been shown that it can also specifically interact with several effector molecules including adenylyl cyclases and GPCR-kinases (see **Table 1**)¹⁹.

Membrane anchors present in the α -subunit as well as in the γ -subunit guarantee the correct localisation of the heterotrimeric G-proteins to the plasma membrane. This is a prerequisite for the interaction with both the activating GPCR and the membrane bound effector molecules.

Functional studies of different G-proteins are facilitated by the possibility to specifically inhibit some members of the family of heterotrimeric GTPases specifically with bacterial toxins. Thus, almost all $G\alpha_i$ proteins are inhibited by pertussis toxin, while $G\alpha_s$ proteins are inhibited by cholera toxin.

1.2.3.1.1. Effector molecules of heterotrimeric G-proteins

The dissociated G_α and $G_{\beta\gamma}$ subunits of heterotrimeric G-proteins can be considered as autonomous signalling molecules. While the majority of effector molecules is either stimulated by the G_α or the $G_{\beta\gamma}$ subunits, some effectors can be regulated independently by both subunits of heterotrimeric G-proteins, as it is the case for K^+ channels³⁵. Several adenylyl cyclases can be influenced by both G_α or the $G_{\beta\gamma}$ subunits as well. Interestingly, the actions of the two subunits are synergistic in the case of the adenylyl cyclase type II, while they are antagonistic in the case of the adenylyl cyclase type I³⁶.

The G_α and the $G_{\beta\gamma}$ subunits are both membrane-bound *via* various lipid anchors. Interaction can only occur with signalling proteins that are also inserted into – or scheduled to – the plasma membrane. Classical effector molecules of heterotrimeric G-proteins comprise adenylyl cyclases (Acs), small GTP binding molecules, phospholipases type C, cGMP phosphodiesterases as well as K^+ and Ca^{2+} channels³⁷.

ACs were the first intracellular proteins identified as targets for heterotrimeric G-proteins, when $G\alpha_s$ was found to stimulate the activity of this enzyme³⁸. Shortly thereafter, $G\alpha_i$ was identified as an inhibitor of ACs³⁹. Throughout the years it became increasingly clear that membrane-bound ACs can be independently regulated by various $G\alpha$ proteins and also $G\beta\gamma$ proteins. Activation of ACs results in an increase of intracellular cAMP, thus activating various protein kinases type A as well as regulating cationic Ca^{2+} channels.

The cAMP phosphodiesterase is another target for some members of the $G\alpha_i$ protein family⁴⁰. The intracellular cGMP level is implicated in the regulation of the activity of cGMP-dependent protein kinases as well as of cationic ion channels.

Additionally, different isoenzymes of the phospholipase C turned out to be subjected to the regulation by $G\alpha$ proteins. Phospholipase C hydrolyses the phosphoester bond of the plasma membrane lipid phosphatidylinositol 4,5-biphosphate generating the ubiquitous second messengers inositol 1,4,5-triphosphate and diacylglycerol⁴¹. Both second messengers stimulate further signalling pathways, including the liberation of Ca^{2+} from the endoplasmatic reticulum by inositol 1,4,5-triphosphate and the activation of protein kinase C by diacylglycerol.

$G\alpha_{12/13}$ proteins can regulate the activity of the small GTPase RhoA *via* activation of various effectors that possess GEF activity^{41,42}. These effectors activate RhoA activity by promoting the exchange of GDP for GTP. By this way, $G\alpha$ -proteins are coupled to different MAP kinase pathways, influencing cell proliferation and differentiation.

While stimulation of downstream effectors of heterotrimeric G-protein was initially thought to be mediated by the $G\alpha$ protein, it is now accepted that the $G\beta\gamma$ protein complex is prone to activate a large number of its own effectors⁴³. The first $G\beta\gamma$ effector class described corresponds to ion channels, including the G-protein-regulated inward rectifier K^+ channel, and various Ca^{2+} channels. Moreover, $G\beta\gamma$ were found to positively and negatively regulate various ACs, various kinases like the phosphoinositide-3' kinase γ , various isoenzymes of the phospholipase C as well as small GTPases.

1.2.3.1.2. Regulation of signalling by heterotrimeric G-proteins

The efficacy of the G-protein signalling depends on the relative amounts of the GDP- and the GTP- bound forms of the heterotrimer. The level of the GTP-bound G-protein is regulated at two different levels: first at the level of the dissociation of GDP from GDP-bound $G\alpha$ protein that in turn becomes available for GTP binding, and second at the level of GTP hydrolysis that determines the duration of G-protein activation.

The former process can be regulated by Guanine nucleotide Dissociation Inhibitors (GDI). These molecules stabilize the inactive GDP-bound form of the $G\alpha$ protein and are able to attenuate signal transduction. The $G\beta\gamma$ heterodimers have been shown to act as GDIs.

The rate of GTP hydrolysis depends on the intrinsic GTPase activity of the $G\alpha$ protein and can be modulated by certain $G\alpha$ effectors such as PLC- β ⁴⁴. In 1996, a novel family of GTPase-accelerating proteins was described and subsequently designated as “regulators of G-protein signalling” (RGS)⁴⁵. The RGS family contains 20 classical members and was found for all families of heterotrimeric G-proteins with the exception of the $G\alpha_s$ family⁴⁶. A structural hallmark of RGS is a ~120 amino acids containing RGS domain that stabilizes the transition state for GTP hydrolysis⁴⁷. This results in a shortening of the duration of the active state of the G-protein and to an attenuated agonist/GPCR-stimulated cellular response *in vivo*. RGS are considered to play a key role in the desensitisation of heterotrimeric G-protein signalling pathways.

1.2.3.2. G-protein-independent signalling by heptahelical receptors

With the development of highly sophisticated methods for the analysis of protein-protein interactions, experimental evidences have emerged showing that GPCRs can interact directly with intracellular partners distinct from G-proteins. These interaction partners, that activate further downstream signalling pathways, include arrestins, SH2 domain-containing signalling- and adaptor-molecules, small GTP-binding proteins, polyproline binding proteins and others⁴⁸.

Upon activation, GPCRs can be phosphorylated by G-protein coupled receptor kinases (GRK). This phosphorylation results in the binding of another family of proteins; the arrestins. GPCR binding to arrestins was initially shown to result in receptor desensitisation of G-protein mediated signalling by hampering the GPCR – G-protein interaction. Later it has been found that arrestins not only negatively regulate the classical G-protein dependent pathway but that they can also couple GPCRs to the activation of Src-like kinases thus creating a direct link with components of the MAPK and JNK pathways⁴⁹.

Several GPCR subtypes are able to associate to SH2 domain-based signalling complexes. Thus, it has been demonstrated that the heptahelical angiotensin AT₁ receptor can associate with the tyrosine Janus-activated kinase JAK2 *via* a SH2 domain containing phosphatase^{50,51}. This example demonstrates that the tyrosine phosphorylation of activated GPCRs allows the possibility to form complexes with various SH- and PTB- domain containing proteins which can then initiate further pathways of signal transduction.

Regulation of small GTP-binding proteins by GPCR mediated signalling was initially interpreted as a result of the classical activation of heterotrimeric G-proteins. However, the activation of phospholipase D by stimulation of the M₃ muscarinic acetylcholine receptor as well as of the H₁ histamine receptor could not be inhibited by classical inhibitors of the heterotrimeric G-protein pathway, but could be effectively abolished by Rho inhibitors⁵². This demonstrates that activation of small GTP-binding proteins Rho consecutive to GPCR activation does not always require the classical heterotrimeric G-protein pathway.

A growing number of GPCRs with a long intracytoplasmic C-terminus was found to interact with PDZ domain-containing proteins. For instance, the β_2 -receptor interacts *via* its C terminal domain with the PDZ domain-containing Na⁺/H⁺ exchange regulatory factor thus directly influencing renal Na⁺/H⁺ exchange independently from classical heterotrimeric G-protein pathways⁵¹.

Finally, several heptahelical receptors contain polyproline rich regions in either their third intracellular loop or in the C-terminus. These regions can mediate interactions with a

variety of conserved protein domains such as SH3 or EHV domains⁵². An example for this apparently quite frequent mechanism is the Ca²⁺ release after stimulation of the metabotropic glutamate receptor through direct EHV domain-mediated binding of the Homer protein to the GPCR as well as to the endoplasmatic-reticulum based inositol triphosphate receptor, thus mediating direct interaction between these two receptors⁵³.

In conclusion, signalling *via* GPCR is a highly complex process that is much more than a simple linear transmission of an extracellular signal to the cytoplasm. The process is subjected to a variety of regulatory influences that can intervene at virtually all levels of signal transduction from the GPCR up to the secondary or tertiary messenger molecule. The fact that the extraordinarily high number of different GPCRs all signal by a limited number of conceptually very similar pathways consisting of a restricted number of intracellular effectors, secondary and tertiary messengers, shows clearly that sophisticated mechanisms are required to maintain the specificity of the signal. The described multiple levels of regulation together with the cell type specific expression of components of the signalling pathways and the strong compartmentalisation and scaffolding of the involved signalling molecules guarantee both for this specificity and for an appropriate cellular response to the initial signal.

1.3. Lysophospholipid receptors

1.3.1. Brief History

The group of lysophospholipid receptors has been historically referred to as EDG receptors. This name, that was an acronym for Endothelial Differentiation Gene receptors, was initially coined in 1990 by Hla *et al.* when they described a set of immediate early response gene products cloned from umbilical vein endothelial cells⁵⁴. Three years later, another GPCR with a 50% identity to the EDG-1 gene was discovered and termed AGR16 gene⁵⁵. The term EDG-2 was then used to describe another structurally related GPCR in 1995⁵⁶. Over the following years, five other receptors of this structural cluster were identified and termed in the order of their discovery EDG-3 to EDG-8, the GPCR initially designated AGR16 being renamed EDG-5.

A seminal discovery was the identification of lysophosphatidic acid (LPA) as ligand for the murine EDG-2 receptor in 1996⁸. Within the following 24 months, EDG-1 and EDG-3 were described as S1P preferring receptors^{57,58}. Soon, the described 8 EDG receptors were identified as lysophospholipid binding receptors, 5 of them with high affinity for S1P and three binding preferentially LPA. Recently, two other LPA receptors have been identified. During the ongoing deorphanization process of GPCRs, additional receptors are still found to

bind various lysophospholipids with high affinity, so that the number of lysophospholipid receptors is still increasing.

1.3.2. Nomenclature and classification

Although the EDG acronym reflected some characteristics of the EDG-1 receptor, this name was used in simple extrapolation for the other receptors without any relevance for their structural or functional characteristics. Therefore, a novel nomenclature for lysophospholipid receptors was proposed and accepted in 2002⁵⁹. According to the guidelines of the International Union of Pharmacology, a receptor is to be named by the international abbreviation for its strongest natural agonist, followed by a subscript arabic number. The order of the numbering reflects the chronology of the publication of family receptors. Thus, EDG-1 became S1P₁ and EDG-2 became LPA₁. The actual nomenclature of lysophospholipids with its typical dichotomy into S1P and LPA receptors is shown in **Figure 4**.

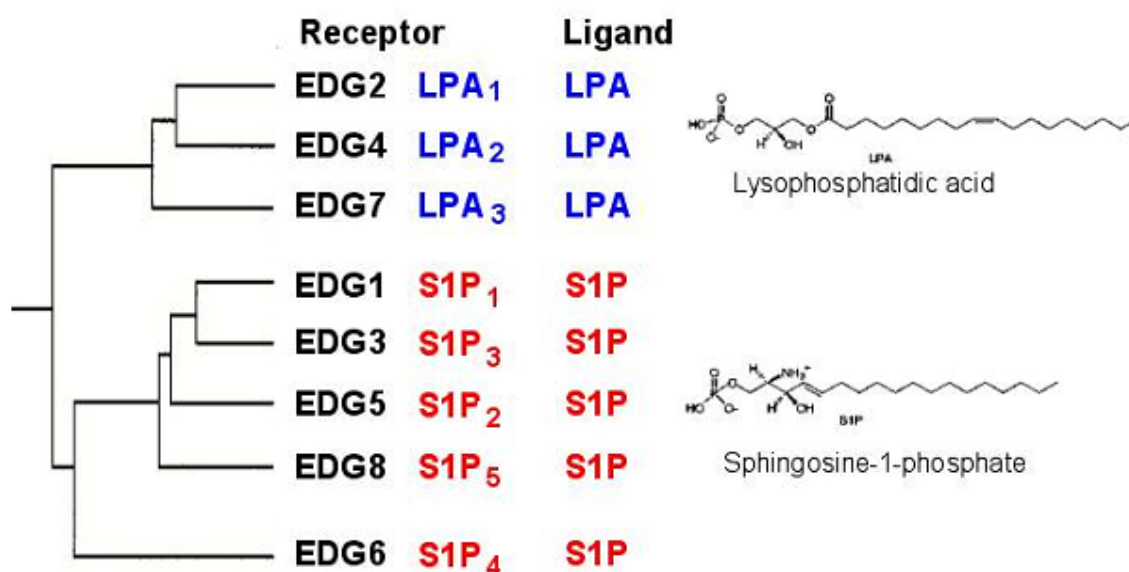


Figure 4: Phylogenetic tree of Lysophospholipid receptors

The S1P and LPA group of lysophospholipid receptors are shown with their respective ligands. The ancient nomenclature is shown for each receptor. The recently characterized LPA receptors LPA₄ and LPA₅ are not depicted due to their phylogenetically distant relation to the 8 classical lysophospholipid receptors.

Comparison of the amino acid sequence of S1P receptors has shown a sequence identity of ~50% while LPA receptors share about 55% identical amino acid sequences⁵⁹. Both groups of receptors exhibit a sequence homology of approximately 30% with each other. The GPCR receptors showing the highest sequence homology to lysophospholipid receptors are the cannabinoid receptors and the receptor for the platelet activating factor.

1.3.3. Sphingosine 1 phosphate receptors

1.3.3.1. S1P₁

S1P₁ has been the first identified receptor for S1P. The murine *s1p1* gene is composed of 2 exons but only exon 2 contains the entire *s1p1* coding region⁶⁰. Both mouse and human S1P₁ contain 382 amino acids (aa) and have an apparent molecular mass of 43 kDa. The mouse *s1p1* gene is localized on chromosome 3⁶⁰. S1P₁ is quite ubiquitously expressed in the adult organism. During embryological development, S1P₁ is weakly and diffusely expressed at E8.5. Higher expression levels are found during the later embryological development in the cardiovascular and nervous system as well as in centres of ossification.

Downstream signalling of S1P₁ differs from that of other S1P receptors in that it couples exclusively to G α_i proteins. Signaling *via* S1P₁ receptors increases the activity of PLC and PI3K and inhibits the activity of AC stimulated by forskoline. S1P₁ mediates intracellular ERK activation and proliferation, Akt activation and cell survival as well as Rac activation and migration (**Figure 5**)⁶¹. The receptor can be phosphorylated by Akt. This phosphorylation is required for Rac activation, cortical actin assembly and cell migration. Rac activation *via*

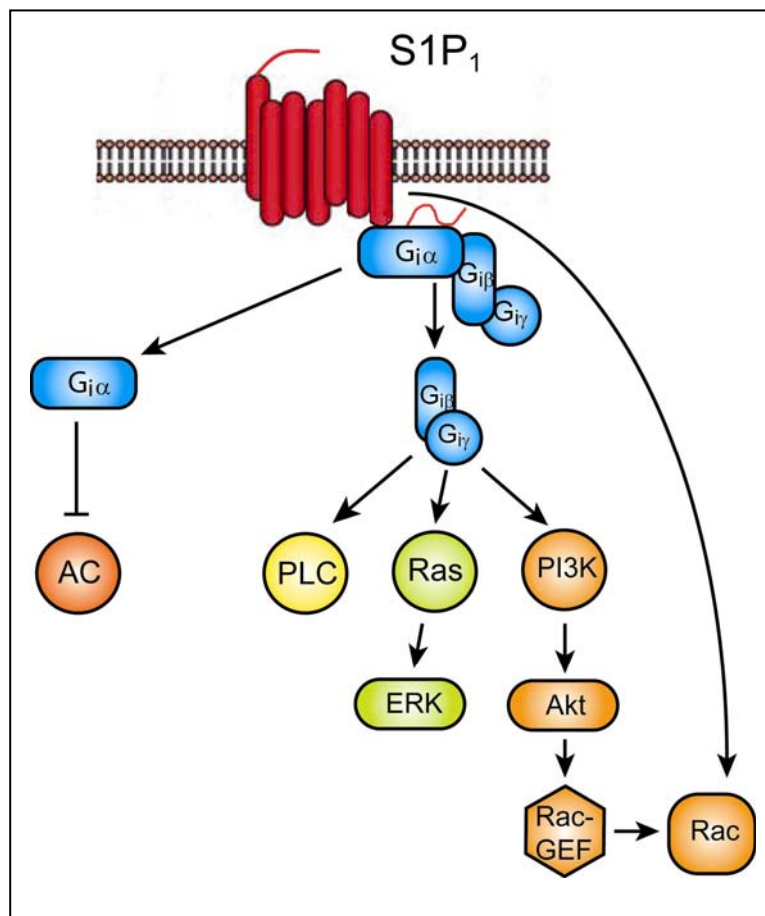


Figure 5: Intracellular signalling pathways of the S1P₁ receptor

AC: adenylate cyclase
 PLC: phospholipase C
 PI3K: phosphoinositide 3-kinase
 ERK: extracellular signal regulated kinase
 GEF: Guanine nucleotide exchange factor

S1P₁, at least in certain cell types, can not be inhibited by pertussis toxin suggesting an Gα_i independent signalling pathway downstream of S1P₁⁶².

S1P₁ deficient mice showed a lethal phenotype *in utero*, dying around day E14.5. Death was due to important embryonic haemorrhage and oedema. However, overall morphology of vasculature appeared normal, indicating unaffected vasculogenesis. Conversely, vascular maturation was shown to be profoundly disturbed, with abnormal migration of vascular smooth muscle cells⁶³. S1P₁-deficient mouse embryonic fibroblasts (MEFs) did not respond to S1P stimulation with Rac activation that has been shown to be crucial for S1P induced cell migration⁶³. Taken together, these findings suggest that the S1P₁ receptor has a crucial role in S1P mediated Rac activation and cell migration.

S1P₁ has wakened much interest for its involvement in the regulation of a broad variety of migrational processes in the immune homeostasis, including T-cell egress from the thymus and secondary lymphoid organs¹ as well as B-cell positioning in the marginal zone of the spleen³. These processes will be described in detail in **chapter 1.7**.

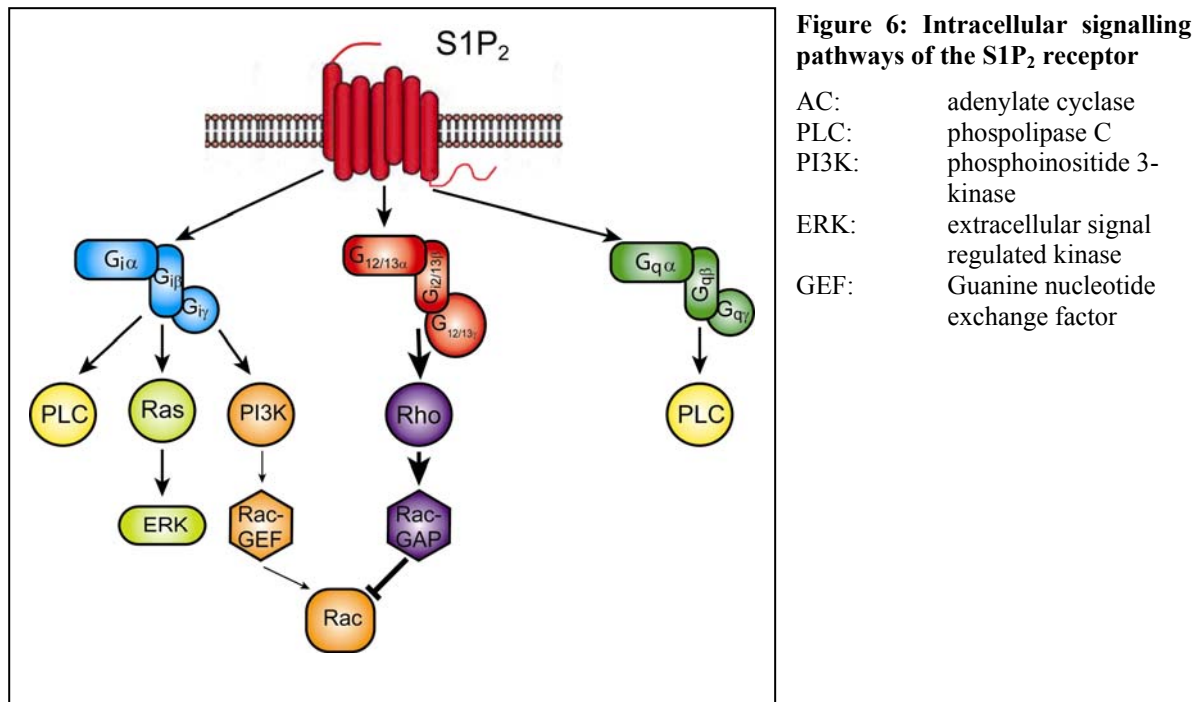
1.3.3.2. S1P₂

The S1P₂ receptor has been initially isolated as an orphan receptor from the rat cardiovascular and nervous system and was later found to be an high affinity receptor for S1P and a low affinity receptor for SPC⁶⁴. The genomic organization of the *s1p2* gene is similar to that of the *s1p1* gene since it contains the entire coding sequence in the second of the two exons. The murine gene is localized on chromosome 9. It encodes for a protein of 352 aa in mice and 353 aa in humans. The apparent molecular weight of this protein is ~39kb.

During embryologic development, S1P₂ expression is particularly strong in the embryonic brain, with an increasing expression level until birth⁶⁵. After a perinatal maximum, expression levels in the brain decrease in the postnatal period. In the adult mouse, expression is quite ubiquitous⁶⁵.

In contrast to S1P₁, S1P₂ interacts with multiple G-proteins including Gα_i, Gα_{12/13} and Gα_q (**Figure 6**). *Via* the activation of its intracellular signalling pathways including ERK activation, AC activation, PLC activation and intracellular Ca²⁺ increase, it can modulate a vast variety of cellular responses like cell-proliferation, -survival and -migration. Depending on the G-protein used in the cellular context, S1P₂ can positively or negatively regulate Rac activation⁶⁶.

Data obtained from S1P₂ deficient mice are partially conflicting and depend on the knock-out mouse strain. While one group reported slightly but consistently diminished litter



size⁵, an independently generated S1P₂^{-/-} mice showed normal litter size⁶⁷. Both mouse strains were normal with respect to appearance, gross anatomy including that of the central nervous system. However, one S1P₂^{-/-} mouse strain presented with spontaneous and sporadic seizures that were occasionally lethal⁶⁷. Electrophysiological exploration of these animals revealed an increased excitability of neocortical neurons.

1.3.3.3. S1P₃

S1P₃ was first isolated as an orphan GPCR from a human genomic cDNA library and was only later shown to be a high affinity receptor for S1P and a low affinity receptor for SPC⁶⁶. The murine and human genes were mapped to chromosome 9 and 13, respectively. Both murine and human S1P₃ contain 378aa with an apparent molecular weight of ~42kDa. Although evolutionary more related to the S1P₁ receptor with protein homology of 67%, the downstream signalling pathways resemble more those of the S1P₂ receptor.

At day E14 of the embryological development, the s1p3 transcript is found at high levels in the lung, kidney, diaphragm and some cartilages⁶⁸. In the adult animal, S1P₃ belongs to the three S1P receptors that are quite ubiquitously expressed.

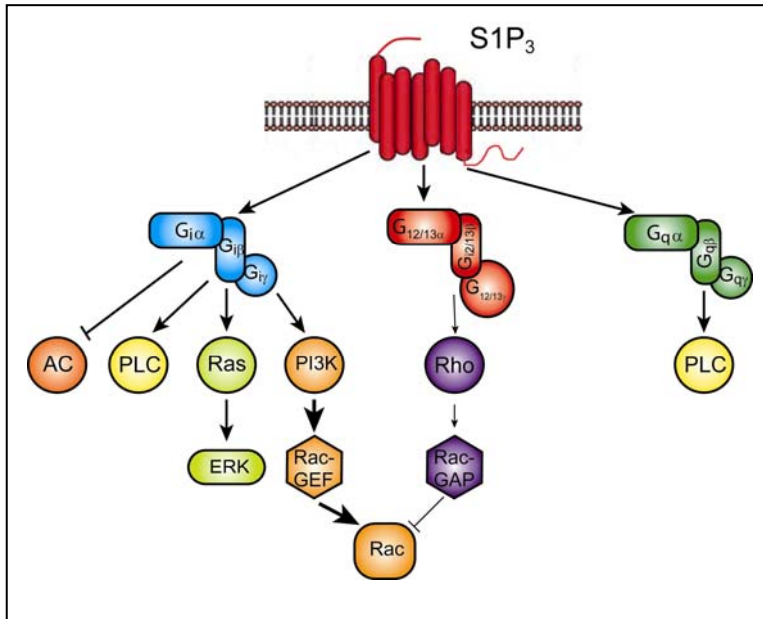


Figure 7: Intracellular signalling pathways of the S1P₃ receptor

AC: adenylate cyclase
 PLC: phospholipase C
 PI3K: phosphoinositide 3-kinase
 ERK: extracellular signal regulated kinase
 GEF: Guanine nucleotide exchange factor

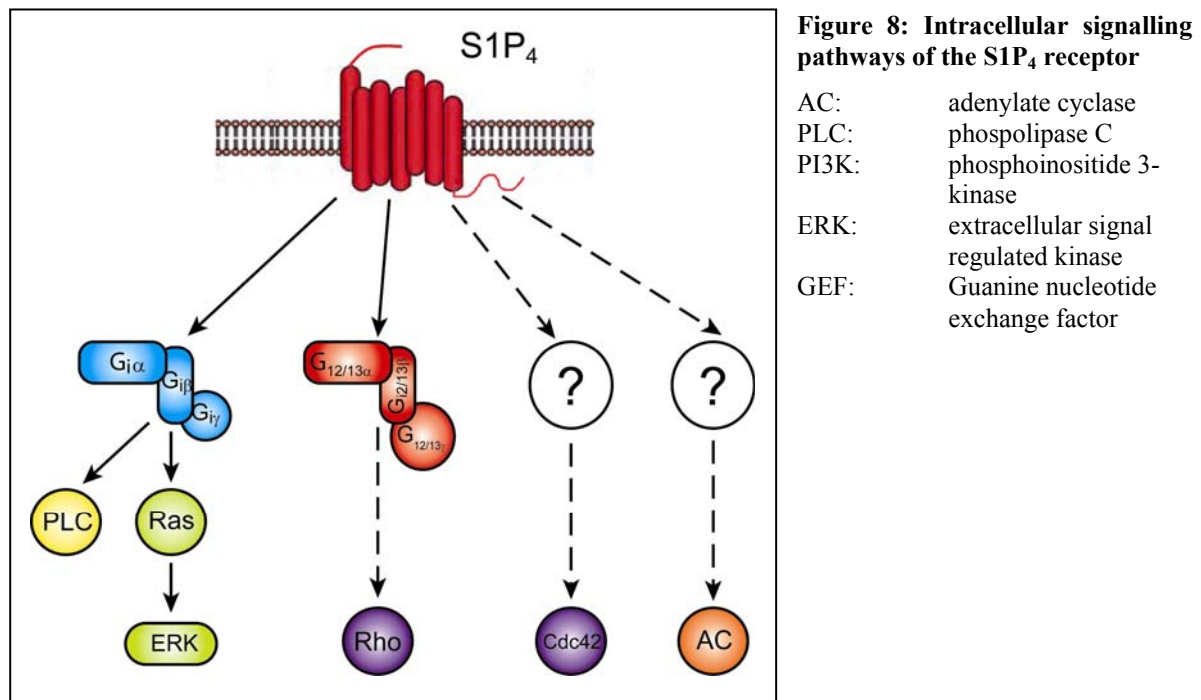
S1P₃ couples to multiple G-proteins including G α_i , G α_q and G $\alpha_{12/13}$. Further downstream signalling resembles those of S1P₂ with the exception of Rac regulation that is positively influenced by S1P signalling *via* S1P₃ (**Figure 7**). Signalling *via* S1P₃ influences a wide spectrum of biological processes including cell-proliferation, -survival, -rounding, ERK activation, regulation of AC activity, PLC activation, Ca²⁺ mobilization and Rho and Rac activation^{64,69}.

S1P₃ deficient mice are born in a classical Mendelian ratio without any gross phenotypical abnormalities, except slightly but consistently reduced litter size⁶⁹. However, S1P₂ and S1P₃ are co-expressed in most tissues, leaving open the possibility of at least partial functional redundancy of both receptors. Indeed, double deficiency for S1P₂ and S1P₃ results in a clear phenotype with markedly reduced litter sizes, and increased early postnatal mortality until the third week. Of note that the remaining survivors were normal. In MEFs, loss of both receptors results in elimination of S1P dependent Rho activation, while specific loss of S1P₃ does not affect Rho activation, and sole S1P₂ deficiency results only in a partial reduction of Rho activation⁵. These observations underline the importance of considering putative compensational phenomenon's in the analysis of S1P receptor knock-out animals. The binding to one and the same ligand, the coupling to similar G-proteins and the frequent co-expression of different S1P receptors on the same cell suggests that partial or even complete receptor redundancy may also occur between all S1P receptors.

1.3.3.4. S1P₄

The S1P₄ receptor was isolated from *in vitro* differentiated human and murine dendritic cells⁹. It binds with high affinity to S1P and with low affinity to SPC. The *slp4* gene encodes a protein consisting of 384aa in humans and 386aa in mice⁶⁴. The receptor shares less sequence homology with the remaining receptors of the S1P group (40-45%) than it is usually seen within this receptor group (48-52%), suggesting that the S1P₄ receptor may have a distinct preferred ligand. Subsequently it was shown that phytosphingosine 1-phosphate has a 50-fold higher affinity than S1P. However, most experimental analysis of S1P₄ function were performed using S1P as activating ligand. The genomic organisation of the *slp4* gene is similar to that of other S1P receptors with the coding region entirely contained within the second exon. The human gene is localized on chromosome 19, while the murine gene maps to chromosome 10⁶⁴.

In contrast to the previously described S1P receptors, S1P₄ expression is restricted to lymphoid and haematopoietic cells and tissues. High expression levels have also been found in the lungs⁹. However, also due to the lack of specific antibodies for S1P₄ that can be used in immunohistochemistry, our knowledge on the exact expression pattern and its temporal and developmental regulations remains patchy. Therefore, detailed data on S1P₄ expression during embryogenesis are yet available.



S1P₄ has been found to interact with various G-proteins including G_i and G_{12/13}, but not G_s or G_q. Data on the further downstream interaction partners is partially conflicting. S1P₄ has been shown to stimulate ERK, PLC and Ca²⁺ increases *via* G_i proteins. S1P₄ stimulation activated Rho and resulted in cytoskeleton rearrangement in one study⁷⁰, while no such effects were observed by other investigators who reported on stimulation of Cdc42 and migration⁷¹ (**Figure 8**).

Data on S1P₄^{-/-} mice have not yet been published. The *in vivo* role of S1P₄ is still scarcely characterized. However, since this molecule is highly expressed on cells of the lymphoid and hematopoietic system, a role of this receptor in the homeostasis of the immune system has been suspected.

1.3.3.4.1. Current knowledge on the role of S1P₄ in the immune homeostasis

Several observations made in experimental settings involving overexpression of S1P₄ implicated this receptor in a broad array of biological processes all contributing to the homeostasis of the immune system.

The influence of S1P₄-mediated S1P signalling on chemotaxis was examined by several investigators. The group of Goetzl showed in two different publications that S1P₄ is not involved in the S1P chemotactic response^{72,73}. In 2002, these investigators showed that only HTC4 rat hepatoma cells overexpressing human S1P₁ but not those overexpressing human S1P₄ migrated towards a S1P gradient. Similarly, only the former cells were able to impact on CXCL1- and CXCL4- induced cell migration at various S1P concentrations while the later were not⁷². The effect of synchronous overexpression of both receptors on the same cell was not assessed in these experiments. Three years later, the same group confirmed their previously reported observations using two different approaches. In two mouse T-cell lines (D10G4.1 and EL4.IL-2) transfected with the murine S1P₄ they did not observe any migrational response to S1P. Also, no S1P-induced modification of the chemotactic response to CCL21 was observed in those cells. Furthermore, in FTY720 treated splenic CD4 T-cells (a treatment which has been shown to down-regulate S1P₁ expression thus maintaining only S1P₄ expression), chemotactic response to S1P was absent and no modification of CCL21-induced chemotactic response occurred. Once again, the cooperative influence of S1P₁/S1P₄ on the migration of lymphocytes was not assessed in this experimental setting. In contrast to the observations of the group of Goetzl, other investigators detected an involvement of S1P₄ in the migrational response of various cell types including lymphocytes. Indeed, Kohne *et al.* showed Cdc42-mediated, S1P induced migration in murine S1P₄ transfected CHO cells⁷¹.

Overexpression of myc-tagged human S1P₄ in Jurkat cells resulted in an increased basal motility without receptor stimulation and a further increased S1P-induced chemotaxis⁷⁰. In contrast to the above mentioned work of Wang *et al*, Matsuyuki *et al*. found significant expression levels of both S1P₁ and S1P₄ in the murine T-cell lines D10G4.1 and EL4.IL-2⁶. In their experimental setting, S1P induced a significant migrational response in these cell lines. Furthermore, Matsuyuki *et al*. produced indirect evidence that S1P₄ influences S1P induced chemotaxis in these cell lines. The source for the discrepancies may reside within the experimental protocols used in these different studies. In particular, exposure to fetal calf serum, that contains physiological amounts of S1P, in the culture medium may have resulted in the desensitisation of S1P receptors preventing a further stimulation by addition of exogenous S1P. In conclusion, the involvement of S1P₄ in the regulation of migrational processes within the immune system remains controversial.

Published data on other S1P₄ mediated processes remains sparse. After stimulation with anti-CD3 and anti-CD28, S1P₄ transfected D10G4.1 and EL4.IL-2 cell lines proliferated less than their WT counterparts. These reports were corroborated by similar observations made in FTY720 treated CD4 T-cells⁷³.

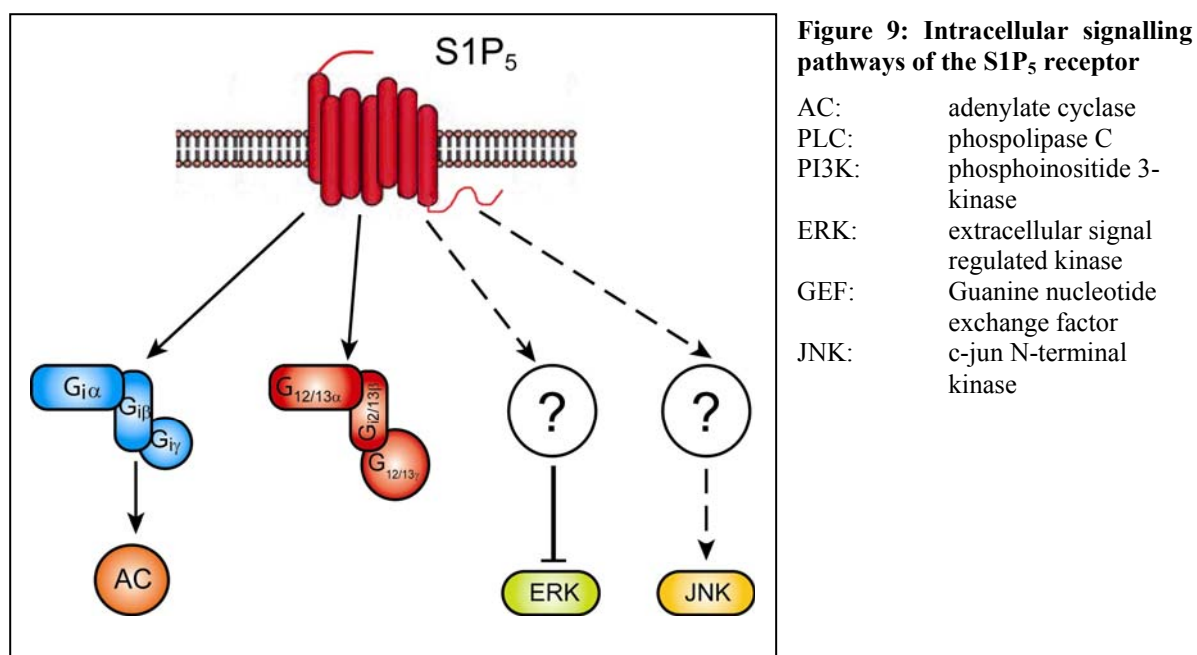
Finally, the influence of S1P signalling via the S1P₄ receptor on cytokine secretion profiles was assessed in the same cell lines. It shows that IL-4 production by anti-CD3/anti-CD28 stimulated S1P₄ transfected D10G4.1 cells was significantly inhibited. In contrast, the secretion of the immunosuppressive cytokine IL-10 was increased in this experimental model. In anti-CD3/anti-CD28 stimulated S1P₄ transfected EL4.IL-2 cells, IL-2 production was reduced. Finally, in FTY720 treated splenic T-cells, interferon γ secretion was diminished⁷³. However, further confirmatory reports of these observations made in a single experimental model have not been published yet.

1.3.3.5. S1P₅

This most recently described S1P receptor was isolated as an orphan GPCR gene from PC12 cells and later shown to be a high affinity S1P and low affinity SPC receptor⁷⁴. As the other S1P receptors, the *slp5* gene contains the coding region in one single exon. The S1P₅ protein contains 398 aa in humans and 400 aa in rodents and has an apparent molecular mass of ~42 kDa⁷⁵.

The study of S1P₅ signalling in CHO cells overexpressing this receptor revealed coupling to G α_i and G $\alpha_{12/13}$ proteins, but no interaction with G α_a and G α_s proteins⁷⁶. S1P₅

mediates activation of JNK, inhibition of AC and negatively regulates ERK activation and cell growth. (Figure 9)



Alike S1P₄, S1P₅ belongs to the S1P receptors with an restricted expression pattern. In humans, S1P₅ expression is found in the brain, the spleen and in peripheral blood leucocytes. In rodents, S1P₅ is expressed in the brain, the skin and the spleen. In rodent brain, the receptor shows particularly abundant expression in the white matter tracts. In contrast to data obtained in S1P₅ overexpressing cellular systems, differentiating oligodendrocytes expressing endogenous S1P₅ showed stimulated ERK activity⁷⁷. According to the differentiation stage of oligodendrocytes, S1P₅ stimulation results in Rho kinase-mediated process retraction (in pre-oligodendrocytes but not in mature oligodendrocytes) or in Akt mediated enhanced survival (in mature oligodendrocytes but not in pre-oligodendrocytes). These observations suggest that S1P₅ has differential cellular effects according to the cellular maturation stage. However, mice deficient in S1P₅ exhibited no behavioural or neuropathological abnormalities⁷⁸.

1.3.4. Lysophosphatidic acid receptors

1.3.4.1. LPA₁

LPA₁ was initially described in 1996 under the name “ventricular zone gene”⁷⁸. It was later found to be a high affinity receptor for LPA. In mammals, the *lpa₁* gene spans about 45kb and contains 5 exons⁷⁹. However, the coding region lays within 2 exons with an intron located within the middle of transmembrane domain VI. The murine gene is located on chromosome 4. LPA₁ contains 364 aa and has an apparent molecular weight of ~41 kDa.

LPA₁ receptors have been shown to couple to G_i, G_q and G_{12/13} proteins although the exact interaction partner may be considerably influenced by the experimental system used. Through activation of these proteins LPA₁ induces various cellular responses. These include inhibition of AC, increase in ERK, Akt, Rho, Rac and PLC activation as well as an increase of intracellular Ca²⁺ concentration⁸⁰.

During embryogenesis, the *lpa₁* transcript was found to be highly expressed in the ventricular zone in the dorsal telencephalon during neurogenesis. The expression disappears from this zone right before birth and reappears in the postnatal nervous system in oligodendrocytes and Schwann cells which are responsible for myelination. The postnatal temporal and spatial expression also correlates with that of myelination suggesting a role of LPA₁ in this process. However, after birth LPA₁ expression occurs widespread outside the nervous system. Significant amounts of LPA₁ mRNA has been found in many adult tissues including brain, heart, lung, testis and to a lesser extent in many other organs⁸¹.

Embryos of LPA1-deficient mice showed in a small percentage frontal haematomas and about half of new born LPA₁^{-/-} pups died within the first three weeks of life⁸⁰. Surviving animals displayed phenotypic abnormalities such as craniofacial dysmorphism and a significant reduction of body weight. Moreover they suffered from a suckling defect that could be a possible explanation for the increased neonatal morbidity and the reduced body weight. Surprisingly, the histopathological examination of the brain did not reveal any neuropathological changes.

1.3.4.2. LPA₂

LPA₂ shows 60% of amino acid homology to LPA₁. The murine *lpa₂* gene contains three exons two of which contain the coding regions with an intron inserted into the transmembrane region VI as it was seen in the *lpa₁* gene. The murine LPA₂ gene is localised on chromosome 8. The LPA₂ receptor contains 348 aa in mice and 350 aa in humans and has an apparent molecular weight of ~39kDa.

LPA₂ was shown to couple to G_i, G_{12/13} and G_q proteins. It uses cellular signalling pathways very similar to those of LPA₁ including an increase of Rho, PLC, ERK and Akt activation as well as increased intracellular Ca²⁺ concentration and inhibition of AC activity thereby influencing stress fibre formation and cell proliferation⁸⁰.

During embryogenesis, high LPA₂ expression is detected in the brain until birth, when expression levels start to decline. In the adult animal, LPA₂ expression is considered ubiquitous⁸⁰. LPA₂^{-/-} mice did not suffer from obvious phenotypical abnormalities⁸². However,

analysis of MEFs established from $LPA_2^{-/-}$ embryos showed significantly reduced AC activation while Rho activation and AC inhibition remained almost unchanged. In spite of almost identical signalling pathways used by LPA_1 and LPA_2 , this phenotype is different from that of MEFs that show in addition an increase of AC inhibition⁸³.

Since both LPA_1 and LPA_2 show ubiquitous expression and signal *via* similar pathways, redundancy between signalling *via* both receptors could not be excluded. However, $LPA_1^{-/-}$ $LPA_2^{-/-}$ double knock-out animals did not reveal additional phenotypic abnormalities as those seen in $LPA_1^{-/-}$ animals with the exception of an increased incidence of frontal cephalic haemorrhage⁸².

1.3.4.3. LPA_3

The *lpa3* gene is composed of 3 exons, two of which contain the coding sequence that is separated by the conserved intron in the transmembrane domain VI and which is a characteristic feature of the LPA receptors 1-3. LPA_3 contains 353 aa in humans and 354 aa in mice with a predicted molecular mass of ~40kDa. This receptor is different from the former by its preference for LPA molecules with unsaturated acyl chains⁷⁵.

The LPA_3 receptor couples to G_i and G_q , but not to $G_{12/13}$. It can mediate PLC activation, ERK activation, increases of intracellular Ca^{2+} concentration and has negative or positive regulatory action on AC activity depending on the cellular context⁸⁴⁻⁸⁶. Its expression is considered to be ubiquitous⁸⁰, but highest expression levels are found in human testis, prostate, heart and frontal cortex^{85,86} and in mouse lung, kidney and testis⁸⁴.

Data on LPA_3 -deficient mice has not been reported yet.

1.3.4.4. LPA_4 and LPA_5

LPA_4 and LPA_5 are two recently described LPA receptors that are structurally distant from the previously described LPA receptors. They show 35% amino acid identity with each other, but only 20-24% of sequence homology with the LPA receptors LPA_{1-3} . Structurally, they are closer to the platelet activating factor receptor than to the previously mentioned LPA receptors^{87,88}.

LPA_4 is encoded by a single exon. Both murine and human receptors contain 370 aa with a molecular mass of ~42 kDa. The coupling preferences of LPA_4 are still poorly understood, although coupling to G_s for AC stimulation was described⁶⁹. LPA_4 mediates LPA-induced Ca^{2+} increase and cAMP accumulation⁶⁹. Low levels of LPA_4 are ubiquitously

expressed, while high expression levels are observed in the ovary⁸⁷. Reports on LPA₄^{-/-} mice have not been published yet.

LPA₅ couples to G_i and G_{12/13} proteins. LPA signalling *via* this receptor leads to increase of intracellular Ca²⁺ and cAMP. As LPA₄, LPA₅ is ubiquitously expressed at low levels. Higher expression is found in small intestine, spleen, dorsal root ganglion cells and embryonic stem cells. Reports on LPA₅^{-/-} mice have not been published yet⁸⁸.

1.3. 5. Other Lysophospholipidreceptors

Further receptors binding to lysophospholipids have been described. However, contradictory data regarding their ligand affinities have prevented their definitive classification in the group of classical lysophospholipid receptors.

A cluster of three S1P and SPC binding GPCRs (GPR3, GPR6 and GPR12) a ~40% homology with the former group of EDG receptors has been described⁸⁹. However, even without ligand binding these receptors show a high intrinsic activity that can be further modified by lysophospholipids. For GPR6 and GPR12, a functional role in the developing central nervous system has been proposed⁹⁰. But also at the outside of the central nervous system, these GPCRs seem to be involved in crucial biological processes. GPR3 and GPR12 are both highly expressed in murine oocytes, where they have been shown by knock-out and siRNA based approaches to be involved in the meiotic arrest of oocytes^{91,92}.

1.4. The ligands: S1P and LPA

1.4.1. Sphingolipids

1.4.1.1. Sphingolipids, a complex network of interconvertible bioactive lipids

S1P belongs to the group of sphingolipids that is highly conserved in all eukaryotic cells and some prokaryotic cells. This group of lipids not only exerts essential biological functions as a major constituent of the eukaryotic plasma membranes, but a number of group members also function as bioactive lipid molecules. Defects of sphingolipid metabolism result in cell death in various experimental settings, but are also implicated in a number of hereditary human pathologies *e.g.* lysosomal storage disease or hereditary sensory neuropathy type I.

Ceramide, ceramide-1-phosphate (C1P), sphingosine (Sph) and S1P are all bioactive lipid molecules with extensive signalling functions. Interestingly, their biological functions are quite different and sometimes even result in opposing effects, although they are interconvertible *via* one- or two-step reactions. Thus, sphingosine and ceramide induce

apoptosis in mammalian cells, while S1P promotes cell proliferation and survival. These opposing functions of interconvertible mediators lead to the development of a “sphingolipid

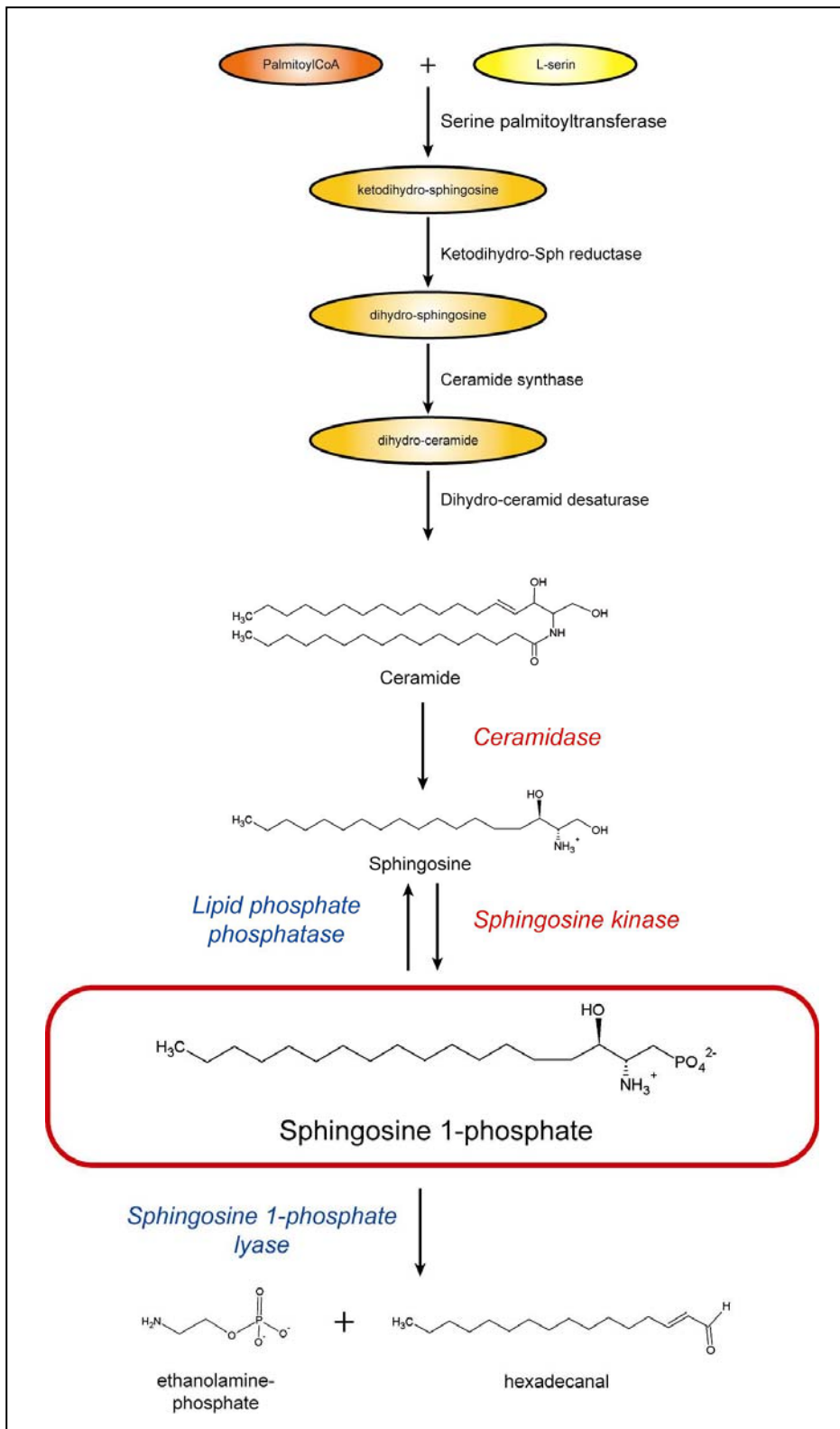


Figure 10:
Metabolism of S1P

rheostat model”, in which the balance between different sphingolipids determines the cell fate⁹³.

The initial step in the *de novo* synthesis of sphingolipids (**Figure 10**) is the serine-palmitoyltransferase-catalysed condensation of serine and palmitoyl-CoA to 3-ketosphinganine. This initial step is the rate-limiting step in the sphingolipid neo-synthesis. It is followed by the reduction of ketosphinganine to dihydrosphingosine, that is further N-

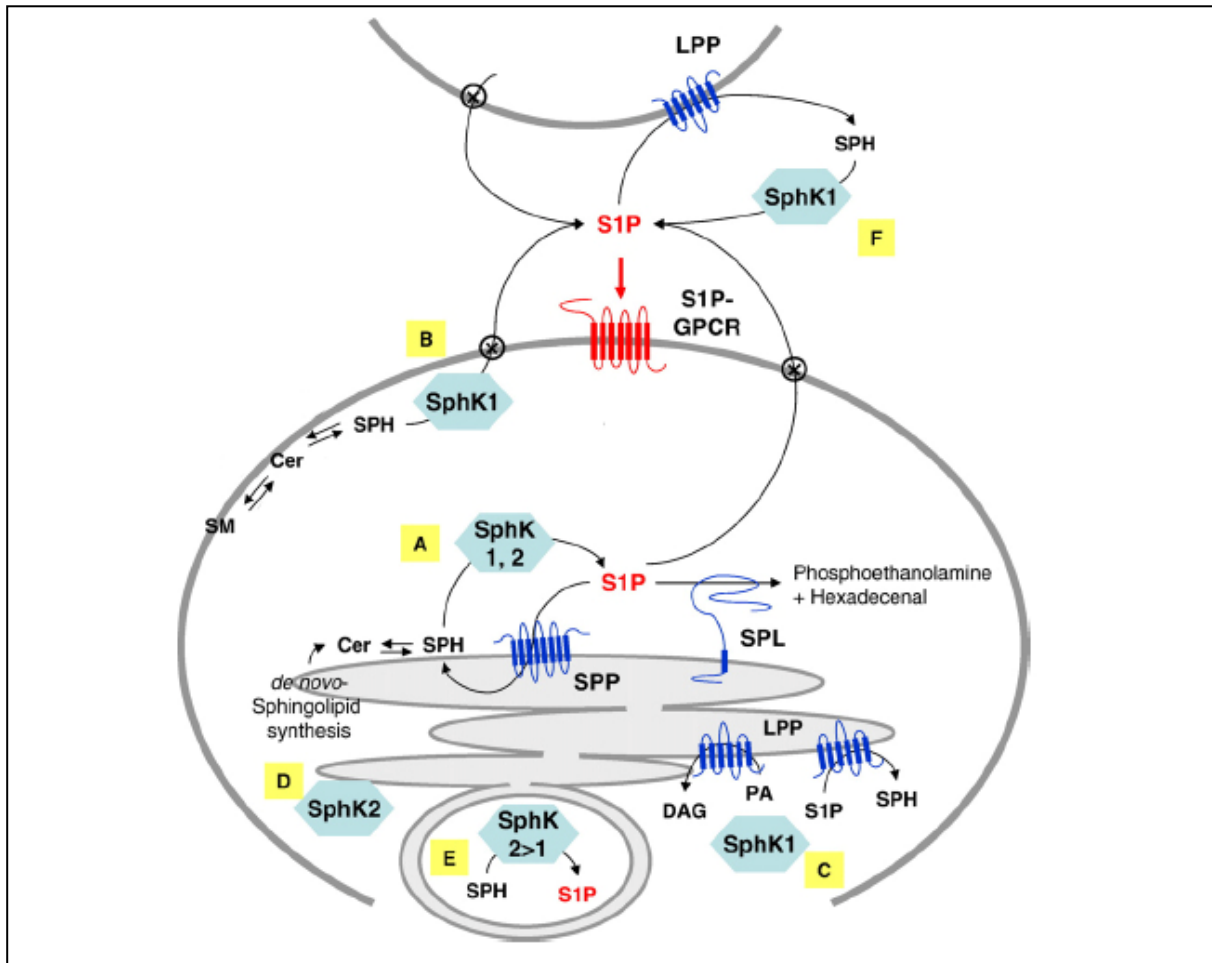


Figure 11: Regulation of intra- and extracellular S1P concentration

S1P availability at G-protein-coupled S1P receptors by localized generation and metabolism of S1P. S1P is formed from sphingosine (SPH) by sphingosine kinases (SphK) and either dephosphorylated by lipid phosphate phosphatases (LPP) and S1P phosphatases (SPP), or irreversibly cleaved by S1P lyase (SPL). SphK1 is a cytosolic enzyme (A) that, upon cellular stimulation, can translocate to the plasma membrane (B) or to other intracellular sites (C). SphK2 is also cytosolic and was observed at the endoplasmic reticulum in serum-depleted cells (D). In some experimental models, it was also found in the plasma membrane. Predominantly SphK2, but also SphK1, can be found in the nucleus (E). S1P can act on intracellular target sites, or it can be excreted, probably by one or more transport mechanisms. Extracellular S1P acting on S1P-GPCRs can thus be derived from auto- or paracrine secretion. In addition, it may be produced by extracellular SphK1 (F). Termination of extra- and intracellular S1P signals is caused by LPPs, SPPs and S1P lyase. LPPs are plasma membrane-bound enzymes with their catalytic activity directed to the extracellular space. LPPs can also be found at the endoplasmic reticulum or other intracellular membranes. SPPs and S1P lyase are endoplasmic reticulum proteins. The catalytic site of S1P lyase is directed towards the cytosol, while that of SPPs has been predicted to be directed towards the lumen of endoplasmic reticulum.

Modified from Meyer zu Heringdorf & Jakobs; *Biochimica et Biophysica Acta*, 2007

acetylated by ceramide synthase to form dihydroceramide. The insertion of a *trans* double bond at C4-C5 by dihydroceramide desaturase results in the generation of ceramide, the central molecule for the synthesis of more complex sphingolipids. Apart from *de novo* synthesis, ceramide can be generated by breakdown of sphingomyelin by sphingomyelinase. Sphingomyelin is the most abundant sphingolipid, and its degradation contributes the major part to the ceramide production. In mammals, sphingosine and S1P are exclusively produced by the degradation of ceramide that thus has a central position in the sphingosine and S1P metabolism. The conversion of ceramide into sphingosine is catalysed by ceramidases (CDase). In mammals, there are 3 types of Cdases that differ in their optimum pH for activity and their subcellular localisation. Ceramide and sphingosine are interconvertible by the action of CDases and ceramide synthase⁹⁴.

The intra- and extracellular concentration of S1P is the result of the activities of the enzymes that catalyse its synthesis and degradation (**Figure 11**). In mammals, these include sphingosinekinase (SphK), S1P lyase and S1P phosphatase. As an highly active cellular mediator that has both extracellular signalling functions *via* G-protein coupled receptors as well as intracellular signalling functions as secondary messenger, the metabolism of S1P is subjected to a high regulation.

1.4.1.2. Sphingosine metabolism

1.4.1.2.1. Sphingosine kinase

SphK catalyse the phosphorylation of Sph to S1P. In mammals, two different SphK isoforms have been described. Human SphK1 is a 42.4 kDa protein that is preferentially expressed in lung, spleen and liver. It is predominantly localised in the cytosol. In contrast, human SphK2 is a 65.6 kDa protein with highest expression levels in liver, brain and heart. In a SphK2 over expressing cell lines, the enzyme was predominantly found in the cytosol, although other studies propose a plasma membrane and nuclear localisation of SphK2⁹⁵⁻⁹⁸. Both isoforms also differ in their substrate specificity. Thus, SphK2 has a higher affinity for D-erythro-dihydrosphingosine than for D-erythro-sphingosine. However, SphK2 seems to be exclusively responsible for the phosphorylation of immunosuppressive S1P agonist FTY720, thus producing the biological active form FTY720 phosphate⁹⁹.

The activities of SphK1 and SphK2 is tightly regulated by a great number of endogenous factors. These include ligands of receptor tyrosine kinases such as platelet derived growth factor, epidermal growth factor, vascular endothelial growth factor or nerve

growth factor, cytokines as tumor necrosis factor, ligands for GPRCs such as acetylcholine, lysophosphatidic acid or cross-linking of immunoglobulin receptors¹⁰⁰.

1.4.1.2.2. Biodegradation of S1P

1.4.1.2.2.1 S1P-specific phosphatase

Two S1P specific phosphohydrolases have been described until yet^{101,102}. Both enzymes show high specificity for sphingosine base phosphate esters and are localized at the endoplasmatic reticulum. They are thus thought to be implicated into the degradation of intracellular S1P. While S1P specific phosphohydrolase 1 is expressed predominantly in liver, placenta and kidney, S1P specific phosphohydrolase 2 shows highest expression levels in kidney and heart. Both enzymes catalyse the dephosphorylation of S1P to Sph (**Figure 10**), favouring the further generation of ceramide by ceramide synthase and thus shifting the “sphingosine rheostat” to the production of ceramide.

1.4.1.2.2.2 Lipid phosphate phosphatases

Lipid phosphate phosphatases (LPP) catalyse the dephosphorylation of numerous lipid phosphates, including LPA, diacylglycerol pyrophosphate and S1P. There are different LPP isoforms that are all integral membrane proteins of the endoplasmatic reticulum or of the plasma membrane. Here, they function as ecto-phosphohydrolases regulating the extracellular S1P level and thus most probably the availability of S1P at the S1P receptors^{80,100}.

1.4.1.2.2.3. S1P lyase

S1P lyase catalyses the degradation of S1P into hexadecanal and phosphoethanolamine and is vitamin B12-dependent. With the exception of erythrocytes and platelets, S1P lyase is ubiquitously expressed with highest levels in liver, kidney, lung heart and brain^{103,104}. As for S1P-specific phosphatases, S1P lyase has been shown to be localized in the endoplasmatic reticulum¹⁰⁵.

1.4.1.3. S1P and its double role as intracellular second messenger and extracellular first messenger

The analysis of the biological actions of S1P is rendered particularly complex by the fact that this sphingolipid not only acts as ligand of the five S1P receptors but also as intracellular second messenger binding to an as yet unidentified intracellular target. Elevation of intracellular S1P levels leads to Ca²⁺ mobilisation from internal sources and seems to

influence a variety of signalling pathways including activation of the ERK pathway, inhibition of the SAPK/JNK pathway or suppression of apoptosis, increased cell proliferation/DNA synthesis and activation of phospholipase D^{57,93,106-108}. Further complexity is added to the system by interactions of intracellular and extracellular S1P. Thus, S1P binding to S1P receptors activates S1P kinase thus resulting in an increased intracellular S1P levels¹⁰⁹. On the other side, it has been shown that an increase of intracellular S1P levels secondary to PDGF induced S1P kinase activation result in an increased para- and autocrine activation of S1P₁. This observation suggested an inside-to-outside signalling paradigm whereby an agonist induces intracellular production of S1P that in turn stimulated its receptor present on the same cell¹¹⁰.

1.4.1.4. Sources of extracellular S1P

Although it is believed that intracellular S1P can be generated to different extents by basically every cell type, the source for extracellular S1P is not well defined. After the detection of SphK1 in culture supernatant of transfected cells some investigators proposed the export of SphK1 into the extracellular space where this enzyme may contribute to the generation of S1P¹¹¹. However, at least in certain cell types, S1P may be released directly into the extracellular space¹¹².

The high plasma levels of S1P are mainly the result of S1P release from platelets, erythrocytes, neutrophils and mononuclear cells. Although platelets were shown to have the highest SphK activity, erythrocytes seem to provide the most important part of plasma S1P due to their great number and to the lack of S1P degrading enzymes¹¹³. The question whether erythrocyte-bound S1P is generated in the red blood cell itself by phosphorylation of Sph, or whether it is taken up by the erythrocytes from another cellular source remains to be answered¹¹⁴.

Interestingly, different cellular sources seem to be responsible for the maintenance of S1P levels in different compartments of the extracellular space. Thus, plasma S1P has been found to be mainly generated by cells of hematopoietic origin, whereas lymph S1P is produced by a radio-resistant non-hematopoietic source¹¹⁵.

1.4.2. Lysophosphatidic acid

The term LPA embraces a mixture of various fatty acids including both saturated (16:0, 18:0) and unsaturated (16:1, 18:1, 18:2, 20:4) fatty acids. Different LPA species appear to exhibit differential biological activities. The different pathways leading to the synthesis of

intra- and extracellular LPA are still poorly understood, and data on the regulation of enzymes involved in the LPA synthesis is scarce. LPA is produced through two major pathways: in cells, LPA is mainly converted from PA, while extracellularly, LPA is mainly produced by deacetylation of LPLs (reviewed in¹¹⁶) (**Figure 12**).

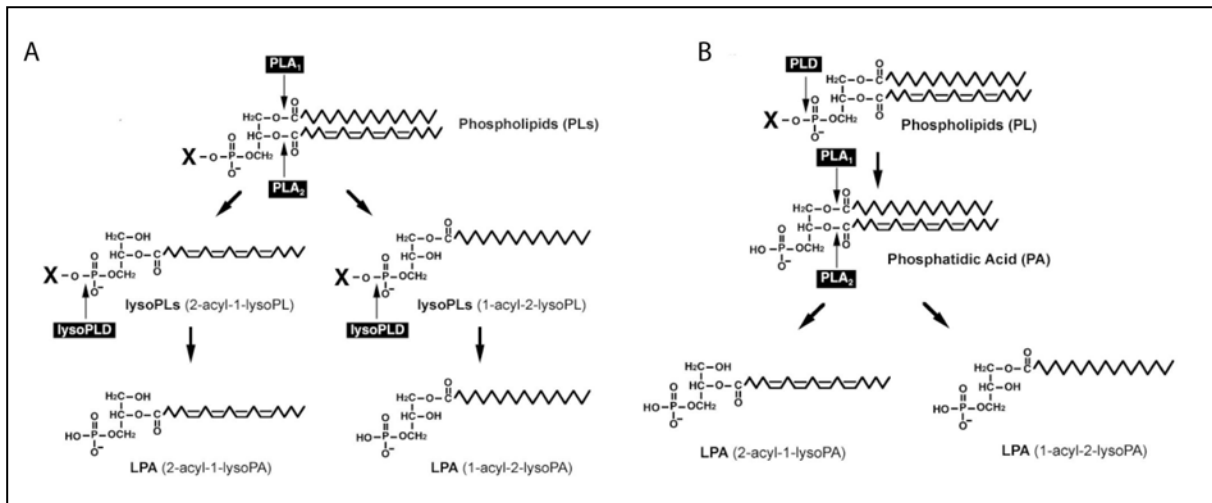


Figure 12: Mechanisms of LPA production

Two hypothetical mechanisms of LPA production in mammals are shown. a) PLA₁/PLA₂-lyso-PLA pathway; b) PLD-PLA₁/PLA₂ pathway. Abbreviations: lysoPL: lysophospholipids; PLA_{1/2}: Phospholipase A1/A2; PLC: phospholipase C; PLD: phospholipase D; lysoPLD: lysophospholipase D

Modified from Aoki *et al*, seminars in Cell & Developmental Biology, 2004

1.4.2.1. Extracellular production of LPA

The major part of extracellularly produced LPA is generated by the action of lysoPLD on lysophospholipids such as LPC, LPE and LPS. These precursors are generated by the action of extracellular phospholipases with PLA₁ and PLA₂ activity.

Although intracellular isoforms of PLA₁ and PLA₂ have been described that were capable of generating intracellular LPC by hydrolysing PC, it remains unclear to what extent their enzymatic action is involved in extracellular LPA production by supplying LPLs to lysoPLD. However, activated platelets and hepatocytes were shown to release LPLs into plasma.

1.4.2.2. Intracellular generation of LPA

The major pathway of intracellular LPA generation consists of two consecutive steps: production of PA and the subsequent conversion of PA into LPA. The first step is catalysed by different isoenzymes of PLD, that can be activated by various agonists including ATP, Ca²⁺ and bombesin. The second step is the under control of PLA₁ and PLA₂ activity. Several

different enzymes doted with these activities but with different specificities and subcellular localisations have been described.

LPA is also an essential intermediate product of the synthetic pathway for phospholipids and triacylglycerol in many cell types. Generation of LPA by acetylation of glycerol 3-phosphate occurs in the endoplasmatic reticulum and mitochondria. Evidence for the release of the produced LPA into the extracellular fluid and the plasma-membrane and thus for its participation in extracellular signalling is lacking.

1.4.2.3. LPA degradation

In mammalian cells, LPA is dephosphorylated by the action of the quite unspecific lipid phosphate phosphohydrolases that are also involved in the degradation of other lipid phosphates such as S1P and PA. Whether this enzyme is also responsible for the termination of LPA signalling, or whether ligand-binding induced internalisation and degradation of the LPA receptors is the prevailing mechanism remains to be shown.

1.4.2.4. LPA as intracellular second messenger

As for S1P, certain authors assigned to LPA a role of an intracellular lipid mediator. Indeed, certain effects of LPA were shown to occur independent from LPA-binding to GPCRs^{117,118}. However, the vast majority of LPA-induced biological effects are mediated *via* LPA binding to one of its specific receptors¹¹⁶.

1.5. Agonist and antagonists of LPL receptors

Molecules that bind to S1P receptors as agonists or antagonists have contributed significantly to our current knowledge in S1P receptor biology. The most frequently used molecule of this group is FTY720. This molecule was developed as a less toxic but more immunosuppressive synthetic analogue of myriocin in the early nineties. This later molecule is an immunosuppressant derived from the fungus *Ischaria sinclarii* and was originally used in Chinese herbal medicines^{119,120}. Both molecules are structural analogues to sphingosine, but unlike myriocin, FTY720 does not inhibit serine-palmitoyl-transferase, which is the initial and rate-limiting enzyme in sphingolipid *de novo* synthesis. In a rodent model, administration of FTY720 induced profound depletion of lymphocytes from the peripheral blood within 3 hours of a single administration. Lymphopenia is reversible after cessation of FTY720 administration¹⁰¹. Clinically, FTY720 lead to significant prolongation of skin and cardiac

allograft survival and to prevention of lethal graft-versus-host reaction in rats¹²¹⁻¹²³. FTY720 does not inhibit T-cell proliferation and T-cell activation and in rodent models does not impair immunity to systemic viral infections¹²⁴. The mechanism leading to the *in vivo* effects of FTY720 has been uncertain for a long time. Initially, FTY720 was thought to induce lymphopenia by increasing apoptotic cell death in lymphocytes^{125,126}. However, this *in vitro* effect occurred only with supra-therapeutic dosages of this molecule which were significantly higher than those found in blood of FTY720-treated animals¹²⁷. In 1998, FTY720-induced lymphopenia was found to be due to increased sequestration of lymphocytes within secondary lymphoid organs¹²⁸. However, the receptors mediating this effect were still unknown at this time. In 2002, two groups reported independently that FTY720 interacts with S1P-GPCRs^{101,129}. It was then shown that *in vivo*, only the phosphorylated form of FTY720 is active as a high affinity agonist at the S1P receptors S1P₁ and S1P₃-S1P₅, but not at S1P₂. Phosphorylation is required for the induction of lymphopenia since sphingosine 2-kinase-deficient mice are resistant to this FTY720 effect⁹⁹. Moreover, the immunosuppressive effect of FTY720 was mimicked by FTY720 phosphonate which cannot be dephosphorylated¹⁰¹. However, it remained still unclear how phosphorylated FTY720 maintains lymphopenia at low nanomolar concentrations in the presence of physiologically higher blood and lymph concentrations of the equipotent S1P¹³⁰. An explanation for this observation was provided by Graeler et al.. Using cell lines stably transfected with human S1P₁₋₅ they showed that FTY720 induced internalisation and degradation of S1P₁ and S1P₅ thus acting as a functional antagonist for these two receptors. S1P₃ and S1P₄ were not concerned by FTY720-induced downregulation¹³¹. However, in this model, several discrepancy to previous reports persist. Thus, FTY720 showed no significant affinity to S1P₄ but bound to S1P₂ that was also internalised. Thus, unsolved questions remain concerning the activity of FTY720 at S1P₄.

Other S1P agonist and antagonists are currently beginning to emerge. However, as yet, none of them had the same impact on S1P receptor research as FTY720. SEW2871 is an agonist at the S1P₁ receptor also capable of inducing lymphopenia in mice¹³². BML-241 and JTE-013 are selective antagonists for the S1P receptors S1P₂ and S1P₃, respectively⁸⁰. Finally, a competitive antagonist for S1P receptors S1P₁ and S1P₃ has been recently described¹³³.

1.6. Lysophospholipidreceptors in the immune system

1.6.1. Lymphocytes

When the number of available publications is used as a quantitative measurement tool, lymphocytes are certainly the immune cells in which S1P and LPA receptor expression and

functions has been most extensively studied. Lymphocytes were reported to express various combinations of S1P and LPA receptors, depending on the subpopulation analysed. The system is further complicated by a complex regulation during lymphocyte development and activation. However, S1P₁ and S1P₄ have been quite consistently reported to be the predominant S1P receptors expressed on human and murine lymphocytes.

1.6.1.1. T lymphocytes

In mature CD4⁺ and CD8⁺ T lymphocytes, S1P₁ consistently shows the highest expression levels of all S1P receptors at the mRNA level, followed by S1P₄. S1P₂₋₅ show only low expression levels in the majority of the studies, or could even not be detected depending on the species investigated^{1,134-136}. During T-cell development, S1P₁ expression is upregulated approximately 1000 times between the double positive and single positive stage. Similarly, the maturation step from single positive, L-selectin^{low} cells to single positive L-selectin^{high} cells is accompanied by a further 30-fold upregulation of the S1P₁ expression. In contrast, none of the other two S1P receptors found at moderated expression levels in this study showed this dependency on the maturation status¹. Interestingly, stimulation of CD4⁺ and CD8⁺ T-cell with anti-CD3/anti-CD28 antibodies *in vitro* resulted in downregulation of both S1P₁ and S1P₄ expression and moderate up-regulation of S1P₃ and S1P₅^{134,135}. *In vivo*, antigen exposure resulted in a transient downregulation of S1P₁ on CD4⁺ T-cells, while S1P₄ expression was not assessed in this experiment¹. In addition to their modulation resulting from T-cell activation, S1P₁ and S1P₄ receptor expression is also down-regulated by exposure to its ligand S1P *in vitro* and *in vivo*. For S1P₁, this agonist-induced receptor internalisation involves phosphorylation of the C-terminus of the S1P₁ receptor by GRK 2¹³⁷. Accordingly, lymphocytes isolated from different lymph nodes or from spleen, where intercellular S1P concentrations are low, showed higher S1P₁ expression than CD4⁺ T-cells from blood and lymph where higher S1P concentrations are found¹³⁸. This observations indicated a cyclic S1P₁ expression on lymphocytes (**Figure 13**).

S1P signalling in lymphocytes is involved in a wide variety of biological processes. Due to findings obtained using the functional S1P antagonist FTY720, special interest was paid to the role of S1P signalling in T-cell migration. *In vitro*, S1P was shown to elicit a strong chemotactic response in lymphocytes at concentrations found in blood and plasma (100-300nM)¹³⁴. Other than this direct chemotactic action, S1P signalling also modulates the chemotactic response of CD4⁺ T-cells to other chemotactic stimuli. Indeed, S1P, at subplasma concentrations of 10nM, increased both CCL5- and CCL7-induced chemotaxis. In contrast,

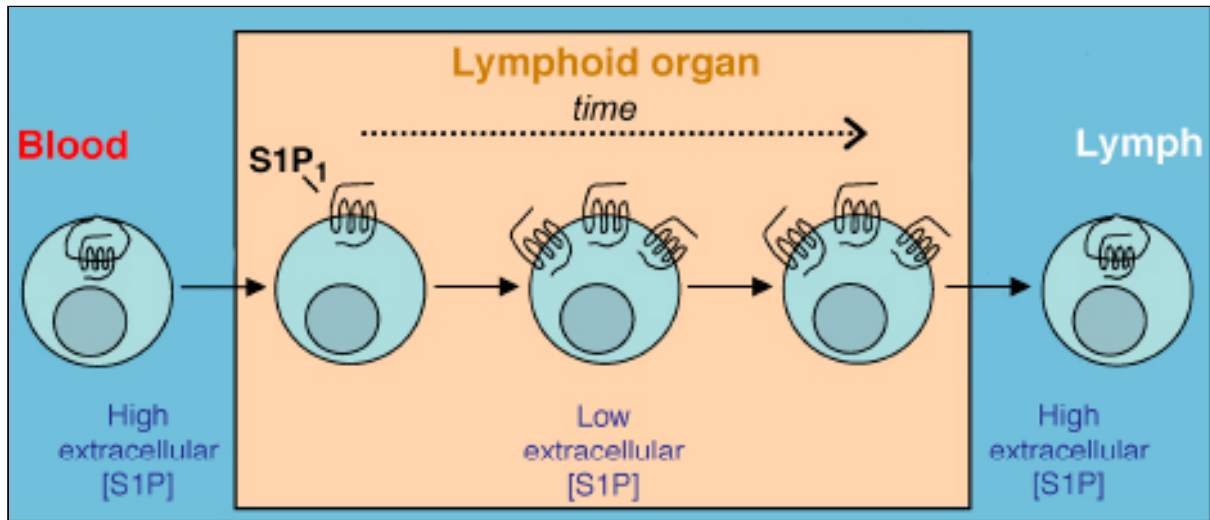


Figure 13: Model for cyclic S1P₁ expression during T cell re-circulation

S1P₁ expression is downregulated in blood where S1P concentration is high (100-300nM). Upon integrin and chemokine controlled T cell migration into the lymph node, S1P₁ is up-regulated after in an environment with low S1P concentration. Only after full up-regulation, T cells become egress competent again (see explanations in the text). The delay between entrance into the lymph node and S1P₁ upregulation guarantees for efficient antigen exposure of the T cell. Modified after *Lo et al. Journal of Experimental Medicine*, 2005

higher S1P concentrations (*i.e.* such as those usually found within the plasma) significantly inhibited CD4⁺ T-cell migration induced by these chemokines⁷². As expected from the modulation of S1P expression by T-cell activation, the chemotactic response of CD4⁺ T-cells and CD8⁺ T-cells to S1P was abolished by T-cell activation *in vitro*¹³⁴.

The identity of the S1P receptors mediating the chemotactic function of S1P on lymphocytes has remained controversial for a long time. Initial experiments using S1P₁- or S1P₄-overexpressing rat HCT4 hepatoma cell lines devoid of endogenous receptor expression revealed that S1P₁ transfectants showed both increased chemokine-induced chemotaxis upon exposure to low levels of S1P and decreased chemotactic response to chemokines upon exposure to higher S1P levels. In contrast, S1P₄ transfectants did not show any modulation of chemokine-induced chemotaxis upon exposure to S1P. These experiments provided the first evidence that the chemotactic action of S1P in lymphocytes is mediated principally by the S1P₁ receptor⁷². In a later report, the same group showed that S1P₄-transfected D10G4.1 and EL4.IL-2 mouse T-cell lines did not show any chemotactic response to S1P gradients, indicating that S1P₄ is not involved in T-cell chemotaxis⁷³. However, the conclusions from this latter report had to be put into perspective in the light of other reports showing that the T-cell lines D10G4.1 and EL4.IL-2 also expressed a variety of endogenous S1P receptors, and showed a chemotactic response to S1P gradients *in vitro*⁶. Moreover, Kohne *et al.* reported that CHO cells stably transfected with S1P₄ showed a clear chemotactic response to S1P gradients⁷¹. More conclusive data on the role of S1P₁ in T-cell migration were provided by the

group of Matloubian *et al.* These authors reported that the chemotactic response of various developmental stages of thymocytes to a S1P gradient *in vitro* showed a correlation with the S1P₁ expression: while DP cells did not migrate to a S1P gradient, single positive immature T-cells showed a positive but only moderate chemotactic response. In fully mature CD4⁺ and CD8⁺ thymocytes, a robust chemotactic response to S1P was observed¹. Using mature S1P₁-deficient CD4⁺ and CD8⁺ cells, they showed that lack of S1P₁ expression resulted in the abolishment of the migratory response to S1P in these cell types.

In conclusion, involvement of S1P₁ in the induction of chemotaxis upon exposure to a S1P gradient has been convincingly shown. In contrast, the role of the remaining S1P receptors expressed on lymphocytes, especially S1P₄, in S1P-induced chemotaxis is far less clear. Especially a modulating influence of these receptors on the S1P₁ mediated chemotaxis has not been assessed yet.

In addition to its action on T-cell chemotaxis, S1P signalling also impacts on T-cell proliferation. Indeed, incubation with S1P used at concentrations ranging from 0.1 to 10 μM, reduced both anti-CD3/anti-CD28- or DC-induced T-cell proliferation¹³⁵. However, some of these *in vitro* experiments used higher S1P concentrations than found in normal tissues. Using S1P₁ and S1P₄ receptor-overexpressing T-cell lines, it was shown that both receptors are involved in a negative regulation of T-cell proliferation induced by anti-CD3/anti-CD28 stimulation *in vitro*^{73,139}.

S1P signalling also influences cytokine secretion as a further aspect of T-cell biology. *In vitro*, T-cells stimulated with anti-CD3/anti-CD28 antibodies significantly increased IL-2 and IFN-γ secretion upon incubation with high levels of S1P (0.1-10 μM)¹³⁵. In contrast, experiments using plasma levels of S1P revealed a differential regulation of cytokine secretion depending on the S1P receptor predominantly expressed. Stimulation of S1P₁ overexpressing T-cells activated with anti-CD3/anti-CD28 antibodies resulted in reduced IL-4 and IFN-γ secretion without any changes in IL-2 secretion¹³⁹. In S1P₄ overexpressing cells, stimulation with plasma levels of S1P resulted in inhibition of IL-2, IFN-γ and IL-4 secretion and in an increase of IL-10 production, a constellation that was shown to be at least partially responsible for the negative effects of S1P₄ stimulation on T-cell proliferation⁷³. In a very recent study performed in a transgenic mouse line expressing both a Ova-specific TCR as well as human S1P₁, incubation of ova-stimulated T-cells with 10 nM to 1 μM S1P induced a significantly increased IL-17 secretion compared to control mice. However, the physiological importance of this latter finding made in a highly artificial experimental system remains to be proven¹⁴⁰.

The role of LPA on T-cell function is as yet far less explored than that of S1P. Unactivated human CD4⁺ T-cells express predominantly LPA₂, and only very low levels of LPA₁. In unactivated human CD8⁺ cells, only LPA₁ expression could be detected by semiquantitative RT-PCR. LPA₃ could be detected neither on CD4⁺ nor on CD8⁺ T-cells^{141,142}. These findings on the mRNA level were confirmed at the protein level. In mouse splenic T-cells, similar expression patterns were found by RT-PCR¹⁴³. Interestingly, LPA₁ was up- and LPA₂ was concomitantly down-regulated after PHA stimulation of CD4⁺ T-cells. In contrast, no changes of the low expression level of LPA₁ occurred after concanavalin activation of CD8⁺ cells¹⁴². The changes in LPA receptor expression observed during phytohemagglutinine (PHA)-induced activation of CD4⁺ T-cells were paralleled by striking changes of their functional response to LPA. While LPA signalling through the LPA₂ receptor predominantly expressed on CD4⁺ cells not activated by PHA resulted in reduced TCR-evoked IL-2 secretion, concomitant LPA signalling through LPA₂ and LPA₁ present on PHA stimulated CD4⁺ cells resulted in increased IL-2 secretion¹⁴². LPA₂ was shown *in vitro* to increase T-cell trans-basement membrane migration, whereas LPA₁ suppresses chemokine-induced T-cell chemotaxis¹⁴⁴. The regulated expression of different LPA receptors during CD4⁺ T-cell activation by PHA can thus modify the biological effect of LPA signalling on CD4⁺ T-cells.

LPA has also been shown to inhibit *in vitro* proliferation of CD4⁺ T-cells stimulated with anti-CD3/anti-CD28 antibodies¹³⁹, but no data on the individual LPA receptor implicated in the mediation of this LPA effect is available.

1.6.1.2. B lymphocytes

S1P receptor expression on B-cells was over a long time out of the focus of scientific interest. Initial studies on S1P receptor expression on these cells were mostly done as “by-product” of T-cell expression studies and did not proceed to a comprehensive analysis of all receptors. Initially, only inconstant expression of S1P₃ with a high variability between individual samples was detected on human B-cells¹⁴¹. However, S1P₄ and S1P₅ expression was not assessed in this investigation. Recently, interest in the role of S1P receptors in B-cell biology has been fuelled by observations made after FTY720 treatment in experimental mouse models that suggest an important implication of S1P in the regulation of the migration of various B-cell populations^{3,145}. In consequence, detailed analysis of S1P receptor expression were performed on numerous B-cell subpopulations.

Follicular B-cells expressed high levels of S1P₁ mRNA, and lower levels of S1P₃ and S1P₄ mRNA. S1P₂ and S1P₃ were not detected on these cells. In marginal zone B-cells, S1P₁

mRNA expression levels were up to threefold higher than in follicular B-cells, and also S1P₃ showed significantly higher expression levels than in follicular B-cells, while S1P₄ was present in comparable amounts. Marginal zone B-cells showed a major chemotactic response to plasma levels of S1P *in vitro*, while only few B-cells migrated to similar S1P gradients. Interestingly, in contrast to T-cells, S1P₁ deficiency of marginal zone B-cells did not result in a significant reduction of the chemotactic response to S1P, suggesting the implication of another receptor. Further experiments confirmed that S1P₃ was critical for S1P-induced chemotaxis *in vitro*³. Interestingly, upon activation with LPS or with the specific antigen in antigen specific, immunoglobulin-transgenic B-cells, all three S1P receptors expressed on marginal B-cells experienced a massive downregulation, leading to a reduced chemotactic response of stimulated marginal zone B-cells to plasma levels of S1P³. Intriguingly, in other mouse strains, quantitative RT-PCR analysis of S1P receptor expression gave a slightly different picture. Although S1P₁ remained the S1P receptor showing the highest expression level, S1P₃ mRNA was only hardly detectable. S1P₄ levels were low but clearly present¹⁴⁵. Peritoneal B-cells showed similar S1P receptor profiles.

LPA receptor expression on B-cells is restricted to LPA₂. In contrast to CD4⁺ T-cells, no modification of LPA receptor profiles was observed after B-cell activation with pokeweed mitogen^{141,142}. Functional data on LPA effects on B-cells is sparse. Immortalized human B lymphoblasts respond to LPA with calcium flux, MAPK activation and IL-2 production¹⁴⁶.

1.6.2. NK cells

NK cells form a first line of defence of the body against certain infectious agents and tumors. They make up approximately 5 – 20% of peripheral lymphocytes in humans. NK cells are doted with a high capacity of cytokine production and cytotoxicity. The two pathways by which NK cells induce apoptosis in their target cells are liberation of cytotoxic granules and ligation of death-receptors. Cytokines released by NK cells , *e.g.* TNF and IFN- γ , affect survival of pathogens and tumour growth and influence the subsequent development and polarization of the adaptive immune response *via* interactions with mature and immature DC.

Basically all S1P receptors with the exception of S1P₃ are expressed to different degrees on NK cells. S1P₁ is the receptor with the highest expression rate. In contrast to the situation on lymphocytes, expression levels, which have only been shown at the RNA level, did not change with the activational status of the cells. In *in vitro* assays, S1P is a chemoattractant for NK cells. Desensitisation after exposure to higher S1P concentrations as seen in other immune cells is not observed in NK cells¹⁴⁷.

NK cells express LPA₁ and LPA₂ in the resting state. Upon activation, LPA₃ expression becomes detectable. Addition of LPA to NK cells *in vitro* induce chemotaxis and Ca²⁺ liberation from intracellular stores in a G-protein-dependent fashion. In contrast to S1P, LPA enhances IFN- γ secretion *in vitro*^{148,149}.

1.6.3. Dendritic cells

The DC is the most potent antigen presenting cell that is profoundly implicated in the regulation of the immune response. DCs are bone marrow-derived cells that reside at the quiescent, immature state sparsely distributed in peripheral tissue. There they can continuously sample the antigenic environment. At this immature stage, DC are particularly specialized for antigen uptake and processing, but they are as yet unable to interact efficiently with T-cells due to the absence of surface expression of MHC complex and costimulatory molecules. After encounter with bacterial antigens or tissue damage, DCs become activated and acquire high capacity for antigen presentation and T-cell activation by up-regulating the expression of surface MHC and costimulatory molecules such as CD80 and CD86. By means of increased expression of chemokine receptor CCR7, maturing DCs migrate towards the peripheral lymph nodes where they efficiently interact with naïve T-cells. According to the nature of the antigen, DC may induce a T_H1 or T_H2 polarized response, or may induce peripheral tolerance^{150,151}.

Lysophospholipids profoundly influence the maturation of immature DC as well as other biological processes in both immature and mature DCs.

Both immature as well as mature human DC express mRNA for S1P₁, S1P₂, S1P₃, S1P₄ and S1P₅^{136,152}. S1P₁, S1P₃, and S1P₅ could be detected in western blot analysis of mature and immature DCs¹⁵³. In *in vitro* systems, addition of S1P increases migration of immature, but not mature human DCs. This effect can be blocked by PTX, indicating a G_i protein-coupled receptor-mediated effect. Similarly, actin polymerisation and Ca²⁺ mobilisation were increased by S1P in immature, but not in mature human DCs. Both biological effects could be abrogated by addition of PTX¹⁵². However, depending on the species the DCs were isolated from, the biological consequences of exposure to S1P varied considerably between the investigators. In contrast to the results obtained with human DCs reported above, Czeloth *et al.* reported that mature murine DCs, but not immature DCs migrated towards S1P¹⁵⁴. While migrational response to S1P appears to be mediated by S1P₄ signalling in lymphocytes, Maeda *et al.* provided first evidence that S1P₃ might be implicated in the migration of mature

murine DCs towards S1P. Moreover, this receptor seems to be implicated in the increased endocytosis seen in matured murine DCs after S1P stimulation¹³⁶.

The chemokines SDF-1 α and RANTES can induce actin polymerisation and chemotaxis in DCs. The S1P analog FTY720 reduced both chemokine-induced actin polymerisation and chemotaxis in both immature and mature DCs by a mechanism independent from chemokine receptor down regulation¹⁵⁵. This observation is in keeping with the reported role of FTY720 as functional S1P antagonist.

IL-12 and TNF- α secretion by mature dendritic cells is inhibited by S1P while IL-10 release is increased. Accordingly, T-cells primed with mature DCs in the presence of S1P showed increased T_H2 polarization (with the release of lower amounts of INF- γ and higher amounts of IL-4 by T-cells)¹⁵². Another group reported that FTY720 reduces IL-12 and increases IL-10 production *in vitro*. Interestingly, FTY720 treatment of DCs seems to inhibit their capacity to stimulate T-cell proliferation by a direct mechanism¹⁵⁵. T-cell differentiation induced by FTY720-treated DCs is biased towards T_H2 polarization. Given the role of FTY720 as functional S1P antagonist, these observations contradict the results seen after direct stimulation with S1P mentioned above. Further elucidation of the mechanisms for FTY720 mediated T_H2 polarisation *in vitro* is therefore necessary.

Very high concentrations of S1P (50 μ M) interfere with the differentiation of human monocytes into competent dendritic cells upon stimulation with IL-4 and GM-CSF. DCs that were differentiated in presence of high concentrations of S1P show reduced expression of several costimulatory molecules upon LPS induced maturation. Moreover, in a context of MLR, these DCs were less potent for the induction of T-cell proliferation¹⁵⁶.

LPA₁, LPA₂ and LPA₃ are expressed on both mature and immature DCs in similar amounts on a mRNA level¹⁵⁷. However, only LPA₂ could be detected in western blot analysis of mature and immature DCs¹⁵³. Addition of LPA to immature human DC resulted in mobilisation of Ca²⁺ from intracellular stores, actin mobilisation and increased chemotaxis by a PTX sensitive mechanism. In contrast, such effects are not observed after addition of LPA to LPS-matured human DCs¹⁵⁷. LPA increases IL-10 release and inhibits IL-12 and TNF- α production in maturing DCs, while basic cytokine production of immature DCs remains unchanged. In the MLR, LPA-treated mature DCs exhibit higher T-cell stimulating capacity. Similar to the effect of S1P, LPA promotes a T_H2 polarized immune response¹⁵⁷.

1.6.4. Monocytes/Macrophages

The mononuclear macrophage system comprises a large number of mononuclear cells that show considerable differences in morphology and functionality according to the tissue localisation. The development of tissue macrophages proceeds by four different stages: bone marrow-derived monoblasts and promonocytes differentiate into monocytes that make up about 5% of white blood cells. Finally, monocytes that migrate into tissue will differentiate into macrophages that fulfil a wide variety of biological functions. Macrophages are equipped for highly effective phagocytosis enabling those cells to clear cell detritus or pathogens with high efficiency. Moreover, macrophages secrete a variety of growth factors and mediators profoundly influencing the physiological function and differentiation of neighbouring cells. Finally, at least under certain conditions, monocytes and macrophages can differentiate into endothelial cells, smooth muscle cells and myofibroblasts¹⁵⁸.

As a consequence of the heterogeneity of the macrophage population, reports on LPL receptor expression and biological function in those cells are largely dependent on the subpopulation studied as well as on the species these cells were isolated from. Expression of various SIP and LPA receptors has been reported on different macrophages subpopulations as

	S1P ₁	S1P ₂	S1P ₃	S1P ₄	S1P ₅	LPA ₁	LPA ₂	LPA ₃	Reference
Human blood monocytes	-	+	+	N.D.	N.D.	+	-	N.D.	159
Human monocytes	+	++	+	++	-	++	++	-	160
Human macrophages	-	++	-	++	-	++	++	-	160
Human alveolar macrophages	++	-	+	-	-	++	++	++	161
Rat alveolar macrophages	-	++	-	+	-	++	+	-	161
Mouse peritoneal macrophages	+	+	-	-	-	+	-	-	159

Table 2: S1P and LPA receptor expression on macrophages and monocytes

S1P and LPA receptor expression was determined at the RNA level by several investigators. ++: high expression level; +: low to very low expression level; -: no detectable expression; N.D.: not determined

shown in **Table 2**. LPA stimulation of human macrophages results in increased oxidative burst and increase of intracellular Ca²⁺ concentration^{160,161}. In mouse peritoneal macrophages, both S1P and LPA stimulation leads to up-regulation of IL-1 β and TNF α , while IL-2 is downregulated¹⁶¹. LPL receptors may be implicated in the migration and correct localisation of macrophages within the SLOs and thus influence the fate of the immune response. In murine spleen, absence of S1P₃ has been shown to result in an aberrant architecture of

marginal sinuses with abnormally organized metallophilic macrophages and MadCAM-1⁺ endothelial cells resulting in a defective immune response¹⁶². Whether this observation is primarily due to the lack of S1P₃ on metallophilic macrophages or whether it is secondary to a defective localisation of MadCAM-1⁺ endothelial cells remains to be shown.

1.6.5. Granulocytes

Various actions on different classes of granulocytes has been reported. Very early, effects of LPL in animal models of allergic disease have been described. In the following paragraphs, knowledge on the different classes of granulocytes will be described.

1.6.5.1. Neutrophil granulocytes

Neutrophils are key mediators in the initiation and regulation of the immune response against invading microorganisms or tissue trauma. In the initial phase of invasion/trauma, neutrophils are the first immune cells arriving at the site of injury, initiating and orchestrating further phases of the inflammatory response. On the one side, they have a bactericidal action themselves by liberating anti-microbial proteins and proteases from their intracytoplasmatic granules and initiating the oxidative burst resulting in massive production of reactive oxygen intermediates upon stimulation *via* Toll-like or complement-receptors. These cells phagocyte pathogens or necrotic cells and restrain pathogens locally by forming pus. On the other side, they interact with a multitude of other key players of the innate as well as the adaptive immune response, thus participating in the shaping and polarization of the immune response¹⁶³. Although the influence of lysophospholipids on the inflammatory responses in animal models or in diverse human pathologies has been described for several decades, comprehensive data on lysophospholipid receptors expression on neutrophils and lysophospholipid metabolism in those cells during inflammatory response are sparse and partially conflicting.

The signalling cascade responsible for the transmission of S1P signals to the neutrophils is not yet finally elucidate. Human neutrophils have been shown to express S1P₄, S1P₁ and to a lower degree also S1P₅ and S1P₂ on a RNA level. In inflammatory states, S1P₃ expression that was detected in very few neutrophils of healthy volunteers was significantly up-regulated. Neutrophils from patients with pneumonia with increased S1P₃ expression exhibited significantly higher chemotaxis towards S1P compared to those from healthy controls, indicating the implication of S1P₃ in S1P-induced chemotaxis. Moreover, pre-treatment of neutrophils with S1P reduced IL-8-induced chemotaxis¹⁶⁴. Furthermore, S1P reduces

neutrophil susceptibility to apoptosis¹⁶⁵. However, S1P has also been implicated in the GPCR-independent increase of calcium influx *via* store-operated calcium entry into neutrophils¹⁶⁶. Chemotaxis of neutrophils *in vitro* could be inhibited *via* blockade of sphingosine-1-kinase and thus S1P production. Similarly, in an *in vivo* model, neutrophil activation (as estimated by increased CD11b expression) was also blocked by sphingosine-1-kinase inhibitors¹⁶⁷. However, whether these biological effects are due to S1P activity at specific GPCRs or secondary to an increase of intracellular Ca^{2+} *via* store-operated calcium entry remains to be shown.

The currently available literature draws a heterogeneous picture of LPA effects on neutrophils. Both *in vitro* and *in vivo* experiments from different investigators showed conflicting results. While some reports described positive *in vitro* effects on chemotaxis in human neutrophils^{164,168}, others reported no such influence of LPA¹⁶⁹. In an animal model, LPA inhalation promoted neutrophil migration into the BAL fluid¹⁷⁰. *In vitro*, oxidative burst of neutrophils was promoted in some experimental settings^{169,171}, while LPA inhibited the generation of reactive oxygen intermediates in others¹⁶⁸. The molecular mechanisms of LPA action in granulocytes are not well characterized. LPA seems to promote Ca^{2+} entry *via* GPCR-independent mechanism¹⁶⁹. Furthermore, LPA increases phospholipase D activation and consecutive degranulation of neutrophils¹⁷². In the only study available assessing LPA receptor mRNA expression in human neutrophils, LPA₂ receptor was the predominantly expressed LPA receptor. LPA₁ was expressed by some individuals on a lower level, but no LPA₃ expression could be detected. Interestingly, LPA₁ expression was significantly upregulated in pneumonia patients. In *in vitro* chemotaxis experiments, these neutrophils showed significantly increased migration towards LPA, indicating that LPA₂ but also LPA₁ mediate chemotaxis in neutrophils. Moreover, signalling *via* LPA₁ and LPA₂ interferes with IL-8-mediated migration of neutrophils *via* a decreased expression of the IL-8 receptor CXCR1¹⁶⁴.

1.6.5.2. Basophil granulocytes

Together with mast cells and eosinophils, basophils are the key players in allergic inflammation. In parasite infections, they represent the major IL-4 producing PBMC in mice as well as in man.

As yet, data on lysophospholipidreceptor expression on basophils is not available in the literature. Distinct biological effects of S1P and LPA on basophils have not been described so far.

1.6.5.3. Eosinophil granulocytes

Blood and tissue eosinophilia is a characteristic sign for helminth infection, allergy and asthma. Eosinophils can release a wide range of inflammatory mediators such as leukotrienes, and also a variety of cytokines such as IL-1, TGF- β , IL-4 or IL-5. In allergic disease and asthma, eosinophils play a pro-inflammatory role.

Human eosinophils express high quantities of S1P₁ and lower amounts of S1P₂ and S1P₃. Upon short-time exposure to S1P, expression of all 3 S1P receptors is up-regulated, while long-term exposure leads to significant down-regulation of S1P₁ compared to basal levels. S1P induces chemotaxis in rat eosinophils *in vivo* as well as in human eosinophils *in vitro*¹⁷³. At least a part of this chemotactic action may be due to a positive S1P effect on CCR3 expression.

Assessment of LPA receptor expression revealed the presence of mRNA for LPA₁ and LPA₃ in human eosinophils. LPA was shown to promote Ca²⁺ mobilisation from intracellular stores, actin remodelling, respiratory burst, chemotaxis and integrin up-regulation in human eosinophils *in vitro*. This effect could be inhibited by pertussis toxin, indicating that the observed effects were mediated by G_i protein coupled receptors¹⁷⁴. Accordingly, in an animal model of asthma, inhalation of LPA promoted invasion of eosinophils¹⁷⁰.

1.6.6. Mast cells

Mast cells play important roles in innate as well as in acquired immunity. Upon crosslinking of Fc γ RI receptors expressed at the cell surface by IgE bound bi- or polyvalent antigens, mast cells release a multitude of mediators from the intracellular stocks (*e.g.* histamine, proteoglycans or proteases) or increase the *de novo* synthesis of bioactive mediators comprising platelet-derived activating factor, leukotriene C₄ or prostaglandine D₂. Furthermore, mast cells produce various cytokines involved in the regulation of many biological processes, including IL-1, IL-3, IL-4, IL-6, IL-10, IL-13, TNF- α , MIP3 α and MCP-1. One of the best explored issues in mast cell biology is their role in IgE-associated immune Type I response. Mast cell activity is responsible for the majority of processes observed during the acute phase of the allergic response, including increased vascular permeability and tissue oedema. Recruitment of granulocytes, which is a prerequisite for the development of late-phase reactions of allergic diseases, is also initiated by factors released by mast cells¹⁷⁵. But mast cells not only play a prominent role in allergic pathology but also in the immune response against certain pathogens, especially against parasites. Thus, mast cell deficient mice

show an impaired clearance of the nematode *Strongyloides venezuelensis*¹⁷⁶. Furthermore, mast cells are involved in the innate immune response. It has been shown that mast cells can be activated directly by complement or certain bacterial components such as lipopolysaccharides^{177,178}.

Both prototypes of lysophospholipids, LPA and S1P are profoundly implicated in the regulation of mast cell responsiveness to biological stimuli.

Interestingly, the biological activity of S1P seems to be mediated by both the binding to S1P receptors on the mast cell surface and also by a direct intracellular action on intracellular signalling cascades. So far, expression of S1P₁ and S1P₂, but not S1P₃, S1P₄ and S1P₅ has been shown on mast cells¹⁷⁹.

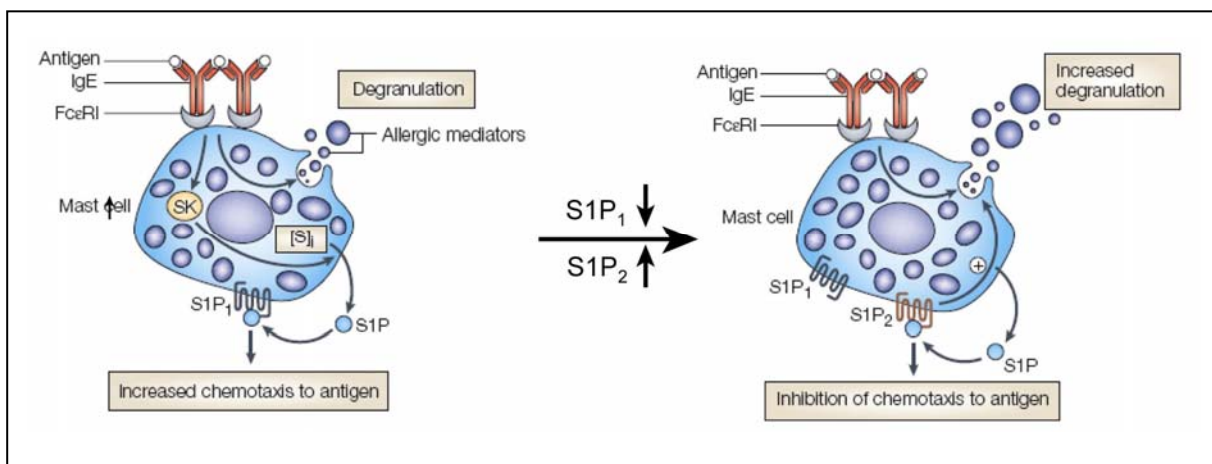


Figure 14: Model for the differential function of S1P signalling during mast cell activation

Upon cross-ligation of the FcεRI receptor, the production and secretion of S1P is increased by augmentation of sphingosine kinase activity. This results on the one hand in decreasing intracellular levels of sphingosine thus promoting leukotriene synthesis and cytokine liberation. On the other hand, increased extracellular levels of S1P result in an intensified chemotaxis to the antigen via stimulation of the S1P₁ receptor. Cross-ligation of the FcεRI receptor also results in increased expression of S1P₂. The increased S1P₁/S1P₂ ratio then gradually leads to diminished chemotaxis and increased degranulation. Modified from Rosen and Goetzl, Nature Reviews Immunology, 2005

The dissection of S1P-mediated signalling is further complicated by the modulation of the activity or/ or expression of several molecules implicated in the metabolism of the ligand S1P or in the signal transduction according to the cellular activation status. Following FcεRI cross ligation, S1P₂ expression is unregulated on a transcriptional level¹⁷⁹. The same stimulus also increases SphK activity by a posttranscriptional mechanism, thus inducing an increase of intra and extracellular S1P concentrations¹⁷⁹. Intracellularly, increased S1P levels function as a second messenger inducing calcium release from intracellular stores¹⁸⁰. Moreover, intracellular S1P counteracts the inhibiting influence of intracellular Sph on leukotriene synthesis and cytokine release, resulting in a MAPK-mediated release of leukotrienes and cytokines¹¹². S1P secreted to the extracellular compartment following activation of SphK I

transactivates S1P₁ and S1P₂ in an autocrine manner resulting in a profound modulation of mast cell function. S1P increases antigen-induced mast cell chemotaxis *via* binding to S1P₁ in a G_i protein-mediated mechanism in an *in vitro* model. In contrast, S1P binding to S1P₂ results in decreased mast cell migration and increased mast cell degranulation as shown in Bone marrow-derived mast cells (BMMCs) of S1P₂^{-/-} mice¹⁷⁹. An attractive *in vivo* scenario for regulation of mast cell activation by S1P is depicted in **Figure 14**. After crosslinking of surface IgE, SphK activation results in increasing S1P and decreasing Sph levels. First, S1P predominantly binds to the highly expressed S1P₁ receptor, leading to increased chemotaxis of mast cells to antigen and decreased secretion of inflammatory mediators. In later stages, S1P binds to the up-regulated S1P₂ resulting in decreased motility at the site of highest antigen concentration and increased liberation of inflammatory mediators¹⁷⁹.

In vitro-derived human mast cells express all three LPA receptors¹⁸¹. LPA induces mast cell proliferation *via* LPA₁ and LPA₃¹⁸². In contrast in IL-4-primed mast cells, LPA binding to LPA₂ results in massive generation of chemokines MIP1 β , MCP-1 and IL-8¹⁸¹.

1.6.7. Regulatory T-cells

Regulatory T-cells are profoundly implicated in the maintenance of a delicate balance between the effective defence against a myriad of potential pathogens and the prevention of excessive immune responses that may be harmful to the host. The classification of these very heterogeneous cell populations is still rapidly evolving. However, there is a main dichotomy between naturally occurring T_{reg} cells and adaptive T_{reg} cells. While naturally occurring T_{reg} cells are generated in the thymus, the very heterogeneous class of adaptive T_{reg} cells is generated in the periphery and exert their regulatory function through different mechanisms¹⁸³. Although there is no “perfect” marker for naturally occurring T_{reg} cells identified as yet, these cells are the best characterized population among all T_{reg} cells classes and are currently identified by the expression of FoxP3 or the double positivity for CD4 and CD25. Their protective action is mediated both through contact-dependent mechanisms involving CTLA4 expression and through secretion of IL-10 and TGF β .

Until now, only this class of T_{reg} cells has been assessed for lysophospholipid receptor expression. However, data on S1P and LPA receptor expression on these cells are partially contradictory. While one group of investigators find only S1P₁ and S1P₄ RNA expression of CD4⁺CD25⁺ regulatory T-cells¹⁸⁴, other investigators report expression of all five known S1P receptors in those cells, although S1P₁ and S1P₄ showed the highest expression levels¹⁸⁵. Also, the relative expression levels on CD4⁺CD25⁺ regulatory T-cells and on CD4⁺CD25⁻ T-cells

showed considerable differences between reports of different groups. While Wang *et al.* showed similar S1P₁ and S1P₄ expression levels on those cell types, Sawicka *et al.* found significantly increased S1P₁ and S1P₄ mRNA levels on CD4⁺CD25⁻ T-cells compared to CD4⁺CD25⁺ regulatory T-cells. The reason for these differences are still poorly understood, but given the lack of a definitive marker for regulatory T-cells, differences in the purity of the cell population may be a possible explanation. Furthermore, differences in the activation status of the cells induced during the isolation procedure may also account for these findings, since activation with anti-CD3/anti-CD28 antibodies or incubation with the functional antagonist FTY720 results, as in CD4⁺CD25⁻ T-cells, in down-regulation of S1P₁ and S1P₄ on CD4⁺CD25⁺ regulatory T-cells.

On the functional level, presence of S1P in concentrations found in lymph and plasma is required for effective IL-10 production and the inhibition of CD4⁺CD25⁻ T-cell proliferation *in vitro*¹⁸⁴. In this experimental setting, the use of the functional S1P antagonist FTY720 decreased IL-10 expression, indicating a negative effect of this drug on the suppressive function of CD4⁺CD25⁺ regulatory T-cells. In contrast to these experiments, Sawacki *et al.* revealed differential effects of FTY720 on CD4⁺CD25⁻ T-cells and CD4⁺CD25⁺ regulatory T-cells. While FTY720 effectively sequesters CD4⁺CD25⁻ lymphocytes from blood and spleen into lymph nodes and Peyer's patches, the percentage of CD4⁺CD25⁺ regulatory T-cells was increased in FTY720 treated mice. Moreover, FTY720 increased T regulatory cell activity in a contact dependent fashion *in vitro* as well as in a murine allergic airway inflammation model¹⁸⁵. The view of an increased activity of CD4⁺CD25⁺ regulatory T-cells following FTY720 exposure was supported by the efficient attenuation of T_H1-mediated colitis in mice after administration of this substance¹⁸⁶. These FTY720 effects were dependent on the presence of functional CTLA4 as well as on IL-10.

In summary, there is growing experimental evidence for a direct involvement of S1P receptor signalling in the control of the activity of CD4⁺CD25⁺ regulatory T-cells. However, the exact molecular mechanisms as well as the individual S1P receptors implicated in this process remain unknown.

1.7. Role of S1P signalling in the immune homeostasis and immune response

Over the last 10 years, a substantial amount of literature has accumulated supporting the *in vivo* function of S1P in immune functions. A major part of experimental settings relayed on

the use of FTY720, an immunosuppressive drug that acts on S1P₁ and S1P₃-S1P₅ and which induces downregulation of S1P₁. Other investigators used S1P receptor deficient animal models to show the implication of specific S1P receptors in certain aspects of the immune response. The resulting picture is dominated by data on S1P influence on immune cell migration and organ-specific localisation. Recently, a growing number of findings on the functional consequences of these aberrant migrational processes have been published. The following chapter will outline the major *in vivo* findings of S1P function.

1.7.1. *In vivo* roles of S1P signalling in the immune homeostasis

1.7.1.1. S1P signalling in T-cell biology *in vivo*

Much of the basic current knowledge on the role of S1P in the generation of the cellular immune response was generated in experimental model using the immunosuppressive drug FTY720, even before the involvement of S1P in these processes was known. In the late 90s, this drug was shown to prolong significantly skin and cardiac allograft survival and to prevent lethal graft-*versus*-host reaction in rats by an unknown mechanism¹²¹⁻¹²³. In 1998, Chiba *et al.* discovered that FTY720 induced a profound lymphopenia in blood and lymph and a reduction in splenic lymphocyte numbers by sequestration of lymphocytes within LNs and Peyer's patches (PP)¹²⁸. Finally, in 2002, Mandala *et al.* showed that the phosphorylated form of FTY720 binds with high affinity to the S1P receptors S1P₁ and S1P₃₋₅¹⁰¹. Both administration of FTY720 as well as of high doses of S1P resulted in the induction of profound peripheral lymphopenia, thus implying a role of S1P in lymphocyte homing to LNs and PPs or in lymphocyte egress from these organs.

Matloubian *et al.* then showed that S1P₁ is involved in the mechanisms leading to FTY720-induced lymphopenia by using reconstitution of lethally irradiated mice with S1P₁^{-/-} foetal liver cells. By transferring single-positive S1P₁^{-/-} T-cells to WT recipients they found that these cells readily homed to SLOs but failed to exit from LNs and Peyer's patches. They furthermore demonstrated that S1P₁ deficiency results in sequestration of mature thymocytes within the thymus by blocking their egress. Interestingly, S1P₁ is up-regulated during T-cell development within the thymus. These two observations clearly suggested that S1P₁ is a S1P receptor crucially involved in T-cell egress from the thymus¹. These findings were later confirmed in animals harbouring a conditional knock-out of S1P₁ in T-cells². There are several reports showing that S1P deficiency and FTY720 do not only affect lymphocyte egress from SOLs but also influence cell entry into these organs. However, these results were partially contradictory^{128,187}.

In line with the observations in S1P₁ deficient models, constitutive over-expression of S1P₁ in T-cells that was not subjected to the cyclic regulation during T-cell migration (see also **chapter 1.6.1.1.**) lead to reduced T-cell numbers in peripheral lymph nodes and increased numbers in blood and spleen. Interestingly, T-cell dependent immune response was impaired in these animals. They developed a reduced swelling to 2,4-dinitrofluorobenzen in the contact hypersensitivity model due to a defect in the initiation phase. In a TCR-transgenic S1P₁ overexpressing mouse model, less antigen-specific T-cells were found in the draining lymph nodes after immunization and finally, development of experimental autoimmune encephalomyelitis was less pronounced in animals with S1P₁-overexpressing T-cells. No intrinsic defects of T-cell proliferation and survival could be found in these animals. Thus, the reduced immune responses were most probably due to an impaired trafficking and/or insufficient retention of S1P₁-overexpressing lymphocytes in the draining LN¹⁸⁸.

1.7.2. S1P is implicated in lymphocyte and mast cell trafficking to the gut epithelium and in the development of food allergy

Intraepithelial T lymphocytes (IEL) are a heterologous cell population consisting of conventional CD4 and CD8 T-cells as well as of unique cells expressing CD8 α as homodimer (CD8 $\alpha\alpha$)¹⁸⁹. S1P was shown to be implicated in the establishment of the specific composition of the IEL population in the small and the large intestine. While FTY720 treatment resulted in a significant reduction of IELs in the large intestine, this reduction was only moderate in the small intestine. Not all IELs were equally affected: while CD4 IELs and CD8 IELs were reduced, CD8 $\alpha\alpha$ were slightly increased in the large intestine. In contrast, in the small intestine only CD4 IELs were reduced, while the other two populations were increased¹⁸⁹. In accordance with observations in conventional T-cells, susceptibility to FTY720 was function of the activation status of the IELs, with naive CD62L^{hi} cells showing the highest sensitivity. Prevention of naive cell homing from the systemic immune compartments to the gut as well as an impaired retention of naive IELs in the intestinal compartment were identified as essential mechanisms of FTY720-induced IEL reduction¹⁸⁹.

S1P signalling is not only implicated in the physiological migration of lymphocytes to the gut, but plays also an important role in pathological conditions like food allergies. In a mouse model, allergic diarrhea can be induced by systemic priming with the OVA antigen and subsequent oral challenges with the same antigen. It has previously been shown that during the sensitisation phase the spleen is indispensable for generation of pathogenic T_H2-primed T-cells¹⁹⁰. Upon oral challenge, these cells migrated preferentially to the large

intestine where they contributed to the development of severe allergic diarrhea. In this experimental setting, FTY720 treatment significantly reduced the migration of activated CD4⁺ T-cells from the spleen to the gut. Interestingly, the mechanism involved was not the exit block of systemically activated CD4⁺ cells from the spleen, but a decreased infiltration of these cells into the lamina propria of the large intestine. Clinically, FTY720 treatment prevented the development of allergic diarrhea in this mouse model. In the same model, OVA-specific proliferation of CD4⁺ T-cells isolated from spleen and mesenteric lymph nodes was not affected by FTY720 treatment. In contrast, IL-4 and IL-5 secretion was significantly reduced, while total and OVA-specific IgE levels remained similar in both treatment groups. Other than lymphocyte infiltration, FTY720 administration also significantly reduced mast cell migration into the lamina propria of antigen-challenged mice. These data indicate that S1P is implicated in the pathogenesis of allergic diarrhea by multiple levels including migration of pathogenic CD4⁺ cells and mast cells to the gut as well as modification of cytokine secretion¹⁹¹.

1.7.3. Implication of S1P signalling in B-cell biology *in vivo* and on the humoral immune response.

Blockade of S1P signalling results in discrepant effects on the generation of the humoral immune response depending on the experimental model. Mice immunized with the T-cell-dependent antigen NP-CGG and treated with high doses of the functional S1P antagonist FTY720 show a significantly reduced IgG1 response while the specific IgM levels are normal. In both spleen and bone marrow of FTY720 treated mice, specific IgG1 AFC are significantly reduced in number. In contrast, specific IgM AFC numbers in these organs were normal. Interestingly, the production of high-affinity IgG1 antibodies was far more affected than those of low affinity IgG1. Taken together, these observations indicate that the initial steps of B-cell activation appear to be less affected, whereas later steps involved in affinity maturation appear to be disturbed¹⁹². Indeed, the formation of germinal centres (GC) where affinity maturation and class switching takes place, is reduced in the spleens, the PPs and the LNs of FTY720 mice compared to untreated animals. However, in another animal model, FTY720 administration at a lower but clinical relevant dose of FTY720 to mice infected with 200 PFU of lymphocytic choriomeningitis virus (LCMV) did not induce any changes in the specific IgM or IgG response¹²⁴. The origin of these discrepant observations remains to be elucidated. Differences in the experimental set-up including different antigens and different dosages of FTY720 may have been involved. In contrast, the humoral response to T-cell-

independent antigens was indistinguishable in FTY720 and mock treated animals on all these experimental models^{124,192,193}.

Blockade of S1P signalling was also implicated in the localisation of B-cell populations within the spleen. So, FTY720 treatment induced delocalisation of marginal zone (MZ) B-cells from the marginal zone to the follicles, a migration pattern reminiscent of that of LPS or pathogen-activated MZ B-cells. The absolute MZ B-cell number in spleen of FTY720 treated and mock treated animals remained constant¹⁹³. S1P₁ was shown to be a S1P receptor critically implicated in this phenomenon. MZ B-cells expressed S1P₁, S1P₃ and S1P₄. Upon activation, S1P₁ and S1P₃ are downregulated. Using S1P₁^{-/-} cells and S1P₁^{-/-}/ wild type chimeras it was shown that S1P₁ deficient B-cells failed to localize to the MZ. S1P₃ deficiency did not result in abnormal localisation of MZ B-cells. The effects of S1P₄ deficiency was not tested in this experimental setting³. Very interestingly, the lack for CXCL13, a chemokine that is crucial for the homing of circulating B-cells to the lymphoid follicles, induced an abolishment of the FTY720-induced delocalisation of MZ B-cells. Taken together, these observations suggest that MZ B-cell localisation in the MZ depends on an equilibrium between S1P and CXCL13 signalling³.

The development of a T-cell-independent immune response is impaired in S1P₃^{-/-} mice. This defect was shown to be due to aberrant localisation of MadCAM-1⁺ endothelial cells in the marginal sinus. This resulted in an abnormal architecture of the MZ and increased numbers of MZ B-cells. LPS induced entry of MZ B-cells into the follicles was increased in these animals¹⁶².

In FTY720-treated mice, the normal migration of ASC from spleen to the bone marrow was impaired. While the entry from the blood to the bone marrow showed no abnormalities in these animals, egress of ASC from the spleen into the blood was significantly reduced under FTY720-treatment. ASCs devoid of S1P₁ showed a similar migrational behaviour to FTY720-treated ASCs implicating the S1P₁ receptor as the essential mediator of the FTY720 effect⁴. Whether these changes in ASC migration induce alterations of the antibody response in this experimental model has not yet been assessed.

1.7.4. S1P impacts on trafficking of peritoneal B-cells

Intraperitoneal application of the functional S1P antagonist FTY 720 lead to a significant decrease in peritoneal B-cell numbers concerning equally all peritoneal B-cell populations assessed (peritoneal B1 and B2 cells). This reduction occurred within 3 hours after single FTY720 application and was reversible, with normal peritoneal B-cell numbers

occurring at day 7 after cessation of FTY720 treatment. A influence of FTY720 on differentiation and viability of peritoneal B-cells or on the B1 B-cell progenitors in the peritoneal cavity or the bone marrow could not be detected. The transfer of labelled peritoneal B-cells into the peritoneal cavity of SCID mice revealed that FTY720 treatment favoured egress of these cells from the peritoneal cavity and accumulation within the parathymic lymph nodes. In parallel, immigration of i.v. transferred peritoneal B-cells into the peritoneal cavity was hampered while their tropism to the bone marrow was favoured. Although peritoneal B-cells are known to be an important source of natural antibodies, the aberrant migrational behaviour and localisation of peritoneal B-cells had no effect on plasmatic immunoglobulin levels. Similarly, the antibody response to T-cell-independent antigens was alike in FTY720 and PBS treated mice. Peritoneal B-cells also contribute to IgA production. Very interestingly, after adoptive transfer of peritoneal B-cells, FTY720-treated SCID mice showed significantly reduced faecal IgA levels than the PBS treated control animals, while IgM levels remained constant. In summary, inhibition of S1P signalling influences peritoneal B-cell trafficking by both favouring exit from the peritoneal cavity and sequestration of these cells in parathymic lymph nodes and by hampering entry from the blood. Intestinal IgA levels are consequently reduced after functional inhibition of S1P signalling¹⁴⁵.

1.7.5. Increased tissular S1P levels induce lymphopenia

During the testing of various food colorants it was observed that THI can induce a peripheral lymphopenia and accumulation of T-cells in thymus. Mice treated with THI have less CD4⁺ and CD8⁺ lymphocytes in blood and lymph but show increased numbers of CD4⁺ and CD8⁺ cells in the thymus and no change in lymph node T-cells compared to untreated animals. Since T-cells in lymph must have passed by the lymph node or the Peyer's patch, a block at the egress level from the lymph node was suspected to be responsible for this clinical picture. As described above, S1P signalling is responsible for lymphocyte egress from lymph nodes and thymus. A mechanism involving S1P was thus suspected. Indeed, THI was shown to inhibit S1P lyase by a mechanism reversible by vitamin B₆. S1P lyase is a cellular enzyme responsible for S1P degradation. Indeed, the vitamin B₆ antagonist DOP was shown to mimic THI action. S1P concentrations in SLOs of DOP or THI treated mice were 100 – 1000 times higher than in untreated control mice. Extracts from organs of DOP treated mice were able to down-regulate S1P₁ expression on test cells over-expressing FLAG-tagged S1P₁ *in vitro*. However, the receptors mediating the biological effects of increased tissue concentrations of S1P have not been formally identified.

2. AIM OF THIS STUDY

S1P signalling plays a crucial role in the homeostasis of the immune system and in the development of the immune response. S1P₁ and S1P₄ being the predominant S1P receptors expressed on immune cells, the vast majority of S1P effects is likely mediated by these receptors. Indeed, as shown in the introductory chapter, S1P₁ plays a pivotal role in many processes of both B- and T-cell biology. In contrast, the biological function of S1P₄ in immune cells is largely unknown. In order to shed more light on this question, a S1P₄-deficient mouse model was generated in our laboratory. The analysis of the immune system of these S1P₄^{-/-} mice constitutes the first focus of this work.

S1P₁ and S1P₄ bind with high affinity the same ligand. Moreover, the intracellular signal transduction involves partially identical signalling pathways. Functional compensation for the lack of one receptor type by another has been shown to occur in the S1P receptor system, as seen in mouse embryonic fibroblasts deficient for S1P₂ and S1P₃⁵. In addition, *in vitro* data from some investigators suggest that S1P₁ and S1P₄ may associate in complexes, at least in cell lines stably expressing these receptors⁶. Therefore, the interpretation of certain observations made in S1P₄^{-/-} animals can be complicated by a possible functional compensation of S1P₄ deficiency by S1P₁. In order to better dissect such an intricate interaction between these two S1P receptors, we decided to generate a novel experimental model in which the expression of both S1P₁ and S1P₄ receptors, would be abolished. Since the S1P₁^{-/-} phenotype results in lethality *in utero*, the double knock-out approach was not possible. Therefore we decided to downregulate S1P₁ expression by siRNA-mediated gene knock-down. The generation of a lentivirus-based vector system for stable shRNA mediated knock-down of S1P₁ constitutes the second focus of this work.

3. MATERIALS

3.1. Bacterial strains

E. coli DH5 α

F-, Φ 80d, *lacZ*, *endA1*, *recA1*, *hsdR17* (rK- mK+), *supE44*, *thi-1*, d-, *gyrA96*, Δ (*lacZYA-argF*), U169

E. coli TOP10F' (Invitrogen)

F'(*lacIqTeeR*), *mcrA*, Δ (*mrr-hsdRMS-*, *mcrBC*), Φ 80*lacZ* Δ M15, Δ *lacX74deoR*, *recA1*, *araD139*, Δ (*ara-leu*)7697, *galU*, *galK*, *rpsL*, *endA1*, *nupG*

3.2. Plasmids

pcDNA 3.1 (+) (Invitrogen)

CMV immediate early promoter, G418 resistance gene, **size: 5.4 kb**

pGEM[®]-T Easy (Promega)

commercially available, pre-linearised vector with T-overhangs for cloning of PCR products with A-overhangs, ampicilline resistance gene, **size: 3.0 kb**

mU6pro (Yu et al, 2002; Univeristy of Michigan, US ¹⁹⁴)

expression vector for expression of hairpin siRNA containing an U6 promoter, ampicilline resistance gene, GFP marker, **size: 4.2 kb**

pLVTHM (Didier Trono, Ecole polytechnique fédérale de Lausanne, Switzerland)

self inactivating lentiviral vector for expression of hairpin siRNA under control of the H1 promoter, contains the GFP reporter gene under control of the EF1-alfa promoter and an ampicilline resistance gene, **size: 11.1 kb**

psPAX2 (Didier Trono, Ecole polytechnique fédérale de Lausanne, Switzerland)

2nd generation packaging plasmid containing the gag, pro and pol genes which code for the main structural proteins and the retrovirus specific enzymes, **size: 10.7 kb**

pMD2G (Didier Trono, Ecole polytechnique fédérale de Lausanne, Switzerland)

envelope plasmid expressing the vesicular stomatitis virus glycoprotein under control of an CMV promoter used to pseudotyp the virus, **size: 10.7 kb**

3.3. Cell lines

NIH3T3

NIH Swiss mouse embryonic fibroblasts (ATCC.CRL-11268TM)

293 T

293HEK cell line expressing the SV40 antigen (ATCC.CRL-11268TM)

COS-7

African green monkey kidney fibroblast-like cell line (ATCC.CRL-1651TM)

TG40

Variant T cell hybridoma cell line lacking the expression of TCR- α and - β chains (Ohno et al., 1991)¹⁹⁵

LBRM-33

Cell line derived from a radiation induced mouse T cell lymphoma (ATCC.TIB-155TM)

3.4. Mice

S1P₄^{-/-} mice on a Balb/C and C57BL/6 background were bred in the animal facilities of the Max-Delbrück-Center for Molecular Medicine, Berlin. Wildtype Balb/C and C57BL/6 mice were either bred in the animal facilities of the Max-Delbrück-Center for Molecular Medicine, Berlin, or purchased from Charles River Germany GmbH, Sulzfeld.

3.5. Primers

PCR primers were purchased from BioTez GmbH, Berlin-Buch, Germany.

Genotyping

mEDG6-F	5`- CGG CCA CAG CCT CCT CAT TGT C -3`
mEDG6-R	5`- ACA GAC CGA TGC AGC CAT ACA CAC -3`
Neo20U	5`- AGA TGG ATT GCA GCA CGC AGG TTC TC -3`
Neo_1457	5`- GTA AAG CAC GAG GAA GCG GTC AG -3`

LightcyclerTM PCR

mG3PDH-F	5`- ACC ACA GTC CAT GCC ATC AC -3`
mG3PDH-R	5`- TCC ACC ACC CTG TTG CTG TA -3`
mu-EDG1 LCn-fow	5`- CTC TGC TCC TGC TTT CCA TC -3`
mu-EDG1 LCn-rev	5`- GCA GGC AAT GAA GAC ACT CA -3`
murEDG6_neu_f	5`-GGC TAC TGG CAG CTA TCC TG-3`
murEDG6_neu_r	5`-GGA GGA CGT GGA GAC TTC TG-3`

Generation of HA-tagged SIP₁

murine_EDG1_HA_F	5`- CAT GGA TCC ATG GGC TAC CCA TAC GAT GTT CCA GAT TAC GCT GGT GGT CCC GTG TCC ACT AGC ATC CC G GAG -3`
murine_EDG1_HA_R	5`- GAT TAG CGG CCG CGA GTT TTT TTT AGG AAG AA G AAT TGA CGT TTC C -3`

3.6. Oligonucleotides

Oligonucleotides for the generation of shRNA were purchased from BioTez GmbH, Berlin-Buch, Germany.

shRNA inserts for mU6prom

siRNA1 Top	5'- TTT GAC TGA CTT CAG TGG TGT TCT TCA AGA GAG AAC ACC ACT GAA GTC AGT TTT TT-3'
siRNA 1 Bottom	5'-CTA GAA AAA ACT GAC TTC AGT GGT GTT CTC TCT TGA AGA ACA CCA CTG AAG TCA GT-3'
siRNA2 Top	5'-TTT GGC ACT ATA TTC TCT TCT GCT TCA AGA GAG CAG AAG AGA ATA TAG TGC TTT TT-3'
siRNA2 Bottom	5'-CTA GAA AAA GCA CTA TAT TCT CTT CTG CTC TCT TGA AGC AGA AGA GAA TAT AGT GC-3'
siRNA3 Top	5'-TTT GGA CCT GTG ACA TCC TGT ACT TCA AGA GAG TAC AGG ATG TCA CAG GTC TTT TT-3'
siRNA3 Bottom	5'-CTA GAA AAA GAC CTG TGA CAT CCT GTA CTC TCT TGA AGT ACA GGA TGT CAC AGG TC-3'
siRNA4 Top	5'-TTT GAT TCA AGA GGC CCA TCA TCT TCA AGA GAG ATG ATG GGC CTC TTG AAT TTT TT-3'
siRNA 4 bottom	5'-CTA GAA AAA ATT CAA GAG GCC CAT CAT CTC TCT TGA AGA TGA TGG GCC TCT TGA AT-3'

shRNA inserts for pLVTHM

siRNA3_tronoTop	5'-CGC GTC CCC GAC CTG TGA CAT CCT GTA CTT CAA GAG AGT ACA GGA TGT CAC AGG TCT TTT TGG AAA T-3'
siRNA3_trono Bottom	5'-CGA TTT CCA AAA AGA CCT GTG ACA TCC TGT ACT CTC TTG AAG TAC AGG ATG TCA CAG GTC GGG GA-3'
siRNA5_trono Top	5'-CGC GTC CCC GCT ACC TTA GGA TCC GTA CTT CAA GAG AGT ACG GAT CCT AAG GTA GCT TTT TGG AAA T-3'
siRNA5_tronoBottom	5'-CGA TTT CCA AAA AGC TAC CTT AGG ATC CGT ACT CTC TTG AAG TAC GGA TCC TAA GGT AGC GGG GA-3'

3.7. Enzymes

Invitrogen:

Superskript™ II RNase H Reverse Transcriptase

NEB GmbH:

Alkalische Phosphatase (CIP), Klenow fragment, T4-DNA-polymerase, Restriktionsenzyme

Roboklon, Berlin:

Taq-DNA-Polymerase

Roche:

T4 DNA-Ligase, DNase I, RNase A

InViTek, Berlin

CombiPol DNA Polymerase

Takara Bio Inc.:

*TaKaRa Ex Taq*TM R-PCR Version 1.0

3.8. Antibodies and conjugates

BD PharmingenTM

Hamster anti-mouse CD3, Biotin, clone 145-2C11; rat anti-mouse CD19, APC, clone 1D3; rat anti-mouse CD21, FITC, clone 76G; rat anti-mouse CD23, PE, clone B3B4; Rat anti-mouse CD25, FITC, clone 7D4; rat anti-mouse IgM, Biotin; clone R 6-60.2; rat anti-mouse CD5, APC, clone: 53-7.3; purified anti-mouse CD3a, clone 145-2C11 and purified anti-mouse CD28, clone 37.51, both for cell culture

Biosource/Invitrogen

Rat anti-mouse IgM, FITC, clone LO-MM-9

Caltag/Invitrogen

Rat anti-mouse CD4, APC, clone RM4-5; rat anti-mouse CD8, PE, clone CT-CD8a; rat anti-mouse B 220, FITC, clone RA3-6B2;

Jackson Laboratories

Streptavidin-PE conjugates, Streptavidin-APC conjugates

Roche

Anti-HA High Affinity Ab, clone 3F10

3.9. Chemicals

BD Bioscience

Mouse collagen type IV

Biochrom KG:

Ficoll, fetal calf serum (FCS), PBS

Biosearch technologies, USA:

NP-O-Su

Calbiochem[®]:

D-erythro-Sphingosine-1-phosphate; Soybean trypsin inhibitor; Serum Bovine Albumin, Fraction V, fatty acid free

ICN Biomedicals Inc.:

Tris-(hydroxymethyl)-aminomethane (Tris)

Intervet:

Ketamin

Invitek GmbH:

2'-Desoxyribonucleoside-5'triphosphates (dATP, dCTP, dGTP, dTTP)

Invitrogen (Gibco BRL and Life Technologies):

TRIZOL®, agarose electrophoresis grade, boric acid, β-mercaptoethanol, penicillin-streptomycin (100X concentrate for cell culture), cell culture medium (DMEM, RPMI 1640), Lipofectamin 2000, SNARF®

Lysoform Dr.Hans Rosemann GmbH:

Lysoformin 2000

MBI Fermentas GmbH:

GeneRuler 1-kb DNA Ladder

E. Merck:

Aluminium hydroxide; Ampicillin; calcium chloride; dinatriumhydrogenphosphate; 0.5% eosin-G; formaldehyde, formamide, glucose, potassium hydrogenphosphate, sodium acetate, sodium-dodecylsulfate (SDS),

Labor Dr. Merk und Kollegen:

Sheep red blood cells

Molecular Probes:

CFDA

MV-pharma:

Xylazine

PAA:

trypsin-EDTA-solution (0.05% trypsin, 0.02%EDTA without calcium and magnesium), cell culture medium (DMEM, RPMI 1640)

Promega:

RNasin

Roche:

SYBR Green I

C. Roth:

Agar-agar, albumin fraction V (BSA); ammonium acetate, ammonium hydrogen carbonate; chloroform, citric acid monohydrate, diethyl ether, dimethylsulfoxide (DMSO), acetic acid, ethanol, ethidiumbromide, ethylenediaminetetraacetic acid (EDTA dinatriumsalt dihydrate), glycerin, glycine, 4-(2-hydroxyethyl)-1-piperazineethanesulfonic acid (HEPES), isopropanol, methanol, 3-(N-Morpholino)-propan-sulfonicacid (MOPS), parafilm (Nescofilm), peptone from casein, phenol, polyvinylpyrrolidone K30, potassium acetate, sodium azide, sodium chloride, sodium citrate, sodium hydroxide, tween-20 and yeast extract.

Sigma-Aldrich:

Albumine dinitrophenyl(DNP-BSA), Albumin chicken egg grade V, Dibutylphthalat, Diethylpyrocarbonate (DEPC), ethylenediaminetetraacetic acid (EDTA tetra-natriumsalt dihydrate), Fluorescein isothiocyanate isomer I (minimum 90%, HPLC), orange-G,

paraformaldehyde, phorbol-12-myristate-13-acetate (PMA), polybrene, propidium iodide, puromycin, sodium butyrate, trypan-blue solution (0.4%) and 4-Deoxypyridoxine hydrochloride (DOP)

3.10. Kits

Agilent:

Agilent RNA 6000 Pico Kit; Agilent RNA 6000 Nano Kit

BD Biosciences:

Mouse IgE ELISA Set,

Miltenyi Biotec:

MACS Separation columns LS and MS; CD4⁺ T cell isolation kit; CD8a⁺ T cell isolation kit

Pharmingen:

OptEIATM Mouse IL-4 Set

Pierce:

BCA Protein Assay Kit

Perbio Science Germany:

SuperSignal[®] West Dura Extended Duration Substrate

Promega:

pGEM-T easy Kit

Qiagen:

RNAeasy mini kit, QIAEX II gel extractions kit, RNase-free DNase kit

Southern Biotech, USA:

SBA Clonotyping System/HRP

Zymed[®] Laboratories:

Mouse MonoAB ID Kit (AP)

3.11. Instruments and consumables:

Agilent Technologis Inc.:

Agilent 2100 Bioanalyzer

Amersham International:

ECLTM Western Blotting Detection Reagents; HybondTM nitrocellulose membrane, HybondTM-ECLTM

BDK Luft- und Reinraumtechnik GmbH:

Laminar ventilation hood for cell culture

Beckman Instruments GmbH:

Centrifuges (GS-6KR und J2-MC), ultracentrifuge tubes (1.5mL, 1x3.5 inches)

Becton-Dickinson GmbH:

Flow cytometer (FACSCalibur, FACScan) and Fac sorter(FACSVantage)

Biometra:

PCR-thermocycler trioblock

Bio-Rad Laboratories:

Gene pulser, GS gene linker, cuvettes, mini trans blot; DNA Engine Dyad[®]

BIO-TEK Instruments, Inc.

Power Wave X Select ELISA reader

Biozym:

Micropipette tips

Braun AG:

Syringes and needles

Buchner Laborservice:

Bacterial petridishes

Corning Inc.:

Cryogenic vial

Coulter:

Cell counter

Eppendorf:

Heat block, reaction tubes 0.5, 1.0 and 2.0 mL, thermomixer 543b, centrifuges 5417C and 5417 R

Fröbel Labortechnik:

Rocking platform

Gilson Medical Electronics:

Pipetman

Greiner:

Microbiological cell culture plates 10-cm, sterile 15- and 50-mL centrifuge tubes, 15-mL bacterial culture tubes

Heraeus:

Incubator, biofuge fresco - cooling centrifuge, cell culture incubator

Hirschmann Laborgerate:

Pipetus-akku

Miltenyi Biotec:

MACS separator

MWG Biotech:

DNA sequencer Long Readir 4200

Nalgene:

Cryo 1°C freezing container

Nunc GmbH:

Freezing cryotubes 2 mL, 96-well microtiterplate (Maxisorb)

Pharmacia Biotech:

Photometer ultrospec, electrophoresis supply

Roche:

LightCycler II, LightCycler capillaries

Roth:

Neubauer-cell chamber (0.1 mm thickness), sterile filters

Schott:

Conical flasks, beakers, glass pipettes and all glass wares

Scientific Industries:

Vortex-Genie 2

Shandon:

Cytospin3

TPP:

Cell culture flasks- 25-cm², 75-cm² and 150-cm², cell culture plates: 6-well, 12-well, 24-well, and 96-well, 10-cm and 15-cm, and sterile 15-mL and 50-mL centrifuge tubes

Whatman Limited:

3-mm paper

3.12. Universal buffers

PBS pH 7.4

0.14 M NaCl

0.14 mM KCl

8.1 mM NaH₂PO₄

1.5 mM KH₂PO₄

TBS pH 7.6

20 mM Tris

140 mM NaCl

4. METHODS

4.1. Molecular Biology Methods

4.1.1. Bacteriological tools

4.1.1.1. Liquide Cultures

LB-media

10 g/l trypton
5 g/l yeast extract
5 g/l NaCl
1ml 1N NaOH

<i>Antibiotic</i>	<i>Stock solution</i>	<i>Solvent</i>	<i>Final concentration</i>
Ampicilline	50 mg/ml	50% Ethanol	100 µg/ml
Tetracycline	12.5 mg/ml	70% Ethanol	12.5 µg/ml

Sterile LB-Media was inoculated with a single bacterial colony from a LB plate or with bacteria from a glycerol stock solution and grown overnight at 37 °C under constant shaking (250 Rpm) in a bacterial shaker. Cultures were grown until they were freshly saturated ($1-2 \times 10^9$ cell/ml). Optimal growth was verified by the measurement of the optical density at 600nm that should be between 1.0 and 1.5 at the end of the culture. If required, a selective antibiotic was added to the culture at the final concentrations shown above.

4.1.1.2. Solide cultures

LB-media

10 g/l trypton
5 g/l yeast extract
5 g/l NaCl
1ml 1N NaOH
15 g agar

LB media containing agar as shown above was autoclaved and allowed to cool down to approximately 55°C. If necessary, antibiotics were added at the final concentrations shown above. When lacZ containing plasmids were used in the following experiments, X-Gal and IPTG were added at 40 µg/ml and 10 µg/ml, respectively. The warm media was then poured into sterile Petri dishes under a laminar flow hood and allowed to solidify. Petri dishes were then dried overnight and subsequently stored at 4°C until further use.

For inoculation, bacteria from a glycerol stock, an overnight culture or freshly transformed bacteria were streaked out with an inoculating loop. Plates were then incubated at

37°C for 8 to 16 hours until single colonies became visible. Plates were then closed with Parafilm[®] and stored at 4°C until further use.

4.1.1.3. Long term storage

For long term storage, bacteria from a liquid culture were mixed with the same volume of glycerol 97% and stored in cryotubes at –80°C.

4.1.1.4. Preparation and transformation of competent cells

4.1.1.4.1. Preparation of competent cells for heat shock transformation

A single colony of DH5 α cells was inoculated to 5 ml of LB medium and grown overnight under moderate shaking (250 rpm) at 37°C. Five hundred μ l of the overnight culture were used to inoculate 50 ml of sterile LB media. This culture was grown at 37°C and under moderated shaking to an OD₆₀₀ of 0.6. All following steps were performed in a cool chamber at 4°C with pre-cooled material. Cultures were incubated for 10 min on ice and centrifuged at 1200 x g for 5 min at 4°C. The supernatant was poured off and the pellet was resuspended in 20 ml of ice-cold 0.05M CaCl₂ solution. After a further incubation step of 15 min on ice, cells were centrifuged for 5 min at 1500 rpm and 4°C. The pellet was resuspended in 2 ml of ice-cold 0.05M CaCl₂ solution. Subsequently, cells were incubated for 1 hour on ice. Subsequently, 20% glycerol was added, and cells were dispensed into pre-chilled sterile polypropylene tubes in 110 μ l aliquots. Aliquots were stored at –80°C until further use.

4.1.1.4.2. Preparation of competent cells for electroporation

Top10F cells were streaked out on an LB plate containing tetracycline at 15 μ g/ml and incubated overnight at 37°C until single colonies became visible. Fifty millilitres of LB media was inoculated with a single colony of Top10F and grown overnight at 37°C in a 250 ml flask in a shaker (250 rpm). One litre of sterile LB media was then inoculated with the overnight culture and grown under constant shaking at 250 rpm in a 2-4 l flask at 37°C for 2-3 hours. When an OD₆₀₀ of 0.5-0.6 was reached, cultures were transferred into 2 pre-cooled 500 ml centrifugation flasks and incubated on ice for 30 min. All following steps were performed in a cool chamber at 4°C with pre-cooled material. In the following step, cultures were centrifuged at 2000 x g for 15 min at 4°C. The supernatant was discarded and the pellet resuspended into 500 ml of ice-cold sterile water. Cells were once again centrifuged at 2000 x g for 15 min at 4°C. The supernatant was discarded and the pellet was taken up into 250 ml of ice-cold water. Once again, cells underwent a centrifugation step at 2000 x g for 15 min at 4°C. The pellet

was then resuspended in 20 ml of ice-cold, sterile 10% glycerol. After a further centrifugation step at 2000 x g for 15 min at 4°C, cells were taken up in 2 ml of ice-cold, sterile 10% glycerol and dispensed into pre-chilled sterile polypropylene tubes in 50µl aliquots. Aliquots were stored at –80°C until further use.

4.1.1.4.3. Introduction of plasmid DNA by heat shock transformation

The half of a ligation preparation or 10-100 ng of plasmid DNA in a volume of 10-25 µl were transferred to 1.5 ml Eppendorf® tube and mixed with 100 µl of competent cells. The mixture was incubated on ice for 30-60 min. Cells were then subjected to a heat shock by placing them into a 42°C water bath for 2 min. Cells were then incubated for further 5 min on ice, before 1 ml of sterile LB media was added. The culture was then incubated under constant shaking at 250 rpm at 37°C for 45 min. Approximately 100 µl of this culture was then streaked out on a pre-warmed LB plate containing the appropriate antibiotic. Plates were incubated at 37°C for 18 to 24 hours until single colonies became visible.

4.1.1.4.4. Introduction of plasmid DNA by electroporation

The half of a ligation preparation or 10-100 ng of plasmid DNA in a volume of 5 µl were transferred to the bottom of a pre-chilled electroporation cuvette. Forty µl of freshly thawed competent cells were added. DNA and cells were thoroughly mixed by tapping the cuvette and incubated for 1 min on ice. The cuvette was then placed in the sample chamber and the electrical pulse was applied. Electroporator settings for cuvettes with 2 mm electrode distance was 2.5 mV, 25 µF and 100 Ω.

After electroporation, 1 ml of LB medium was rapidly added to the electroporated sample and incubated at 37°C under constant shaking at 250 rpm for at least 30 minutes. Approximately 100 µl of this culture was then streaked out on a pre-warmed LB plate containing the appropriate antibiotic. Plate were incubated at 37°C for 18 to 24 hours until single colonies became visible.

4.1.2. DNA preparation and manipulation

4.1.2.1. Isolation of plasmid DNA from bacterial cultures

4.1.2.1.1. Minipreps of plasmid DNA: alkaline lysis miniprep

Buffer P1	Buffer P2	Buffer P3
50 mM Tris-HCl	200 mM NaOH	3 mM potassium acetate
10 mM EDTA	1 % SDS	
100µg/ml Rnase A		

RNase stock solution

10 mM Tris HCl (pH 7.5)

15 mM EDTA

10 mg/ml RNase A

For preparation of small quantities of plasmid DNA, i.e. for analytical purposes, the alkaline lysis method was used. Five ml of sterile LB medium with the appropriate selective antibiotic were inoculated with one colony of the plasmid containing bacteria and grown overnight under moderate shaking (250 rpm) at 37°C. The cells were then harvested by centrifugation at 6000 x g for 5 min. The supernatant was discarded and the pellet was suspended in 200 µl of buffer P1. Thereafter, 200 µl of buffer P2 were added. The tube was thoroughly mixed by inverting and incubated for 5 min at RT. After the addition of 200 µl of buffer P3 and a further incubation of 5 min on ice, the tubes were centrifuged at 20000 x g and 4°C for 15 min in order to pellet chromosomal DNA, cell debris and bacterial proteins. The plasmid DNA contained in the clear supernatant was then precipitated by addition of 1/10 volume of 3M potassium acetat (pH 4.8) and 2.5 volumes of 96% ethanol. The samples were then incubated at -20°C for at least 30 min and then centrifuged at 15000 rpm for 30 min at 4°C. Pellets were washed twice in 70% ethanol, air-dried and resuspended in 50 µl of sterile water.

4.1.2.1.2. Large scale preparation of plasmid DNA: alkaline lysis protocol followed by anion exchange chromatography

The basis for this protocol is also an alkaline lysis of the plasmid containing bacterial culture. The plasmid DNA is purified by binding to an anion exchange resin under appropriate pH and low-salt conditions. This procedure was usually performed with the QIAGEN Plasmid Midi Kit®.

Fifty ml of sterile LB media containing the appropriate selective antibiotic were inoculated with a colony from a solid culture or with bacteria from a glycerol stock and grown overnight at constant shaking (250 rpm) at 37°C until an OD₆₀₀ of 1-1.5 was reached. Cells were then harvested by centrifugation at 6000 x g for 10 min and 4°C. Supernatant was taken off completely and the pellet was resuspended in 4 ml of buffer P1. Buffer P2 was then added and the sample was thoroughly mixed by inverting the tube. After a 5 min incubation at RT, 4 ml of solution 3 was added, followed by a further incubation step of 5 min on ice. The samples were then centrifuged at 20000 x g for 15 min and 4°C. Whenever the supernatant was not clear, the centrifugation step was repeated under the same conditions. The clear

supernatant was then applied to the previously equilibrated anion exchange columns. The columns were then washed twice with buffer QC. After the washing steps, plasmid DNA was eluted with 5 ml of buffer QF. Eluted plasmid DNA was precipitated by addition of 0.7 volumes of isopropanol and centrifuged at 15000 x g for 30 min at 4°C. Pellets were washed twice with 70% ethanol, air dried and finally resuspended in an appropriate volume of either sterile water or 10mM Tris-HCl (pH 7.5).

4.1.2.2. Preparation and analysis of plasmid DNA

4.1.2.2.1. Clean-up of DNA by phenol extraction

Nucleic acids may be separated from contaminating proteins by a phenol/chloroform extraction. Nucleic acids in aqueous solutions are mixed with the identical volume of Phenol/Chloroform (saturated with 0.1M Tris-HCl pH 8.0) and vigorously vortexed. The organic and aqueous phases are separated by spinning the sample for 5 minutes at maximum speed at RT in a table top centrifuge. The proteins remain in the organic phase. The aqueous phase is carefully removed with a micropipette. If desired, a further extraction step with chloroform can be performed in order to remove small quantities of remaining phenol. The DNA in the aqueous phase is then precipitated with ethanol.

4.1.2.2.2. Ethanol precipitation of DNA

For purification and concentration, DNA can be precipitated by addition of salt and 100% of ice cold ethanol. Currently used salt solutions for this purpose are potassium acetate at a final concentration of 0.25M or ammonium acetate at a final concentration of 0.3M. After addition of the salt solution to the aqueous DNA solution, 2.5 volumes of 100% ethanol were added. If small DNA quantities were to be precipitated, the sample was incubated for 30 min at -20°C. Finally, the DNA was pelleted by centrifugation at maximal speed and 4°C for 30 min. The pellet is washed twice with 70% ethanol and resuspended in an appropriate volume of sterile water or 10mM Tris-HCl (pH 7.5).

Alternatively, isopropanol can be used instead of ethanol. In this case, 0.7 x the volume of the DNA solution was added. Since some salts were less soluble in isopropanol than in ethanol and precipitated along with the DNA, care was taken to remove them by washing with 70% ethanol.

4.1.2.2.3. Determination of nucleic acid concentration

The concentration of nucleic acids (DNA and RNA) was determined by the photometric measurement of the absorption at 280 nm. An absorption value of 1 corresponds to 50µg/ml of double stranded DNA and 40 µg/ml of RNA. The purity of the solution can be determined by concurrent measurement of the absorption at 260 nm. Pure DNA solutions are characterized by a Abs₂₆₀/Abs₂₈₀ ratio between 1.8 and 2.0. The characteristic Abs₂₆₀/Abs₂₈₀ ratio of pure RNA solutions is between 1.9 and 2.1.

4.1.2.2.4. Separation of DNA fragments on agarose gels by electrophoresis

10 x TBE buffer	6 x loading buffer
0.9 M Tris-HCl	40 % saccharose
0.9 M boric acid	0.2 % bromphenol blue
50 mM EDTA	

Analytical and preparative separation of DNA fragments were done by agarose gel electrophoresis. In function of the size of the DNA fragment to be separated, 0.8 – 2% agarose in 1x TBE was used. Ethidiumbromide was added to the gels at a final concentration of 0.5 µg/ml for subsequent detection of DNA fragments under UV light (366nm).

Samples were mixed with 1/6 volume of loading buffer. The voltage settings were chosen in function of the electrode distances (6-10 V/cm) and were comprised between 80 and 180V. The separated and stained DNA bands were visualized under UV light and photographed.

4.1.2.2.5 Extraction of DNA fragments from agarose gels

Extraction of DNA fragments from preparative agarose gels was done by means of the QIAEX[®] Kit from Qiagen according to the protocol provided by the manufacturer. Briefly, the target band of DNA was cut out mechanically from the agarose gel and transferred to an 2 ml Eppendorf[®] tube. The agarose gel was then solubilized by addition of the appropriate volume of buffer QX1 and adsorbed to an appropriate volume of silica-gel particles added to the sample. Silica-gel particles were pelleted by centrifugation at maximum speed for 30 seconds and subjected to 3 further washing steps with buffer QX 1 and buffer PE. Finally, DNA was eluted by addition of an appropriate volume (usually 20µl) of 10mM Tris-HCl (pH 8.5).

4.1.2.3. Enzymatic manipulation of plasmid DNA

4.1.2.3.1. Digestion of DNA with restriction endonucleases

Restriction endonuclease cleavage was done by incubating the DNA with the desired restriction endonuclease under the conditions recommended by the manufacturer. As a general rule, 1 unit of restriction endonuclease was used per μg of plasmid DNA and restriction site present in the plasmid. The volume of restriction endonuclease added to the reaction mix should be inferior to 1/10 of the total reaction volume in order to prevent exceedingly high glycerol concentrations in the reaction mix. The sample was then incubated for at least 1 hour at the reaction temperature recommended by the manufacturer. Complete digestion was verified by agarose gel analysis of an aliquot of the reaction mix. The reaction was then stopped by heating the samples to 65-70°C. Digested plasmid DNA was then purified by phenol/chloroform extraction and subsequent ethanol precipitation. The pellet was resuspended in an appropriate volume of sterile water.

4.1.2.3.2 Dephosphorylation of plasmid DNA with Calf Intestine Phosphatase

In order to prevent self-ligation of vector termini, 5'-ends of digested vectors were dephosphorylated by incubation with CIP. After restriction endonuclease cleavage, 1 unit of CIP per μg plasmid DNA was added directly to the reaction mix. After a incubation time of 30 min at 37°C, the reaction mix was heated at 70°C for 10 min in order to inactivate the CIP. Digested and dephosphorlated plasmid DNA was then purified by phenol/chloroform extraction and subsequent ethanol precipitation. The pellet was resuspended in an appropriate volume of sterile water.

4.1.2.3.3. Fill-in of 5'-protruding ends with Klenow Polymerase

When ligation of DNA fragments cleaved with incompatible restriction endonucleases was required, the 5'-protruding ends of the DNA fragment were converted to blunt ends by a fill-in reaction with Klenow fragment. In a reaction volume of 20 – 100 μl , 0.1 – 4 μg of cleaved plasmid DNA were incubated with 1 x Klenow-buffer as provided by the manufacturer, dNTPs with a final concentration of 50 μM each and 1-5 units of Klenow fragment at 30°C for 15 min. The sample was then heated to 75°C for 10 min in order to heat-inactivate the Klenow fragment. DNA fragments were purified by phenol/chloroform extraction and subsequent ethanol precipitation. The pellet was resuspended in an appropriate volume of sterile water.

4.1.2.3.4. Removal of 3' protruding ends with T4-DNA-polymerase

When ligation of DNA fragments cleaved with incompatible restriction endonucleases was required, the 3'-protruding ends of the DNA fragment were removed by the strong 3'→5' exonuclease activity of the T4 DNA polymerase in order to obtain blunt ends. In a reaction volume of 20 µl, up to 5 µg of previously cleaved plasmid DNA were incubated in 1 x T4-polymerase reaction buffer as recommended by the manufacturer with a final concentration of 200 µM each dNTP and 1 unit of T4 DNA polymerase per µg of plasmid DNA for 20 min at 11°C. Subsequently, the reaction was stopped by heat inactivation at 75°C for 10 minutes. DNA fragments were then purified by phenol/chloroform extraction and subsequent ethanol precipitation. The pellet was resuspended in an appropriate volume of sterile water.

4.1.2.3.5. Ligation of DNA fragments

Ligation was performed using T4 Ligase to catalyse the formation of phosphodiester bonds between juxtaposed 5'-phosphate and a 3'-hydroxyl termini in duplex DNA. The specific reaction conditions chosen were dependent on the characteristics of the ends of the DNA fragments. In general, ligation was performed overnight at 14°C. However, when compatible overlapping ends were to be ligated, incubation time was 2 hours at RT. When blunt end ligation was to be performed, vector was dephosphorylated in order to prevent self-ligation and the insert was added in excess. After ligation and before electroporation, salt was removed by ethanol precipitation and two washing steps with 70% ethanol. Transformation was always performed the same day.

4.1.2.4. Isolation and manipulation of genomic DNA

Lysis buffer pH 8.5

100mM Tris-HCl pH 8.5
5 mM EDTA pH 8.0
200mM NaCl
0.2 % SDS

Isolation of genomic DNA for genotyping was done from tail tissue of 4 week old mice pups. Five hundred µl of lysis buffer with 20 µl of proteinase K (10mg/ml) were added per mouse tail and incubated at 55°C overnight. Probes were then centrifuged at 20000 x g and RT for 5 min. Four hundred µl of the supernatant were transferred to a new tube. After addition of 400µl of isopropanol, a white DNA precipitate becomes visible. Genomic DNA was pelleted by centrifugation at 20000 x g at RT for 5 min and washed twice with 70% ethanol. The pellet was then air-dried and dissolved in 100 µl of TE-buffer. Samples were stored at 4°C.

4.1.2.5. DNA sequencing with the chain termination method of Sanger

TBE long run buffer 10x (1l)

1,34 M	Tris-HCl
0.45 M	boric acid
25 mM	EDTA
Water ad 1l	

Sequencing of plasmid DNA was done with the “Thermo Sequenase cycle Dye primer Sequencing Kit” commercialised by Amersham/USB. The protocol is based on a PCR reaction with a fluorescence labelled primer and under addition of 2',3'-dideoxynucleotide triphosphates in order to obtain random chain termination. The fluorescence labelled reaction products were then separated by vertical gel electrophoresis and detected by the laser system of the LICOR system.

Sequencing reactions were run in small plastic tube compatible with thermal cycling. Per kb of plasmid, approximately 100 ng of plasmid DNA were used per reaction. DNA, 2 pmol of fluorescent labelled primer and 1.4 µl of DMSO and an appropriate volume of H₂O were prepared as a master reaction mix in a final volume of 21µl. 1.5 µl of the termination mix A, C, G, and T containing the respective 2',3'-dideoxynucleotide triphosphates were transferred to each of the tubes labelled A, C, G, and T, mixed with 4.5 µl of the previously prepared master mix and overlaid with mineral oil. PCR conditions used for the sequencing reaction are shown in **Table 3**.

Step	Duration	Temperature	Cycling
Initial Denaturation	2'	95°C	
Denaturation	15''	95°C	
Annealing	15''	60°C	30x
Polymerisation	30''	70°C	
Final Denaturation	15''	95°C	

Table 3: PCR parameters used in sequencing reactions with the “Thermo Sequenase cycle Dye primer Sequencing Kit”

Separation and analysis of the fluorescence labelled PCR products were done by vertical electrophoresis in a denaturing polyacrylamid gel. The length of the gel was depended on the length of the DNA fragment to be sequenced. The composition of a 33, 41 and 66cm gel is shown in **Table 4**. Immediately prior to pouring, 400µl of APS and 40 µl of TEMED are added to the gel mix.

After the termination of the sequencing reaction, 2 µl of loading buffer were added per sample. The samples were then loaded onto the polyacrylamid gel and separated by vertical

gel electrophoresis in the LICOR system. Fluorescence labelled PCR products were detected contemporaneously by the laser of the LICOR system.

Gel Length	66 cm plates	33 or 41 cm plates
Spacer thickness	0.25 cm	0.25 cm
Gel composition	4% Long Ranger 7M Urea/1.2 x TBE	6% Long Ranger 7M Urea/1.2 x TBE
Urea	25.2 g	25.2 g
Long Ranger 50% Gel Solution	4.8 ml	7.2 ml
10 x TBE	7.2 ml	7.2 ml
dd water	fill to 60 ml	fill to 60 ml

Table 4: Composition of the polyacrylamid gel mix for the LICOR system

4.1.3. RNA preparation and manipulation

4.1.3.1. Isolation of RNA from primary cells and cell lines

RNA isolation from primary cells or cultured cell lines was done either by using the selective binding of RNA to a silica-based membrane (“Rneasy Mini[®]” or “Rneasy Micro[®]” Kit from Qiagen) or using a phenol/chloroform extraction with consecutive precipitation of RNA (Trizol[®]).

4.1.3.1.1. Isolation of RNA with Trizol

Approximately $1-5 \times 10^6$ primary cells or cells from established cell lines were pelleted at $300 \times g$ and $4^\circ C$ for 5 minutes. The supernatant was taken off completely. Cells in the pellet were lysed by addition of 1 ml of TRIZOL reagent. Homogenized samples were incubated for 5 min at room temperature to allow for complete disruption of nucleoprotein complexes. Now, 0.2 ml chloroform per ml TRIZOL reagent were added, the tube was shaken vigorously for at least 15 seconds and then centrifuged at $12000 \times g$ at $4^\circ C$ for 15 min. The aqueous phase was transferred to a new tube and RNA was precipitated by addition of 0.5 ml isopropyl alcohol per ml of TRIZOL reagent initially used. Samples were incubated at RT for 10 min and centrifuged at $12000 \times g$ at $4^\circ C$ for 15 min. The pelleted RNA was washed with 75% ethanol and pelleted by centrifugation at $7500 \times g$ and $4^\circ C$ for 5 min. After washing, the supernatant was taken off and the RNA was air-dried briefly and resuspended in an appropriate volume of RNase free water. A small aliquot was put aside for quality assessment and concentration measurement, the remaining RNA was stored at $-80^\circ C$ until further use.

4.1.3.1.2. Isolation of RNA with the RNeasy Kit

RNA was extracted following the RNeasy protocol provided by the manufacturer and using exclusively the reagents included in the kit. Briefly, approximately $1-5 \times 10^6$ primary cells or cells from established cell lines were pelleted at $300 \times g$ and 4°C for 5 minutes. The supernatant was taken off completely. Cells in the pellet were lysed by addition of $350 \mu\text{l}$ of RLT buffer. Samples were then homogenized by passing them 10 times through a 20-gauge needle. After homogenisation, 1 volume of 75% ethanol was added to the sample which was subsequently transferred to the RNeasy spin column. After centrifugation at $8500 \times g$ for 15 seconds, the flowthrough was discarded and the RNA on the silica-based membrane was washed with $350 \mu\text{l}$ of buffer RW1. After this washing step, on-column DNase I digestion was performed in order to remove remaining traces of DNA. For DNase I digestion, $80 \mu\text{l}$ of DNase I solution was transferred onto the silica-based membrane of the RNeasy column and incubated for 15 min at RT. Columns were then washed with another $350 \mu\text{l}$ of RW1 buffer, followed by two washing steps with $500 \mu\text{l}$ RPE buffer each with centrifugation parameters as described above. RNeasy columns were then dried by a further centrifugation step at full speed for 1 min. Afterwards, RNA was eluted by addition of an appropriate volume of RNase-free water ($20-50 \mu\text{l}$) and centrifugation at $8500 \times g$ for 1 min. A small aliquot of RNA was put aside for quality assessment and concentration measurement, the remaining RNA was stored at -80°C until further use.

4.1.3.2. Quality assessment and quantification of RNA

Quality and concentration of all RNA samples were assessed using the Agilent RNA 6000 Nano Kit[®] or the Agilent RNA 6000 Picco Kit[®]. Only RNA samples with a RNA integrity number superior to 9 have been used for further experiments.

4.1.3.3. Reverse transcription

Complementary DNA was generated from total RNA by reverse transcription. One to $4 \mu\text{g}$ of RNA in a volume of $6 \mu\text{l}$ were transferred to an Eppendorf[®] tube and mixed with $2 \mu\text{l}$ of random hexamers ($0.5 \mu\text{g}/\text{ml}$). Samples were heated to 70°C for 10 min, incubated on ice for 1 min and finally incubated at RT for further 10 min. In another Eppendorf[®] tube, a master mix containing the following components was prepared (per sample): $2 \mu\text{l}$ of DTT (100mM), 40 units of RNAsin, $1.6 \mu\text{l}$ of dNTP mix (12.5mM each), $2 \mu\text{l}$ of Superscript T II polymerase, $4 \mu\text{l}$ of $5\times$ RT buffer and dd water ad $12 \mu\text{l}$. Twelve μl of the master mix were then added to the tube containing the RNA with annealed random primers and incubated for 10 min at RT

followed by an incubation period of 1 hour at 40°C. Reverse transcriptase was inactivated by a 5 min incubation at 95°C. After another 5 min incubation on ice, RNA was precipitated by addition of 55 µl H₂O, 0.5 volumes of 7.5M ammonium acetate and 2.5 volumes of 100% ethanol. The efficiency of the precipitation was increased by the addition of 0.5 ml linear acrylamid carrier. Samples were centrifuged at 20000 x g for 30 min at RT. The pellet was washed twice with 80% ethanol, air-dried, resuspended in an appropriate volume (usually 30 µl) of water and stored at -80°C until further use.

4.1.4. Polymerase chain reaction

PCR was used to amplify specific double stranded DNA sequences, to genotype the S1P₄^{-/-} mice and to introduce a HA-tag at the 5' end of the murine slp₁ gene. Primers for amplification of murine S1P₁ harbouring a 5' HA-tag were designed manually by comparison with the published cDNA sequence (accession number NM_007901). Primers for genotyping were generated using Primer3 software.

The quantity of template DNA was variable: 500-1000 ng for genomic DNA and 1-100 pg for plasmid DNA. In a 50 µl reaction volume, template DNA was mixed with 100 pmol of each primer, 5µl of 10x Optizyme[®] reaction buffer, desoxynucleotides at a final concentration of 100-200 µM each, 1.5 µl of MgCl₂ (1.5mM), 10µl of Optizyme[®] Enhancer and 1 µl of Combizyme DNA polymerase. If required, reaction volumes were up-scaled to 100µl or down-scaled to 25 µl for certain applications. Optimal MgCl₂ were titrated for each primer pair. Similarly, optimal annealing temperatures were determined by temperature gradient PCR starting at the theoretical annealing temperature which was calculated based on the number of each nucleotides present in the primer sequence:

$$T_{anneal} (^{\circ}C) = (4 \times (\text{number of } G \text{ and } C)) + (2 \times (\text{number of } A \text{ and } T))$$

When the primer contained unpaired sequences not present in the template, the annealing temperature of the initial 5 amplification cycles was adapted to the theoretical value calculated at the basis of the overlapping sequences only. In the case of unsatisfactory amplification results, 5% DMSO was added to the reaction mix in order to facilitate annealing of the template and the primer.

The typical PCR protocol consisted of: Step 1) an initial denaturation step for 2 min at 95°C, followed by Step 2: a shorter heat denaturation step of 40 seconds at 95°C; Step 3: annealing of primer and template at the annealing temperature calculated as shown above and Step 4: polymerisation at 72°C. Step 2 to 4 were repeated 30-35 times, depending on the amplification efficiency of the specific reaction conditions. The polymerisation step of the last

amplification cycle was extended to 2 minutes. An aliquot of the PCR product was used for analysis by agarose gel electrophoresis. The remaining PCR product was purified by phenol/chloroform extraction, ethanol precipitated and subcloned in the pGEMT cloning system for sequencing.

4.1.5. Quantitative polymerase chain reaction

Real-time quantitative PCR was conducted to quantify the levels of S1P₁ and S1P₄ mRNA expression. Starting material was single stranded cDNA prepared as described in 4.1.3.3.. The reaction was carried out in a reaction volume of 20 μ l as described below:

Template cDNA	25-500ng	2	μ l
dNTP mix	2 mM each	2	μ l
Ex Taq PCR buffer	10 x	2	μ l
Primer pair	10 μ M	2	μ l
MgCL ₂	50 μ M	variable	
BSA	5 mg/ml	1	μ l
Ex Taq DNA polymerase	5 U/ μ l	0.2	μ l

All PCR reactions were carried out with a LightCycler® (Roche Diagnostics, Germany) according to the manufacturer's instructions. Samples were initially denatured for 60 s at 95°C, followed by a denaturation step at 95°C for 5 s, a annealing step at variable temperatures depending on the primer pair used (**table 5**) for 15 s, and a polymerisation step at 72°C for 15 s. Depending on the primers used, step 2 to 4 were repeated 30 –35 times. At the end of the final cycle, PCR products were annealed at 65°C for 15 s, then heated slowly to 95°C at 0.1°C/s under continuous fluorescence measurement to determine the melting curves of PCR products, followed by final cooling.

Target gene	Size of expected fragment	MgCl ₂ concentration	T _{ann}	T _{melt}
GAPDH	452 bp	4.0 mM	62 °C	89.7 °C
S1P ₁	173 bp	4.0 mM	60 °C	87.6 °C
S1P ₄	214 bp	3.0 mM	62 °C	88.5 °C

Table 5: Specific reaction parameters for semiquantitative Lightcycler PCRs

T_{ann}: Annealing temperature; T_{melt}: melting temperature

Quantification was performed by online monitoring fluorescence and identification of the exact time point at which the logarithmic linear phase could be distinguished from the background signal (crossing point). The relative amount of cDNA was normalized to the expression level of the housekeeping gene β 2-microglobuline. Copy numbers for all samples

were calculated from a virtual standard curve which was derived by plotting the known input concentrations of a pertinent PCR product (serial dilutions) on a logarithmic scale to the PCR-cycle number reached at the crossing point. The relative expression of a particular target between samples was determined by employing Microsoft Excel. The data of two or three independent analyses for each target were averaged and presented as normalized mean expression ratios.

4.1.6. siRNA related techniques

4.1.6.1. Selection of appropriate target sequences for shRNA

Suitable target sequences for shRNA mediated knock-down of the murine S1P₁ gene were selected using the Ambion siRNA Converter. From the proposed candidate sequences, four sequences were chosen manually according to the following criteria: GC content of larger than 50%, repartition of the five target sequences along the whole mRNA sequence but not within 100 base pairs from start and stop codon; absence of 4 or more consecutive Ts in the chosen target sequence. Furthermore, a blast search was performed to exclude homologies with other known genes. After identification of appropriate potential target sequences, these were used to design hairpin shRNA oligonucleotides in which the antisense strand and sense strand of the siRNA were joined by a loop sequence consisting of the TTCAAGAGA sequence published by Brummelkamp et al.¹⁹⁶. The ends of the designed oligonucleotides are designed to create compatible overhangs for cloning in the restriction sites of the shRNA vectors.

4.1.6.2. Cloning of shRNA oligonucleotides into the shRNA vectors

Annealing buffer 10x

100	mM	Tris-HCl pH 7.4
1	M	NaCl

The following components were mixed in a final reaction volume of 50 µl: oligonucleotides 1 and 2 at a final concentration of 100 nmol/ml, 5 µl of annealing buffer 10x, water ad 50 µl. The following incubations were performed in a PCR machine: 4 min at 90°C, followed by 10 min at 70°C, followed by incubation at slowly decreasing temperatures at rate of 0.1°C/min down to 4°C and a final incubation step at 4°C for 10 min. The annealed oligonucleotides are then diluted 1:4000 in annealing buffer. The shRNA vector was cleaved by the appropriate restriction endonucleases and gel purified. One µl of the diluted annealed

oligonucleotides was used for ligation with 30-50 ng of the gel purified shRNA vector in a final volume of 10 μ l. Ligation was done overnight at 16°C.

4.1.7. Lentiviral techniques

All experimental procedure involving manipulation of lentiviral vectors were performed under BL 2 conditions in order to limit the hazardous potential of these vectors.

4.1.7.1. Large scale virus production

Production of lentiviral shRNA vectors was performed in 100 mm or 150 mm cell culture dishes. The day before transfection, 4.5×10^6 (100 mm dish) or 12×10^6 293T cells were plated to the cell culture dish and incubated at 37°C and 5% CO₂ overnight. The next day, lentiviral transfer plasmids, envelope and packaging plasmids were co-transfected into the 293T cells by calcium phosphate transfection. The quantities of lentiviral plasmid DNA used for transfection are shown in **Table 6**.

	100 mm cell culture dish	150 mm cell culture dish
Transfer plasmid	7 μ g	20 μ g
Packaging plasmid: psPAX ₂	5 μ g	15 μ g
Envelope plasmid: pMD2G	2 μ g	6 μ g

Table 6: Amount of plasmid DNA used for transient transfection of 293T cells

Four hours after Calcium phosphate transfection, media was taken off, cells were washed twice with warm PBS and DMEM media containing 3% FCS. Sodium butyrate at a final concentration of 10mM was added to the cells in order to stimulate lentiviral production. After 12 hours of further incubation, the sodium butyrate containing media was removed, cells were washed twice with warm PBS, and 8 ml (100 mm dishes) or 20 ml (15 m dishes) of fresh DMEM with 3% FCS was added. Transfected cell were returned to the incubator for further 24 hours. Forty and 52 hours after the initial transfection, the cell culture supernatant containing the viral particles was harvested and centrifuged at 900 x g for 7 min at 4°C. The supernatant was then passed through a 0.45 μ m filter. Virus particles were either further concentrated by ultracentrifugation or stored at -80°C until further use.

After the virus has been harvested, transfection efficiency was monitored by FACS analysis of transfected 293 T producer cells expressing GFP. Transfection efficiencies of >90% were characteristic of efficient virus production.

4.1.7.2. Concentration of lentiviral particles by ultracentrifugation

Virus particles were further concentrated by ultracentrifugation in order to obtain high lentiviral titres.

Thirty ml of viral supernatant were transferred to a Beckman conical tube and spun at 26000 rpm for 2 hours at 4°C in a Beckman SW28 rotor. After the spin, supernatant was discarded and the virus was resuspended in an appropriate volume (usually 300 ml) of serum-free medium. Resuspension was done at 4°C for 2 hours under constant shaking.

4.1.7.3. Determination of lentiviral titers

Titration of viral supernatants was performed in 6-well plates. Twenty four hours prior to viral transfection, 293T cells at a density of 1×10^5 cells were plated in each well of a 6-well plate. Cells were incubated at 37°C with 5% CO₂ overnight. The following day, ten-fold serial dilutions of each viral stock in 1 ml serum-free media with polybrene at a final concentration of 8 µg/ml were prepared. For non-concentrated vector, the initial dilution was 10^{-1} , for concentrated vector it was 10^{-3} . At least 3 dilution steps were done for each viral stock. Cells were infected by addition of 1 ml diluted lentiviral vectors and incubated at 37°C with 5% CO₂ overnight. A negative control consisting of DMEM with polybrene at a final concentration of 8µg/ml was included in each experiment. After 12 hours, 1 ml of DMEM with 10% FCS was added to each well. At day 4 after lentiviral transduction, cells were harvested and the percentage of transduced GFP expressing cells was determined by FACS analysis. Viral titer was calculated as follows:

$$\text{Viral titer [Infectious units (IU)/ml]} = \frac{\text{GFP}^+ \text{ cells} \times \text{cell number}_{\text{Day2}} \times \text{Dilution of virus stock}}{\text{volume of diluted stock [ml]}}$$

4.1.7.4. Infection of eukaryotic cells with lentiviral vectors

4.1.7.4.1. Infection of adherent cells with lentiviral vectors

Adherent cells were transfected at a MOI of 1 to 5, depending on the target cell line. Eighteen to 24 hours prior to infection, $1.5 - 4 \times 10^5$ adherent cells were plated per well of a 6-well plate and incubated at 37°C with 5% CO₂ overnight. The next day, cell culture media was removed and virus supernatant at a MOI of 1-5 diluted in the appropriate cell culture medium containing polybrene at a final concentration of 8µg/ml was added on the cells. After 24 hours, virus particle containing media was taken off, cells were washed twice with warm

PBS and incubated with fresh cell culture medium supplemented with FCS and P/S at 37°C with 5n% CO₂ for three further days. Infection efficiency was then assessed by FACS analysis for GFP⁺ cells.

4.1.7.4.2. Infection of nonadherent cells with lentiviral vectors

Infection of nonadherent cells was performed by spinoculation at an MOI of 5-10. At the day of infection, 5-10 x 10⁶ nonadherent cells were diluted in 2 ml of appropriate serum free cell culture medium containing virus particles at an MOI of 5-10 and polybrene at a final concentration of 8 µg/ml. Cells were then centrifuged for 2 hr at 2000 x g at RT to perform spinoculation. After centrifugation, supernatant was taken off and replaced by 2 ml of fresh medium with FCS and P/S. Cells were incubated for further 3 days in cell culture flasks of an appropriate size. Infection efficiency was then assessed by FACS analysis for GFP⁺ cells.

4.1.8. Protein isolation, manipulation and analysis

4.1.8.1. Protein isolation from cell lines and primary cells

Lysis Buffer

	PBS pH 7.2
1 %	Triton X-100
5 mM	EDTA
1 mM	PMSF

An appropriate number of cultured cells or primary cells (1-5 x 10⁷ cells) were lysed by addition of 500 – 1000 µl of lysis buffer. Lysis was performed for 45 min at 4°C under slow overhead rotation. Subsequently, cellular debris were pelleted by centrifugation at 20000 x g for 10 min. The supernatant containing the proteins was transferred to a pre-chilled Eppendorf[®] tube and stored at –80°C until further use. A small aliquot was taken for concentration measurement.

4.1.8.2. Determination of protein concentration using the BCA method

Protein concentration was determined using the BCA assay. The method is based on the reaction of Cu²⁺ to Cu¹⁺ by protein in an alkaline medium (biuret reaction). The cuprous ion chalets with two molecules of BCA resulting in a colorimetric reaction (purple). This complex exhibits a strong absorbance at 562 nm that is nearly linear with increasing protein concentrations over a broad working range (20-2000 µg/ml).

Ten µl of the unknown protein sample were incubated with 100 µl of a 50:1 mixture of solution A and B in duplicate and incubated for 30 min at 37°C. Standard dilutions from 125-

2000 µg/ml BSA in duplicate were included in 96 well plate. Absorption was then measured at a wave length of 562 nm and protein concentrations in the unknown samples were determined according to the values of the standard curve.

4.1.8.3. Protein separation by denaturing discontinuous gel electrophoresis

Separation gel 12%

1,5 mM Tris-HCl pH8.8:	1.5 ml
30% acrylamide:	2 ml
dd water:	2.5 ml
10% ammonium persulfate:	50 µl
TEMED:	10 µl

Stacking gel 5%

1,5 mM Tris-HCl pH6.8:	900 µl
30% acrylamide:	600 µl
dd water:	2.5 ml
10% ammonium persulfate:	50 µl
TEMED:	1 µl

Laemmli buffer 5x (1l)

15.1 g	Tris-HCl
72 g	glycine
5 g	SDS

Sample buffer (100ml)

40 ml	glycerine
2.5 g	Tris HCl pH adjusted to 6.8
4 ml	β-mercaptoethanol
2 mg	bromophenol blue
4 g	SDS
Aqua ad 100 ml	

Proteins can be separated according to their size by one-dimensional gel-electrophoresis under denaturing conditions (Laemmli gel method). The vertical polyacrylamide gel consists of an upper stacking gel that serves to focus proteins and a lower separation gel in which the separation of proteins according to their size occurs.

The polyacrylamide gel-electrophoresis was performed in a Bio-Rad vertical minigel system. After assembly of the glass plates and the spacers, the separation gel was poured into the lower $\frac{3}{4}$ of the mounted glass plates and immediately overlaid by 100% ethanol. After polymerisation of the separation gel, the ethanol was removed, the stacking gel was poured and the comb inserted.

The protein sample (1-10 mg of protein) was prepared by adding $\frac{1}{4}$ volume of sample buffer and subsequent heating of the sample to 40°C for 15 min. After removal of the comb, the acrylamid gel was transferred to the electrophoresis chamber and a 5 minute pre-run at 2 W for 5 minutes was started. After the pre-run, samples were loaded to the gel and run at 7 W as long as full separation of the pre-stained marker had occurred.

4.1.8.4. Protein transfer to membranes (Western blot) with a tank transfer system

Blotting buffer (II)

3.03 g	Tis-HCl
14.4 g	Glycine
20 %	Methanol

After protein separation in the polyacrylamid gel, proteins were transferred to a nitrocellulose membrane by blotting in a tank (Bio-Rad mini-tank blot) of buffer with the gel in a vertical orientation.

A nitrocellulose membrane was submerged into blotting buffer and applied to the gel surface. On both sides of the gel/membrane sandwich, a pre-wetted sheet of Whatman paper and a sponge was applied. The whole montage was then installed into the Bio-Rad mini-tank system. Blotting was performed at 300 mA for 105 min. Successful transfer of proteins was verified by reversible Ponceau staining of membrane bound proteins.

4.1.8.5. Immunodetection of specific proteins

After blotting, specific proteins on the nitrocellulose membrane were detected by incubation with specific antibodies. For prevention of non-specific antibody binding, membranes were blocked with 2% BSA in TBS-T or 5% milk powder in TBS-T (depending on the antigen to be detected) for 30 min (see **Table 7**). Membranes were then incubated overnight with the primary Ab at the appropriate dilution (see **Table 7**) at 4°C and under constant shaking.

Antigen	Blocking reagent	Primary Ab	Dilution primary Ab	Secondary Ab	Dilution secondary Ab
HA-tag	5% milk powder	Rat anti-HA	1:4000	Goat anti-rat HRP labelled	1:15000
S1P ₁	2% BSA	rabbit polyclonal anti-S1P ₁	1:2000	goat anti-rabbit HRP labelled	1:10000
S1P ₄	2% BSA	rabbit polyclonal anti-S1P ₄	1:2000	goat anti-rabbit HRP labelled	1:10000

Table 7: Blocking reagents, primary and secondary Ab used for immunodetection of S1P receptors on western blots

After at least 3 washing steps in TBS-T, membranes were incubated with the appropriate HRP labelled secondary Ab for 1 hour at RT. After at least 3 further washing steps in TBS-T, proteins were visualized with luminescent substrates using the ECL-kit from Amersham according to the recommendations of the manufacturer. Briefly, Solution A and B

were mixed in equal quantities and applied on the nitrocellulose membrane at 0,125 ml/cm². After a 1-min-incubation, membranes were removed, drained, and wrapped into clear plastic wrap. In the dark room, membranes were put onto films in a cassette. Films were exposed for an appropriate length of time, ranging from seconds to several hours.

4.2. Cell Biology Methods

4.2.1. Culture of eukaryotic cells

4.2.1.1. Cell culture conditions and media

All cell lines and primary cells that were used in the present work were cultured in an humidified 5% CO₂ incubator at 37°C. Adherent cells (293 T, NIH3T3, cos α) were cultured in DMEM supplemented with 10% FCS, 100 U/ml penicillin and 100 μ g/ml streptomycin. For certain applications, FCS content was reduced to 3%. Cells were grown to 80-90% confluency and then spitted 1/4 – 1/8. Suspension cell lines (LBRM, TG40) were cultured in RPMI 1640 medium supplemented with 10% FCS, 100 U/ml penicillin and 100 μ g/ml streptomycin. When cells reached a density of 3-5 x 10⁵ cells/ml, cells were diluted 1/5 – 1/10 in fresh culture medium. Primary lymphocytes were cultured in RPMI 1640 supplemented with RPMI 1640 medium supplemented with 10% FCS, 100 U/ml penicillin, 100 μ g/ml streptomycin and 0.1mM β -mercaptoethanol.

4.2.1.2. Splitting of adherent cell lines

When adherent cell lines reached a density of 80-90%, cells were washed with warm PBS and detached from the support by addition of enough warm trypsin/EDTA solution to cover the adhering cell layer. Cells were then detached by rinsing with warm PBS, transferred to a 50 ml falcon tube and pelleted by centrifugation at 300g for 5 min. Cells were then resuspended in warm culture medium, diluted and transferred to a new cell culture bottle.

4.2.1.3. Determination of the cell number and viability

Cells were counted in a Improved Neubauer hemacytometer. Before loading the hemacytometer, cells were mixed with an equal volume of 0.1% trypan blue. Under the microscope, cells in the four large squares were counted. Living cells could be identified by their unstained appearance, while dead cells were stained dark blue by trypan blue. The cell number was calculated according to the following formula:

$$\text{cells/ml} = \frac{\text{counted cell number}}{2} \times 10^4 \times \text{dilution}$$

4.2.1.4. Storage, freezing of eukaryotic cells, thawing and recovery of eukaryotic cells

For long term storage, cells were washed in PBS and pelleted by centrifugation at 300 x g for 5 min. The cell pellet was then resuspended in pre-chilled freezing medium at a concentration of 10^6 to 10^7 cells/ml. Cryovials were then transferred to a isopropanol-filled freezing container to guarantee for a gradual temperature drop. The freezing container was stored at -80°C overnight and cryovials were transferred to liquid nitrogen (-196°C) the following day.

When cryopreserved cells were needed for study, they were thawed rapidly, diluted in at least 10 ml of the appropriate pre-warmed medium and pelleted at 300g for 5min. The cell pellet was then resuspended in 7-15 ml of pre-warmed cell culture medium and plated into the appropriately sized cell culture flask.

4.2.2. Transfection of eukaryotic cells

4.2.2.1. Calcium phosphate method

<i>2 x HEBS</i>	<i>CaCl₂ solution</i>
280mM NaCl	2.5 mM CaCl ₂
1 mM KCl	
1 mM Na ₂ HPO ₄ x 12 H ₂ O	
10 mM Dextrose	
40 mM HEPES	
pH 7,05	

Calcium phosphate transfection was usually performed in 100 mm culture dishes, but reaction volumes can be up- or downscaled.

On the day before transfection, 4.5×10^6 cells were plated to a 100 mm culture dish and incubated overnight at 37°C and 5% CO₂. On the day of transfection, cells should be at 50-

60% confluence. In a sterile tube, 2 – 20 µg of plasmid DNA is mixed with 50 µl of 2.5mM CaCl₂, water is added to reach a final volume of 500 µl. Five hundred µl of 2 x HEBS are placed in a sterile conical 15-ml tube. A Pasteur pipette attached to a mechanical pipettor is used to bubble the 2 x HEBS while the DNA/CaCl₂ solution is added dropwise in the tube. The mixture is incubated for 10 min at RT while a fine precipitate is forming. Thereafter, the calcium phosphate/DNA solution is added dropwise on the cells while swirling the culture plate to be transfected. After a 15-24 hour incubation period, medium was taken off and cells were washed twice with PBS. Ten ml of complete medium were added and cells were further incubated for at least 2 further days before transfection efficiency was assessed by FACS or by Western blot.

4.2.2.2. Cationic lipid-mediated transfection

Liposome based techniques were used for transient transfection of adherent cells mostly in the 6-well plate format. However, cell cultures in different formats can be transfected by adapting the quantity of reagents in proportion to the relative surface area.

On the day before transfection, 2-4 x 10⁵ cells in 2 ml of complete medium were plated to each well of a 6-well plate and incubated overnight at 37°C and 5% CO₂. On the day of transfection, cells should be at 80-90% confluence. Two to 6 µg of plasmid DNA were diluted in 250 µl of OptiMEM medium. In a separate tube, 10 µl of Lipofectamine™ 2000 were diluted in 250 µl of OptiMEM. After a five minute incubation step, diluted DNA and diluted Lipofectamine™ 2000 were combined, gently mixed and incubated for further 20 minutes. Complexes were then transferred onto the cells. Cells were incubated overnight at 37°C in a 5% CO₂ incubator before culture media was changed. Cells were further incubated for at least 2 further days before transfection efficiency was assessed by FACS or by Western blot. If necessary, cells were split at day 2 after transfection.

4.2.3. Isolation of primary lymphocytes from blood and lymphatic organs

4.2.3.1. Isolation of mononuclear cells from lymphatic organs

Single cell suspensions from freshly removed organs (spleen, thymus, Peyer's patches and lymph nodes) were prepared by mechanically dissociating the tissue structure with a syringe plunger in a 60 mm cell culture dish containing 5 ml of PBS with 1% FCS. Bone marrow cells from the femur and the tibia were removed by flushing these bones with 5 ml of PBS.

Clumps were dispersed by drawing the cell suspension several times in a glass pipette. The cell suspension was then passed through a 70 µm nylon mesh to remove remaining cell clumps and fibrous material. Finally, cells were pelleted by centrifugation at 300 x g for 5 min at 4°C. Cell pellets were resuspended in an appropriate volume of PBS with 1% FCS and stored on ice until further use. If required for the later experimental procedures, cell suspensions from spleen containing high numbers of erythrocytes were subjected to a Ficoll gradient centrifugation or erythrolysis in order to remove red blood cells.

4.2.3.2. Isolation of mononuclear cells from peripheral blood

Blood was obtained by retroorbital puncture with a heparinized Pasteur pipette or by intracardiac puncture of the deeply anaesthetised animal with a heparin flushed syringe. Erythrocytes were removed by Ficoll gradient centrifugation or by lysis of erythrocytes.

4.2.3.3. Ficoll gradient

Suspensions of splenic cells were depleted of contaminating red blood cells by Ficoll gradient centrifugation. Care was taken that all materials and reagents were brought to room temperature. Spleen cell suspensions were diluted with PBS to a volume of 7 ml. On the bottom of a 15 ml conical tube, 4 ml of Ficoll solution (density: 1.077 g/ml) was deposited. Very slowly, the Ficoll solution was overlaid by the cell suspension. Subsequently, the gradient was centrifuged at 900 x g for 30 min at RT without break. Mononuclear cells localised in the interphase were harvested, washed twice in PBS, resuspended in an appropriate volume of PBS with 1% FCS and stored on ice until further use.

4.2.3.4. Erythrocyte lysis

ACK lysis buffer (1l)

8.29 g NH₄Cl
1.0 g KHCO₃
37.2 mg Na₂EDTA
Ad 1 l H₂O, pH 7.3

Alternatively, red blood cells were removed from peripheral blood and spleen cell suspensions by erythrolysis with ACK lysis buffer. Five ml of ACK lysis buffer was added per spleen or per 500 µl mouse blood. After a 5 min incubation period at RT, 9 ml of PBS were added and mononuclear cells were pelleted by centrifugation at 300 x g for 5 min at RT. After one further washing step with PBS, the cell pellet was resuspended in an appropriate volume of PBS with 1% FCS and stored on ice until further use.

4.2.4. Flow cytometry

FACS Buffer

PBS, pH 7.2 with 1% FCS

Detection of cell surface markers but also of intracellular markers was done by cell cytometry with an FACS Calibur. Usually, $5 \times 10^5 - 10^6$ cells in a volume of 100 μ l FACS buffer were used per sample. Washing steps consisted in addition of at least 200 μ l of FACS buffer and subsequent centrifugation at 300 x g for 5 min. Staining procedures were usually performed in 96 well plates, unless large quantities of cells were stained for subsequent cell sorting. In those cases, the volume of the cell suspension was up-scaled.

4.2.4.1. Detection of surface epitopes

Non-specific binding of the specific antibody was blocked by incubating the cells with anti-Fc γ III/II antibody diluted 1: 200 in PBS at RT for 20 min. After removal of the blocking Ab, the primary antibody was added in an appropriate dilution in 100 μ l FACS buffer and incubated for 20 min at RT. After 3 washing steps with at least 200 μ l of FACS buffer, cells were resuspended in an appropriate volume of FACS buffer and analysed by flow cytometry. When a unlabelled or biotinylated primary Ab was used, washing steps were followed by incubation with an appropriate secondary antibody or with streptavidine fluorochrome conjugate, respectively, for 20 min at RT, followed again by 3 washing steps and subsequent FACS analysis.

The optimised dilutions of the Ab used in this work are shown in **Table 8**.

4.2.4.2. Detection of intracellular epitopes

Detection of intracellular epitopes was performed after fixation and permeabilisation. Briefly, cells were pelleted and resuspended into an appropriate volume of freshly prepared 4% paraformaldehyde solution in PBS and incubated for 15 min on ice. Cells were then washed 3 times in at least the 4 fold volume of ice-cold PBS. Blocking was done by incubation for 20 min with anti Fc γ III/II Ab diluted 1:200 in PBS with 0.1% saponin. After removal of the blocking agent, cells were stained with the primary Ab diluted in PBS with 0.1% saponin for 20 min at RT. After 3 washing steps with PBS with 0.1% saponin and one further washing step with PBS, cell were ready for analysis by flow cytometry.

Specificity	Type	Species and Isotype	Conjugate	Dilution
anti-CD3	primary	Hamster IgG1	Biotin	1:100
anti-CD4	primary	Rat IgG2a	APC	1:100
anti-CD8	primary	Rat IgG2a	PE	1:100
anti-CD19	primary	Rat IgG2a	APC	1:200
anti-CD45R (B220)	primary	Rat IgG2a	FITC	1:200
anti-CD21	primary	Rat IgG2b	FITC	1:100
anti-CD23	primary	Rat IgG2a	PE	1:200
anti-CD25	primary	Rat IgM	FITC	1:100
anti-CD5	primary	Rat IgG2a	APC	1:100
anti-IgM	primary	Rat IgG2a	Biotin	1:200
anti-IgM	primary	Rat IgG2a	FITC	1:200

Table 8: Antibodies used for FACS staining

All shown antibodies are directed against murine epitopes.

4.2.5. Cell separation techniques

4.2.5.1. MACS

MACS Buffer

PBS, pH 7.2 with 0.5% FCS

2 mM EDTA

CD4⁺ and CD8⁺ T cells were isolated by magnetic labelling and subsequent removal of non-T cells using the negative selection kits from Miltenyi Bioscience. Briefly, Ficoll gradient purified mononuclear cells were suspended in MACS buffer (40 ml per 10⁷ cells). Ten µl of the appropriate Biotin-antibody cocktail were added and samples were incubated for 10 min at 4°C. After incubation, 30 µl of MACS buffer and 20 µl of anti-biotin MicroBeads were added per 10⁷ cells. These were incubated for further 15 min at 4°C. After thorough washing with MACS buffer, cells were resuspended in 500 µl of MACS buffer per 10⁸ total cells. Then, labelled cells were removed by loading of the cell suspension to a LS column placed in the magnetic field of a MACS separator. After appropriate washing of the columns, the unlabelled fraction in the flow-through was harvested, pelleted and resuspended in an appropriate volume of MACS buffer. An aliquot was analysed by FACS in order to determine purity. At least a 90% purity was required for further experiments.

4.2.5.2. Cell sorting by FACS

FACS sorting was performed with a FACSVantage™SE either after labelling of the target population with specific antibodies or by assessing green fluorescence due to GFP expression. Sorted cells were assessed for purity. At least 95% purity was required for further utilisation of sorted cells in subsequent experiments.

4.2.6. Enzyme-linked immunosorbent assay

Coating buffer

8.4 g NaHCO₃
3.56 g Na₂CO₃
H₂O ad 1 l

Wash buffer

PBS with 0.05 Tween 20%

Different ELISA systems were used to detect specific antibodies, soluble antigens or for antibody isotyping. In general, commercial ELISA kits have been used. Only exception was the indirect ELISA for detection of SRBC specific antibodies which was done by using freshly prepared SRBC antigen combined with the SBA Clonotyping™ system/HRP Kit from Southern Biotech.

4.2.6.1. Isotype determination by sandwich ELISA

Blocking solution

25% BSA in PBS
0.05% NaN₃

Determination of the class and subclass of murine antibodies in mouse plasma and serum was done using the Mouse MonoAB ID Kit (AP) from Zymed and the BD OptEIA™ Set Mouse IgE from BD Bioscience.

For the MonoAB ID Kit (AP), the capture EIA protocol was used. Briefly, 50 µl of diluted goat anti-mouse IgGAM antibody was added per well of a 96 well plate and incubated overnight at 4°C. Wells were then blocked with 200 µl of blocking solution at 37°C for 1 hour. Thereafter, 50 µl of appropriately diluted serum / plasma as well as serial dilutions of murine Ab solutions of known concentration were transferred to the plate and incubated at 37°C for 1 hour. After 4 washing cycles, one drop of subclass specific rabbit detection Ab was added. Blanks (1 drop of TBS pH 7.5) and negative controls (1 drop of normal rabbit serum) were included in each assay. Plates were incubated at 37°C for 1 hour and washed 4 times with TBS-Tween. Thereafter, 50 µl of diluted AP labelled anti-rabbit IgG was added and incubated for 1 hour at 37 °C. After 4 washing cycles, 100 µl of substrate solution

(contained in the kit) was added and incubated at RT for 30 min. Absorbance was then read at 405 nm in an ELISA reader. Isotype concentrations in the samples were calculated based on the standard curve obtained from the dilutions of standards.

IgE concentrations were determined using the BD OptEIA™ Set Mouse IgE from BD Bioscience. Briefly, 100 µl of diluted anti IgE capturing AB was added to a 96 well plate and incubated overnight at 4°C. After washing and blocking, 100 µl of standards and appropriately diluted samples were added and incubated at RT for 2 hours. After thorough washing, HRP labelled anti-mouse detection Ab was added and incubated for 1 hour at RT. After 7 further washing cycles, 100 µl of substrate solution consisting of tetramethylbenzidine and hydrogen peroxide were added and incubated for 30 min at RT in the dark. The reaction was then stopped with 50 µl of stop solution and absorbance was read at 450 nm and 570 nm in an ELISA reader. Target concentrations in the samples were calculated based on the standard curve of the standard dilutions.

4.2.6.2. Antibody-sandwich ELISA to detect soluble antigen

Assay diluent

PBS with 10% FCS

IL-4, IL-5 AND IFN- γ concentration was determined by sandwich ELISA. Appropriate sample dilutions were determined by initial optimisation experiments. An appropriate number of 96 well plates was coated with the capturing Ab by adding 100 µl of diluted capturing Ab solution (Dilution: 1:250). Plates were incubated overnight at 4°C. The wells were then aspirated, washed 3 times with wash buffer and blocked with assay diluent for 1 hour at RT. Again, plates were washed 3 times. Sample and standard dilutions were transferred to the wells and incubated for 2 hours at RT. After 5 washing steps, 100 µl of diluted HRP conjugated detection Ab was added and incubated for 1 hour at RT. Plates were then washed 7 times. Hundred µl of substrate solution consisting of tetramethylbenzidine and hydrogen peroxide were added and incubated for 30 min at RT in the dark. The reaction was then stopped with 50 µl of stop solution and absorbance was read at 450 nm and 570 nm in an ELISA reader. Target concentrations in the samples were calculated based on the standard curve of the standard dilutions.

4.2.6.3. Indirect ELISA for detection of specific antibodies

SRBC specific antibodies in serum of immunized mice were detected by indirect ELISA. Briefly, 100 µl of diluted soluble SRBC antigen (5µg/ml) prepared as described in paragraph 4.3.7. was transferred to each well of a 96 well plate and incubate overnight at 4°C.

After 3 washing cycles, samples were blocked with 1% BSA in PBS for 1 hour. After 3 washing cycles, a volume of 100 μ l serially diluted serum samples (1:2) were added to the wells and incubated for 1 hour at RT under moderate shaking. After 3 washing cycles, 100 μ l of diluted HRP conjugated isotype specific detection Ab was added per well and incubated at RT for 1 hour. Now, plates were washed 5 times and 100 μ l of substrate solution were added per well. After 10 and 20 min, optical density was measured at 405 nm with an ELISA reader. Since no standards were available, a semi-log graph was created in order to verify whether it was S-shaped. Then, the linear portion was identified by a log-log curve fit. Once the linear region was determined, the dilution value at OD = 0.5 was interpolated and recorded. The reported results represent the titer of the sample and are the reciprocal of the serum dilution which has a OD value of 0.5.

4.2.7. Cytospin

About $2.5-5 \times 10^5$ cells of interest were resuspended into 200 μ l of cold PBS. Pre-labelled slides were then mounted with filters and cuvettes in a metal holder. Two hundred μ l of the cell suspension were then transferred to the cuvette and spun at 500 rpm for 5 min in a Shandon cytopsin 3. Cells were immediately fixed by submersion in acetone at -20°C for 10 min. Cells were stained with May-Grünwald-Giemsa. Briefly, slides were fixed in methanol for 15 minutes and stained in May-Grünwald staining solution for 5 minutes. Slides were then placed in H₂O for 1 minute and afterwards stained in 10% Giemsa solution for 7 to 10 minutes. Slides were then washed twice in H₂O. After dehydration, slides were mounted with Entalan[®].

4.2.8. In-vitro proliferation assay

Replicate suspensions of 2×10^5 CD4⁺ and CD8⁺ T cells purified by immunomagnetic beads from spleens of S1P₄^{-/-} and wild type littermates were incubated in 0.2 ml of RPMI 1640 medium with 10% FCS, penicillin and streptomycin in 96-well plates. Some wells had been precoated with 0.2 μ g each of anti-CD3 mAb and anti-CD28 mAb to stimulate T cells through the TCR. Other wells received 2×10^5 irradiated mixed mononuclear leukocytes from spleens of C57Black/6 mice to evoke a MLR. After 48 hours, cell proliferation was measured by a non-radioactive assay using the Celltiter 96[®] Aqueous One Solution Cell Proliferation Assay from Promega. Briefly, 2 ml of the MTS solution and 100 μ l of the PMS solution both contained in the kit were mixed immediately before addition to the culture plate. Then, 40 μ l of the combined PMS/MTS solution was added to each well containing 200 μ l of cell

suspensions. Cells were then incubated for further 4 hours. During this period, the MTS tetrazolium compound is bio-reduced by living cell into a coloured formazan product. Absorbance was then read at 490 nm using an ELISA reader. Absorbance is proportional to the number of living cell in the culture well.

4.2.9. In vitro chemotaxis assay

Chemotaxis of mouse splenocytes was quantified using 12-well Transwell chambers with 5 µm pore size filters (Costar) coated with 20 µg/ml collagen type IV overnight at 4°C. Filter chambers were washed four times with 500 µl of PBS, air-dried, and filled with 100 µl of suspensions of 1×10^7 cells/ml in RPMI 1640 supplemented with 25 mM HEPES, pH 7.4, 0.1% fatty acid-free BSA, and 1x penicillin/streptomycin. Bottom compartments were filled with 600 µl of the same medium containing different concentrations of S1P. An aliquot of the cell suspension put to the upper chamber was put aside for later FACS analysis. Cells that migrated to the bottom chamber in 4 h at 37°C in 5% CO₂ in air were stained with anti-CD3 and anti-CD19 antibody and analysed by FACS. Absolute cell numbers were assessed by using BD TruCOUNT™ tubes.

4.3. Animal experimentation

All animal care practices and experimental procedures were performed in accordance with the German animal protection law.

4.3.1. Genotyping of S1P₄^{-/-} animals

A 3 mm tail clip was cut from 4 week old mice pups. Genomic DNA was extracted as described above. Animals were genotyped by PCR with primer pairs detecting S1P₄ and the neo-cassette present in S1P₄^{-/-} animals. The PCR reaction was performed in a 25 µl volume.

The PCR reaction mix was prepared as follows:

Polymerase Buffer	10 x	2.5	µl
dNTP mix	12.5 mM	0.4	µl
Taq polymerase	5 U/µl	0,25	µl
Primer pair S1P ₄	50 µM	0.2	µl
Primer pair neo	50 µM	0.2	µl
DMSO		1.23	µl
Genomic DNA		2	µl

The PCR programme contained the following steps:

Initial denaturation	3 min	94°C
Denaturation step	40 sec	94°C
Annealing step	40 sec	60.5°C
Polymerisation step	40 sec	72°C
Final denaturation	3 min	72°C

PCR products were analysed by agarose gel electrophoresis.

4.3.2. Anesthesia and sacrifice

For surgical procedures, mice were anaesthetised by intraperitoneal injection of a ketamine/xylazine mixture. This mixture was prepared by adding 1 ml of xylazine (20mg/ml) to 10 ml of ketamine (100 mg/ml). This solution was diluted 1 : 5. Each mice received 2.5-7.5 ml/kg body weight of the diluted solution to induce anaesthesia for 15 to 20 min.

In general, euthanasia was done by carbon dioxide asphyxiation. When terminal blood collection was required, animals were deeply anaesthetized and exsanguinated by cardiac puncture.

4.3.3. Gastrointestinal lavage

Gastrointestinal lavage buffer

25 mM	NaCl
10 mM	Na ₂ SO ₄
10 mM	KCl
20 mM	NaHCO ₃
50 mM	EDTA
162mg/ml	PEG
1 mM	PMSF
0.1 mg/ml	Soybean trypsin inhibitor

Animals were killed by carbon dioxide asphyxiation. The small intestine was removed from the gastro-duodenal junction to the ileocaecal junction. Mesenterium was discarded. Intestinal tubes were clipped on both ends with an haemostat and washed abundantly in PBS to remove peripheral blood. The cleaned gut was then opened longitudinally. The gut and faeces was then transferred to a 5 ml FACS tube. Two ml of gastrointestinal lavage buffer was added. The tube was then vigorously vortexed and incubated for 5 min on ice. The tube was then centrifuged at 700 x g for 10 min at 4 °C. The supernatant was transferred to a new Eppendorf tube. PMSF at a final concentration of 1mM was added. The supernatant was then centrifuged at 20000 x g for 20 min at 4°C. The supernatant was transferred to a new

Eppendorf tube. PMSF at a final concentration of 1mM was again added. The supernatant was then aliquoted and stored at -20°C until further use.

4.3.4. Bronchoalveolar lavage

Animals were killed by carbon dioxide asphyxiation. The trachea was exposed surgically. A appropriately sized canula was introduced into the trachea and fixed with a silk suture. Depending on the following experiments, 750 μl or 500 μl of PBS was gently injected into the trachea, pulled-back, reinjected and finally recovered. This procedure was repeated with another 750 (500) μl of PBS. The BALF fluid was centrifuged at 500 x g for 10 min at 4°C . The supernatant was aliquoted and stored at -20°C until further use. The cell pellet was resuspended in PBS and used for cytospin.

4.3.5. Type IV hypersensitivity assay

<i>NP-O-Su solution</i>	<i>Borate buffer saline</i>
2 % NP-O-Su	15 mM sodium borate
In DMSO	0.15M NaCl
	pH 8.5 with NaOH

At day 0, mice were anaesthetised by intraperitoneal injection of a ketamine/xylazine mixture as described in paragraph 4.3.2.. In each flank, 50 μl NP-O-Su solution was injected subcutaneously, followed by subcutaneous injection of 0.1 μl of borate buffer saline in dorsal midline skin. At day 6, NP-O-Su challenging solution for the DTH challenge was prepared by diluting 20 μl of the original NP-O-Su in 400 μl of PBS, pH 7.8. DTH challenge was performed by injecting 25 μl of NP-O-Su challenging solution in the right rear footpad. Twenty five μl of PBS alone were injected into the left rear footpad for comparison. After 24 and 48 hours, footpad thickness of both rear footpads was assessed with a specialized caliper.

4.3.6. Contact hypersensitivity assay

At day 0, 400 μl of 0.5% FITC in acetone/diputylphtalat (1:1) was applied epicutaneously to the previously shaved abdomen of $\text{S1P}_4^{-/-}$ and wild type animals. At day 6, base line ear thickness of both ears was measured with specialized caliper. Following ear measurement, each face of the right ear was treated epicutaneously with 10 μl of 0.5% FITC in acetone/diputylphtalat (1:1). As negative control, the left ear was treated with solvent only. After 24 and 48 hours, ear thickness was measured and recorded.

4.3.7. T-cell-depended antibody response to sheep red blood cell antigens

S1P₄^{-/-} and wild type mice were immunized with 2 x 10⁸ SRBCs in 200 µl intraperitoneally on days 0 and 15. At days 0, 14, 21, 28, 49 and 70, blood was drawn by retro-orbital puncture. Titer of anti-SRBC antibodies was determined in the serum by ELISA as described in paragraph 4.2.6.3.

For the ELISA, soluble SRBC antigen was prepared from sheep erythrocytes. Six ml of SRBC were lysed hypotonically by suspension in 12 ml of distilled water. The lysate was then centrifuged at 20000 x g for 15 min at 4°C. The pellet was washed 3 times with PBS. The pellet was then resuspended in 4 ml of PBS and sonicated on ice with a sonic probe for 30 seconds with 30% intensity and 50% intervals. The sample was then centrifuged at 30000 x g for 60 min. The supernatant was aliquoted and stored at 20 °C for further use. A small aliquote was taken for measurement of the protein concentration.

4.3.8. Ovalbumin induced asthma

Hundred µg of ovalbumin was adsorbed to 10 mg of AL(OH)₃ in a volume of 3ml of a 0.9% NaCl solution. Age and sex matched, six to twelve weeks old female S1P₄^{-/-} and WT mice were systemically sensitised by intra-peritoneal injection of 300 µl of this solution on day 1, 8 and 14. At days 21, 22 and 23, animals were challenged by inhalation of aerosolised 2% ovalbumin in PBS for 30 min. Twenty four hours after the last airway challenge, mice were sacrificed and BAL was performed as described in paragraph 4.3.4. The left lung was included into TissueTek and stored at -80°C, the right lung was fixed in 4% paraformaldehyde and included into paraffin for later histological examination.

4.3.9. 4'-deoxypyridoxin induced peripheral lymphopenia

Six to twelve weeks old female S1P₄^{-/-} and their WT littermates were put on special pyridoxine-poor diet (<5 mg/kg) for 7 days. DOP treated mice received drinking water with 100 mg/l DOP and 10 g/l glucose for 3 days. Control animals received drinking water with 10 g/l glucose only for the same period. At day 4, mice were sacrificed. Spleen, peripheral lymph nodes, thymus were removed and snap frozen in liquid nitrogen and stored at -80°C until determination of S1P content by chromatography. Peripheral blood lymphocytes were isolated from a small aliquot of peripheral blood, stained with anti-B220 and anti-CD3 antibody and analysed by FACS. The remaining blood was separated in corpuscular components and plasma by centrifugation at 2500 x g for 5 min. Plasma and cell pellet were

then snap frozen in liquid nitrogen and stored at -80°C until determination of S1P content by chromatography.

4.4. Determination of S1P content by chromatography

Samples were adjusted to 1 ml volume with 1 M NaCl and transferred into a glass centrifuge tube. After addition of 1 ml methanol and 100 μl of 37% hydrochloric acid, the samples were vortexed. Chloroform (2 ml) was added, and the samples were mixed for 30 min at 50 rpm in a test tube rotator. Samples were centrifuged for 3 min at 1900 x g, and the lower chloroform phase was transferred into a new glass centrifuge tube. After repeating the lipid extraction with another 2 ml of chloroform, the two chloroform phases were combined and vacuum-dried in a SpeedVac for 45 min at 48°C . Eighteen mg FMOCl were dissolved in 5 ml dioxane. Vacuum dried samples were dissolved in 200 μl dioxane with subsequent addition of 200 μl of 70 mM dipotassiumhydrogenphosphate in H_2O and 200 μl FMOCl solution. Chromatographic detection of sphingolipids was performed using the Merck-Hitachi Elite LaChrom System (VWR; Darmstadt, Germany). The injection pump delivery rate was 1.3 ml/min. The eluent was 82 to 95% methanol, 5 to 0% 70 mM dipotassiumhydrogenphosphate, and 13 to 5% H_2O , forming a gradient over a period of 68 min. A 10 μl sample volume was injected using the cut injection method. Separation of sphingolipids with reversed phase chromatography was done using a 250 x 4.6 mm Kromasil 100–5 C18 separation column and a 17 x 4 mm Kromasil 100–5 C18 precolumn. Column temperature was 35°C ; detection was performed with a fluorescence detector at 263 nm excitation and 316 nm emission wave length.

4.5. Statistical analysis

Statistical analysis of the experimental data was performed using the SPSS 12.0 software package (SPSS Inc., Chicago, IL, USA) statistical software. Graphs were generated with GraphPad PRISM[®] (GraphPad Software Inc). For comparison of continuous variables, the Student's t test or the Mann Whitney-U test was applied. A significance level of $p < 0.05$ was considered significant.

5. RESULTS

5.1. Alterations of the homeostasis of the immune system in S1P₄-deficient mice and their consequences on immune reactivity

5.1.1. S1P₄ deficiency in mice: immune phenotype

5.1.1.1. Phenotypic analysis of primary and secondary lymphoid organs in S1P₄^{-/-} mice by FACS

S1P₄ was shown to be highly expressed on lymphoid cells. Another member of the S1P receptor family that is highly expressed on immune cells, namely S1P₁, was demonstrated to regulate the migration of immune cells such as lymphocytes and dendritic cells (DCs).

Therefore, in order to assess whether S1P₄ has a similar action and whether its absence would modify the cellular composition of the major lymphoid organs, cells from primary lymphoid organs (bone marrow (BM) and thymus), secondary lymphoid organs (peripheral lymph nodes (pLN (inguinal and axillary)) and mesenteric lymph nodes (mLN)) as well as from peripheral blood were stained for characteristic surface markers and analysed by multicolour FACS analysis.

In bone marrow, no significant difference was observed between cells from both experimental groups except for CD8⁺-expressing T-cells which were systematically 50%-increased in S1P₄^{-/-} mice (**Table 9**).

	S1P ₄ ^{-/-}	WT	p
Granulocytes [% of MNC]	23.25 ± 2.07	25.38 ± 2.69	0.151
Monocytes [% of MNC]	2.89 ± 0.68	6.93 ± 1.13	1.000
CD4⁺ [% of lymphocytes]	2.89 ± 0.45	2.17 ± 0.8	0.151
CD8⁺ [% of lymphocytes]	3.07 ± 0.81	1.56 ± 0.6	0.016
CD19⁺ [% of lymphocytes]	42.72 ± 3.46	49.14 ± 7.58	0.222
CD19⁺ IgM⁺ [% of lymphocytes]	18.99 ± 2.43	19.3 ± 4.38	0.841
CD19⁺ IgM⁻ [% of lymphocytes]	23.06 ± 1.75	28.87 ± 4.33	0.056

Table 9: Cell populations in the Bone marrow cells

Medullary cells was stained with monoclonal Ab against CD4, CD8, CD25, CD19 and IgM. Five animals were analysed per group.

In the thymus, frequencies of single positive CD4⁺ and CD8⁺ as well as double positive CD4⁺CD8⁺ were similar in WT and S1P₄^{-/-} animals (**Table 10**).

	S1P ₄ ^{-/-}	WT	p
SP CD4 ⁺	14.41 ± 3.93	12.19 ± 2.21	0.31
SP CD8 ⁺	2.02 ± 0.84	1,61 ± 0.34	0.58
CD4 ⁺ CD8 ⁺	73.90 ± 9.28	78.1 ± 2.78	0.69

Table 10: Lymphocyte populations in the thymus

Single cell suspensions from thymus were stained with monoclonal Ab against CD4 an CD8. Five animals were analysed per group.

In the spleen of S1P₄^{-/-} cells, no aberrant distribution of lymphocyte populations was observed when compared with controls (**Table 11**).

	S1P ₄ ^{-/-}	WT	p
CD4 ⁺	39.11 ± 2.34	36.98 ± 1.72	0.222
CD8 ⁺	16.20 ± 1.23	14.34 ± 0.93	0.056
CD4 ⁺ CD25 ⁺	4.71 ± 0.24	4.48 ± 0.41	0.151
CD19 ⁺	38,32 ± 5,02	40.63 ± 4.02	0.548

Table 11: Lymphocyte populations in the spleen

Single cell suspensions from spleens were stained with monoclonal Ab against CD4, CD8, CD25, CD19 and IgM. Five animals were analysed per group.

Interestingly, both in pLN and mLN, the frequency of CD19⁺-expressing cells -likely representing B lymphocytes- was reduced by roughly 30% in S1P₄^{-/-} mice. While this difference reached statistical significance in the pLN (p=0.032), the same tendency was noted in mesenteric nodes, yet not statistically significant (p=0.063). (**Tables 12 and 13**).

	S1P ₄ ^{-/-}	WT	p
CD4 ⁺	66,02 ± 3,06	63.55 ± 3,56	0.548
CD8 ⁺	24.39 ± 2.62	24.74 ± 1.44	1.000
CD4 ⁺ CD25 ⁺	6.12 ± 0.41	6.73 ± 0.72	0.151
CD19 ⁺	6.75 ± 0.81	9.05 ± 2.1	0.032

Table 12: Lymphocyte populations in the pLN

Single cell suspensions from pLN were stained with monoclonal Ab against CD4, CD8, CD25, CD19 and IgM. Five animals were analysed per group.

Cell frequencies of CD4⁺, CD8⁺ and CD19⁺ cells within Peyer's patches of S1P₄^{-/-} animals and WT controls were indistinguishable (**Table 14**).

	S1P ₄ ^{-/-}	WT	p
CD4⁺	19.90 ± 1.37	19.67 ± 9.85	0.629
CD8⁺	5.40 ± 1.00	5.99 ± 3.67	0.857
CD4⁺CD25⁺	2.22 ± 0.25	2.53 ± 1.02	0.857
CD19⁺	53.44 ± 3.55	56.88 ± 10.22	0.486

Table 14: Lymphocyte populations in the Peyer's patches

Single cell suspensions from Peyer's patches were stained with monoclonal Ab against CD4, CD8, CD25, CD19 and IgM. Four animals were analysed per group.

Finally in peripheral blood, granulocytes, monocytes, CD19⁺ B-cells, CD4⁺, CD8⁺ as well as CD4⁺CD25⁺ T-cells were equally frequent in both groups. In the BM, CD8⁺ T-cells were consistently more frequent in S1P₄^{-/-} mice while CD19⁺IgM⁻ cells were more frequent in WT animals (**Table 15**).

	S1P ₄ ^{-/-}	WT	p
Granulocytes [% of PBMC]	23.63 ± 10.33	33.32 ± 6.44	0.200
Monocytes [% of PBMC]	2.68 ± 0.63	2.50 ± 1.46	0.886
CD4⁺ [% of lymphocytes]	56.03 ± 8.81	59.23 ± 6.38	0.686
CD8⁺ [% of lymphocytes]	14.00 ± 3.00	15.02 ± 2.20	0.686
CD19⁺ [% of lymphocytes]	25.44 ± 12.41	19.41 ± 4.69	0.886

Table 15: Cell populations in the peripheral blood mononuclear cells

PBMC were stained with monoclonal Ab against CD4, CD8, CD25, CD19 and IgM. Five animals were analysed per group.

In conclusion, *in vivo* S1P₄-deficiency in mice does not lead to profound alteration in immune cell populations either in primary or secondary lymphoid organ, as well as in peripheral blood. Nevertheless in S1P₄^{-/-} mice, we could noticed discrete, yet significant, modifications in the percentages of medullary CD8⁺ T-cells (50% increase) and CD19⁺ B-cells in lymph nodes (30% decrease).

5.1.1.2. Comparative analysis of cell populations in the bronchoalveolar lavage fluid

S1P levels have been shown to be increased in bronchoalveolar lavage (BAL) fluids from asthmatic patients and in animal models of asthma.

We therefore wondered whether S1P signalling could contribute to the migrational control of cell populations to the lung and whether the lack of S1P₄ might impact on the relative abundance of cells found in the BAL fluid in normal conditions.

Thus, bronchoalveolar lavage was performed in S1P₄^{-/-} and WT animals. Cells were centrifuged onto microscope slides, stained by the May-Grünwald method and subsequently counted under a light microscope. This staining allows to determine the relative numbers of alveolar macrophages, lymphocytes and granulocytes per 1000 counted-cells. No statistically significant differences were observed between S1P₄^{-/-} and WT animals (**Figure 15**).

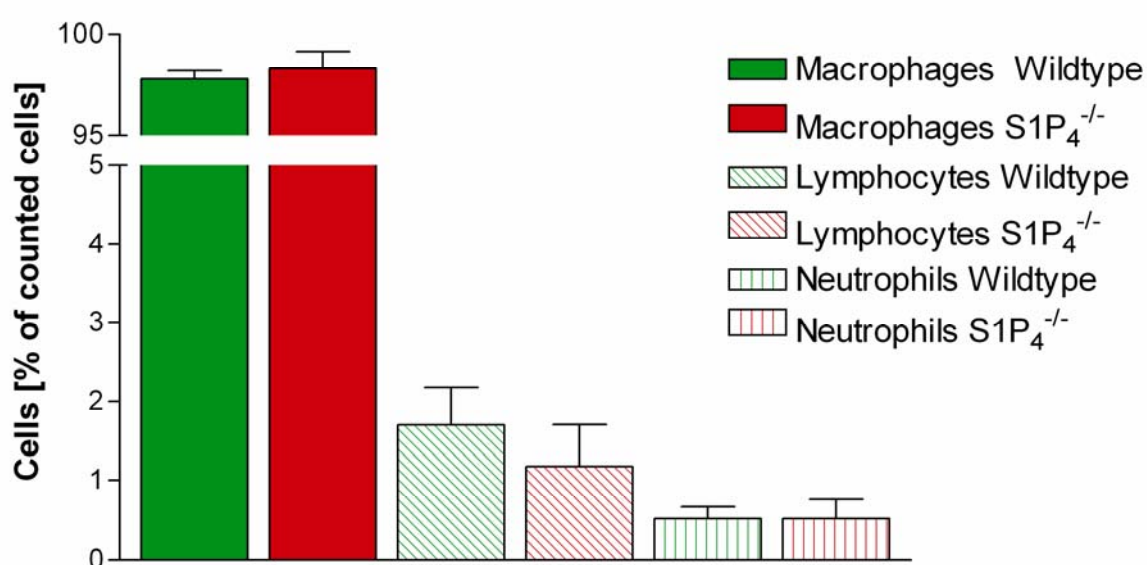


Figure 15: Cell populations in the bronchoalveolar lavage fluid

Relative cell numbers were determined per 1000 cells after May-Grünwald staining. Results are representative of 5 animals per group.

5.1.1.3 Comparative evaluation of Ig levels in plasma and serum of WT and S1P₄^{-/-} mice

To further characterize the “immune phenotype” of S1P₄^{-/-} mice, we evaluated by ELISA the levels of the different immunoglobulin (Ig) isotypes in the serum of WT and S1P₄^{-/-} mice. Briefly, it is known that the spectrum of Ig isotypes is regulated primarily by cytokines released from antigen-stimulated T helper (Th) cells at the B-cell-Th-cell interface. The T_H2 prototype cytokine IL-4 favours the isotype switch towards IgG1 and IgE, while IFN-γ, mostly secreted by T_H1 cells, predominantly induces IgG2a.

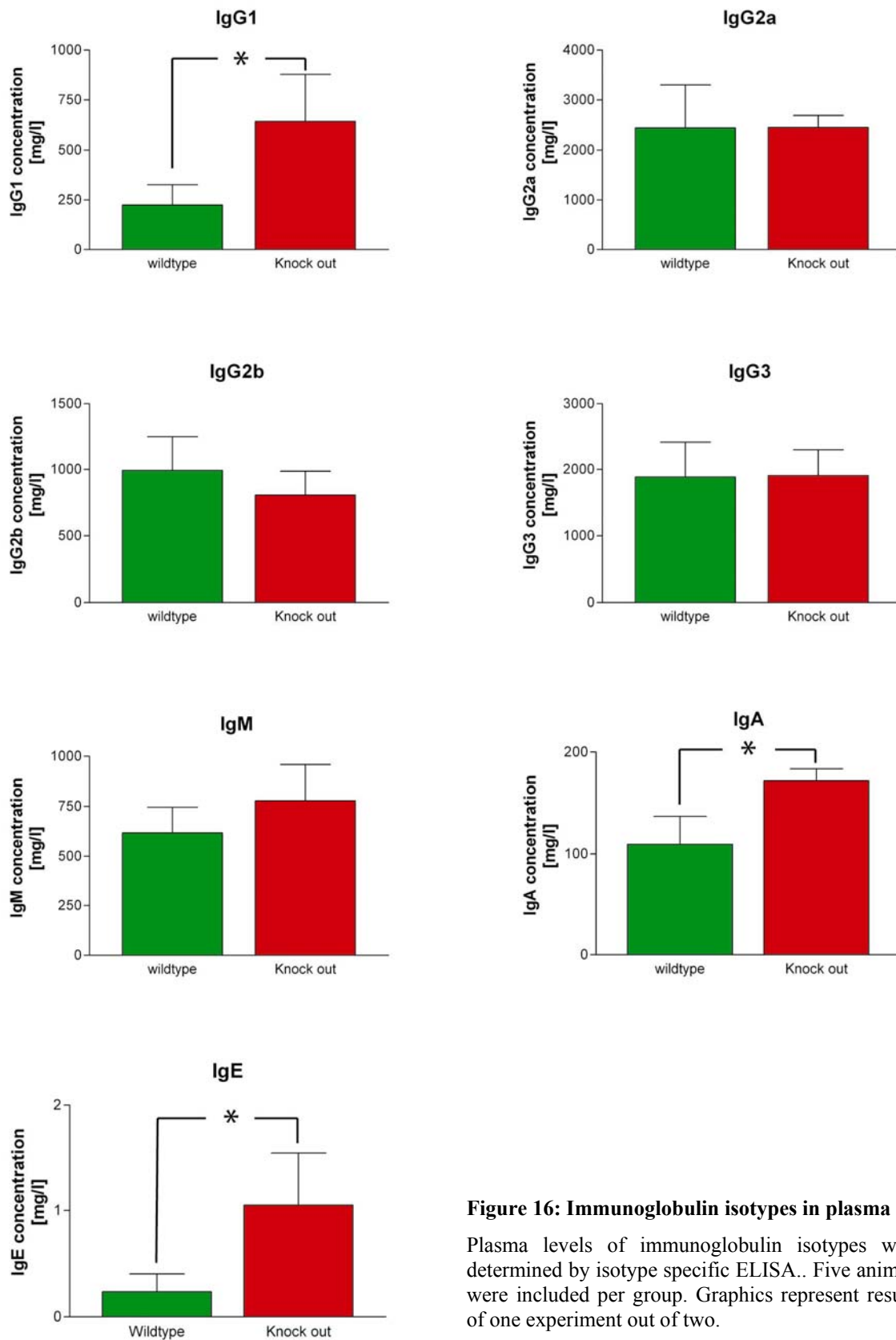


Figure 16: Immunoglobulin isotypes in plasma

Plasma levels of immunoglobulin isotypes were determined by isotype specific ELISA.. Five animals were included per group. Graphics represent results of one experiment out of two.

In $S1P_4^{-/-}$ mice, a significant increase of IgG1, IgE and IgA immunoglobulins was found in plasma compared with WT animals (**Figure 16**). Differences of the same magnitude were also observed in the serum of other independent cohorts of WT and $S1P_4^{-/-}$ mice.

In summary, $S1P_4$ -deficiency in mice leads to an increase in T_H2 -associated immunoglobulin isotypes (IgG1, IgE and IgA). This might signify that $S1P_4$ would be involved in T_H2 polarization.

5.1.1.4. Determination of mucosal IgA levels

Since we observed differences between $S1P_4^{-/-}$ and WT regarding blood IgA levels, we decided to compare the concentrations of local IgA in the bronchoalveolar tract (BAT) and the gastrointestinal tract (GIT)

In order to measure bronchoalveolar IgA levels, 5 WT and 5 $S1P_4^{-/-}$ mice were sacrificed and bronchoalveolar lavage (BAL) was performed with 500 μ l PBS. No statistically significant differences in IgA levels between WT and $S1P_4^{-/-}$ mice were observed (**Figure 17**).

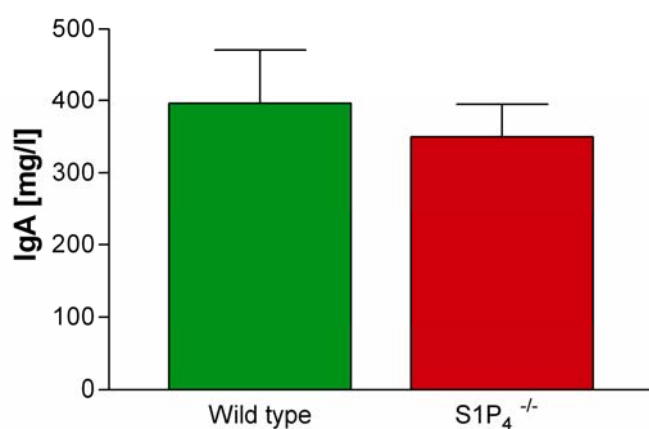


Figure 17: IgA levels in broncho-alveolar lavage fluid

IgA levels were assessed in WT and $S1P_4^{-/-}$ mice by ELISA. (n=5)

For comparative analysis of IgA levels in the gastrointestinal tract, gastrointestinal lavages (GIL) were performed in 5 WT and 5 $S1P_4^{-/-}$ mice. IgA levels were determined by ELISA. In contrast to systemic IgA levels, intestinal IgA in $S1P_4^{-/-}$ mice was reduced compared with wild type animals (65.1 ± 11.4 in $S1P_4^{-/-}$ mice and 94.1 ± 12.1 in WT mice, (**Figure 18**). These differences were statistical significant ($p=0,008$).

In conclusion, IgA levels in the BAL were indistinguishable in animals of both phenotypes, while GIL fluid from $S1P_4^{-/-}$ animals showed significantly reduced IgA levels. These results are in contrast with our findings in plasmas and serum. These observations

suggest that the mechanisms governing systemic and local IgA production are differentially influenced by S1P signalling via the S1P₄ receptor.

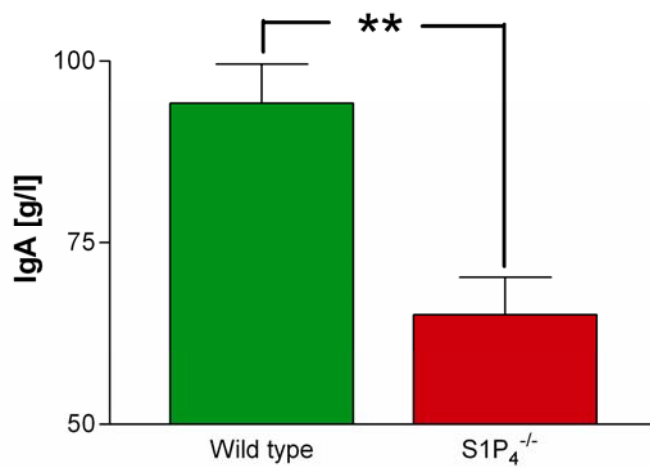


Figure 18: IgA levels in gastro-intestinal lavage fluid
IgA levels were assessed in WT and S1P₄^{-/-} mice by ELISA. Results are representative of 5 animals per group.

5.1.1.5. Quantitative assessment of the B-cell development in S1P₄^{-/-} and WT mice

We showed that S1P₄-deficiency resulted in higher systemic IgG1, IgA and IgE levels. In addition, reinforcing a putative role of S1P₄ in B-cell biology, S1P₄^{-/-} mice present less IgA locally both in BAT (not significant) and GIT (significant).

Thus, in order to assess whether B-cell development is affected by the lack of S1P₄, a quantitative analysis of various developmental stages of B-cells in bone marrow and spleen was performed.

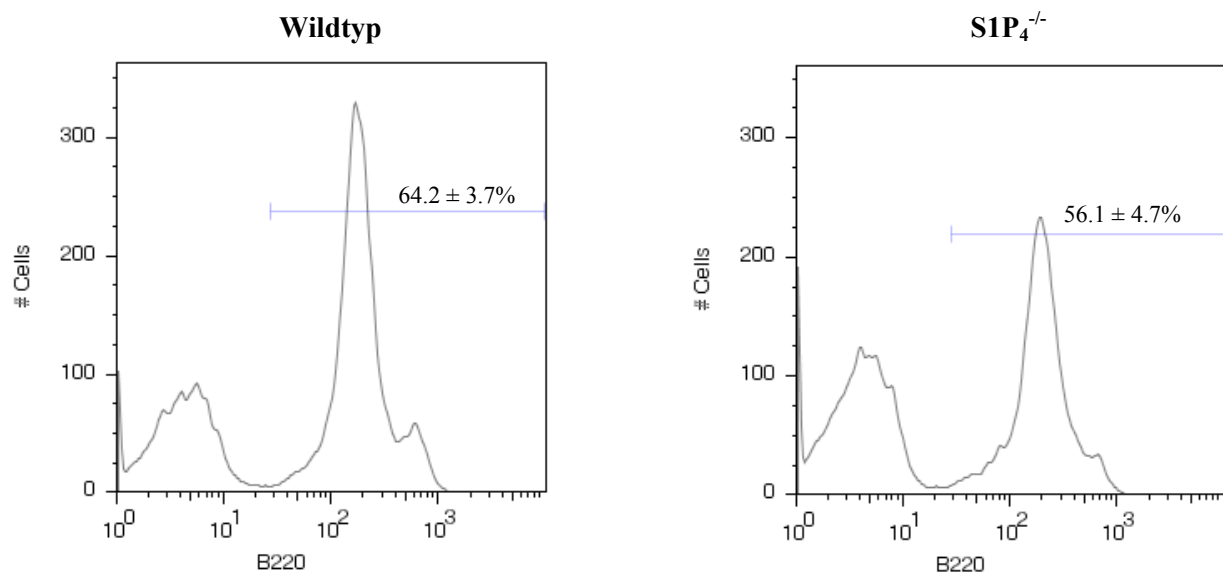


Figure 19: Reduction of total B cells derived from bone marrow

Bone marrow cells from WT and S1P₄ deficient mice were stained with B220 and analysed by FACS. Percentages indicate B220+ cells in gated lymphoid populations. (n = 5 per group)

First, in bone marrow cells were stained with anti-IgM Ab and anti-B220 Ab and analysed by FACS. Bone marrow of S1P₄^{-/-} contained slightly less total B220⁺ B-cells than that of WT mice ($56.1 \pm 4.7\%$ versus $64.2 \pm 3.7\%$ in S1P₄^{-/-} and WT, respectively, $n=5$, $p=0.016$, **Figure 19**) Although this difference is relatively tiny, it is reproducible, statistically significant and is in line with our previous observation of reduced CD19⁺IgM⁺ cell numbers in S1P₄^{-/-} animals (**see paragraph 5.1.1.1**).

Subsequently, the development of the B-cell lineage including pro-/pre- B-cells, immature B-cells and mature B-cells was examined. It showed that the B220⁺ IgM⁻ cell population (containing both pro- and pre- B-cells) was slightly but significantly reduced in S1P₄^{-/-} animals ($24.9 \pm 4.3\%$ versus $32.5 \pm 5.0\%$ in S1P₄^{-/-} and WT mice, respectively; $n = 5$; $p = 0.036$, **Figure 20**). Immature B-cells, characterized as IgM⁺B220^{int} cells, were equally present in the bone marrow of S1P₄^{-/-} and WT mice ($14.1 \pm 2.2\%$ and $16 \pm 1.4\%$ in S1P₄^{-/-} and WT mice, respectively). Furthermore, the population of mature B-cells (IgM⁺B220^{hi}) were indistinguishable in S1P₄^{-/-} and WT mice ($9.4 \pm 4.0\%$ and $7.2 \pm 1.1\%$ in S1P₄^{-/-} and WT mice, respectively).

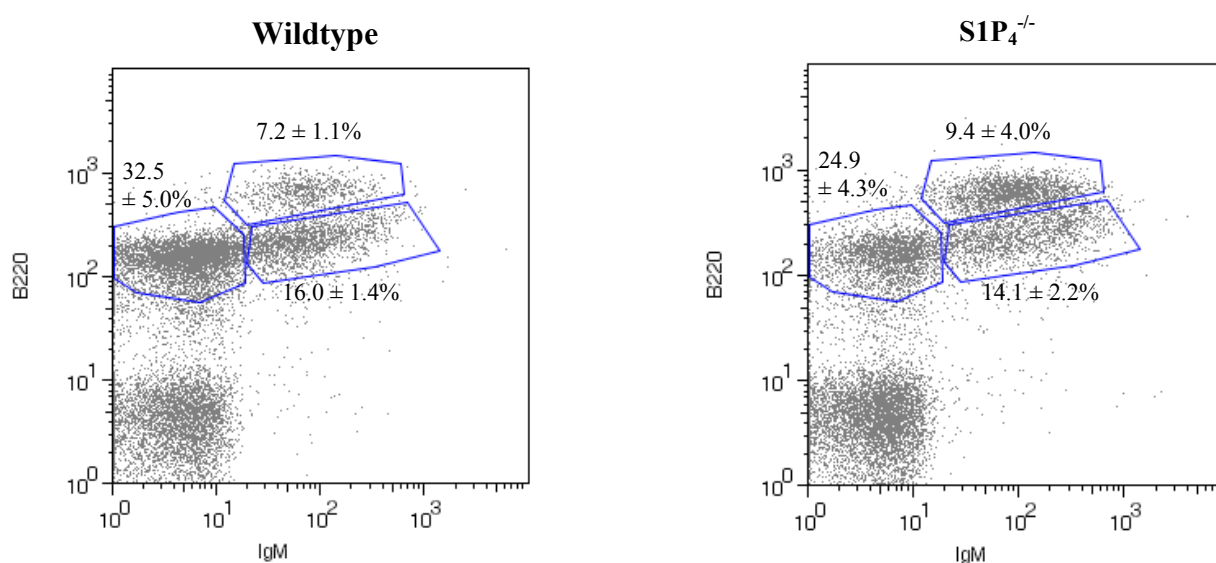


Figure 20: Identification of developmental B cell stages in the bone marrow

The B220⁺ IgM⁻ B cell population was more frequent in WT than in S1P₄ deficient mice. Immature (IgM⁺B220^{int}) and mature (IgM⁺B220^{hi}) B cell frequencies were indistinguishable in animals of both genotype. ($n = 5$ per group)

Second, the analysis of B-cell stages was performed in the spleen. We looked for the transitional type 1 B-cells (CD21^{lo}CD23⁻, IgM^{hi}), transitional type 2 B-cells (CD21^{hi}CD23⁺, IgM^{hi}) and mature B-cells. The two types of mature B-cells residing in the

spleen comprise mature follicular B-cells ($CD21^{int}CD23^+, IgM^{lo}$) and marginal zone (MZ) B-cells ($CD21^{hi}CD23^-, IgM^{hi}$).

It showed that, when gating on lymphocytes, the percentages of $CD19^+$ B-cells in both mice strains were indistinguishable. Similarly, no differences concerning the percentage of transitional type 2 B-cells ($3.9 \pm 1.5\%$ and $2.3 \pm 0,2 \%$ in $S1P_4^{-/-}$ and WT mice, respectively) and of mature follicular B-cells ($37.1 \pm 0.4\%$ and $38.3 \pm 1.8\%$ in $S1P_4^{-/-}$ and WT mice, respectively) were observed. In contrast, the frequency of marginal zone B-cells in the spleen was significantly increased in the $S1P_4^{-/-}$ mice compared to WT animals ($2.2 \pm 0.3\%$ and $1.3 \pm 0,1\%$, **Figure 21**). Transitional type 1 cells were less frequent in $S1P_4^{-/-}$ mice compared to WT ($1.1 \pm 0.3\%$ and $2.0 \pm 0,1 \%$, **Figure 21**).

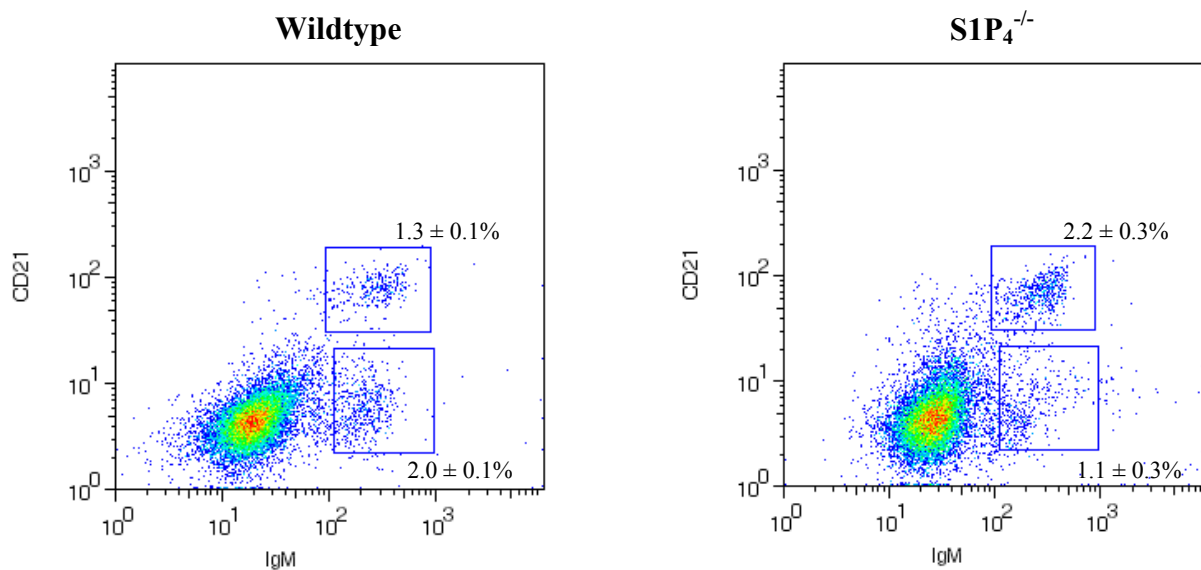


Figure 21: Increase of Marginal zone B cells in $S1P_4$ -deficient mice

Splenocytes from WT and $S1P_4$ deficient mice were stained with anti-IgM, anti-CD21 and anti-CD23. In cells gated on $CD23^-$, marginal zone B cells ($CD21^{hi}CD23^-, IgM^{hi}$) and transitional type I B cells ($CD21^{lo}CD23^-, IgM^{hi}$) are shown. Percentages indicate cells in gated lymphoid populations. (n = 5 per group)

In order to confirm the observation of increased marginal zone B-cell numbers, splenocytes were stained by anti-CD19, anti-CD21 and anti-CD23 antibodies. Marginal zone B-cells were identified as $CD19^+$, $CD21^{hi}$ and $CD23^{lo}$ cells. Here again, marginal zone B-cells were significantly increased in $S1P_4^{-/-}$ mice compared to WT mice. ($14.0 \pm 2.8\%$ versus $10.2 \pm 1.4\%$ of $CD19^+$ cells in $S1P_4^{-/-}$ mice and to WT mice, n=5; p=0.028) (**Figure 22**).

In conclusion, a reduction of distinct developmental stages of B-cells was observed comprising very early B-cell progenitors (pre-/pro-B-cells) and transitional type I B-cells. In contrast, splenic mature B-cells were not affected by this reduction. Follicular B-cells showed normal frequencies, and MZ B-cells were increased by almost 70%.

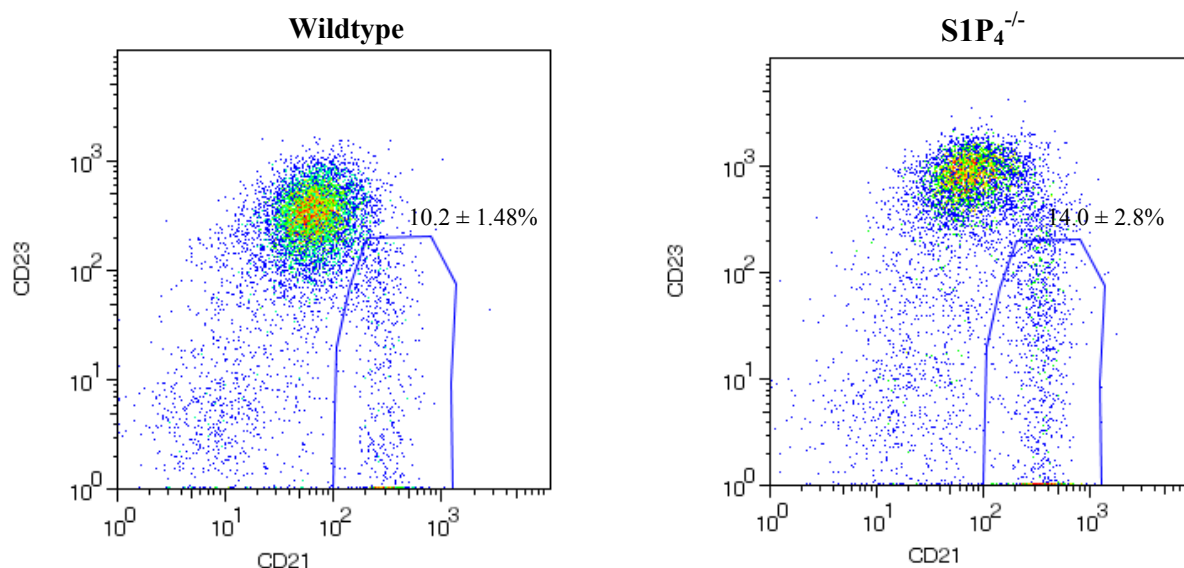


Figure 22: Increase of Marginal zone B cells in S1P₄-deficient mice

Splenocytes from WT and S1P₄-deficient mice were stained with anti-CD19, anti-CD21 and anti-CD23. In cells gated on CD19⁺, marginal zone B cells (CD21^{hi} and CD23^{lo}). Percentages indicate cells in gated lymphoid populations. (n = 5 per group)

5.1.1.6. Comparative analysis of peritoneal B1 cells

B1 cells represent a CD5-expressing B-cell sub-population mainly found in body cavities (pleural /peritoneal cavity). These cells are described to be the major producer of natural IgM antibodies, but also produce significant amounts of IgA. Natural antibodies are produced in the absence of exogenous antigenic stimulation, are poly-reactive, weakly auto-reactive and react with many common pathogen associated antigens.

In order to determine whether the observed differences in plasma IgA levels as well as in local IgA levels in S1P₄^{-/-} mice are partly due to changes in the development/maintenance of the B1 cell compartment, B1 cells of the peritoneal cavity were identified by CD5/IgM double staining and quantified by FACS analysis. The CD5⁺IgM⁺ B1 cells were observed in equal quantities in both S1P₄^{-/-} mice and WT mice (19.4 ± 1.7 % versus 21.2 ± 3.0 %, respectively; **Figure 23**).

The quantitative development of the B1 cells seemed thus uninfluenced by S1P₄ deficiency.

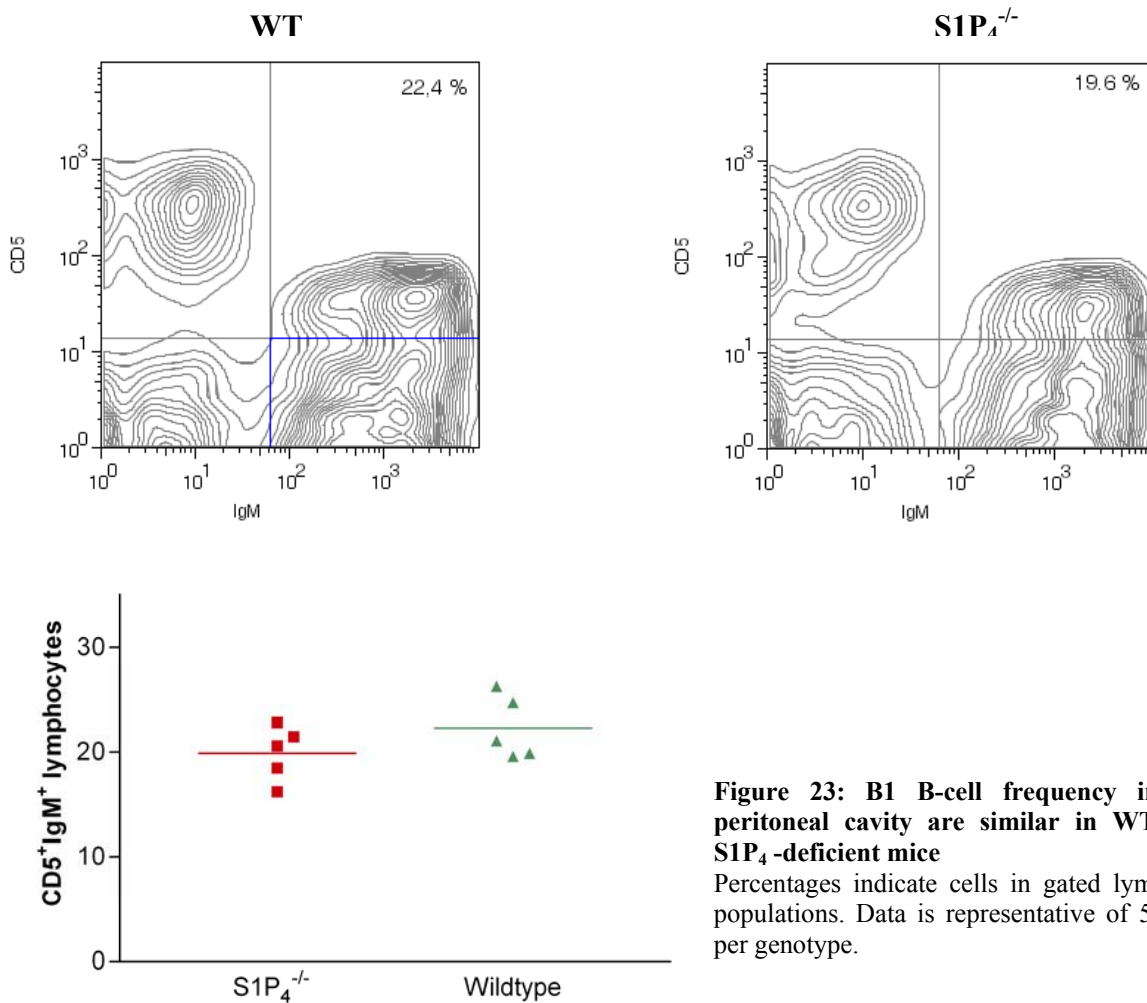


Figure 23: B1 B-cell frequency in the peritoneal cavity are similar in WT and SIP₄-deficient mice

Percentages indicate cells in gated lymphoid populations. Data is representative of 5 mice per genotype.

5.1.2. SIP₄ deficiency in Mice: functional consequences in the immune system

In the previous chapter we have detailed the consequences of SIP₄ deficiency on the immune system at a descriptive level. We have found quantitative differences concerning various stages of B-cell development in bone marrow and spleen, a small but reproducible reduction of CD19⁺ B-cell numbers in peripheral and mesenteric lymph nodes as well as a systemic Ig profile (increase of IgG1, IgE and IgA) suggestive of a T_H2 deviation of the immune response. In contrast, mucosal IgA levels showed an inverse tendency to reduced IgA levels.

In the following part, we have assessed the functional consequences of the observed differences in *in vitro* assays as well as different *in vivo* models of T_H1 or T_H2 dominated immune responses.

5.1.2.1. S1P₄ deficiency does not impact on the proliferative potential of CD4⁺ and CD8⁺ T-cells

In an *in vitro* model over-expressing S1P₄, S1P signalling *via* this receptor has been previously reported to impact on the proliferation of CD4⁺ T-cells⁷³.

To test whether S1P₄-deficiency influences the proliferative capacity of CD4⁺ and CD8⁺ T-cells, these cells were isolated by a negative selection based MACS procedure and stimulated with anti-CD3 and anti-CD28 antibody or incubated with irradiated splenocytes from C56Bl/6 mice to induce a MLR reaction. Proliferation was assessed after 2 days in culture by a colorimetric reaction with a tetrazolium substrate.

Our results show that WT and S1P₄^{-/-} CD4⁺ cells exhibit a similar proliferative response both after anti-CD3/anti-CD28 stimulation and in the MLR (**Figure 24**).

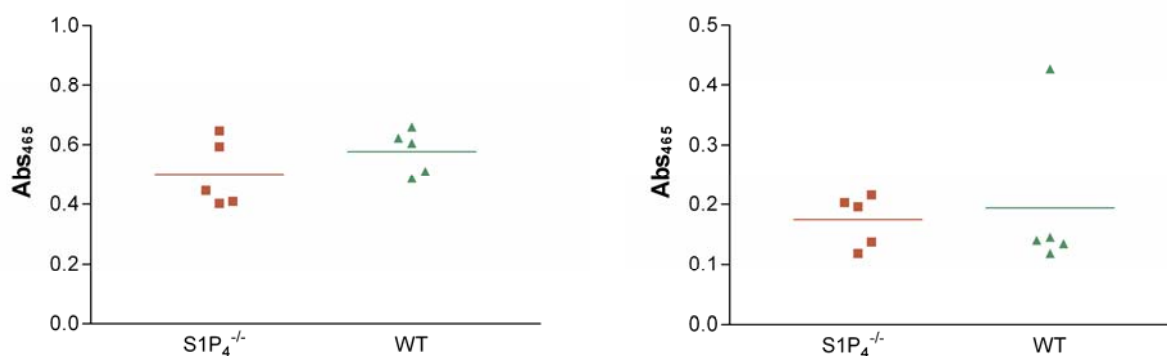


Figure 24: *In vitro* proliferation of CD4⁺ T-cells after stimulation with CD3 (left) or MLR (right)

Similarly in CD8⁺ T-cells, no differences in proliferation after stimulation with either anti-CD3/anti-CD28 or in a MLR was detected after 2 days of culture (**Figure 25**).

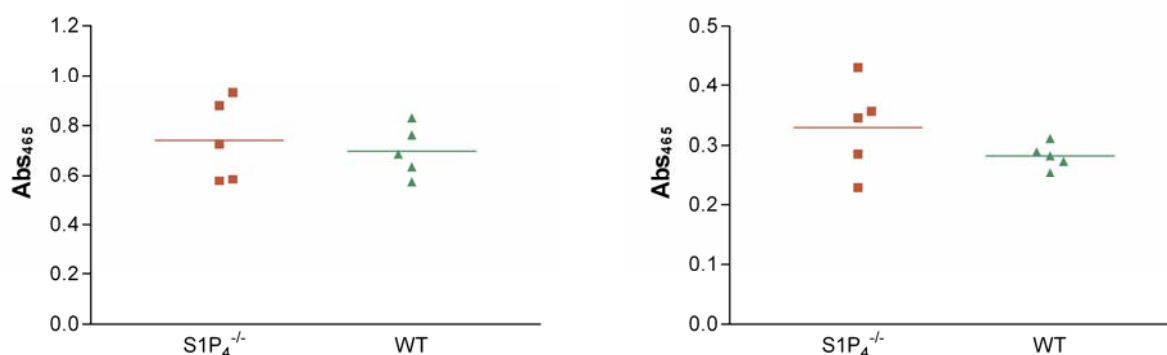


Figure 25: *In vitro* proliferation of CD8⁺ T-cells after stimulation with CD3 (left) or MLR (right)

5.1.2.2. S1P₄ deficiency deviates cytokine secretion *in vitro*

Stable overexpression of S1P₁ and S1P₄ in T-cell lines was shown to influence the panel of cytokines secreted. We therefore assessed whether *in vitro* cytokine secretion of S1P₄^{-/-} T helper cells differed from that of WT lymphocytes.

CD4⁺ T-cells were isolated from spleens of S1P₄ and sex- and age-matched controls and stimulated with anti-CD3/anti-CD28 antibodies for 48 hours. The cell culture supernatant was assayed for IL-4, IL-5 and IFN γ .

IL-4 and IFN γ showed no statistically significant differences between S1P₄^{-/-} and WT controls (IL-4: 804.2 \pm 418.7 pg/ml versus 639.2 \pm 267.3 pg/ml; IFN γ : 80 \pm 22.6 ng/ml versus 50 \pm 9.3 ng/ml in S1P₄^{-/-} and WT animals. Interestingly, IL-5 concentration in the cell culture supernatants of S1P₄-deficient animals was significantly increased compared to that of control animals (869.6 \pm 560.0 pg/ml versus 255.1 \pm 33.7 pg/ml in S1P₄^{-/-} and WT animals, respectively; p = 0.044) (**Figure 26**).

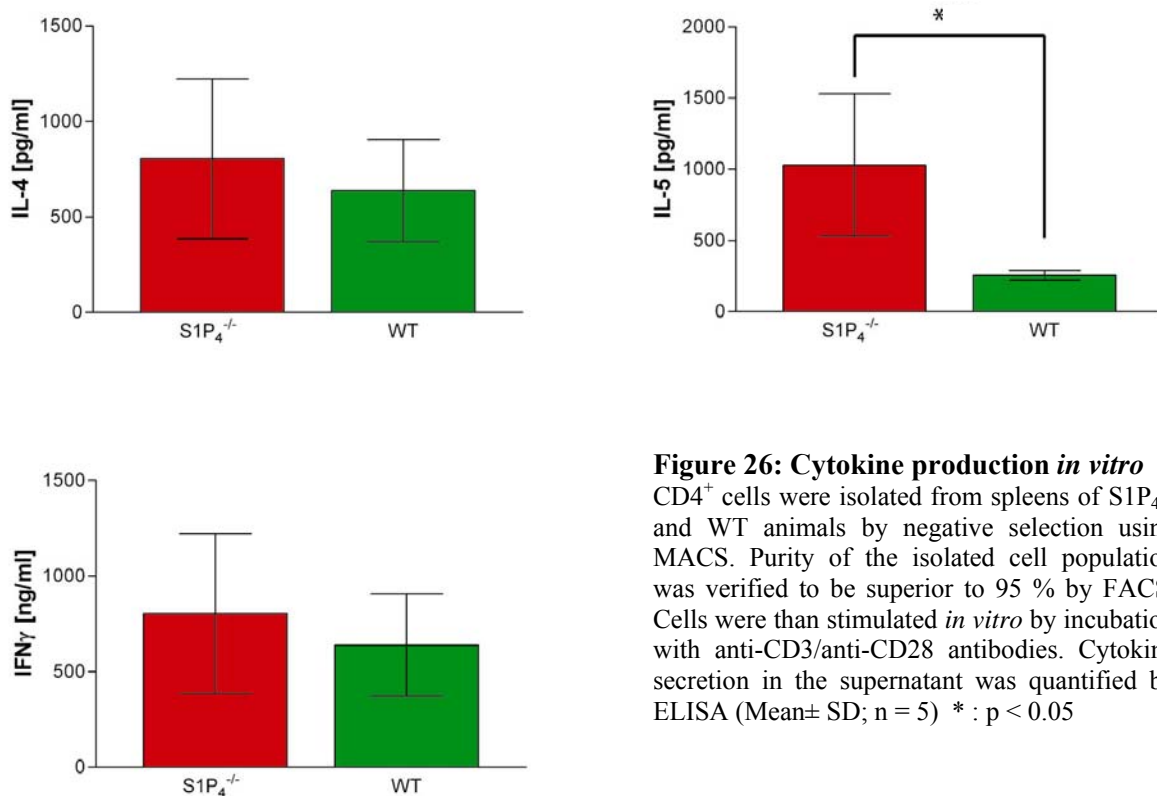


Figure 26: Cytokine production *in vitro*
 CD4⁺ cells were isolated from spleens of S1P₄^{-/-} and WT animals by negative selection using MACS. Purity of the isolated cell population was verified to be superior to 95 % by FACS. Cells were then stimulated *in vitro* by incubation with anti-CD3/anti-CD28 antibodies. Cytokine secretion in the supernatant was quantified by ELISA (Mean \pm SD; n = 5) * : p < 0.05

5.1.2.3. Assessment of plasma and blood cell S1P concentrations

The ligand for S1P₄, S1P, is present in blood and lymph fluid at concentrations ranging from 100 to 500 nM. Plasma S1P is generated by cells of hematopoietic origin, while lymph S1P is synthesized by a radio-resistant non-hematopoietic source¹¹⁵. Extracellular S1P has

been shown to stimulate Sphingosine kinase activity thus increasing its own production. The identity of the receptors mediating this effect is still unknown.

In order to evaluate whether S1P levels are similar in WT and S1P₄^{-/-} mice, levels of S1P in both plasma and blood cells (thrombocytes, erythrocytes and PBMC) were assessed by chromatography.

We showed that concentrations of S1P₁ from in both plasma and blood cells are similar in WT and S1P₄^{-/-} mice and lay within the range of published S1P plasma concentrations (Figure 27).

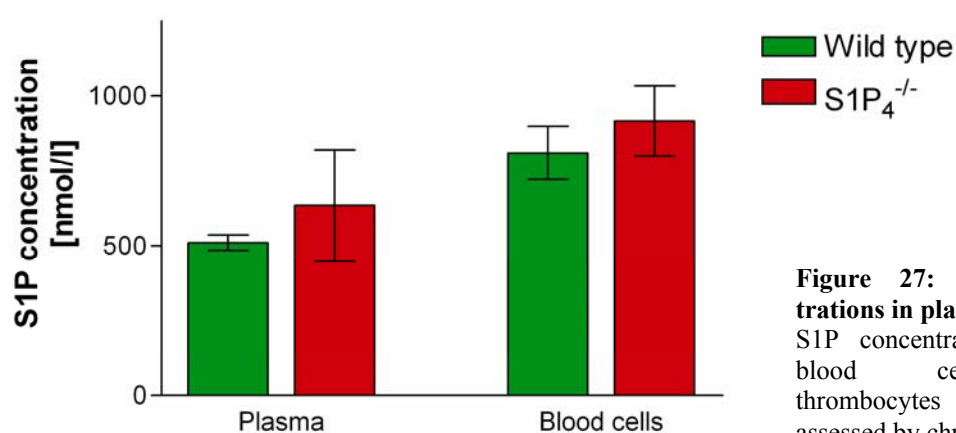


Figure 27: Basal S1P concentrations in plasma and blood cells
S1P concentrations in plasma and blood cells (erythrocytes, thrombocytes and PBMC) were assessed by chromatography.

5.1.2.4. Vitamin B6 antagonist DOP induced similar peripheral lymphopenia in WT and S1P₄^{-/-} mice

Schwab *et al.* demonstrated that inhibition of S1P lyase by the Vitamin-B6 (Vit-B6) antagonists 4'-deoxyypyridoxin (DOP) or 2-acetyl-4-tetrahydroxybutylimidazol (THI) resulted in peripheral lymphopenia. The mechanism implicated was supposed to be the loss of the S1P gradient between tissues where S1P concentrations were shown to be very low, and the plasma and/or the lymph for which S1P levels are higher. Higher concentrations of tissular S1P were shown to result in S1P₁ downregulation at the cell surface and to reduce migration of B and T lymphocytes towards S1P¹⁹⁷. The implication of other S1P receptors in the induction of lymphopenia by Vit-B6 antagonists has not been assessed so far.

We thus wondered whether S1P₄ may play a role in this process. WT as well as S1P₄^{-/-} were treated with DOP p.o. for 3 days. Mice were sacrificed on day 3 and PBMC were isolated from blood after erythrocyte lysis. Before erythrocyte lysis, 10 µl of APC-labelled calibration beads were added per 100µl of blood for quantification purposes. Induction of

peripheral lymphopenia was assessed by FACS analysis of anti-CD3/anti-B220 double stained PBMC (**Figure 27**).

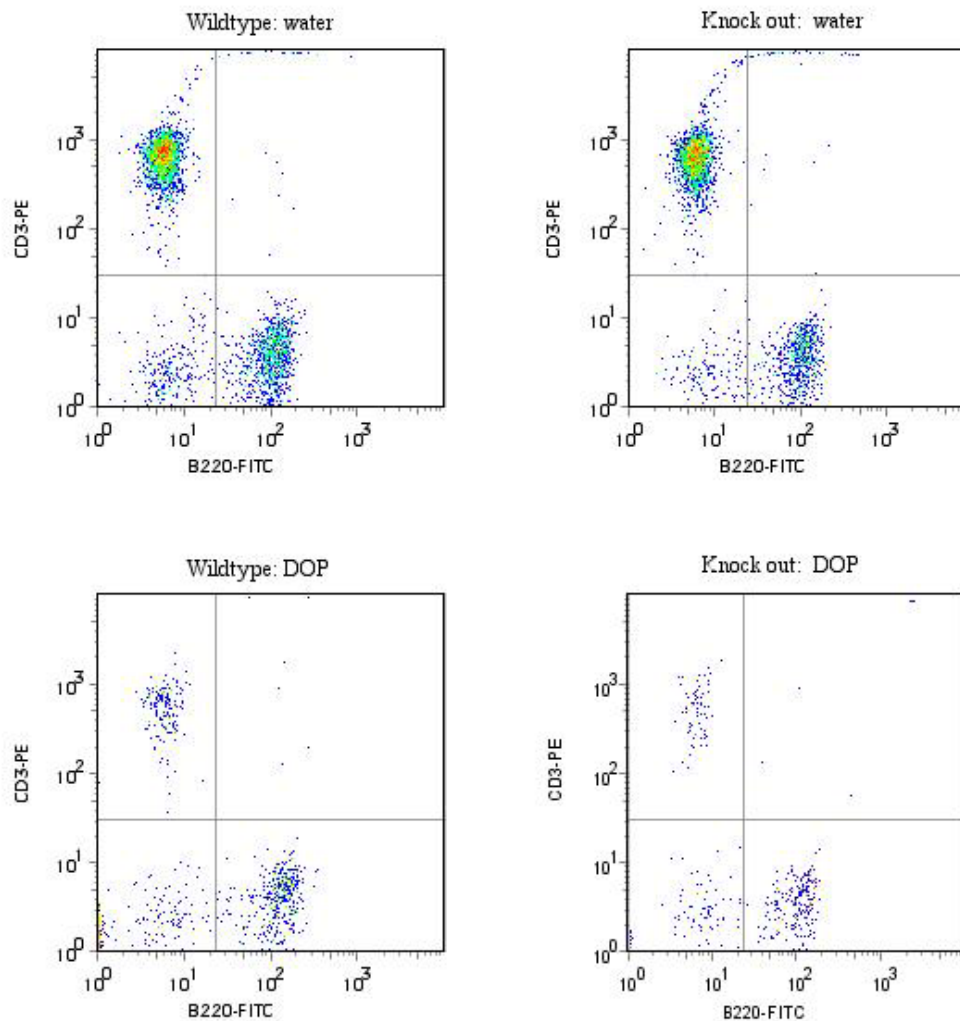


Figure 27: DOP induced peripheral lymphopenia in Wild type and $S1P_4^{-/-}$ mice.

After 3 days of DOP application p.o., animals were sacrificed and blood drawn by intracardiac puncture. Before lyses of erythrocytes, 10 μ l of APC labelled calibration beads were added per 100 μ l of blood. After lyses of erythrocytes and staining with PE-labelled anti-CD3 Ab and FITC labelled anti-B220 Ab, cells were analysed by FACS. The dot blots shown above are gated on lymphocytes. For quantification of absolute cell numbers, APC labelled beads were acquired in a separate gate. Acquisition was stopped at 20000 APC labelled beads.

It showed that DOP induced peripheral lymphopenia in both WT and $S1P_4^{-/-}$ mice. Indeed, the absolute number of CD3⁺ cells were significantly reduced in animals of both genotypes. Interestingly, the reduction of CD3⁺ T-cells was more pronounced in $S1P_4^{-/-}$ than in WT mice, with lower absolute numbers of CD3⁺ cells in the peripheral blood after DOP treatment (116 ± 42 CD3⁺ cells/ 17000 APC⁺ beads versus 245 ± 86 CD3⁺ cells/ 17000 APC⁺ beads in $S1P_4^{-/-}$ and WT animals, respectively, $p = 0.036$). In contrast, the absolute number of B220⁺ cells in WT and $S1P_4^{-/-}$ mice after DOP treatment did not show significant differences

(396 ± 206 B220⁺ cells/ 17000 APC⁺ beads versus 616 ± 336 B220⁺ cells/ 17000 APC⁺ beads in S1P₄^{-/-} and WT animals, respectively, $p = 0.307$) although a reduction occurred in animals of both genotypes compared to the untreated control group. (**Figure 28**)

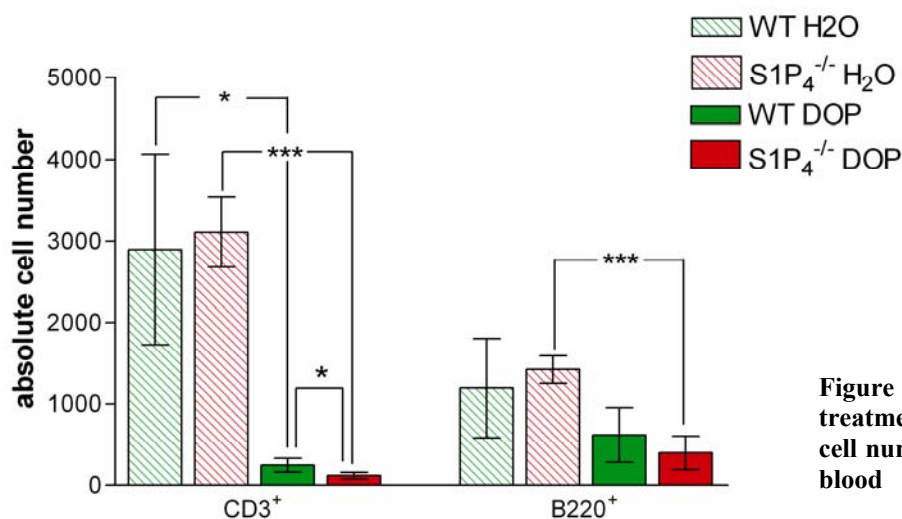


Figure 28: Effects of DOP treatment on absolute B and T cell numbers in the peripheral blood

The differences in the absolute numbers of T and B-cells would suggest that T-cells undergo a stronger decrease in peripheral blood upon DOP exposure than B-cells. In order to better question that point, we calculated the B/ T-cell ratio (**Figure 29**). While this ratio was 0.39 ± 0.07 and 0.47 ± 0.17 in untreated WT and S1P₄^{-/-} animals, respectively; it was inverted to 2.4 ± 0.6 and 3.3 ± 0.54 in DOP-treated WT and S1P₄^{-/-} mice, respectively. Most interestingly, there was a tendency to even higher B/T-cell ratios in DOP-treated S1P₄^{-/-} mice than in DOP-treated WT animals, suggesting a more pronounced differential effect on B and T-cells in S1P₄^{-/-} mice compared to the WT.

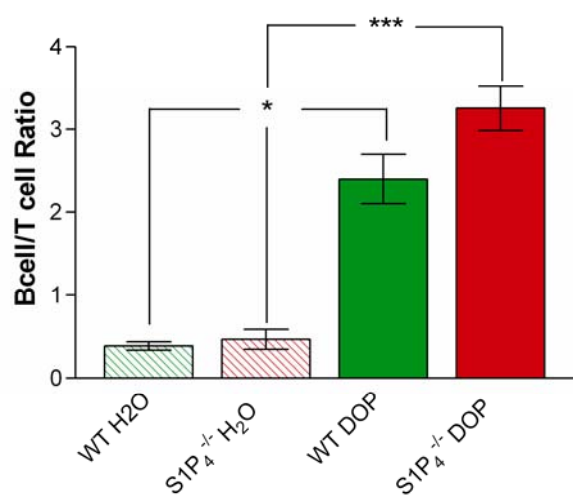


Figure 29: B- and T-cells are differentially affected by DOP

A B/T-cell ratio was calculated by dividing absolute B and T cell numbers. DOP effects on T-cells seem to be more pronounced than those on B-cells.

The observed differences between the WT and the S1P₄^{-/-} animals can be due to direct consequences of the S1P₄ deficiency on migrating cells. However, S1P₄-deficiency may also influence the effects of DOP on S1P levels in different organs thus indirectly influencing the migrational behaviour of lymphocytes. In order to test the latter possibility, the levels of S1P were determined in WT and the S1P₄^{-/-} mice, in various lymphatic organs (lymph node, thymus, spleen) as well as in plasma and total blood cells (**Figure 30**).

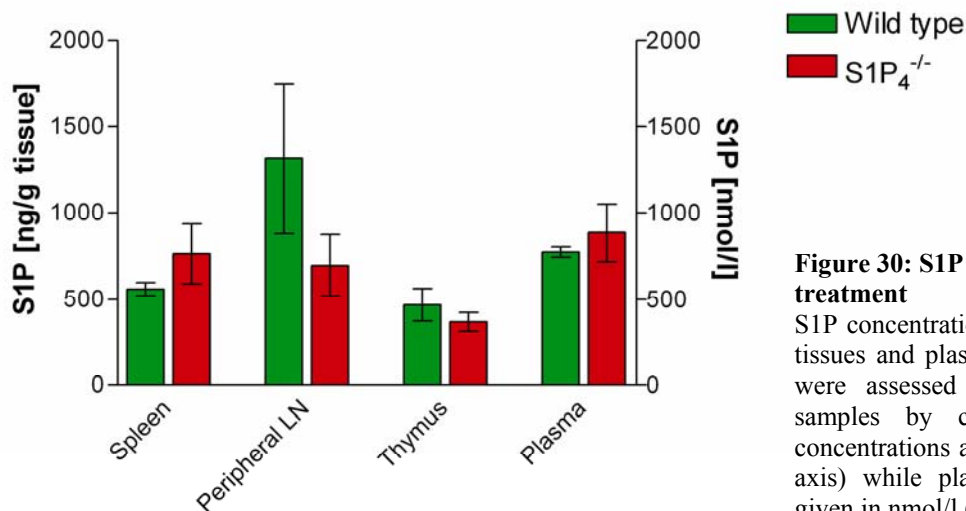


Figure 30: S1P levels following DOP treatment

S1P concentrations in various lymphatic tissues and plasma after DOP treatment were assessed in snap frozen tissue samples by chromatography. Tissue concentrations are given in ng/g (left Y-axis) while plasma concentrations are given in nmol/l (right Y-axis)

S1P levels in lymphatic tissues as well as in plasma did not vary between animals of both genotypes. Plasma levels of S1P in DOP treated animals were only slightly elevated compared to untreated control animals (control: $510 \pm 26,5$ nmol/l versus DOP: $772,3 \pm 59.1$ nmol/l and control : 633.2 ± 187.2 nmol/l versus $885.0 \pm 330,5$ nmol/l in WT and S1P₄^{-/-} mice, respectively). Only in WT mice, this difference reached statistical significance at $p < 0.05$. The obtained results suggest that S1P₄ does not induce modification in S1P metabolism and that the effects we showed on B and T-cells are likely due a direct effect of S1P₄ deficiency on the migratory capacity of lymphocytes. Therefore we next tested this hypothesis.

5.1.2.5. S1P₄ deficiency affects *in vitro* migration of CD4⁺ and CD8⁺ lymphocytes

In vitro migration experiments with S1P₄ overexpressing murine T-cell lines devoid of endogenous S1P receptor expression suggested that S1P₄ is not implicated in the regulation of a chemotactic response to S1P.

However, the results shown in paragraph 5.1.2.4. indicate clearly that WT and S1P₄^{-/-} T-lymphocytes react differently to the increase of interstitial S1P concentration in lymphatic

tissues. We therefore assessed *in vitro* in a transwell migration assay the chemotactic response of CD4⁺, CD8⁺ and CD19⁺ splenocytes to S1P.

Single cell suspensions of spleen from naive WT and S1P₄^{-/-} animals were prepared. After 4 hours of migration, cell having migrated along a 0 nM, 1nM, 10 nM or 100 nM S1P gradient through a collagen-coated transwell membrane (pore size 5µm) were quantified by FACS. Interestingly, S1P₄^{-/-} CD4⁺ cells showed a significantly stronger chemotactic response to a 10 nM and 100 nM S1P gradient than their WT counterparts (**Figure 31A**). While only 6.7 % ± 2.7 % and 6.1 % ± 1.0 % of WT CD4⁺ cells migrated along a gradient of 10 nM and 100 nM S1P, respectively, the corresponding percentages of migrated S1P₄^{-/-} cells were 14.8 % ± 6.2 % and 31.0 % ± 14.3 %, respectively. These differences were statistically significant (p= 0.027 and p = 0.005, respectively). A similar migrational response to S1P occurred in CD8⁺ cells. 12.1 % ± 8.5 % and 28.2 % ± 14.9 % of S1P₄^{-/-} CD8⁺ lymphocytes migrated to a 10 nM and 100 nM S1P gradient, compared to 4.8 % ± 1.6 % and 5.1 ± 1.1 % of WT lymphocytes respectively (**Figure 31B**). These differences were statistically significant at a gradient of 100 nM (p = 0.008). In contrast, WT as well as S1P₄^{-/-} CD19⁺ lymphocytes did not show a significant chemotactic response to S1P (**Figure 31C**).

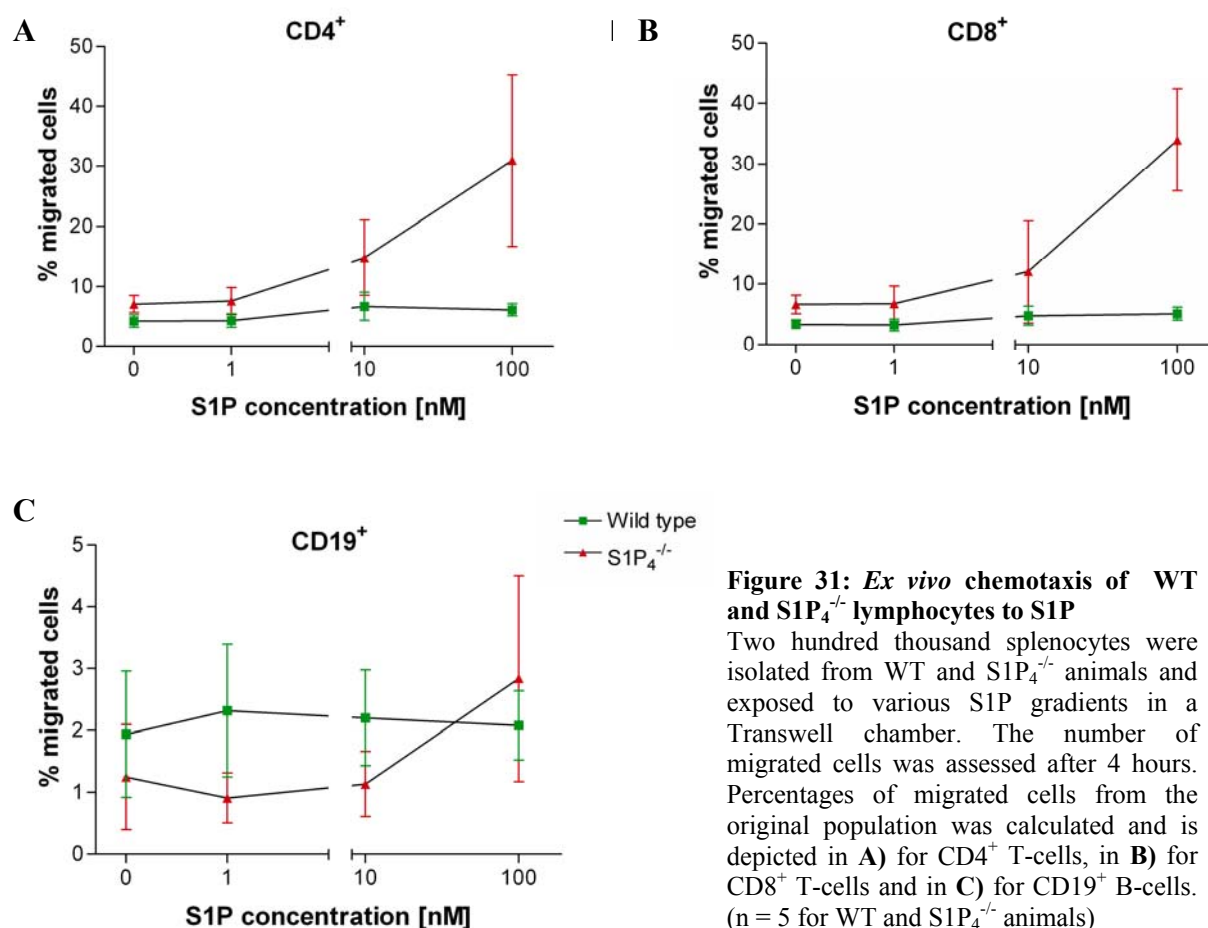


Figure 31: Ex vivo chemotaxis of WT and S1P₄^{-/-} lymphocytes to S1P

Two hundred thousand splenocytes were isolated from WT and S1P₄^{-/-} animals and exposed to various S1P gradients in a Transwell chamber. The number of migrated cells was assessed after 4 hours. Percentages of migrated cells from the original population was calculated and is depicted in **A**) for CD4⁺ T-cells, in **B**) for CD8⁺ T-cells and in **C**) for CD19⁺ B-cells. (n = 5 for WT and S1P₄^{-/-} animals)

In conclusion, the results of the experiments shown in paragraphs 5.1.2.4. and 5.1.2.5. strongly indicate that S1P₄ is implicated in the regulation of CD4⁺/CD8⁺ T-cell migration. Since the receptor S1P₁ has also been shown to influence lymphocytes migration both to S1P gradients as well as to chemokine gradients, it would be particularly interesting to perform further experiments with S1P₁/S1P₄ double deficient lymphocytes to better dissect the individual participation of the two receptors.

5.1.2.6. T-cell dependent antibody production is normal in S1P₄-deficient animals

T-cells provide key help for B-cell maturation in germinal centres. Cytokines, in particular T_H2 cytokines such as IL-4, IL-5, IL-6, IL-10 and IL-13 are critically involved in B-cell proliferation and class switching.

IgG1 and IgE, which are antibody isotypes characteristic of a T_H2-deviated immune response, were found to be increased in the S1P₄^{-/-} mice (cf. Figure 16). Therefore we wondered whether the antibody response to a T-cell dependent antigen would show differences in S1P₄^{-/-} animals compared to WT mice.

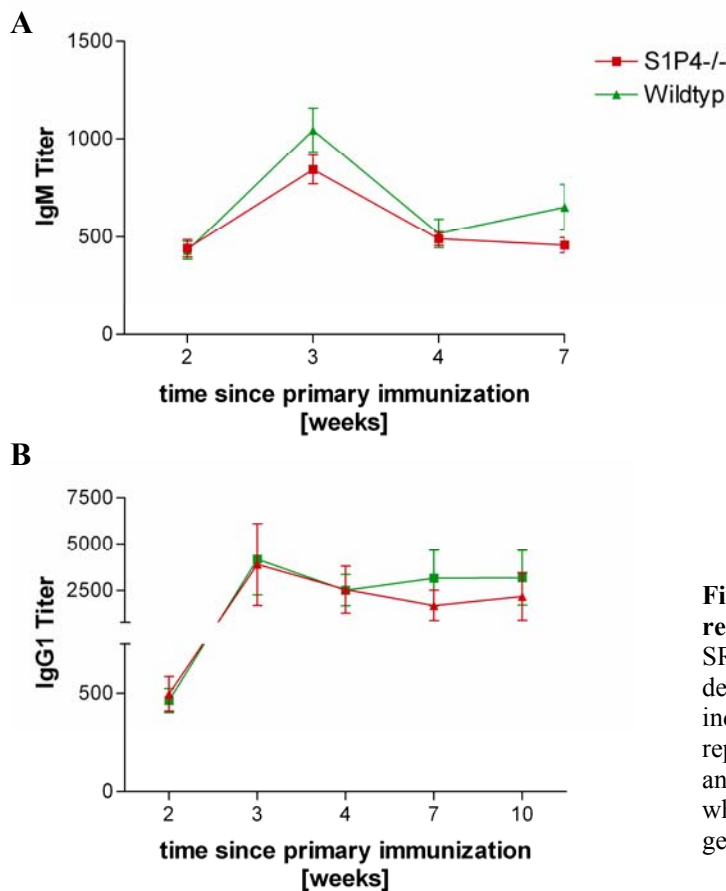


Figure 32: SRBC-specific IgM and IgG1 response

SRBC-specific IgM (A) and IgG1 (B) were detected in plasma from immunized mice by indirect ELISA at the time points shown. The reported results represent the titer of the sample and are the reciprocal of the serum dilution which has a OD value of 0.5. (n = 5 per genotype)

WT and $S1P_4^{-/-}$ animals were immunized by intraperitoneal injection of SRBC at day 0. A boost was given at day 14 after the primary injection. Serum was taken at day 0 and 14, each time before immunization, and at days 21, 28, 49 and 70. Titers of specific anti-SRBC IgM and IgG1 antibodies were determined by ELISA.

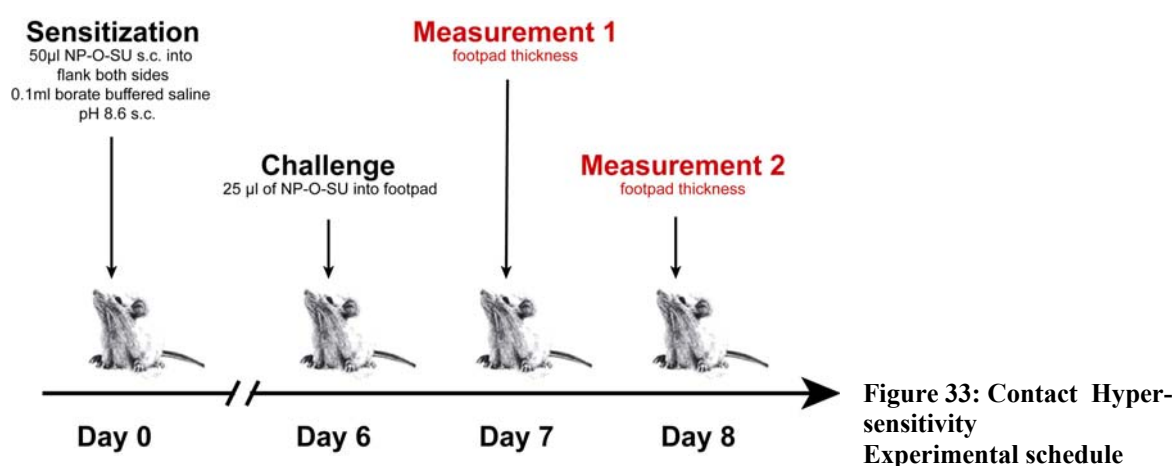
It showed that $S1P_4$ -deficiency caused no abnormalities concerning the amplitude or the dynamics of the SRBC specific IgM and IgG1 antibody response in our experimental model (**Figure 32**).

5.1.2.7. $S1P_4$ deficiency results in an increased contact hypersensitivity

$S1P_4$ -deficient mice present a plasmatic isotype Ig profile reminiscent of a T_H2 -polarized immune response (cf. Figure 16). In order to test the hypothesis that $S1P_4$ -deficiency results in conditions promoting a T_H2 immune response, we used the well known T_H -dependent system of contact hypersensitivity (CHS).

Indeed, dependent on the antigen used to sensitise the animal, the pathophysiological cascade leading to local oedema, swelling and cellular infiltration can be predominated by T_H1 - or T_H2 -type mechanisms. As an example, FITC has been shown to be a typical T_H2 -type sensitizer¹⁹⁸.

Aiming to assess the capacity of the $S1P_4^{-/-}$ animals to develop a T_H2 -dominated CHS reaction, both $S1P_4^{-/-}$ and WT mice were sensitised by epicutaneous application of 0.5% FITC in Aceton/Dibutylphtalat at the ear after previous sensitisation with the same antigen. Ear swelling was measured after 1 and 2 days following challenge with FITC (**Figure 33**).



It showed that $S1P_4^{-/-}$ mice developed a significantly increased ear swelling at day 1 compared to WT animals ($144 \pm 26\mu\text{m}$ versus $97 \pm 28\mu\text{m}$, respectively, $p = 0,007$; **Figure**

34). At day 2 after epicutaneous challenge, the difference observed at day 1 was still present, but did not reach statistical significance.

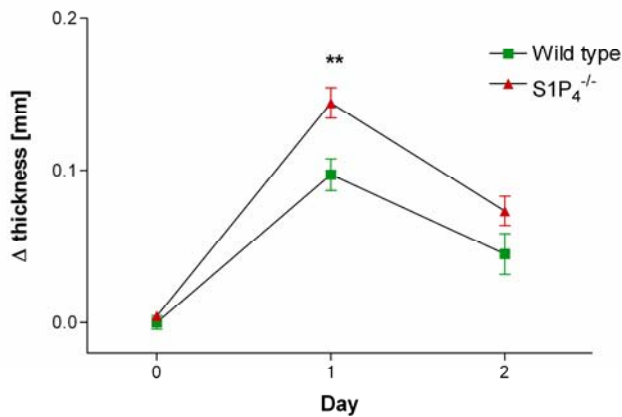


Figure 34: Contact Hypersensitivity

Ear swelling of the right ear at day 1 and day 2 after challenge were assessed and normalized against the non-challenged left ear. Results are representative of 7 animals per group. (Mean ± SD between animals per group)

***p* < 0.01

5.1.2.8. S1P₄ deficiency results in a reduced classical Type IV hypersensitivity response

After having tested the ability of the S1P₄^{-/-} mice to develop a T_H2-polarized immune response in the FITC contact hypersensitivity model. We next wondered whether S1P₄^{-/-} mice were able to develop a normal T_H1 response. In order to address this question, we performed a classical Type IV hypersensitivity model by injecting NP-O-SU in the footpad of previously sensitised mice. Footpad swelling was measured at day 1 and day 2 after intradermal challenge. Our experimental procedure is depicted in **Figure 35**.

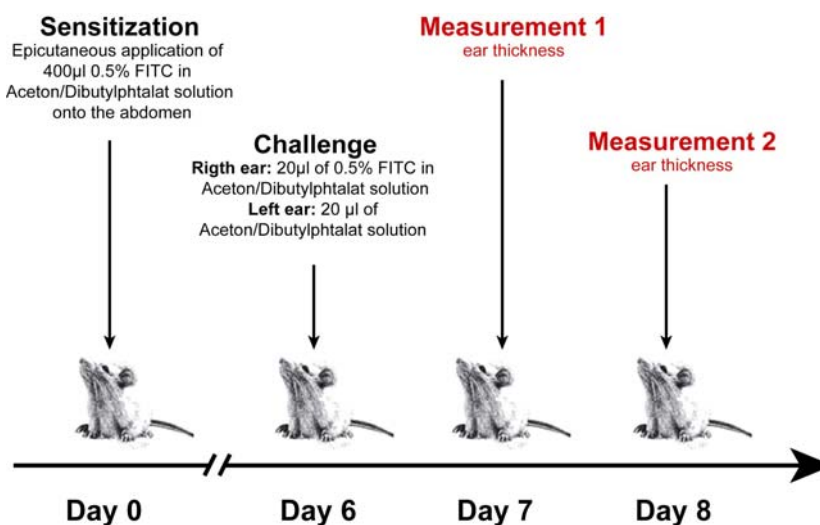


Figure 35: Type IV Hypersensitivity Experimental schedule

At day 1 after NP-O-SU challenge, WT animals developed an important swelling of the injected footpad compared to the contralateral foot treated with solvent control. In contrast, $S1P_4^{-/-}$ mice developed significantly less swelling following NP-O-SU challenge ($0,28 \pm 0.03$ mm versus 0.6 ± 0.01 mm in $S1P_4^{-/-}$ mice and WT mice, respectively; $p = 0.002$). At day 2 after challenge, these differences remained statistically significant (**Figure 36**).

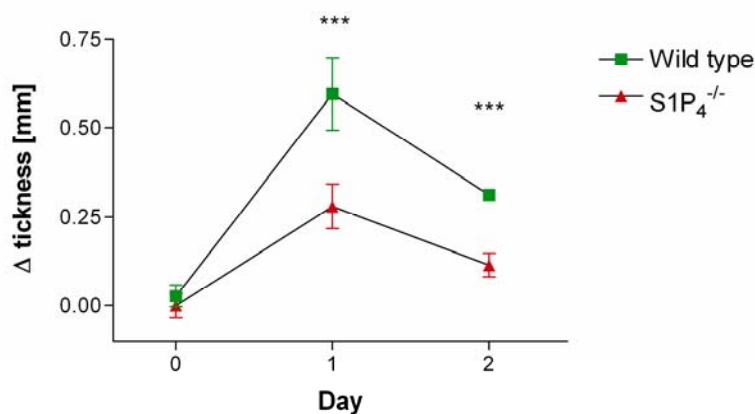


Figure 36: Type IV Hypersensitivity

Differences of foot thickness between the left (NP-O-SU) and right (solvent control) foot were measured at day 1 and day 2 after challenge. Results are representative of 2 independent experiments with 4 animals per group each. ***: $p < 0.005$

In conclusion, we showed that, as might have been expected from the phenotypic alterations reported in the first descriptive part, that KO mice are more prone to develop a T_H2 -type of response (CHS-FITC experiment), while those animals have reduced ability to develop a T_H1 -type of response (Typ IV hypersensitivity).

5.1.2.9. $S1P_4$ deficiency results in increased eosinophilic infiltration in a murine asthma model

Asthma is an allergic condition that is caused by a dysregulated T_H2 -biased immune response to environmental allergens. The disease is associated with elevated levels of T_H2 cytokines and increased production of IgE. An histopathological hallmark of asthma is the infiltration of the respiratory mucosa with eosinophils^{199,200}.

$S1P_4^{-/-}$ lymphocytes have shown an increased capacity for IL-5 secretion after anti-CD3/anti-CD28 stimulation *in vitro*. Moreover, $S1P_4^{-/-}$ mice show a decreased reaction in a murine model of T_H1 type immune response, as well as an increased contact hypersensitivity against a T_H2 sensitizer. We therefore wondered whether the lack of $S1P_4$ expression would result in an distinct behaviour of the $S1P_4^{-/-}$ mice in a murine asthma model.

$S1P_4^{-/-}$ and WT animal were sensitised by intraperitoneal administration of 10 μ g chicken egg ovalbumin (OVA) coupled to alum hydroxyd. Animals were than stimulated with inhalative ovalbumine (**Figure 37**). The inflammatory response was than measured by

quantifying the cellular infiltrate and cytokine levels in the bronchoalveolar lavage fluid (BALF).

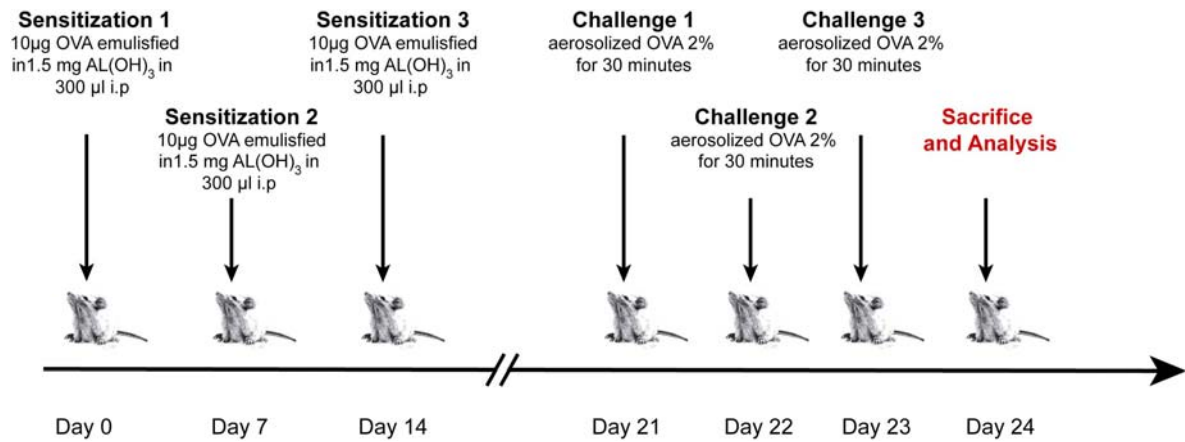


Figure 37: Murine asthma model: Experimental setting

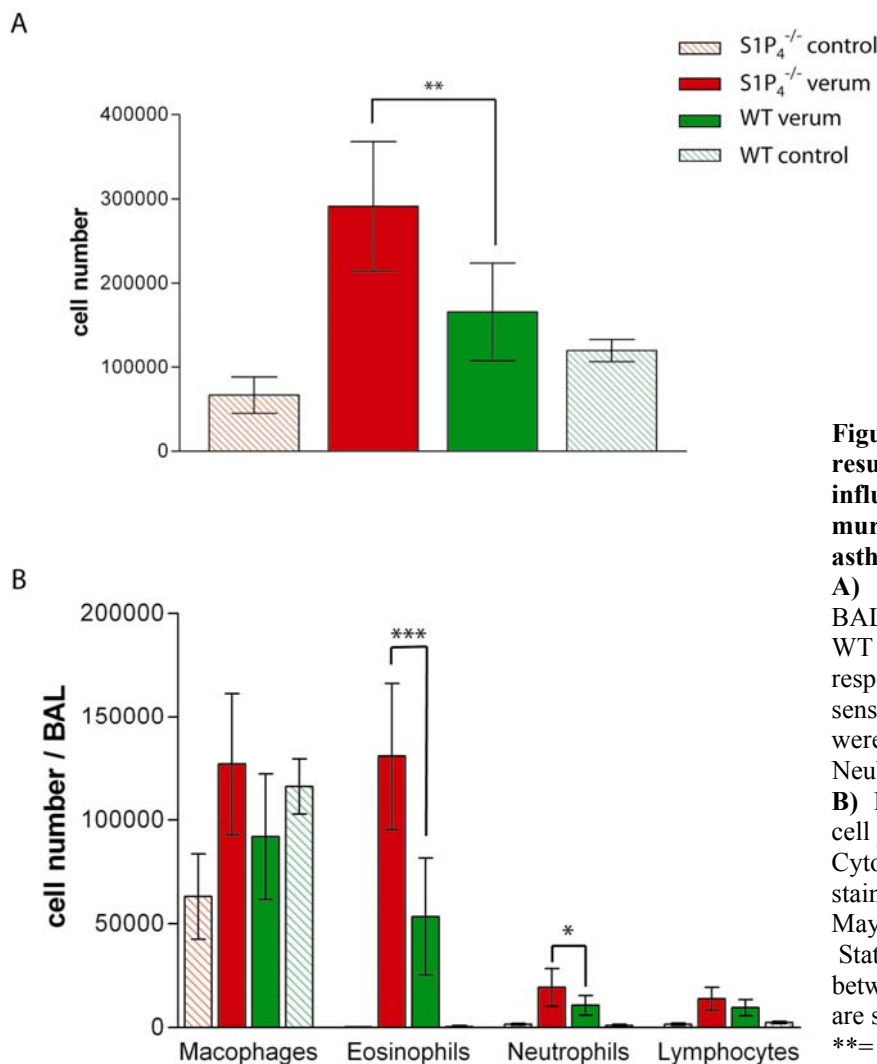


Figure 38: $S1P_4$ deficiency results in an increase cellular influx into the BALFs of a murine model of OVA induced asthma

A) Total cell numbers in the BALFs of $S1P_4^{-/-}$ mice (red) and WT animals (green) and the respective controls in non-sensitised but challenged animals were assessed with in Improved Neubauer hemacytometer

B) Differential cell count of the cell populations in the BALFs. Cytospins of the BAL cells were stained according to the method of May-Grünwald. (n = 8).

Statistically significant differences between the two sensitised groups are shown.

***= p < 0.005

The bronchial lavage fluid of S1P₄-deficient mice contained significantly higher total cell numbers than that of WT animals. While BAL from the lung of OVA challenged S1P₄^{-/-} animals contained a mean of $29.1 \pm 7.6 \times 10^4$ total cells, challenged WT mice showed only $16.6 \pm 5.8 \times 10^4$ cells (**Figure 38a**). In contrast to BALF from normal subjects that predominantly contains macrophages and minute numbers of lymphocytes and granulocytes, the cellular population of BALF from asthmatic subjects is predominantly composed of eosinophils and macrophages and to a lesser extent of neutrophils and lymphocytes. In order to assess whether the increase of the global cell number seen in S1P₄ animals was due to the increase of a single cell type or to a global and unspecific increase of all cell types, a differentia count of the BALF was performed (**Figures 38b and 39**).

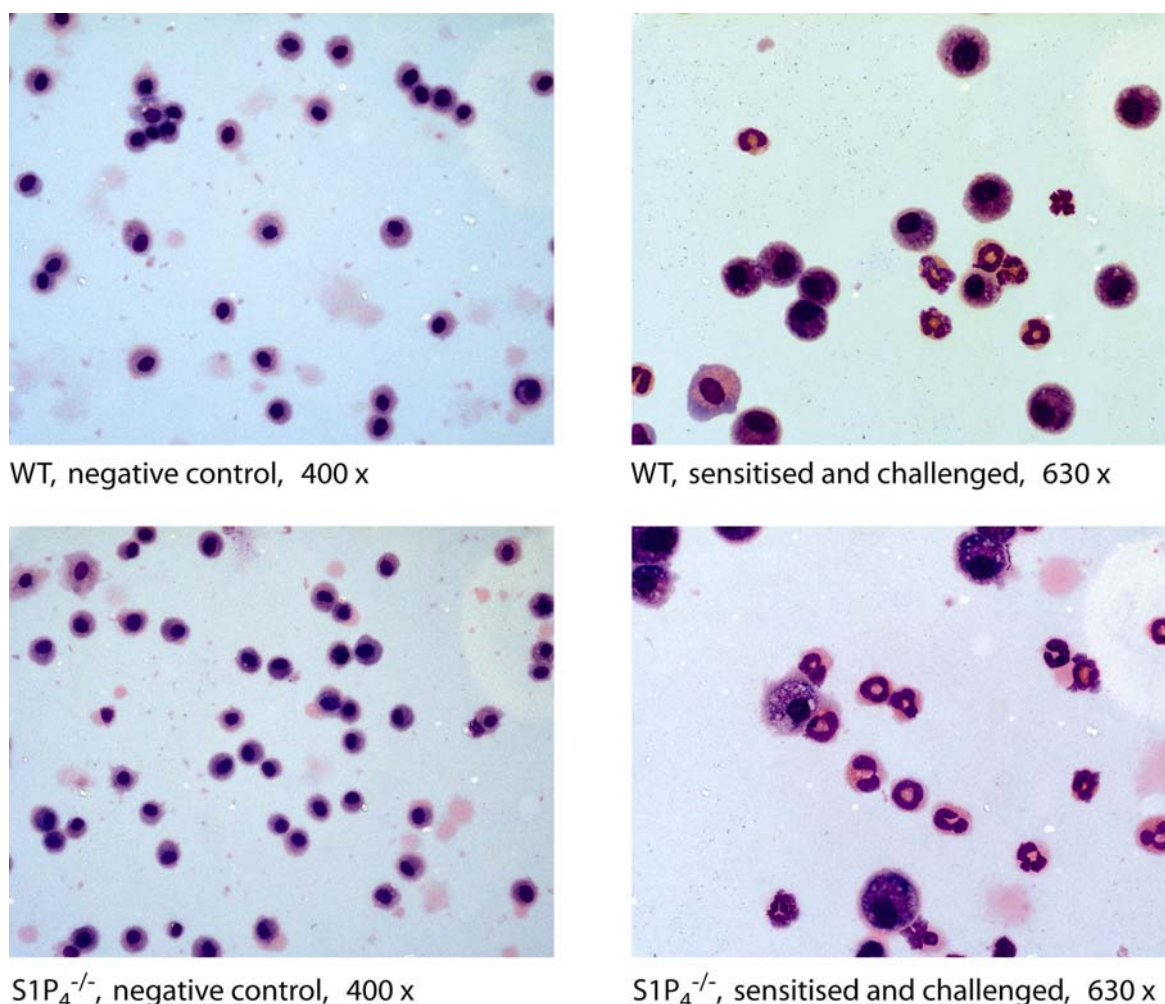


Figure 39: Cell populations in the BALF of S1P₄^{-/-} and WT animals suffering from OVA induced asthma Cytospins from BAL cells were stained according to the method of May-Grünwald. In the negative controls shown at a magnification of 400 x, no eosinophils can be found among a high number of macrophages (left). In contrast, numerous eosinophils are clearly visible in sensitised and OVA-treated animals. Higher ratios of eosinophils to macrophages were observed in S1P₄^{-/-} animals compared to WT animals (magnification 630 x; right).

Very interestingly, the higher total cell numbers seen in the BALF of S1P₄^{-/-} animals compared to WT animals was almost entirely due to a strong increase of infiltrating eosinophils ($13.1 \pm 3.5 \times 10^4$ versus $5.3 \pm 2.8 \times 10^4$ eosinophils in S1P₄^{-/-} versus WT animals, respectively; $p = 0,001$). A smaller but still significant difference was seen in neutrophils numbers ($1.9 \pm 0.9 \times 10^4$ versus $1.0 \pm 0.4 \times 10^4$ neutrophils in S1P₄^{-/-} versus WT animals, respectively; $p = 0,029$). In contrast, no significant differences were found in macrophage (12.6 ± 3.4 versus $9.2 \pm 3.0 \times 10^4$ macrophages in S1P₄^{-/-} versus WT animals, respectively) and lymphocyte cell numbers (1.4 ± 0.4 versus $1.0 \pm 0.4 \times 10^4$ lymphocytes in S1P₄^{-/-} versus WT animals, respectively).

The cytokine profile in the BAL was assessed by ELISA. The IL-4 levels showed no statistically significant differences between the sensitised and challenged S1P₄^{-/-} and WT mice (62.2 ± 26.2 pg/ml versus 104.7 ± 55.5 pg/ml, respectively; $p = 0.121$). In contrast, S1P₄^{-/-} mice showed significantly increased IL-5 levels compared to WT animals (482.1 ± 109.7 pg/ml versus 353.3 ± 112.8 pg/ml, respectively; $p = 0.029$) (**Figure 40**).

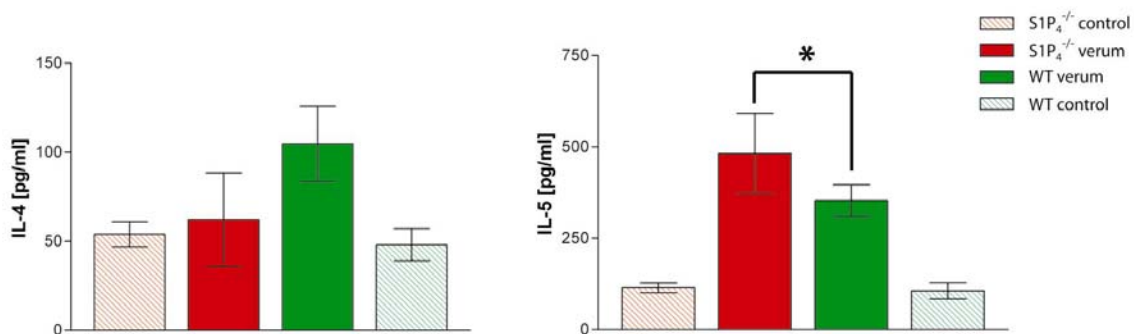


Figure 40: Cytokine production in the murine, ovalbumin-induced asthma model

IL-4 and IL-5 levels were determined in the BALF at day 1 after the last challenge with nebulised ovalbumin ($n = 8$). *: $p < 0.05$

5.2. Knock-down of the S1P₁ receptor in S1P₄^{-/-} mice

S1P₁ and S1P₄ are the predominant S1P receptors on human and murine lymphocytes. Both share the same high affinity ligand and signal *via* similar but not totally identical pathways.

The results of our *in vitro* and *in vivo* analysis of S1P₄^{-/-} mice, which we showed in the first part of the Results section, suggested that at least in some aspects of their development and functionality, the responsiveness of B- and T-cells to S1P signalling could be the integrated resultant of signal transduction *via* both receptors. In some processes, this interaction may be synergistic, in others, like for instance T-cell migration, it may be antagonistic. In order to dissect this intricate interaction between both receptors, a experimental model for a differential knock-down of these two receptors was required. The S1P₁^{-/-} phenotype was shown to be lethal *in utero* due to serious malformations of central vascular structures⁶³. Possible alternatives that have been used in experiments done to elucidate the biological function of S1P₁ are the generation of conditional S1P₁^{-/-} animals showing the lack of the gene of interest only in specific cell types e.g. lymphocytes, or the transfer of S1P₁^{-/-} foetal hematopoietic cells to WT animals.

However, with the advent of the siRNA technology, a further method became available for downregulation of S1P₁. Since this tool would be easily operational in various genetic backgrounds, our strategy was to employ a siRNA-based technology to stably knock-down S1P₁ in S1P₄^{-/-} and WT lymphocytes.

5.2.1. Generation of an expression vector for HA-tagged murine S1P₁

When this study was initiated, detection of endogenous S1P₁ expression was complicated by the lack of a S1P₁ specific antibody. In order to facilitate the functional assessment of various siRNA candidate sequences, we decided to generate an expression vector for HA-tagged murine S1P₁.

Total RNA was extracted from lung tissue isolated from Balb/c mice. After reverse transcription, the S1P₁ ORF was amplified by PCR. Primers were designed complementary to the 5' and 3' end of the S1P₁ ORF published in the NCBI Nucleotide database (accession number NM 007901). The 5'-primer contained the HA coding sequence as well as a BamH1 restriction site. The 3'-primer contained a Not I restriction site for subsequent subcloning of the PCR product (**Figure 41**).

5'-Primer

5'- CAT GGA TCC ATG GGC TAC CCA TAC GAT GTT CCA GAT TAC GCT GGT GGT CCC GTG TCC ACT AGC ATC CCG GAG -3'
BamH1 splice site HA-tag Complementary sequence

3'-Primer

5'- GAT TAG CGG CCG CGA GTT TTT TTT AGG AAG AAG AAT TGA CGT TTC C -3'
BamH1 splice site Complementary sequence

Figure 41: Primer design for HA tagged murine S1P₁

Primer for PCR amplification of the murine S1P₁ gene were designed based on the sequence published in the NCBI Nucleotide database. The 5'-primer contained the HA tag in order to guarantee for easy detection of HA at the cell surface. A BamH1 and Not I splice site were integrated in order to facilitate subsequent subcloning.

The PCR product that was obtained was subcloned into the pGEMT easy vector system. The PCR product was sequenced and 2 clones containing the correct sequence were identified. The insert of one of these clones containing the correct sequence was subcloned into the BamH1 / Not1 sites of the pcDNA3.1(+) expression vector (**Figure 42A**) thus generating the S1P₁ expression vector pcEDG1muHA.

The functionality of this expression vector was tested by transient transfection in cos7 cells (**Figure 42B**). As shown by western blot analysis, the anti-HA as well as an anti-S1P₁ antibody revealed the same band at ~42kD (**Figure 42C**). In addition, cell surface expression of HA-tagged S1P₁ was shown by FACS analysis of nonpermeabilized cos7 cells stained with an FITC labelled anti-HA antibody (**Figure 42D**).

After those verifications on the quality and specificity of our pcEDG1muHA expression vector, we used it in subsequent experiments to test the efficiency of various S1P₁-specific siRNA sequences.

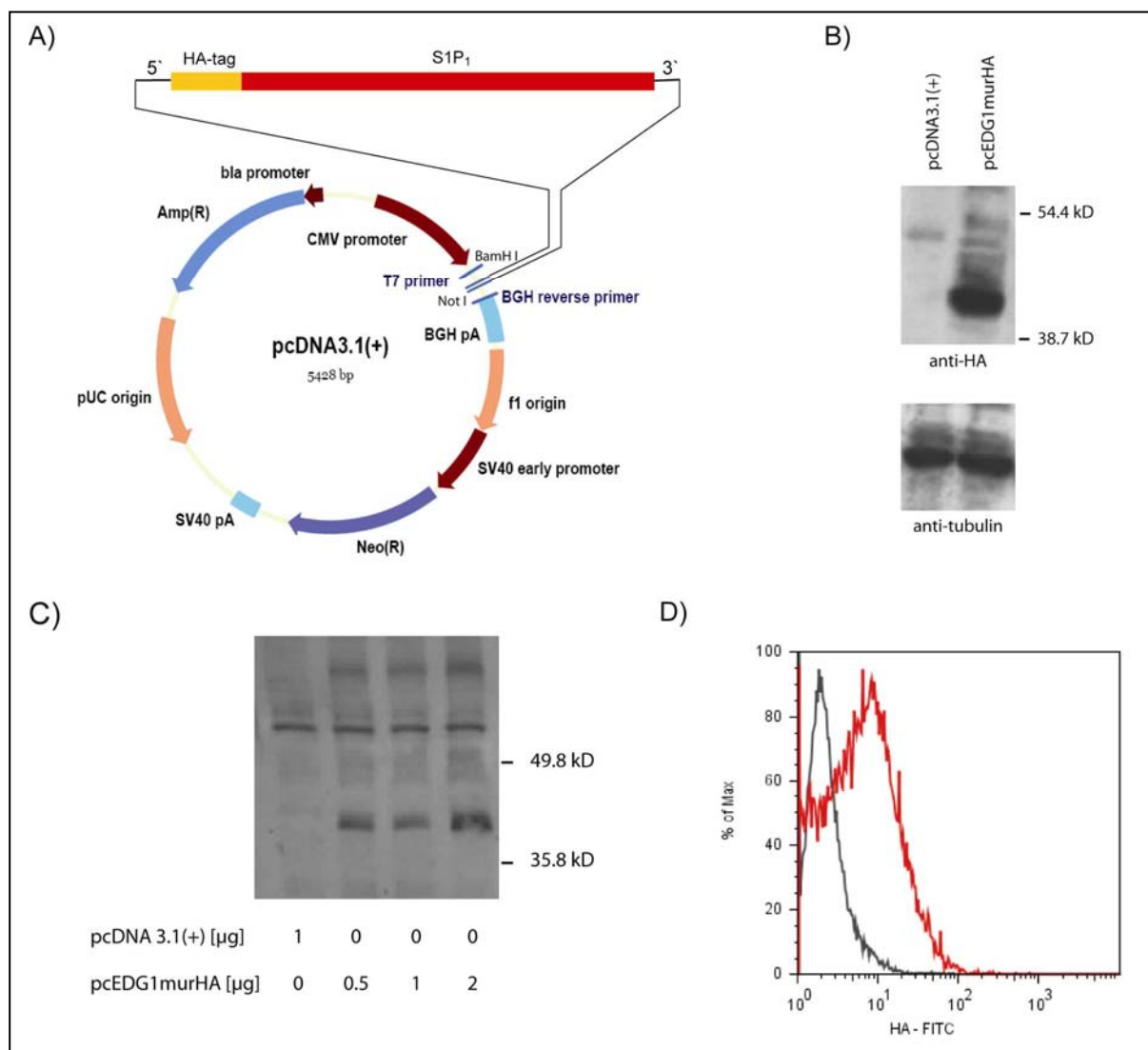


Figure 42: Generation of a plasmid expression vector for HA-tagged S1P₁

A) The PCR product was subcloned from the pGEMT easy plasmid into the NotI / BamHI restriction sites of the pcDNA3.1(+) vector. **B)** Transient transfection of the resulting pcEDG1murHA plasmid into cos7 cells resulted in the expression of a ~42kb protein detectable with a high affinity anti-HA antibody. **C)** A protein of identical size (~42 kb) was detected with an anti-S1P1 antibody. **D)** The HA tag at the amino-terminus of the S1P₁-HA protein could be easily detected by staining of nonpermeabilized, transfected cells with the FITC labelled anti-HA.

5.2.2. Identification of effective shRNA sequences for S1P₁ knock-down

5.2.2.1. Selection of potential siRNA targets within the S1P₁ ORF

SiRNA-mediated gene knock-down became increasingly popular during the past 4 years, leading to the development of various strategies for siRNA generation and delivery into living cells. Today, an increasing number of rules for the basic structure of efficient siRNAs is starting to emerge. Nevertheless, the effectiveness of potential siRNA sequences have still to be assessed experimentally since not every siRNA designed according to the current knowledge, induces satisfying gene knock-down. When the current project was initiated, only few empirical rules for efficient siRNA design were known. The potential target sequence

should contain 21 nucleotides starting with two adenosine nucleotides. Furthermore, it should not be situated within the first 100 nucleotides from the start- and the stop-codon. Moreover, the GC content should be contained within 30 % - 50 %. And finally, an exhaustive BLAST search should exclude the presence of the chosen target sequence in any other gene than the targeted one.

Applying these criteria and using the Ambion siRNA Target Finder, four potential target sequences in the S1P₁ ORF were selected. The localisation of the chosen targets within the S1P₁ gene and the target sequence are shown in **Figure 43**.

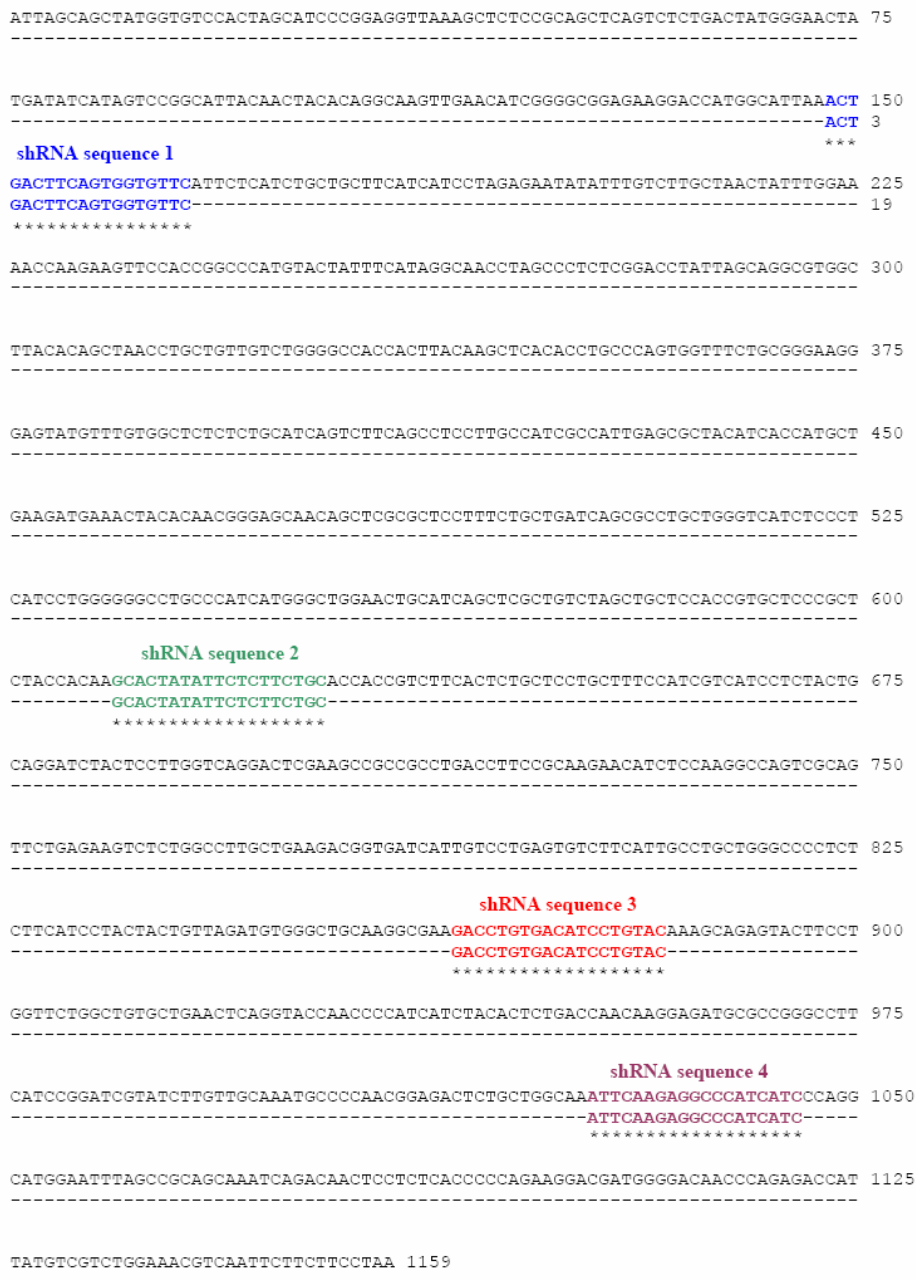


Figure 43: Localisation of potential shRNA sequences within the *s1p1* ORF: Multiple potential target sequences for shRNA specific for *s1p1* were generated using the Ambion siRNA Target Finder. A further pre-selection was done according to the criteria enumerated in the text. The finally selected shRNA sequences and their localisation within the *s1p1* ORF are shown.

5.2.2.2. Generation of expression plasmids for production of S1P₁-specific shRNA

SiRNA mediated knock-down in mammalian cells is transient. Depending on the proliferative status, siRNA activity persists only for 3-7 days in proliferating cells. However, in our experimental setting, a stable S1P₁ knock-down was required for long-term transfer experiments in the S1P₄ knock-out animals. Therefore, we decided to adopt a strategy for long-term vector-based suppression of S1P₁ expression. For this purpose, the selected siRNA target sequences were used to generate a vector system in which short hairpin RNAs were

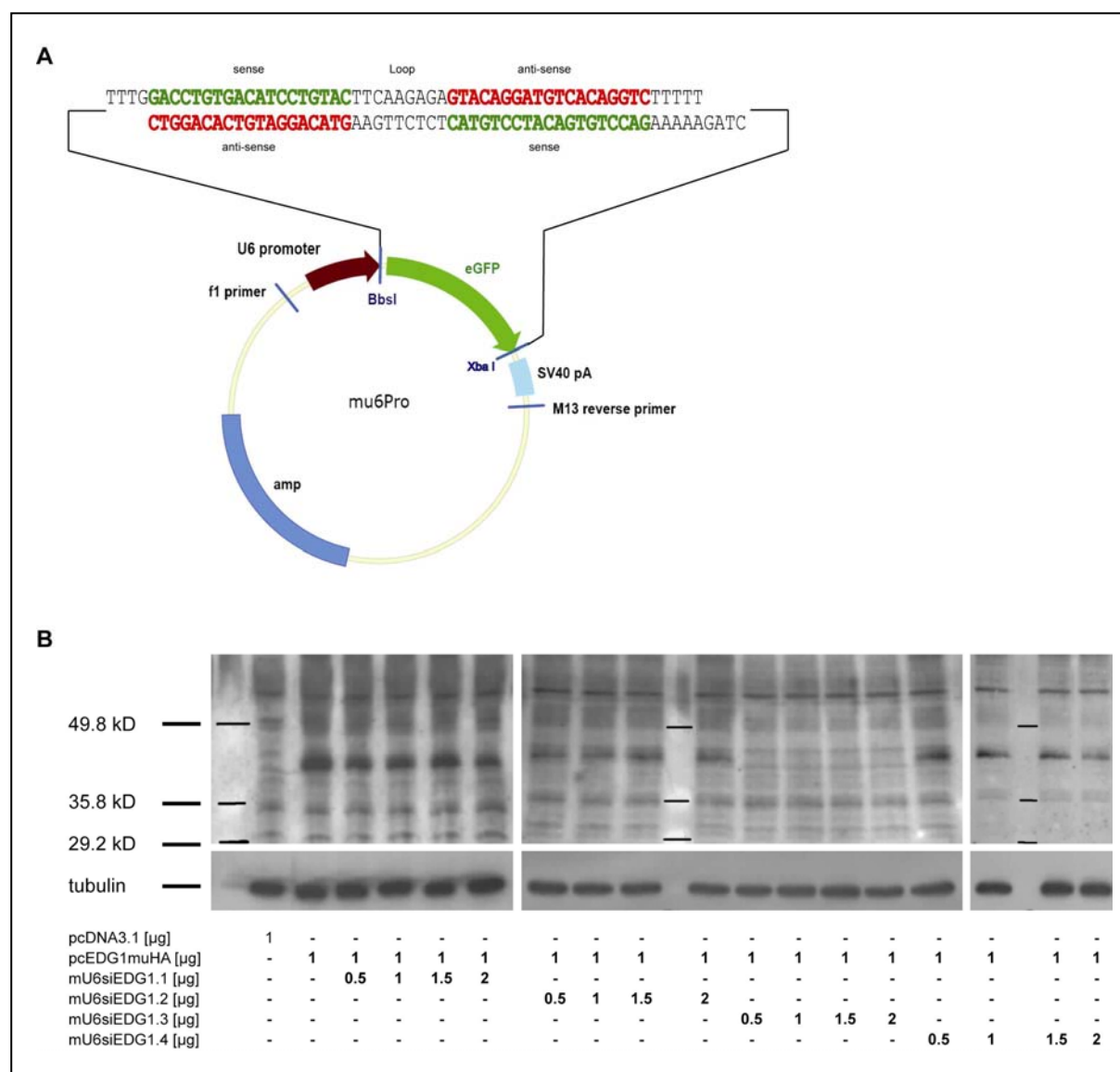


Figure 44: Generation of a plasmid expression vector for S1P₁ specific shRNA

A) Annealed oligonucleotides specific for the previously identified target sequences were cloned into the Bbs I /Xba I restriction sites of the m6pro plasmid. **B)** The potential for efficient shRNA-mediated S1P₁ knock-down was tested by transient co-transfection of pcEDG1muHA and the mu6prom –based shRNA constructs. Only sequence 3, that is contained within the shRNA plasmid mU6siEDG1.3, induced efficient suppression of HA-tagged S1P₁.

expressed under the control of the murine U6 promoter. The design of the short DNA fragment coding for the shRNA is depicted in **Figure 44a**. Briefly, this fragment consisted of the identified 19-nt sequences from the target transcript (sense) and the reverse complement of the same sequence (anti-sense), separated by a short 9-nt spacer as published by Brummelkamp *et al.*¹⁹⁶. After annealing of this oligonucleotide with a partner oligonucleotide of complementary sequence, the resulting short DNA fragments were cloned in the mu6prom vector downstream of the murine U6 promoter. The resulting constructs were sequenced for verification of the correct sequence of the siRNA fragment. In total, 4 plasmid constructs corresponding to the previously defined target sequences were generated (mU6siEdg1.1 – mU6siEdg1.4).

5.2.2.3. Assessment of the efficiency of the selected candidate siRNA sequences for S1P₁ knock down

The potential of each of the above mentioned shRNA constructs to suppress expression of HA-tagged S1P₁ in cos7 cells transiently transfected with pcEDG1muHA was assessed in a cell-culture system. This showed that transient transfection of pcEDG1muHA resulted in efficient S1P₁ expression. Oppositely, transient co-transfection of pcEDG1muHA and either mu6Edg1.1, mu6Edg1.2 or mu6Edg1.4 resulted in no (mU6siEdg1.1) or unsatisfying (mU6siEdg1.2 and mU6siEdg1.4) knock-down of S1P₁. However, co-transfection of pcEDG1muHA and mU6Edgsi1.3 resulted in an almost complete abolishment of S1P₁ expression. This effect was stable for a molecular mu6Edg1.3/pcEDG1muHA ratio used for transient transfection from 0.8 – 3 (**Figure 44B**).

We thus have shown that the siRNA sequence of mU6siEdg1.3 has a high potential for knock-down of S1P₁. Therefore, this sequence was chosen for all further cloning steps and experiments involving siRNA-mediated S1P₁ knock-down.

5.2.3. Generation of a retroviral vector for shRNA mediated knock-down of S1P₁

Efficient delivery of siRNAs or shRNA constructs into mammalian cells is primordial for efficient knock-down of the target gene. However, both lymphocyte cell-lines and freshly isolated primary lymphocytes or bone marrow cells constitute difficult targets for classical transfection methods. Here, retroviral or lentiviral vectors represent a promising alternative for efficient delivery of shRNAs. Moreover they offer the advantage of stable integration of the viral genome into the host cell genomic DNA, resulting in stable expression of the shRNA.

At the time of the initiation of this project, no retroviral vectors for shRNA expression were available. We thus decided to create our own retroviral shRNA vector system based on the pMP71linker system published by Engels *et al.* This vector system has previously been shown to infect very efficiently both T-cell lines (62 % of transduced cells at an MOI of 5) as well as primary lymphocytes (34 % of transduced cells at a MOI of 5). Furthermore, it contains the marker gene GFP under the control of the 5'-LTR, thus facilitating the identification of transduced cells (**Figure 45A**).

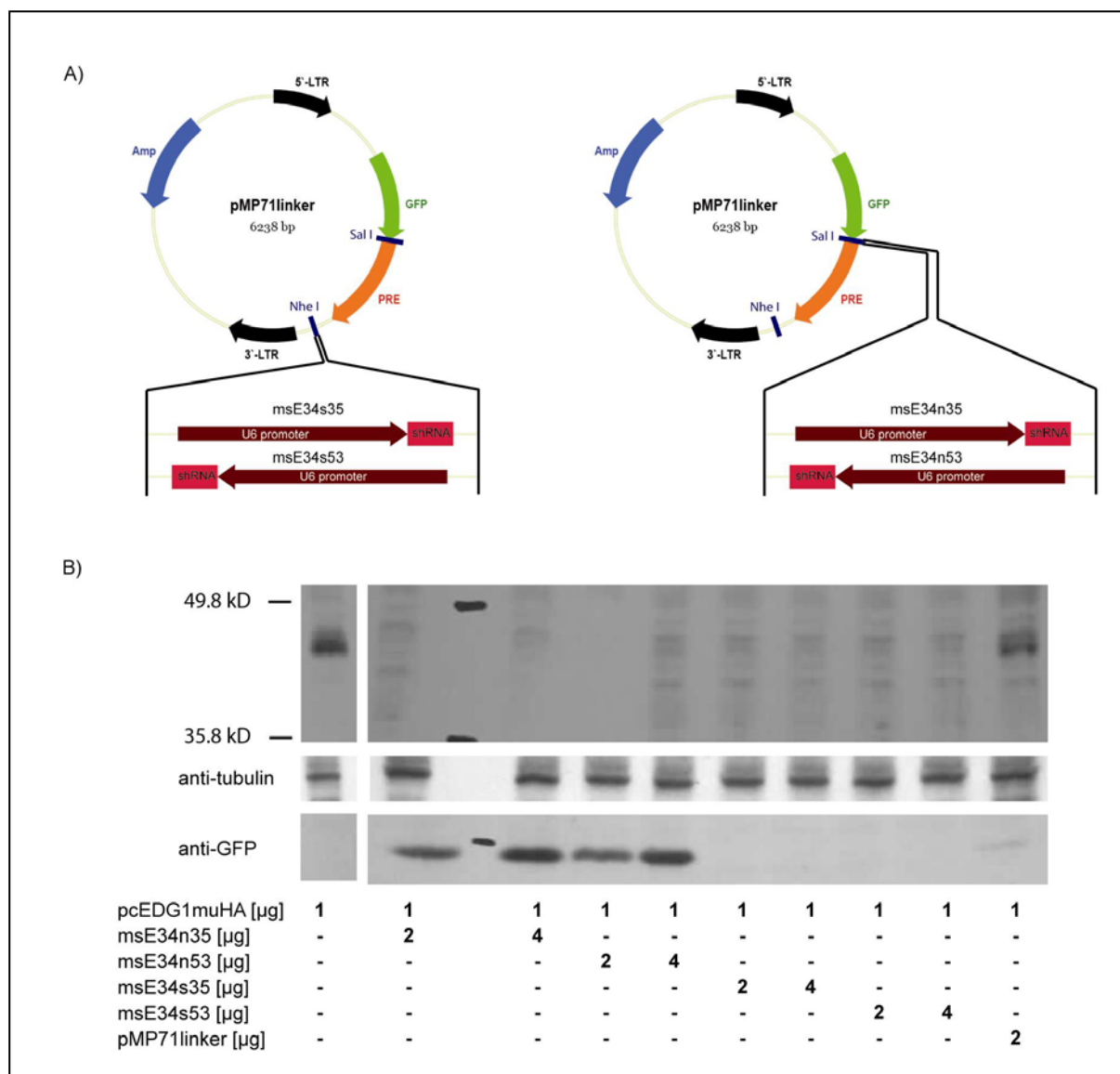


Figure 45: Generation of a retroviral vector for S1P₁ specific shRNA

A) A fragment containing the murine U6 promoter as well as the shRNA fragment 3 that has been shown to be highly effective for S1P₁ knock down were cloned into the retroviral plasmid pMP71linker. Four different constructs were generated. The fragment was cloned into the Sal I or the Nhe I restriction site of the pMP71 linker, in each case in both 5'→3' as well as 3'→5' orientation. **B)** The potential for efficient shRNA-mediated S1P₁ knock-down as well as expression of the marker gene GFP was tested by transient co-transfection of pcEDG1muHA and each of the generated constructs into cos7 cells. Constructs containing the insert in the Sal I restriction site did not show GFP expression. Constructs containing the insert in the Nhe I site both efficiently suppressed S1P₁ expression and induced GFP expression.

Expression of shRNAs requires a polymerase III promoter, *i.e.* the H1 or the U6 promoter. Since the original pMR71linker did not contain a polymerase III promoter, a fragment from the mU6siEdg1.3 plasmid containing U6 promoter and the shRNA sequence was cloned either in the Nhe I or the Sal I splice site of the pMP71linker (**Figure 45A**). In both sites, the inserts were cloned either in 5'→3' or 3'→5' orientation, giving rise to a total of four different constructs: msE34s53, msE34s35, msE34n53 and msE34n35.

The potential of each of the four constructs was assayed in cos7 cells co-transfected with pcEDG1muHA and the pMP71 linker-based shRNA constructs. As shown in **Figure 45B**, each of the four shRNA construct efficiently suppressed the expression of HA-tagged S1P₁. However, cloning of the U6 promoter-shRNA-fragment in the Sal I splice site immediately upstream of the PRE enhancer of pMP71linker completely abolished the expression of the GFP reporter gene, while it was maintained after cloning in the Nhe I splice site (**Figure 45B**).

In order to maintain the possibility to identify infected cells by the presence of the marker gene GFP, msE34n35 and msE34n53 were used for all subsequent experiments involving retroviral shRNA transfer.

For large scale virus production, the retroviral vectors msE34n35 and msE34n53 were co-transfected with pWL_{neo} into the ecotropic packaging cell-line GP+E86. Stably transfected cells were selected by a 10 day selection with G418. After the selection, bulk cultures were expanded and used to generate high-titer retrovirus-producing cells by two rounds of fluorescence activated cell sorting of high-fluorescence producing packaging cells (**Figure 46**).

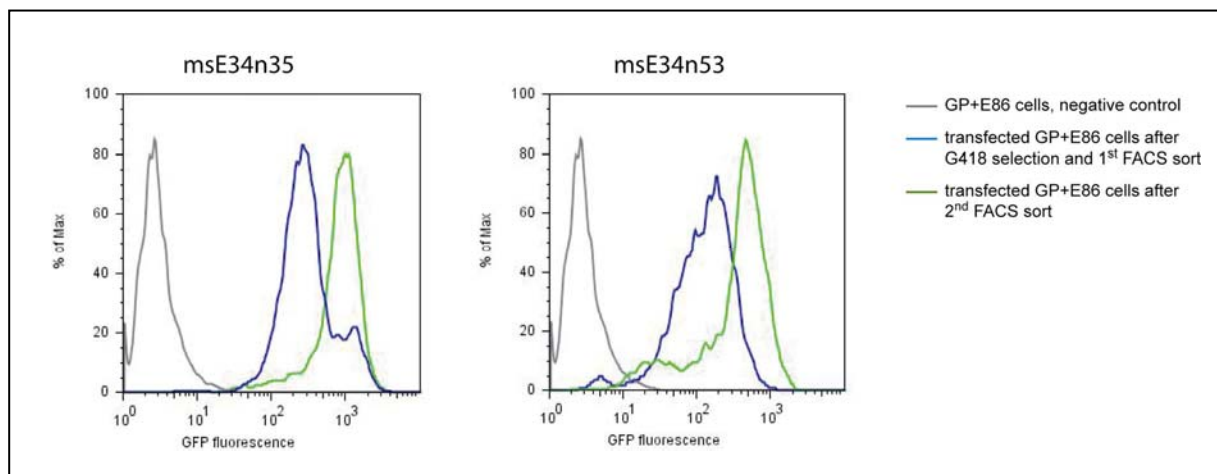


Figure 46: Generation of a stable packaging cell line for large scale virus production

The packaging cell line GP+E48 was stably transfected with the retroviral plasmids msE34n35 or msE34n53 as well as the pWL_{neo} plasmid. After a 10 day selection under G418, packaging cells with the highest GFP expression were isolated by two rounds of FACS sorting. These cells were subsequently used for large scale virus production.

The virus titer in the cell-culture supernatant was determined by infection of NHI 3T3 cells. Surprisingly, the virus titer produced by the highly GFP⁺ producer cells were extremely low (*i.e.* $21.9 \pm 4.9 \times 10^3$ GFU/ml). Multiple modifications of the experimental protocol including virus production by transient transfection of the packaging cell-line did not result in a substantial increase of virus titer. Given the fact that an MOI comprised between 5 and 10 is a minimum requirement for efficient infection of primary lymphocytes, the obtained virus titer were insufficient for the planned experimental settings.

We therefore decided to abandon the generation of the retroviral vector system, and to chose an alternative viral vector system.

5.2.4. Generation of a lentiviral vector for shRNA mediated knock-down of S1P₁

Human immunodeficiency virus-based vectors are increasingly used to transduce a wide variety of cells. In contrast to classical retroviral vectors, lentiviral vectors offer the advantage to transduce non-dividing and terminally-differentiated cells. Moreover, pseudotyping of the

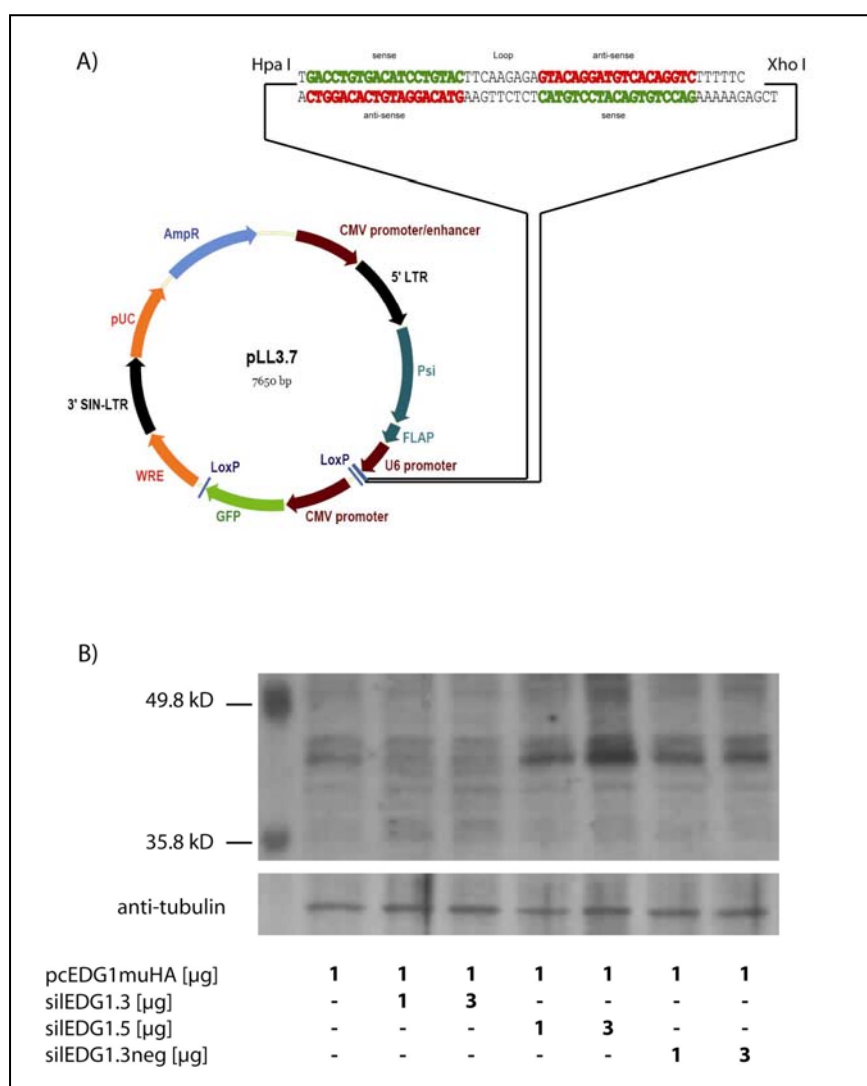


Figure 47: Generation of a lentiviral vector for S1P₁-specific shRNA

A) The oligonucleotides containing the shRNA sequence 3 was cloned into the Hpa I / Xho I restriction sites of the pLL3.7 plasmid.

B) The potential for efficient shRNA-mediated S1P₁ knock-down was tested by transient co-transfection of pcEDG1muHA and the silEDG1.3 plasmid.

silEDG1.3: contains the shRNA sequence 3; *silEDG1.5*: contains the nucleotides of the shRNA sequence 3 in a random order; *silEDG1.3neg*: contains the shRNA sequence 3 with 4 nucleotide exchanges

viral envelop with Vesicular Stomatitis Virus Glycoprotein (VSVG) protein offers the possibility to concentrate virus supernatants by ultracentrifugation, resulting in a titer increase of up to two logs.

As evoked in paragraph 5.2.3., we encountered massive problems to produce an appropriate virus titer in our retroviral vector system. We thus decided to generate a lentiviral vector system pseudotyped with VSVG. For that purpose, the shRNA sequence 3 was cloned in the Hpa I / Xho I site of the lentiviral pLL3.7 vector (**Figure 47**). As negative controls, two further shRNA inserts were generated: shRNA sequence 5 contains the nucleotides of the shRNA sequence 3 in a random order, and shRNA 3 neg contains 4 nucleotide exchanges within the original shRNA sequence 3.

Lentiviral vectors were produced by transient co-transfection in 293T cells as described in Materials and Methods. Virus titers varied between 1.2 and 6.7×10^6 GFU/ml. Concentration of virus particles by ultracentrifugation resulted in an about 10-fold increase of the virus titer of the initial preparation.

The capacity of silEDG1.3 vectors to transduce lymphocytes was first assessed in cultured murine T-cell lines. Depending on the T-cell line used in the assay, the transduction efficiency was between 75 - 85 % at a MOI of 5 (**Figure 48**).

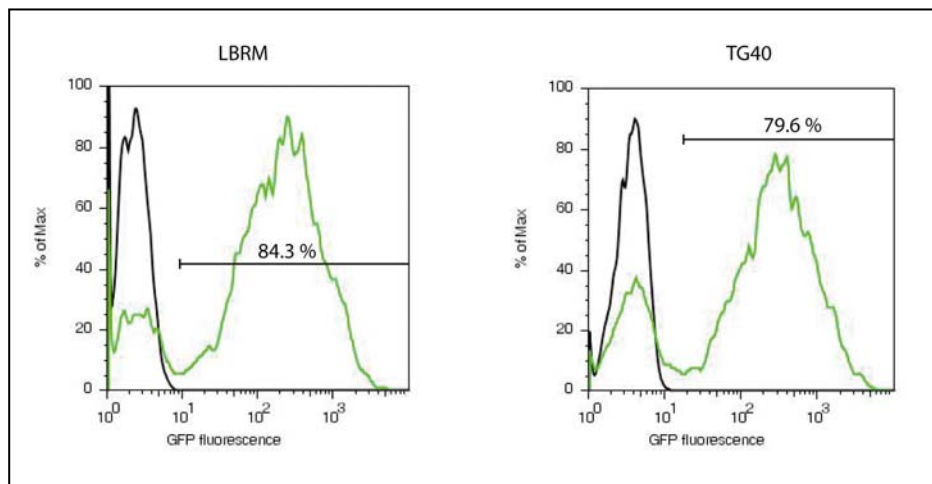


Figure 48: Transduction efficiency of lentiviral shRNA vectors
The murine T-cell lines LBRM (left) and TG40 (right) were transduced with the lentiviral vector silEDG1.3 at an MOI of 5. The percentage of GFP⁺ cells was assessed by FACS.

Next, we tested shRNA-mediated knock-down of the endogenous S1P₁ expression in the murine T-cell lines TG40 and LBRM. Cells were transduced with silEDG1.1 (containing the shRNA fragment 3), silEDG1.5 (containing the shRNA fragment 5 as first negative control) and the silEDG1.3 neg (containing the shRNA fragment 3neg as second negative control). After 1 week in culture, GFP⁺ cells were sorted by FACS and analysed for S1P₁ expression by semi-quantitative Ligthcycler[®] PCR. Transduction with silEDG1.3 resulted in a reduction of S1P₁ RNA expression of 10 %-25% of that of cells transduced with negative controls (**Figure 49**).

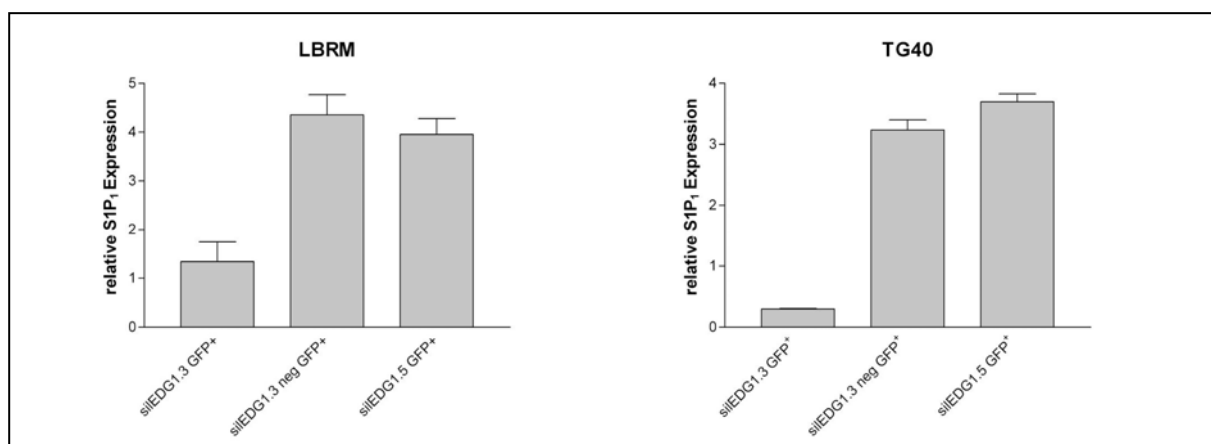


Figure 49: Highly efficient knock down of S1P₁ expression by lentiviral shRNA vectors

The murine T-cell lines LBRM (left) and TG40 (right) were transduced with the lentiviral vector silEDG1.3 as well as with the negative control vectors silEDG1.5 and silEDG1.3neg at an MOI of 5. GFP⁺ cells were isolated by FACS sorting. Relative S1P₁ expression in GFP⁺ cells was assessed by Lightcycler-PCR.

In order to assess whether expression of the GFP reporter gene correlates with the shRNA-mediated knock-down of S1P₁, LBRM cells were transduced with silEDG1.3 and silEDG1.3neg at a MOI of 5. After 1 week, bulk cultures were sorted in a GFP⁻ and GFP⁺ fraction. After additional 3 days in culture, endogenous S1P₁ expression was measured by semi-quantitative Lightcycler[®] PCR in both sorted fractions (**Figure 50**).

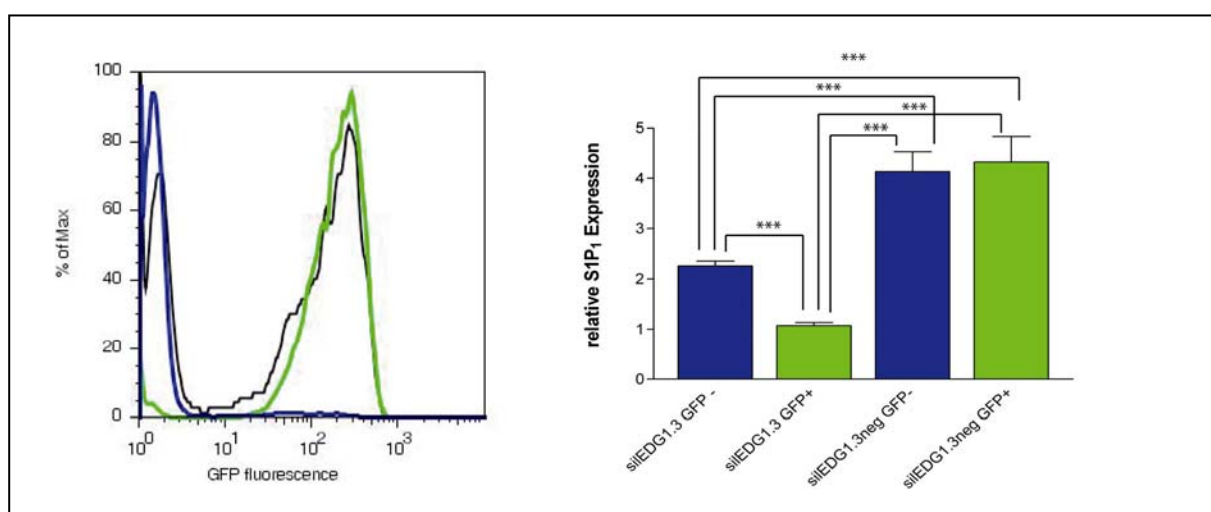


Figure 50: Correlation of S1P₁ knock-down and expression of the marker gene GFP

The murine T-cell lines LBRM (left) was transduced with the lentiviral vector silEDG1.3 and the negative control vector silEDG1.3neg at an MOI of 5. Bulk cultures of transformed cells were sorted in a GFP⁺ fraction (green) and GFP⁻ fraction (blue). Relative S1P₁ expression in both fractions were assessed by Lightcycler-PCR.

As expected, GFP⁺ cells transduced with silEDG1.3 expressed less S1P₁ than GFP⁻ silEDG1.3 transduced, silEDG1.3neg transduced GFP⁺ or GFP⁻ cells. Surprisingly, GFP⁻ silEDG1.3 cells expressed less S1P₁ than GFP⁺ or GFP⁻ cells transduced with the negative control virus. Thus, in some transduced cells, shRNA seems to be produced under the control

of the U6 promoter, while the expression of the marker gene GFP under the control of the CMV promoter seems to be absent.

An advantage of stable integration of lentiviral shRNA vectors in the genome of the transduced cells is the long-term expression and the persistent down-regulation of the target gene expression. In order to assess whether our vector system induces long-term S1P₁ down-regulation, TG40 and LBRM cells were transduced with silEDG1.3 and silEDG1.3neg at a MOI of 5. After one week, GFP⁺ cells were isolated from bulk cultures by FACS sorting.

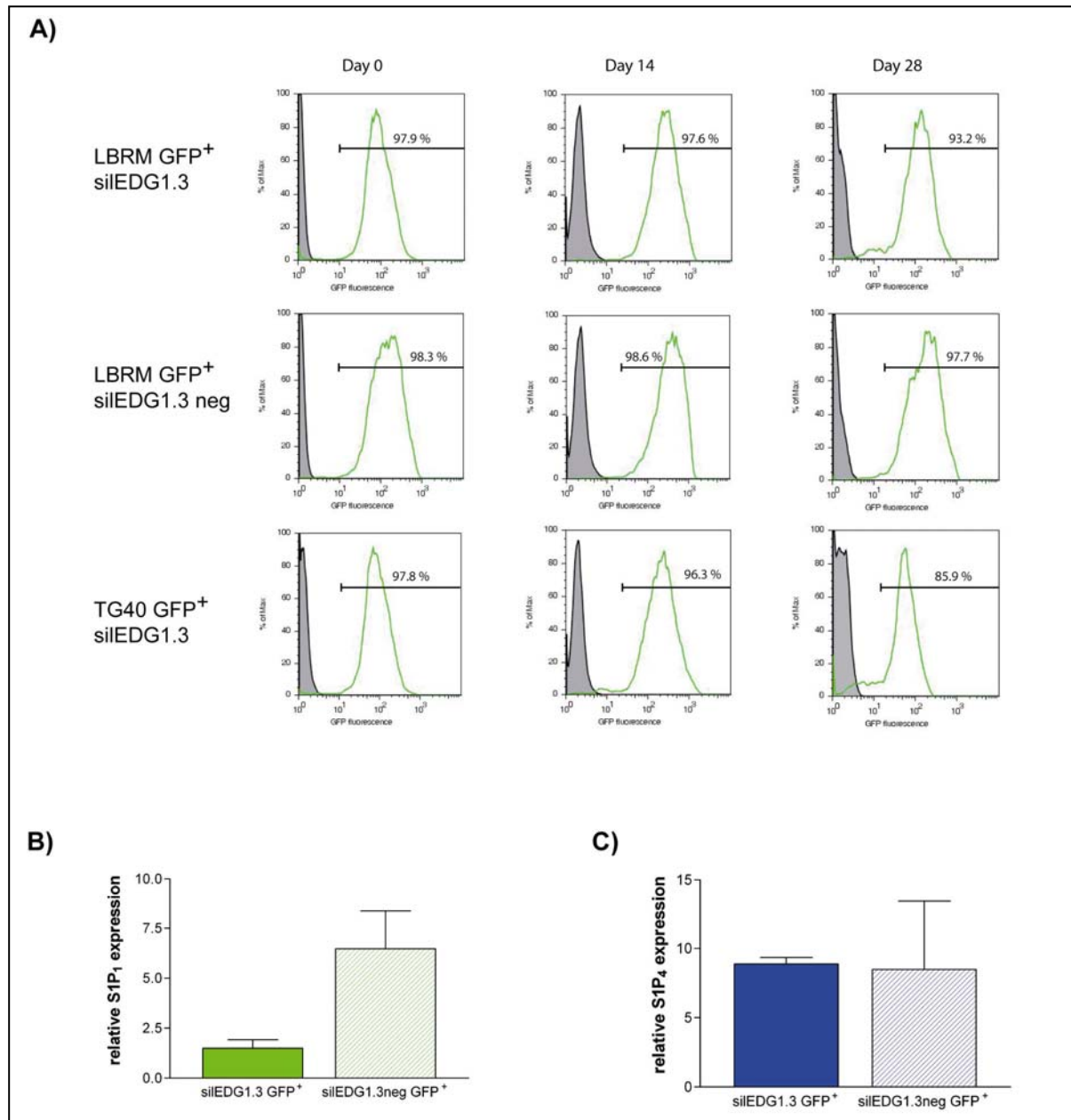


Figure 51: Long-term persistence of shRNA mediated S1P₁ knock-down

The murine T-cell lines LBRM (left) and TG40 (right) were transduced with the lentiviral vector silEDG1.3 and the negative control vector silEDG1.3neg at an MOI of 5. GFP⁺ cells were isolated from bulk cultures by two rounds of FACS sorting. GFP⁺ cells were cultured for 4 further weeks and GFP expression was assessed weekly by FACS. (A) RNA was extracted from GFP⁺ cells at the end of the 4 weeks culture period and relative expression of S1P₁ (B) and S1P₄ (C) were assessed by Lightcycler-PCR.

After 3 additional days in culture, the cells showing the highest GFP expression were sorted by FACS. These sorted GFP^{hi} cells were cultured for further 4 weeks under standard conditions and assessed for GFP expression by FACS at weekly intervals.

In LBRM cells, GFP expression remained almost constant over the observation period, and only 0.5 - 4.7 % of cells lost GFP (**Figure 51A**). In TG40 cells, slightly more cells lost GFP expression (up to 15 %) but the vast majority remained GFP⁺. After long-term culture, S1P₁ expression was assessed in GFP⁺ cells by Lightcycler PCR. As shown in **Figure 51B**, S1P₁ knock-down in GFP⁺ cells remained effective after 28 days in culture. Of note that levels of S1P₄ mRNA were not affected by transduction of the cells with the lentiviral S1P₁ specific shRNA vector (**Figure 51C**).

6. DISCUSSION

The present work aims at the delineation of the physiological role of the G-protein coupled receptor S1P₄ by means of the phenotypic characterisation of a S1P₄-deficient mouse model (S1P₄^{-/-}). Until present, the *in vivo* role of this receptor remains largely unknown. During the progress of this work, an important amount of seminal work on other S1P receptors has been published, inciting us to reconsider certain observations previously made in our model in the new light of recent findings.

In the first following chapter, we will discuss the biological significance of the findings made in our experimental S1P₄^{-/-} model in the context of the current knowledge on the role of S1P signalling in the immune system.

6.1. Functions of S1P₄ expression in the immune system

6.1.1. S1P₄ deficiency only marginally affects B and T-cell distribution within lymphatic organs.

In recent years, S1P signalling has received growing interest for its implication in lymphocyte trafficking. A seminal event in S1P-related research was the finding that FTY720, an immunosuppressive drug synthesized in the mid-1990's, was a high affinity ligand for the S1P receptors S1P₁, S1P₃, S1P₄ and S1P₅¹²⁹. Administration of FTY720 to rats results in a redistribution of lymphocytes between the circulatory (lymph and blood) and secondary lymphoid tissue compartments. T- and B-cell numbers were reduced in the blood, the lymph of the thoracic duct and to a considerably lesser extent in the spleen, while their numbers were largely increased in peripheral and mesenteric lymph nodes (respectively pLN and mLN) as well as the Peyer's patches (PP). The exact mechanism of the induction of peripheral lymphopenia remained matter of an intense scientific debate for a long time. In 2004, Matloubian *et al* showed that S1P₁ deficient lymphocytes transferred to lethally irradiated WT animals showed a distribution similar to that of FTY720-treated lymphocytes. Moreover, lethally irradiated WT recipients reconstituted with S1P₁^{-/-} foetal liver cells showed peripheral T-cell lymphopenia due to an impaired thymic emigration¹. These observations suggested that S1P₁ might be a S1P receptor with crucial implication in the regulation of lymphocyte trafficking. The apparent contradiction that the binding of the agonist FTY720 to the S1P₁ receptor results in a phenotype identical to that induced by a deficiency of the same receptor was resolved by findings of Graeler *et al*, who showed in an *in vitro* model that FTY720 induced a S1P₁ desensitisation by internalisation of this receptor¹³¹.

The role of the second S1P receptor present at high levels on lymphocytes, S1P₄, in these lymphocyte distribution has never been assessed *in vivo*. Our S1P₄^{-/-} mice offered an appropriate model answer to this question. We therefore assessed the cellular composition of primary and secondary lymphatic organs by FACS. No major aberrations of T and B-cell distribution within blood, spleen and thymus could be detected. In contrast, CD19⁺ B-cell numbers in peripheral lymph nodes were significantly reduced by ~25 % in S1P₄ deficient mice. A similar tendency occurred in the mesenteric lymph nodes, but failed to reach statistical significance. Quite interestingly, after FTY720 administration or in experiments with S1P₁^{-/-} lymphocytes, an accumulation of B-cells in the pLN and mLN was observed, although this accumulation was less pronounced than that of T-cells^{1,129}. This finding may suggest opposing functions of the two predominant lymphocyte S1P receptors at the B-cell level. These opposing effects of S1P₁ and S1P₄ deficiency were also observed in some functional assays that were performed in this work and which will be discussed later. However, the observed quantitative differences in B-cell numbers in mLN and pLN can originate at least from two different mechanism. First, S1P₄ deficiency may influence the migrational behaviour of B lymphocytes. Second, S1P₄ deficiency may influence B-cell activation and proliferation. The results of the *in vitro* migration assays argue against the former hypothesis. Moreover, all organs assessed showed slightly reduced B-cell numbers, proposing a reduced total number of peripheral B-cells rather than an imbalance of cell distribution.

In the bone marrow, the fraction of CD8⁺ cells was increased in S1P₄^{-/-} animals compared to their wild type littermates. An implication of S1P signalling in the organ distribution of CD8⁺ cells in spleen, pLN, mLN and PP has been reported in the literature, however, a role in the regulation of CD8⁺ trafficking to the bone marrow has not been shown yet. The biological implication of our observation is as yet unknown.

6.1.2. Signalling via S1P₄ impacts on T- but not on B-cell migration

The question whether S1P₄ mediates migratory response to S1P is still a matter of debate. *In vitro* assays using S1P receptor transfectants or the functional and non-selective S1P receptor antagonist FTY720 gave conflicting results. While Wang *et al* found neither migration to S1P gradients nor modification of chemokine induced migration in S1P₄ transfectants, Matsuyuki *et al* reported opposite findings^{6,73}.

Our *in vitro* migration experiments performed with S1P₄^{-/-} lymphocytes indicate that S1P₄ is implicated in the regulation of CD4⁺ and CD8⁺ cell migration. Both S1P₄^{-/-} CD4⁺ and

CD8⁺ cells showed an increased migration to a S1P gradient compared to their wild type counterparts. In contrast, S1P₄^{-/-} and WT B-cells showed no differences in their migrational behaviour in response to a S1P gradient. The clear reduction of T-cell migration in cells with functional S1P₄ suggests an inhibitory role for this receptor. In our experimental model, WT CD4⁺ and CD8⁺ showed no migratory response to a S1P gradient in the tested range (0-100 nM). This type of response is usually seen in activated lymphocytes or after exposure to S1P concentrations susceptible to down-regulate the presence of S1P₁ on the lymphocyte surface. We cannot exclude that cells have encountered elevated S1P concentrations during isolation from mice spleen. However, even if partial down-regulation of S1P₁ might have had occurred in both experimental groups, the conclusion remain unchanged, clearly proposing a functional antagonism between S1P₄ and S1P₁ in the regulation of S1P-induced migration.

A second experimental model provides additional data in favour of an implication of S1P₄ in cell migration. In a murine model, Schwab *et al* has shown that administration of the vitamin B6 antagonist DOP results in peripheral lymphopenia due to reduced egress of T lymphocytes from the thymus and sequestration of lymphocytes in secondary lymphoid organs. This sequestration was shown to result from an inhibition of cellular S1P lyase with a consecutive increase of tissular S1P concentration. In their model, this increase of local S1P concentrations resulted in agonist-induced desensitisation of S1P₁, leading to in reduced S1P₁ mediated egress from thymus and peripheral lymph nodes. The role of S1P₄ in their system has never been assessed¹⁹⁷.

In our experimental model, oral administration of DOP resulted also in induction of peripheral lymphopenia. As described by Schwab *et al*, T-cell numbers were much more potently reduced than B-cell numbers, as shown by an inversion of the B-cell/T-cell ratio in peripheral blood of DOP-treated animals compared to control mice. However, while DOP treatment similarly reduced B-cell numbers in the peripheral blood of S1P₄^{-/-} and WT mice, the reducing effect on T-cell numbers was stronger in the peripheral blood of DOP-treated S1P₄^{-/-} animals than in DOP-treated control mice. The interpretation of this finding in this complex model is difficult. Measurement of tissue and plasma S1P levels in our mice showed that the physiological S1P gradient (i.e.: higher plasma and lower tissue S1P concentrations) found in untreated animals is actually inversed after DOP treatment. In this perspective, the described finding is in line with our *in vitro* observation of an increased migration of S1P₄^{-/-} CD4⁺ and CD8⁺ lymphocytes in response to an S1P gradient. Accordingly, S1P₄^{-/-} and WT B-cells showed no differences in the migrational response to S1P *in vitro*, and those cells were similarly affected by *in vivo* DOP treatment in WT and S1P₄^{-/-} mice. However, further

experiments are required to better characterize the experimental model and to ascertain this interpretation of our findings. The amplitude and the kinetics of ligand-induced internalisation of S1P₁ and S1P₄ under DOP-treatment should be assessed in WT lymphocytes. However, the generation of S1P₁/S1P₄ double deficient lymphocytes and S1P₁ deficient lymphocytes using our lentiviral system for shRNA mediated S1P₁ knock down will allow for a more sophisticated dissection of the intricate roles of S1P₁ and S1P₄ in lymphocyte migration.

6.1.3. S1P₄ does not impact on tissular S1P levels

S1P signalling *via* Gi coupled S1P receptors has been shown to result in intracellular sphingosine kinase activation and in an increase of intracellular S1P¹⁰⁹. The specific S1P receptor mediating this response has not been identified yet. We therefore measured plasma and blood cell S1P levels in order to assess a potential implication of the S1P₄ receptor in the regulation of S1P synthesis. Neither under basal conditions nor after blockage of the S1P degrading enzyme S1P lyase by DOP, we could reveal any difference in S1P concentration between S1P₄ and WT control animals whatever the tested compartment. These data suggest that S1P₄ is not the receptor responsible for S1P mediated sphingosine kinase activation.

6.1.4. Signalling via S1P₄ does not impact on T-cell proliferation

Several reports have clearly shown that S1P negatively affects T-cell proliferation^{135, 139}. In order to evaluate whether S1P₄ is implicated in this inhibition, we assessed proliferation of CD4⁺ and CD8⁺ T-cells after stimulation with anti-CD3/anti-CD28 antibody or in mixed lymphocyte reaction (MLR). In both stimulating conditions, no differences were found between the proliferative activity of S1P₄^{-/-} CD4⁺ and CD8⁺ lymphocytes and that of the corresponding WT control cells. This clearly indicates that S1P₄ is not involved in the transmission of negative S1P signalling on T-cell proliferation. This finding is at odds with the report of Wang *et al* who showed that proliferation of the T-cell lines EL-4.IL-2 and D10G4.1 both stably transfected with S1P₄ was inhibited by S1P in a dose-dependent manner⁷³. However, both cell lines were later shown to express significant levels of endogenous S1P receptors other than S1P₄, rendering questionable the conclusion that the observed inhibition was mediated by S1P₄ in the experimental setting of Wang *et al*⁶. Other investigators have shown in various transgenic models, that the S1P₁ receptor is crucially implicated in the transmission of negative S1P signals on T-cell proliferation^{139,201}.

In conclusion, our data clearly show that S1P₄ is not the S1P receptor transducing negative S1P signals on T-cell proliferation and by exclusion suggest that the S1P₁ is the S1P

receptor implicated in this process. The use of our lentiviral vector system for shRNA mediated S1P₁ knock-down might allow to confirm this conclusion.

6.1.5. S1P in humoral immune response

6.1.5.1. S1P₄^{-/-} mice show increased IgG1, IgA and IgE levels

Experiments involving immunisation of FTY720 treated mice suggest that S1P signalling is implicated in the development of humoral immune response¹⁹². The determination and quantification of the isotypes of plasmatic immunoglobulins was therefore an obvious next step in the characterisation of the S1P₄^{-/-} immune phenotype. Naive S1P₄^{-/-} mice had significantly higher IgG1, IgE and IgA plasma levels compared to their wild type littermates. The other isotypes showed similar levels in knock-out and WT animals. These relative differences were also found in plasma.

Ig class switching is the process by which B-cells shift from IgM production to production of IgE, IgA or to one of the IgG subclasses. It involves deletional DNA recombination between the switch region of the μ gene of the Ig heavy chain and the switch regions situated upstream of each remaining immunoglobulin heavy chain gene. Certain cytokines have been shown to directly push B-cells towards switching to specific isotypes. Thus, IL-4, *via* STAT6 activation, induces Ig class switching to IgG1 and IgE. TGF- β induces preferentially the switch to IgA and IgG2b. And finally, IFN- γ promotes the Ig class switch to IgG2a and IgG3 (reviewed in²⁰²). Conversely, each of these chemokines is also capable of inhibiting the production of specific Ig classes. Indeed, IL-4 inhibits production of IgM, IgG2a and IgG3; IFN- γ inhibits production of IgM, IgG1 and IgE and TGF- β inhibits IgM and IgG3 production. Other stimuli are capable of increasing production of certain Ig classes upstream from the step of Ig class switching. Thus, IL-5 increases IgA secretion by promoting the maturation of post-switch surface IgA positive cells²⁰³.

In the S1P₄^{-/-} model, increased plasma and serum levels of those Ig classes is found whose generation is induced/supported by the T_H2 cytokines IL-4 and IL-5. This observation suggests that S1P₄ mediated S1P signalling may be implicated in the T_H1/ T_H2 polarisation of the immune response. This hypothesis that will be discussed in chapter 6.1.7. in the light of further findings. Whether this Ig profile is due to an effect on T helper cell/ B-cell interaction, on the intrinsic T helper cell function or an event located even more upstream at the dendritic cell (DC) level remains to be shown.

A further explanation for the observed differences is a direct effect at the B-cell level. That B-cells may be influenced by S1P₄ deficiency is suggested by the quantitative

differences found within the peripheral lymph nodes and, to a lesser and not statistically significant extent, in the mesenteric lymph nodes. This possibility urged us to analyse in greater detail the B-cell compartment in our mouse model, including the bone marrow and the spleen. These findings will be discussed in chapter 6.1.6.

Interestingly, Graeler *et al* found significantly increased basal IgE levels in a transgenic mouse model overexpressing human S1P₁²⁰¹. The identical change of basal IgE levels in an S1P₁ overexpressing model and in S1P₄ deficient animals makes it particularly tempting to speculate that there is an opposing effect of these receptors on IgE production.

Increased IgE levels are also found during parasite infections. Thus, elevated IgE levels could also be due to isolated helminth infection of the S1P₄^{-/-} group. However, screening for helminth infection is routinely performed in our animal facility.. Moreover, the close contact between S1P₄^{-/-} animals and WT controls in the animal facility renders an isolated infection of one of the two groups unlikely.

6.1.5.2. The humoral response to SRBC is normal in S1P₄^{-/-} mice

Han *et al.* have previously shown that blockade of S1P signalling with FTY720 reduced the T-cell dependent (TD) IgG1 response by inhibiting germinal centre reaction while the IgM response remained unaffected. In contrast, the T-cell independent (TI) humoral immune response was not affected¹⁹². Other investigators using different antigens and FTY720 dosages found no such effect on the TD humoral immune response¹²⁴. The specific S1P receptor mediating this effect is as yet unknown.

In order to assess whether S1P₄ deficiency impacts on the regular TD immune response, we immunized S1P₄^{-/-} mice and WT control mice with sheep red blood cells, an antigen known to induce a strong germinal center reaction. Neither the primary response (measured 14 days after primary immunisation i.p). nor the secondary response to a booster immunization (15 days after the primary immunisation) showed significant differences in SRBC-specific plasma IgM or IgG1 levels. Similarly, no differences in the kinetics of the Ab response could be detected between both genotypes. These findings suggest that S1P₄ deficiency has not impact on the development of the humoral immune response to T-cell dependent antigens. However, the interpretation of our findings should be done with caution. The antigen SRBC was chosen for its capacity to induce a strong germinal reaction. Its strong drawback in our model is its polyclonality. Although Ag-specific Ab to soluble SRBC antigen can be detected by ELISA, it was not possible to differentiate between high- and low-affinity antibodies. Given the fact that FTY720 treatment had a much stronger impact on high-affinity antibodies to TD antigens suggesting a defect of affinity maturation, our

experimental model might lack sufficient sensitivity to detect these differences¹⁹². Further experiments to assess the TD response to more defined TD antigen such as NP-CGG that allows for differentiation between low- and high-affinity antibodies are required and presently under investigation.

6.1.5.3. S1P₄ deficiency affects intestinal IgA levels

Mucosal IgA levels in the bronchoalveolar lavage fluid (BALF) of S1P₄^{-/-} animals were indistinguishable from those of WT animals, and IgA levels in the gastrointestinal lumen fluid (GILF) of S1P₄^{-/-} animals showed a significant reduction of almost 31% compared to WT control mice. These findings were quite unexpected given the moderate but significant increase of plasma IgA levels found in S1P₄-deficient animals.

The majority of antibody-secreting cells (ASC) after immunization by the intestinal route is found in the intestinal lamina propria as well as in Peyer's patches. A significant fraction of these ASC's derive from B1 cells, that are usually induced to undergo class switch and plasma cell differentiation locally. Other ASC's in the lamina propria and Peyer's patches derive from classical follicular B-cells that have been activated by T-cells in the Peyer's patches. In response to activation, these ASC leaves the intestine *via* the mesenteric lymph nodes and start to produce antibodies while circulating through the spleen. Finally, they home to the intestinal lamina propria and contribute to the production of mucosal IgA. The homing of the activated B-cells/plasma cells is a complex process essentially controlled by chemokines and adhesion receptors. Thus, CCR9-mediated CCL25 signalling and CCR10-mediated CCL28 signalling have been shown to be involved. Homing to the mucosa is further ensured by specific adhesion molecules, like $\alpha_4\beta_7$ integrin (reviewed in²⁰⁴). Further "players" in the induction and maintenance of intestinal IgA levels are intraepithelial lymphocytes (IEL). Gamma/delta IELs were shown to enhance antigen-specific as well as polyclonal IgA response in the lamina propria of the gut²⁰⁵. The reduction of GILF IgA levels may stem from an impact of S1P₄ deficiency at various levels. First, the frequency of B1 B-cells or follicular B-cells in the Peyer's patches may be reduced, thus reducing the number of potential ASC precursors. Secondly, the complex migrational process of follicular B-cells from the point of activation, namely the Peyer's patch to the point of final antibody secretion in the lamina propria may be disturbed. And finally, a disturbed trafficking of IEC to the gut, including a disturbed B-cell/IEL interaction can be the source of the observed differences.

In order to evaluate the first hypothesis, the frequency of peritoneal B1 B-cells was assessed. No differences between S1P₄^{-/-} and WT controls were found. Similarly, no difference in B-cell frequency was found in the Peyer's patch of both strains. It is thus

improbable that quantitative differences in the number of potential ASC cells explain the divergence in intestinal IgA levels. Numbers of CD4⁺ T helper cells in Peyer's patch were also similar in both genotypes. The second hypothesis has as yet not been assessed in our model, but is an urgent next step in the further analysis of our model. Recently, Kunisawa *et al* reported that S1P signalling plays a crucial role in the migration of both B1 B-cell and follicular B-cell derived ASCs into the lamina propria. In this model, impaired S1P signalling resulted in significantly reduced faecal IgA levels¹⁴⁵. Finally, the same group reported that inhibition of S1P signalling resulted in diminished trafficking of certain types of IEL to the lamina propria, and is also implicated in the retention of these cells in this location. In our model, we have not yet assessed the influence of S1P₄ deficiency on IEL.

In conclusion, S1P₄ deficiency results in reduced mucosal IgA levels. The exact mechanisms leading to this effect remain to be established by further experiments. These include a meticulous analysis of ASCs in the lamina propria and the Peyer's patches as well as their migrational properties. Furthermore, IEC numbers and phenotype require further investigation in our model.

6.1.6. S1P in B-cell lineage development

Decreased B-cell numbers in peripheral LN and differences in plasma Ig levels suggested that the B-cell compartment may have been affected by the lack of S1P₄ expression. We therefore performed a more detailed analysis of quantitative aspects of B-cell development.

6.1.6.1. S1P₄^{-/-} deficiency results in reduced number of pre-/pro-B-cells in the bone marrow

FACS staining of bone marrow cells with anti-IgM and anti-B220 antibody allowed for the identification of various early stages of the B-cell development, including pre-/pro-B-cells (B220⁺IgM⁻), immature B-cells (B220^{int}IgM⁺) and recirculating mature B-cells (B220^{hi}IgM⁺). Interestingly, total numbers of B220⁺ B-cells were slightly but consistently reduced in the bone marrow. Analysis of the different developmental stages revealed that this decrease is mainly due to a reduction of the compartment of pre-/pro-B-cells, while immature and recirculating mature B-cell numbers were similar in animals of both genotypes.

In the bone marrow, hematopoietic stem cells develop from multipotent progenitors early B-cell precursors to immature B-cells. The developmental stages are shown in **Figure 52**. Various factors have been shown to be essential for the development of B-cell precursors. Thus, CXCL12 signalling is essential for the earliest stage of B-cell development (pre-pro-B-cells). Moreover, it is implicated in the bone marrow colonization of haematopoietic stem

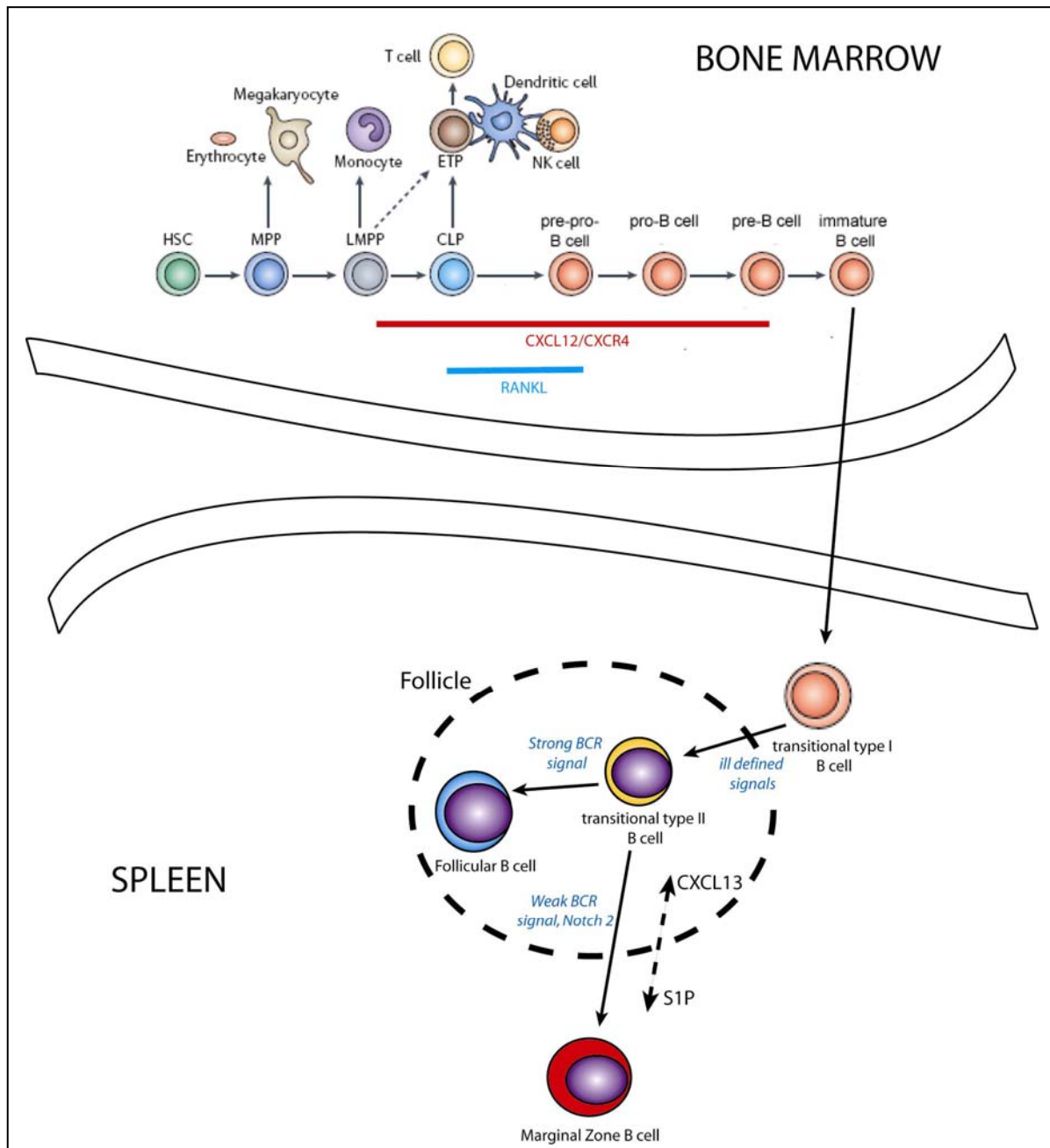


Figure 52: B cell development in bone marrow and spleen

Hematopoietic stem cells (HSC) give rise to non-self-renewing hematopoietic multipotential progenitors (MPP). Lymphoid-primed multipotential progenitors (LPMP) retain myeloid-cell, B and T cell potential but are devoid of erythro-megacaryocytic differentiation potential. The common lymphoid progenitor (CLP) can give rise to B and T cells, but not to myeloid cells. B cell progenitors run through discrete developmental stages during which they undergo successive rearrangement of Ig heavy- and light-chain genes. These steps are controlled by a number of factors including FLT3L and CXCL12.

Immature B cells leave the bone marrow and migrate to the spleen where they develop to mature B cells via different developmental stages. The nature of the signals leading to the transition from transitional type I to transitional type II B cells are still ill defined. Transitional type II B cells can then differentiate into mature follicular B cells or MZ B cells. The decision towards a MZ or follicular B cell fate depends crucially from the strength of the BCR mediated signal during differentiation. ETP: early T cell lineage progenitors

Modified from Nagasawa, Nature Reviews Immunology, 2006 and Pillai *et al*, Annu. Rev. Immunol., 2004

cells and in the retention of haematopoietic precursors within the bone marrow (reviewed in²⁰⁶). Interestingly, B-cell precursors are significantly reduced in bone marrow of chimeric

wild-type mice that have been reconstituted with CXCR4 deficient fetal cells²⁰⁷. Moreover, pre-B-cells were increased in the blood of CXCR4 deficient animals, indicating that retention of the B-cell precursors within the bone marrow is dependent on CXCR4²⁰⁸. S1P signalling has been shown to act in synergy with CXCL12 induced migration of splenic T-cells, at least at low to intermediate nanomolar concentrations of S1P²⁰⁹. On the other side, in an *in vivo* model, Kabashima *et al* proposed a functional antagonism between S1P₁-mediated S1P signalling and CXCR4 signalling in plasma cell egress from secondary lymphoid organs. However, these data suggest a putative interaction between S1P and CXCR4 signalling *in vivo*. The precise nature of this interaction is certainly dependent on several factors, including local S1P concentration and the expression profile of the different S1P receptors on the cell surface.

The precise mechanism by which S1P₄ deficiency results in reduced pre- and pro-B-cell numbers is not yet clear. Whether a reduced migration of progenitor cells, a reduced retention within the bone marrow or the lack of a trophic signal for the early progenitors is the main mechanism remains to be shown.

6.1.6.2. S1P₄^{-/-} deficiency results in reduced number of splenic transitional type II cells but increased numbers of MZ B-cells

B-cell development is not completed within the bone marrow. Instead, immature B-cells leave the bone marrow and migrate to peripheral lymphoid tissues where they serve as developmental intermediate for the generation of mature peripheral B-cells. This development occurs in multiple discrete steps, shown in **Figure 52**. The molecular mechanisms driving the development from transitional type I stage to the transitional type II stage are still not well defined. Immature B-cells are subjected to a high turnover, with a 50% renewal rate in the periphery. Only 5% of newly formed BM B-cells successfully enter the mature B-cell compartment^{210,211}. Thus, the results of the analysis of immature B-cell stages in the spleen is a snapshot of a highly dynamic process. The mechanisms that leads to the observed reduction of transitional type I B-cells can act on various levels. In the light of normal immature B-cell frequencies in the bone marrow, a reduced production of these cells seems improbable. A further possibility is a reduced migration from bone marrow to the spleen, or a reduced survival of cells in this developmental stage. Further investigations are necessary to define the exact mechanism leading to our observation of reduced transitional type I B-cells in the spleen^{210,211}. While transitional type I B-cells had a reduced frequency in our knock out model, transitional type II B-cells showed a normal frequency in our S1P₄ deficient animals. At a first sight, this appeared disturbing, given that in the well-accepted models of peripheral B-cell

development, transitional type I and type II B-cells are consecutive developmental stages (**Figure 52**). However, the CD21^{hi}CD23⁺ cell fraction has been previously shown to be enriched in proliferating cells²¹². This opens the possibility that in our knock out model, proliferative processes at the transitional type II level compensated for the moderately reduced precursor frequency in the transitional type I compartment.

Marginal zone (MZ) B-cells were significantly increased in spleen of the S1P₄^{-/-} mice. Compared to the other type of mature splenic B-cells, the follicular B-cells, MZ B-cells are equipped with a number of divergent functional specificities. They do not recirculate through blood or lymph and show a higher capacity for antigen presentation, therefore likely involved in early stages of *in vivo* T-cell activation. Also due to their localisation in the marginal zone, they are perfectly exposed to circulating antigens, and they participate very early in immune response. In B-cell clones specific for T-cell independent antigens, MZ B-cells are enriched. This observation has led to the conclusion that MZ B-cells are mainly involved in the response to T-cell independent antigens. However, MZ B-cells also participate in the response to T-cell independent antigens (reviewed in^{213,214}). *In vitro* it has been shown that MZ B-cells cultured in minimal conditions switched preferentially to the IgA phenotype²¹⁵.

Interestingly, blockade of S1P signalling by FTY720 was shown to reduce MZ B-cell numbers in their typical location, although total splenic MZ B-cell numbers remained constant¹⁹³. Experiments with S1P₁ deficient MZ B-cells revealed a dislodgment of MZ B-cells from the marginal zone to follicles. Again, total splenic B cell numbers were not affected³. In our knock out model, the total numbers of MZ B-cells were reduced, suggesting a different mechanism from that found in the reports mentioned before. Immunohistochemical studies are currently ongoing in order to assess the intrasplenic localisation of MZ B-cells in the S1P₄ deficient mice. The functional consequences of reduced MZ B-cell numbers in our S1P₄^{-/-} mice have not been formerly shown. However, since MZ B-cells are crucially implicated in the generation of IgA plasma levels, it is tempting to speculate that the increased numbers of these cells is involved in the increased plasma IgA levels found in the S1P₄^{-/-} animals.

6.1.6.3. S1P₄^{-/-} deficiency does not impact on B1 B-cell numbers in the peritoneal cavity

Beside follicular B-cells and MZ B-cells, B1 B-cells are the third type of mature B-cells. Alike MZ B-cells, B1 B-cells do not recirculate in blood or lymph but are restricted to the pleural and peritoneal cavity. Together with MZ B-cells, they are early participants in the T-cell independent immune response and give rise to the early wave of plasma cells in these

responses²¹⁶. In addition, B1 B-cells can take part in the early phases of T-cell dependent immune responses²¹⁷. B1 B-cells are crucially implicated in the generation of natural antibodies, and IgM and IgG3 Ig plasma levels are considered to be strongly influenced by the B1 B-cell compartment²¹⁸. B1 B-cells are also participating in the generation of systemic and local IgA levels. Transfer experiments have shown that up to 50 % of lamina propria ASC derive from B1 B-cells. Similar experiments revealed that up to 50% of plasma IgA are produced by the B1 B-cell lineage^{219,220}.

In our S1P₄^{-/-} mice, peritoneal B1 B-cells were present with a frequency similar to that of WT animals. However, this finding does not exclude the possibility that B1 B-cell migration to the lamina propria of the gut is impaired in these animals, resulting in reduced intestinal IgA levels found in S1P₄^{-/-} mice. Further experiments are required to assess this possibility. Furthermore, the normal B1 B-cell number suggest that the increased plasma IgA levels found in S1P₄^{-/-} animals do not result from quantitative increases of the B1 B-cell compartment. The observed increase in MZ B-cells within the spleen is here a more likely candidate to explain this observation.

6.1.7. S1P in polarisation of the immune response

6.1.7.1. S1P₄ deficiency results in an increased intrinsic capacity for secretion of the T_H2 cytokine IL-5 by CD4⁺ T-cells

The type of plasma Ig profile found in the S1P₄^{-/-} animals was strongly suggestive of a T_H2 deviation of the immune response in our mouse model. In order to investigate this possibility, we measured the intrinsic capacity for T_H1 and T_H2 cytokine secretion of S1P₄^{-/-} and WT CD4⁺ T-cells after stimulation through the TCR-coreceptor pathway. Both IL-4 and IFN- γ secretion was slightly increased in S1P₄^{-/-} CD4⁺ cell cultures, but without reaching statistical significance. Interestingly, the secretion of the T_H2 cytokine IL-5 was significantly increased in S1P₄^{-/-} CD4⁺ cell cultures.

Our findings are in keeping with those made by Wong *et al.*⁷³. In S1P₄ overexpressing T-cell lines, they found reduced levels of IL-4 and IFN- γ secretion after anti-CD3/anti-CD28 stimulation. However, as mentioned earlier, doubts persist concerning their experimental model regarding the endogenous expression of other S1P receptors in their T-cell lines. To our knowledge, S1P-induced modification of IL-5 secretion has not been reported by other investigators. Thus, the increased IL-5 secretion was a new finding in our experimental model, that may account for the observed differences in plasma IgA levels. However, whether the observed differences in intrinsic cytokine secretion in helper T-cells is sufficient to induce

the changes in the Ig profile observed in our animals remains to be proven. The polarization of naïve T-cells requires interaction with dendritic cells. During this interaction, at least three signals are required for the successful differentiation of the naïve T-cell towards the T_{H1} or T_{H2} profile. Signal 1 is the antigen-specific recognition of peptides in the context of major histocompatibility complex on the DC by the T-cell receptor. Signal 2 is provided by the interaction of costimulatory molecules on the DC surface with receptors on the T-cell. And finally, signal 3 that directs the response toward the T_{H1} or T_{H2} issue is the cytokine environment provided by the DC to the T helper cells. Thus, IL-12 and IL-27, two members of the IL-12 family of cytokines polarise of T-cell toward the T_{H1} phenotype^{221,222}. In contrast, exposure to IL-4 results into a polarisation toward the T_{H2} phenotype^{223,224}. However, there is recent evidence that further cell types are implicated in regulating the secretion of T_{H1} / T_{H2} polarizing cytokines by DC, including mast cells or NKT cells^{225,226}. A prerequisite for the interaction between DC and naïve T cells is the migration of the DC from the peripheral tissue, where the antigenic sampling takes place, to the secondary lymphoid organs, where they will interact with naïve T-cell to induce their activation and their polarisation toward either the T_{H1} or the T_{H2} types. S1P signalling has been shown *in vitro* to impact on both processes, *i.e.* DC migration and cytokine secretion by DC^{136,152,154,155}. It is thus indispensable to assess the role of DC on the T_{H1} / T_{H2} polarisation in our $S1P_4^{-/-}$ model. Experiments relevant to this question are currently ongoing.

In order to further substantiate our hypothesis that $S1P_4$ deficiency results in a T_{H2} -deviated immune response, we performed experimental models in which immune responses are either dominated by T_{H1} or T_{H2} mechanisms. The results of those relatively complex models are discussed in the following paragraphs.

6.1.7.2. $S1P_4$ in contact hypersensitivity and type IV hypersensitivity

Contact hypersensitivity (CHS) is a T-cell mediated cutaneous immune response to reactive haptens. Depending on the antigen involved, the immune response is predominated by T_{H1} or T_{H2} mechanisms. The mechanisms leading to the development of a T_{H1} versus a T_{H2} driven response are yet poorly defined. A crucial role in this selection is played by the nature of the antigen. While some antigens like oxazolone or dinitrofluorobenzene induce preferentially T_{H1} -dominated responses, fluorescein isothiocyanate (FITC) was shown to induce a T_{H2} -dominated reaction²²⁷. Therefore, we chose FITC in our experimental model to induce a T_{H2} dominated CHS. $S1P_4^{-/-}$ animals developed a significantly stronger CHS response reflected by an increased swelling of the FITC-treated ear compared to WT animals. This result confirms our hypothesis of a T_{H2} -deviated immune response in $S1P_4$ -deficient

mice. However, the precise mechanism by which lack of S1P₄ induces the observed differences can not yet be defined with certainty. The mechanism of CHS can be divided into two distinct phases (reviewed in^{228,229}). During the sensitisation phase, Langerhans cells (LCs) take up haptenated proteins. Following this up-take, LCs are activated by inflammatory cytokines, *i.e.* IL-1 β and TNF- α . In contrast, IL-10 acts as functional antagonist in this process. Activated LCs further mature and migrate to the local LNs, where they interact with hapten-specific T cells. The migration of LCs from the periphery to the LN is critically regulated by the up-regulation of CCR7 that allows the migration of LCs to the CCL19 gradient present in the LN. The elicitation phase is initiated by the reexposure to the sensitising hapten. In response, antigen specific T-cells undergo clonal proliferation, differentiation and migration to the site of antigen exposure. Potential impact points of S1P₄ deficiency in the sensitisation phase and elicitation phase are multiple. First, S1P has been shown to affect DC migration as well as chemokine-induced chemotaxis in dendritic cells^{152,154}. Second, S1P signalling in S1P₄-overexpressing T cell lines was shown to increase IL-10 secretion. Thus, reduced IL-10 production in the S1P₄^{-/-} mice could be a further mechanism in the sensitisation phase leading to increased CHS. Finally, an impact of S1P signalling on the cytokine profile of DC may contribute to the T_{H2} polarisation of the effector CD4⁺ T cells^{152,155}. However, since no individual S1P receptors have been assigned to these effects seen in *in vitro* experiments with DCs, these hypothesis remains speculative. Finally, not excluding the other mechanisms, the migration of the effector T cells to the zone of hapten reexposure may be modified by S1P₄ deficiency.

After the demonstration that S1P₄ deficiency leads to an increased reaction in an experimental model of T_{H2} dominated immune response, we tested the S1P₄^{-/-} mice in an experimental setting of T_{H1} dominated immune response. In accordance with our previous findings, S1P₄^{-/-} animals showed a reduced delayed type hypersensitivity compared to WT control animals. From a mechanistic point of view, the sensitisation and elicitation phases of the contact hypersensitivity and the type IV hypersensitivity model are very close but involve different type of antigen and probably different antigen presenting cells. However, the potential impact points of deficient S1P₄ signalling in these two models should be quite similar.

In conclusion, the two models of T_{H1}- and T_{H2}-driven immune responses demonstrate clearly that the T_{H1}/ T_{H2} balance in the S1P₄^{-/-} mice is preferentially shifted towards the T_{H2} side. The exact mechanism underlying this observation remains to be defined. Furthermore,

these models underscore the necessity to deepen the analysis of the effects of S1P₄ deficiency on the function of various DC populations.

6.1.7.3. Role of S1P₄ in asthma

Allergic asthma is an inflammatory lung disease characterized by reversible airway obstruction, presence of an inflammatory infiltrate and non-specific airway hyperresponsiveness. Pathological and histopathological hallmarks of allergic asthma include elevated levels of T_H2 cytokines, increased production of IgE and eosinophilic airway infiltration^{199,200,230}. Transfer experiments with T-cell receptor transgenic T_H1 and T_H2 cells have clearly shown that airway inflammation is dependent on the transfer of the latter but not of the former cells²³¹. Thus, a critical role of T_H2 cell is widely accepted today²³².

In our S1P₄^{-/-} mice we have observed increased IgE plasma levels as well as strong indications for a predisposition towards T_H2 dominated immune responses. We therefore hypothesised that these animals might show a stronger response in an ovalbumin (Ova)-induced asthma model. Indeed, previously sensitised S1P₄^{-/-} animals exhibited a stronger response to the inhalative challenge with nebulized antigen than their WT littermates as assessed by a significantly increased cellular infiltrate.

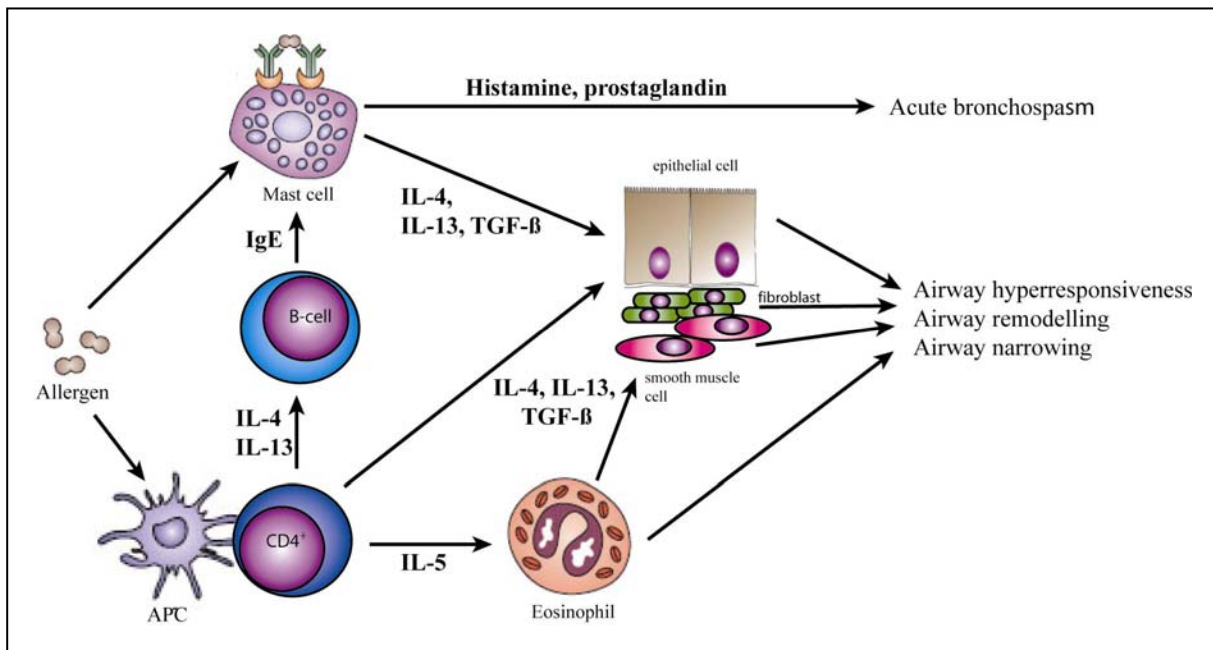


Figure 53: Overview of the cellular potential interactions between cell types implicated in the pathogenesis of asthma

(modified from Larché et al, J Allergy Clin Immunol, 2003)

Multiple cells participate in the induction of epithelial damage and cellular infiltration observed in asthma, *i.e.* T_H2 cells, eosinophils, mast cells, basophils and indirectly dendritic cells and B cells. A schematic overview of cellular interactions during the asthma

pathogenesis is depicted in **Figure 53**. Presentation of the antigen by DCs to T cells induce their differentiation into T_H2 cells. These cells elaborate a panel of T_H2 cytokines including IL-4 and IL-13 thus increasing IgE production by B cells, and which have direct effects on airway smooth muscle cells, fibroblasts and epithelial cells resulting in airway hyperresponsiveness and chronic airway remodelling. The T_H2 cytokine IL-5 induces activation and chemotaxis of eosinophils, promoting the development of an eosinophilic infiltration. Activated eosinophils secrete additional mediators including TGF- β , IL-4 and IL-13, and contribute directly to airway remodelling and airway hyperresponsiveness. The interaction of the antigen with specific IgE bound to the surface of mast cells results in mast cell degranulation, leading to the liberation of further pro-inflammatory mediators such as histamine, prostaglandins, TGF- β , IL-4 and IL-13.

Given this complex pathogenic mechanism, it is difficult to define the precise point of impact that leads to the increased infiltrative response seen in $S1P_4^{-/-}$ mice. In the contrary, it is even possible, that multiple mechanisms participate in the final read-out observed in our model. First, $S1P_4^{-/-}$ $CD4^+$ cells stimulated *via* the TCR-coreceptor pathway *in vitro* secreted significantly elevated quantities of IL-5 than WT controls. IL-5 is crucially implicated in enhancing eosinophilic accumulation and activation during allergen-induced inflammation²³³. This increased intrinsic capacity for IL-5 secretion seen in $S1P_4^{-/-}$ $CD4$ T cells may account partly for the observed phenotype. However, other potential mechanism should also taken into consideration, and special attention should be concentrated at examining the effect of $S1P_4$ -deficiency on the function of lung DCs. Very recently, Idzko *et al* reported abrogation of Ova-induced asthma by local administration of the immunosuppressive drug and structural S1P agonist FTY720. Interestingly, local administration of FTY720 did not result in detectable systemic levels of this drug, and the peripheral lymphopenia seen during systemic administration of FTY720 for immunosuppressive purposes was not seen in this model. Here, local administration resulted in an reduced migration of lung DCs to mediastinal LNs as well as in a reduced priming of T_H2 cells *in vivo* and *in vitro*. Lung DCs in this experimental setting expressed mRNA of all 5 known S1P receptors, and a specific S1P receptor responsible for the mediation of the observed FTY720 effects was not identified by the authors²³⁴. Given that FTY720 was shown to be a functional antagonist of S1P mostly for the $S1P_1$ and $S1P_5$ receptor, it is tempting to speculate that there is a functional antagonism between $S1P_1$ and $S1P_4$ in lung DCs, leading to an increased response in situations with functional $S1P_1$ and $S1P_4$ deficiency, and to a reduced response in situations with $S1P_1$ blockade (FTY720) and partially preserved $S1P_4$ signalling. However, FTY720 has not been

shown to be a selective antagonist for S1P₁, and further experiments designed to assess the biological behaviour of S1P₄ deficient lung DC are required. Furthermore, selective knock-down of S1P₁ with the lentiviral shRNA system will further facilitate the dissection of S1P₁/S1P₄ interaction in this model.

Eosinophils and mast cells are two other cell types implicated in the pathogenesis of asthma. It should be kept in mind that S1P signalling has also been described in these cells. In eosinophils, S1P induces chemotaxis *in vivo* (rats) and *in vitro* (humans)¹⁷³. However, only S1P₁, S1P₂ and S1P₃ mRNAs were detected in eosinophils. Expression or absence of S1P₄ and S1P₅ have not been reliably reported. Therefore, physiological S1P₄ expression on eosinophils should be reassessed and if present, the influence of S1P₄ deficiency on eosinophil migration should be assessed.

Mast cells express S1P₁ and S1P₂, while none of the remaining 3 S1P receptors could be detected. While S1P₁ affects mast cell chemotaxis, S1P₂ activation results in increased mast cell degranulation and reduced chemotaxis¹⁷⁹. Interestingly, S1P₂ is up-regulated during mast cell activation upon cross-linking of FcεR-bound IgE. Similarly, sphingosine kinase 1 and 2 are activated by the same stimulus, resulting in increased S1P production and an rise of intracellular and extracellular S1P concentration²³⁵. Interestingly, S1P concentration in the BALFs of asthmatic patients is significantly increased, probably due to the above described mechanism²³⁶. However, since S1P₄ was not detected, it is very unlikely that the observed increase of inflammatory response in our asthma model is due to mast cell inherent mechanisms.

In conclusion, the asthma model once more confirms our finding of an Th2-orientated immune response in S1P₄^{-/-} mice. Further experiments are required to determine the precise cellular mechanisms. Especially lung DCs may be a promising target for further investigations.

6.2. Generation of a lentiviral vector system for shRNA-mediated S1P₁ knock-down

The analysis of the immune system of the S1P₄^{-/-} mice allowed us to reveal distinct functions of the S1P₄ receptor in the immune system. However, the fact that the same ligand, S1P, binds with high affinity to all S1P receptors, that some of these receptors show a quite ubiquitous expression pattern and that ligation of the receptor by the ligand can in some systems induce the intracellular generation of the ligand itself renders the interpretation of the experimental system particularly complex. S1P₄ as one of the predominant S1P receptor on

immune cells shares this localisation with S1P₁, that is also expressed in other tissues. Within the S1P receptor family, it has been previously shown that in knock-out models lacking the expression of one S1P receptor, other members of this receptor group can compensate this deficiency on a functional level⁵. Moreover, it has been proposed that S1P₁ and S1P₄ can associate in complexes on the surface of stably transfected cells *in vitro*⁶. The biological significance of this observation still remains to be shown. Both observations suggest that there could be an intricate interaction of both receptor subclasses, leading to functional redundancy or, as another possibility, to antagonistic functions. Indeed, some of the findings in our S1P₄^{-/-} mice suggest antagonistic functions of both receptors on lymphocyte migration and polarization of the immune response. In order to better dissect the S1P effects transduced by S1P₁ and S1P₄ in the cells of the immune system, we have generated a vector system for RNA-mediated knock-down of the S1P₁ gene.

Initially, we have created a plasmid for transient expression of HA-tagged murine S1P₁. This tool facilitated the identification of siRNA sequences which suppressed transient expression of HA-tagged S1P₁ with high efficiency. However, siRNA mediated knock-down in mammalian cells is transient, lasting for only for 3-7 days in proliferating cells. In our planned experimental *in vivo* models involving reconstitution of mice with S1P₁/S1P₄ double deficient bone marrow cells and transfer of S1P₁/S1P₄ double deficient lymphocytes, a stable knock down of S1P₁ was required. We thus decided to apply retro-/lentivirus based vectors for efficient and stable delivery of shRNA sequences.

As a first approach, we used a retroviral vector system optimised for transduction of T-cell lines and primary T-cells to generate a retroviral shRNA vector system by introducing a cassette containing the murine U6 promoter and the S1P₁ specific shRNA. This cassette was cloned into the pMP71linker by two different cloning strategies upstream (msE34s35 and msE34s53) and downstream (msE34n35 and msE34n53) of the PRE element. Although all generated vector plasmids proved to suppress transient expression of HA-tagged murine S1P₁ with high efficiency in a cell culture system when transfected by lipofection, their further use was not possible due to a lack of expression of the reporter gene GFP (msE34s35 and msE34s53) and the incapacity to produce high virus titers (msE34n35 and msE34n53). The reasons for these deficiencies have not been further assessed. However, the lack of GFP transcription after transfection with msE34s35 and msE34s53 may be due to the localisation of the shRNA cassette in this construct. Cloning upstream of the PRE elements enlarges the distance between the GFP and the PRE element, thus possibly influencing the functional activity of this element.

In a second approach, we have generated a lentiviral shRNA vector system that inhibited expression of HA-tagged murine S1P1 with high efficiency. Two T-cell lines were transduced with high efficiency and endogenous S1P₁ expression in these cell lines was reduced to 10 %-25% of that of control cells. In long term experiments, S1P₁ knock-down was shown to persist for at least 4 weeks. Finally, we have also demonstrated that expression of the reporter gene GFP identifies cells with most efficient S1P₁ knock-down. The expression of the reporter gene GFP will thus allow for easy identification of S1P₁-deficient cells in experiments involving adoptive cell transfer of reconstitution of lethally irradiated animals. In conjunction with the S1P₄^{-/-} mouse model, this tool will enable us to delineated far more precisely the individual part of each receptor in the biological effects of S1P signalling seen in our experimental system.

7. CONCLUSIONS AND PERSPECTIVES

The analysis of the immune phenotype of our S1P₄-deficient mice revealed specific functions of the S1P₄ receptor in the immune system. As most salient findings, we have shown its implication in lymphocyte migration, marginal zone B-cell biology and in the T_H1/T_H2 polarisation of the immune response. It has been previously shown that another member of the S1P receptor family, namely the S1P₁ receptor, also plays a pivotal role in the same immunological processes. However, in many models, the changes induced by S1P₄-deficiency resembled those induced by S1P₁-activation or S1P₁ over-expression reported in the literature. Therefore one could conclude that these receptors may transduce opposite effects of S1P signalling in certain cell types. In contrast, it is also known from the literature that S1P receptors may mutually compensate their function in knock-out models. Furthermore, some experimental data from stably S1P₁/S1P₄ over-expressing cells demonstrate the existence of a close physical interaction between both receptor subtypes. In the next future, it will thus be essential to dissect the interplay between S1P₁- and S1P₄-mediated signalling. With the generation of our lentiviral vector system for shRNA-mediated knock-down of S1P₁, we have provided a tool for further experiments aimed at differentiating S1P₁- and S1P₄-mediated biological effects. These included the generation of murine models with a S1P₁/S1P₄ double-deficient hematopoietic system, but also the comparative *in vitro* assessment of biological functions of S1P₁-, S1P₄- or double deficient immune cells, i.e. lymphocytes, eosinophils and, most importantly, dendritic cells that are crucial in the induction and orientation of any immune response.

The observations made in our S1P₄-deficient mouse show that assessment of S1P₄ function in other cells of the immune system is required. Being the antigen processing and presenting cells which secrete the majority of T_H1/T_H2-polarizing cytokines, dendritic cells may be at the origin of the observed T_H2 deviation of the immune response in our knock-out model. The analysis of the *in vivo* and *in vitro* functions of dendritic cells in a context of S1P₄ deficiency, is currently ongoing. Eosinophils have a causal implication in the pathogenesis of asthma and were found in significantly increased numbers of S1P₄^{-/-} mice in our asthma model. Therefore, an intrinsic action of S1P₄ in the biology of these cells should be deeper evaluated.

S1P signalling was shown to be involved in a variety of immune pathologies such as asthma or hypersensitivity. A better understanding of the role of S1P₁ and S1P₄ in those processes is a prerequisite for the development of interventional strategies targeted at these

receptors. The induction of immunosuppression in transplantation by the unselective agonist FTY720 is a first example for such treatments, but the search for more specific agonists/antagonists is currently ongoing. The rationale for their use in human would have to be based on the complete knowledge on S1P₁ and S1P₄ receptor biology.

8. BIBLIOGRAPHY

1. **Matloubian, M, Lo CG, Cinamon G, Lesneski MJ, Xu Y, Brinkmann V, Allende ML, Proia RL, Cyster JG.** Lymphocyte egress from thymus and peripheral lymphoid organs is dependent on S1P receptor 1. *Nature* **2004**, 427, 355-60.
2. **Allende, ML, Dreier JL, Mandala S, Proia RL.** Expression of the sphingosine 1-phosphate receptor, S1P1, on T-cells controls thymic emigration. *J Biol Chem.* **2004**, 279, 15396-401.
3. **Cinamon, G, Matloubian M, Lesneski MJ, Xu Y, Low C, Lu T, Proia RL, Cyster JG.** Sphingosine 1-phosphate receptor 1 promotes B cell localization in the splenic marginal zone. *Nat Immunol* **2004**, 5, 713-20.
4. **Kabashima, K, Haynes NM, Xu Y, Nutt SL, Allende ML, Proia RL, Cyster JG.** Plasma cell S1P1 expression determines secondary lymphoid organ retention versus bone marrow tropism. *J Exp Med* **2006**, 203, 2683-90.
5. **Ishii, I, Ye X, Friedman B, Kawamura S, Contos JJ, Kingsbury MA, Yang AH, Zhang G, Brown JH, Chun J.** Marked perinatal lethality and cellular signaling deficits in mice null for the two sphingosine 1-phosphate (S1P) receptors, S1P(2)/LP(B2)/EDG-5 and S1P(3)/LP(B3)/EDG-3. *J Biol Chem.* **2002**, 277, 25152-9.
6. **Matsuyuki, H, Maeda Y, Yano K, Sugahara K, Chiba K, Kohno T, Igarashi Y.** Involvement of sphingosine 1-phosphate (S1P) receptor type 1 and type 4 in migratory response of mouse T cells toward S1P. *Cell Mol Immunol.* **2006**, 3, 429-37.
7. **Pieringer, RA, Bonner H, Jr., Kunnes RS.** Biosynthesis of phosphatidic acid, lysophosphatidic acid, diglyceride, and triglyceride by fatty acyltransferase pathways in *Escherichia coli*. *J Biol Chem.* **1967**, 242, 2719-24.
8. **Hecht, JH, Weiner JA, Post SR, Chun J.** Ventricular zone gene-1 (vzg-1) encodes a lysophosphatidic acid receptor expressed in neurogenic regions of the developing cerebral cortex. *J Cell Biol.* **1996**, 135, 1071-83.
9. **Graeler, MH, Bernhardt G, Lipp M.** EDG6, a novel G-protein-coupled receptor related to receptors for bioactive lysophospholipids, is specifically expressed in lymphoid tissue. *Genomics* **1998**, 53, 164-9.
10. **Flower, DR.** Modelling G-protein-coupled receptors for drug design. *Biochim Biophys Acta.* **1999**, 1422, 207-34.
11. **Bargmann, CI.** Neurobiology of the *Caenorhabditis elegans* genome. *Science.* **1998**, 282, 2028-33.

12. **Plakidou-Dymock, S, Dymock D, Hooley R.** A higher plant seven-transmembrane receptor that influences sensitivity to cytokinins. *Curr Biol.* **1998**, 8, 315-24.
13. **Dohlman, HG, Thorner J, Caron MG, Lefkowitz RJ.** Model systems for the study of seven-transmembrane-segment receptors. *Annu Rev Biochem.* **1991**, 60, 653-88.
14. **Vernier, P, Cardinaud B, Valdenaire O, Philippe H, Vincent JD.** An evolutionary view of drug-receptor interaction: the bioamine receptor family. *Trends Pharmacol Sci.* **1995**, 16, 375-81.
15. **New, DC, Wong JT.** The evidence for G-protein-coupled receptors and heterotrimeric G proteins in protozoa and ancestral metazoa. *Biol Signals Recept.* **1998**, 7, 98-108.
16. **Bockaert, J, Pin JP.** Molecular tinkering of G protein-coupled receptors: an evolutionary success. *Embo J.* **1999**, 18, 1723-9.
17. **Farrens, DL, Altenbach C, Yang K, Hubbell WL, Khorana HG.** Requirement of rigid-body motion of transmembrane helices for light activation of rhodopsin. *Science.* **1996**, 274, 768-70.
18. **Jensen, AD, Guarnieri F, Rasmussen SG, Asmar F, Ballesteros JA, Gether U.** Agonist-induced conformational changes at the cytoplasmic side of transmembrane segment 6 in the beta 2 adrenergic receptor mapped by site-selective fluorescent labeling. *J Biol Chem.* **2001**, 276, 9279-90.
19. **Wess, J.** G-protein-coupled receptors: molecular mechanisms involved in receptor activation and selectivity of G-protein recognition. *Faseb J.* **1997**, 11, 346-54.
20. **Zeng, FY, Wess J.** Identification and molecular characterization of m3 muscarinic receptor dimers. *J Biol Chem.* **1999**, 274, 19487-97.
21. **Cvejic, S, Devi LA.** Dimerization of the delta opioid receptor: implication for a role in receptor internalization. *J Biol Chem.* **1997**, 272, 26959-64.
22. **Hebert, TE, Bouvier M.** Structural and functional aspects of G protein-coupled receptor oligomerization. *Biochem Cell Biol.* **1998**, 76, 1-11.
23. **Bai, M, Trivedi S, Brown EM.** Dimerization of the extracellular calcium-sensing receptor (CaR) on the cell surface of CaR-transfected HEK293 cells. *J Biol Chem.* **1998**, 273, 23605-10.
24. **AbdAlla, S, Zaki E, Lothar H, Quitterer U.** Involvement of the amino terminus of the B(2) receptor in agonist-induced receptor dimerization. *J Biol Chem.* **1999**, 274, 26079-84.
25. **Romano, C, Yang WL, O'Malley KL.** Metabotropic glutamate receptor 5 is a disulfide-linked dimer. *J Biol Chem.* **1996**, 271, 28612-6.

26. **Dwyer, ND, Troemel ER, Sengupta P, Bargmann CI.** Odorant receptor localization to olfactory cilia is mediated by ODR-4, a novel membrane-associated protein. *Cell*. **1998**, 93, 455-66.
27. **McLatchie, LM, Fraser NJ, Main MJ, Wise A, Brown J, Thompson N, Solari R, Lee MG, Foord SM.** RAMPs regulate the transport and ligand specificity of the calcitonin-receptor-like receptor. *Nature*. **1998**, 393, 333-9.
28. **Ferguson, SS.** Evolving concepts in G protein-coupled receptor endocytosis: the role in receptor desensitization and signaling. *Pharmacol Rev*. **2001**, 53, 1-24.
29. **Claing, A, Laporte SA, Caron MG, Lefkowitz RJ.** Endocytosis of G protein-coupled receptors: roles of G protein-coupled receptor kinases and beta-arrestin proteins. *Prog Neurobiol*. **2002**, 66, 61-79.
30. **Kristiansen, K.** Molecular mechanisms of ligand binding, signaling, and regulation within the superfamily of G-protein-coupled receptors: molecular modeling and mutagenesis approaches to receptor structure and function. *Pharmacol Ther*. **2004**, 103, 21-80.
31. **Luttrell, LM, Lefkowitz RJ.** The role of beta-arrestins in the termination and transduction of G-protein-coupled receptor signals. *J Cell Sci*. **2002**, 115, 455-65.
32. **Carman, CV, Parent JL, Day PW, Pronin AN, Sternweis PM, Wedegaertner PB, Gilman AG, Benovic JL, Kozasa T.** Selective regulation of G α (q/11) by an RGS domain in the G protein-coupled receptor kinase, GRK2. *J Biol Chem*. **1999**, 274, 34483-92.
33. **Sterne-Marr, R, Dhimi GK, Tesmer JJ, Ferguson SS.** Characterization of GRK2 RH domain-dependent regulation of GPCR coupling to heterotrimeric G proteins. *Methods Enzymol*. **2004**, 390, 310-36.
34. **Simon, MI, Strathmann MP, Gautam N.** Diversity of G proteins in signal transduction. *Science*. **1991**, 252, 802-8.
35. **Codina, J, Yatani A, Grenet D, Brown AM, Birnbaumer L.** The alpha subunit of the GTP binding protein G α opens atrial potassium channels. *Science*. **1987**, 236, 442-5.
36. **Tang, WJ, Gilman AG.** Type-specific regulation of adenylyl cyclase by G protein beta gamma subunits. *Science*. **1991**, 254, 1500-3.
37. **Neer, EJ.** Heterotrimeric G proteins: organizers of transmembrane signals. *Cell*. **1995**, 80, 249-57.
38. **Ross, EM, Gilman AG.** Resolution of some components of adenylyl cyclase necessary for catalytic activity. *J Biol Chem*. **1977**, 252, 6966-9.

39. **Hildebrandt, JD, Sekura RD, Codina J, Iyengar R, Manclark CR, Birnbaumer L.** Stimulation and inhibition of adenylyl cyclases mediated by distinct regulatory proteins. *Nature*. **1983**, 302, 706-9.
40. **Arshavsky, VY, Lamb TD, Pugh EN, Jr.** G proteins and phototransduction. *Annu Rev Physiol*. **2002**, 64, 153-87.
41. **Longenecker, KL, Lewis ME, Chikumi H, Gutkind JS, Derewenda ZS.** Structure of the RGS-like domain from PDZ-RhoGEF: linking heterotrimeric g protein-coupled signaling to Rho GTPases. *Structure*. **2001**, 9, 559-69.
42. **Booden, MA, Siderovski DP, Der CJ.** Leukemia-associated Rho guanine nucleotide exchange factor promotes G alpha q-coupled activation of RhoA. *Mol Cell Biol*. **2002**, 22, 4053-61.
43. **Clapham, DE, Neer EJ.** G protein beta gamma subunits. *Annu Rev Pharmacol Toxicol*. **1997**, 37, 167-203.
44. **Berstein, G, Blank JL, Jhon DY, Exton JH, Rhee SG, Ross EM.** Phospholipase C-beta 1 is a GTPase-activating protein for Gq/11, its physiologic regulator. *Cell*. **1992**, 70, 411-8.
45. **Siderovski, DP, Hessel A, Chung S, Mak TW, Tyers M.** A new family of regulators of G-protein-coupled receptors? *Curr Biol*. **1996**, 6, 211-2.
46. **Neubig, RR, Siderovski DP.** Regulators of G-protein signalling as new central nervous system drug targets. *Nat Rev Drug Discov*. **2002**, 1, 187-97.
47. **Tesmer, JJ, Berman DM, Gilman AG, Sprang SR.** Structure of RGS4 bound to AIF4-activated G(i alpha1): stabilization of the transition state for GTP hydrolysis. *Cell*. **1997**, 89, 251-61.
48. **Hall, RA, Premont RT, Lefkowitz RJ.** Heptahelical receptor signaling: beyond the G protein paradigm. *J Cell Biol*. **1999**, 145, 927-32.
49. **McDonald, PH, Chow CW, Miller WE, Laporte SA, Field ME, Lin FT, Davis RJ, Lefkowitz RJ.** Beta-arrestin 2: a receptor-regulated MAPK scaffold for the activation of JNK3. *Science*. **2000**, 290, 1574-7.
50. **Marrero, MB, Schieffer B, Paxton WG, Heerdt L, Berk BC, Delafontaine P, Bernstein KE.** Direct stimulation of Jak/STAT pathway by the angiotensin II AT1 receptor. *Nature*. **1995**, 375, 247-50.
51. **Hall, RA, Premont RT, Chow CW, Blitzer JT, Pitcher JA, Claing A, Stoffel RH, Barak LS, Shenolikar S, Weinman EJ, Grinstein S, Lefkowitz RJ.** The beta2-

- adrenergic receptor interacts with the Na⁺/H⁺-exchanger regulatory factor to control Na⁺/H⁺ exchange. *Nature*. **1998**, 392, 626-30.
52. **Pawson, T, Scott JD.** Signaling through scaffold, anchoring, and adaptor proteins. *Science*. **1997**, 278, 2075-80.
53. **Tu, JC, Xiao B, Yuan JP, Lanahan AA, Leoffert K, Li M, Linden DJ, Worley PF.** Homer binds a novel proline-rich motif and links group 1 metabotropic glutamate receptors with IP3 receptors. *Neuron*. **1998**, 21, 717-26.
54. **Hla, T, Maciag T.** An abundant transcript induced in differentiating human endothelial cells encodes a polypeptide with structural similarities to G-protein-coupled receptors. *J Biol Chem* **1990**, 265, 9308-13.
55. **Okazaki, H, Ishizaka N, Sakurai T, Kurokawa K, Goto K, Kumada M, Takuwa Y.** Molecular cloning of a novel putative G protein-coupled receptor expressed in the cardiovascular system. *Biochem Biophys Res Commun*. **1993**, 190, 1104-9.
56. **Masana, MI, Brown RC, Pu H, Gurney ME, Dubocovich ML.** Cloning and characterization of a new member of the G-protein coupled receptor EDG family. *Receptors Channels*. **1995**, 3, 255-62.
57. **Lee, MJ, Van Brocklyn JR, Thangada S, Liu CH, Hand AR, Menzeleev R, Spiegel S, Hla T.** Sphingosine-1-phosphate as a ligand for the G protein-coupled receptor EDG-1. *Science*. **1998**, 279, 1552-5.
58. **An, S, Bleu T, Huang W, Hallmark OG, Coughlin SR, Goetzl EJ.** Identification of cDNAs encoding two G protein-coupled receptors for lysosphingolipids. *FEBS Lett*. **1997**, 417, 279-82.
59. **Chun, J, Goetzl EJ, Hla T, Igarashi Y, Lynch KR, Moolenaar W, Pyne S, Tigyi G.** International Union of Pharmacology. XXXIV. Lysophospholipid receptor nomenclature. *Pharmacol Rev*. **2002**, 54, 265-9.
60. **Liu, CH, Hla T.** The mouse gene for the inducible G-protein-coupled receptor edg-1. *Genomics*. **1997**, 43, 15-24.
61. **Okamoto, H, Takuwa N, Gonda K, Okazaki H, Chang K, Yatomi Y, Shigematsu H, Takuwa Y.** EDG1 is a functional sphingosine-1-phosphate receptor that is linked via a Gi/o to multiple signaling pathways, including phospholipase C activation, Ca²⁺ mobilization, Ras-mitogen-activated protein kinase activation, and adenylate cyclase inhibition. *J Biol Chem*. **1998**, 273, 27104-10.
62. **Lee, MJ, Thangada S, Paik JH, Sapkota GP, Ancellin N, Chae SS, Wu M, Morales-Ruiz M, Sessa WC, Alessi DR, Hla T.** Akt-mediated phosphorylation of the G protein-

- coupled receptor EDG-1 is required for endothelial cell chemotaxis. *Mol Cell*. **2001**, 8, 693-704.
63. **Liu, Y, Wada R, Yamashita T, Mi Y, Deng CX, Hobson JP, Rosenfeldt HM, Nava VE, Chae SS, Lee MJ, Liu CH, Hla T, Spiegel S, Proia RL.** Edg-1, the G protein-coupled receptor for sphingosine-1-phosphate, is essential for vascular maturation. *J Clin Invest* **2000**, 106, 951-61.
64. **Fukushima, N, Ishii I, Contos JJ, Weiner JA, Chun J.** Lysophospholipid receptors. *Annu Rev Pharmacol Toxicol*. **2001**, 41, 507-34.
65. **Zhang, G, Contos JJ, Weiner JA, Fukushima N, Chun J.** Comparative analysis of three murine G-protein coupled receptors activated by sphingosine-1-phosphate. *Gene*. **1999**, 227, 89-99.
66. **Yamaguchi, F, Tokuda M, Hatase O, Brenner S.** Molecular cloning of the novel human G protein-coupled receptor (GPCR) gene mapped on chromosome 9. *Biochem Biophys Res Commun*. **1996**, 227, 608-14.
67. **MacLennan, AJ, Carney PR, Zhu WJ, Chaves AH, Garcia J, Grimes JR, Anderson KJ, Roper SN, Lee N.** An essential role for the H218/AGR16/Edg-5/LP(B2) sphingosine 1-phosphate receptor in neuronal excitability. *Eur J Neurosci*. **2001**, 14, 203-9.
68. **Ishii, I, Friedman B, Ye X, Kawamura S, McGiffert C, Contos JJ, Kingsbury MA, Zhang G, Brown JH, Chun J.** Selective loss of sphingosine 1-phosphate signaling with no obvious phenotypic abnormality in mice lacking its G protein-coupled receptor, LP(B3)/EDG-3. *J Biol Chem* **2001**, 276, 33697-704.
69. **Ishii, I, Fukushima N, Ye X, Chun J.** Lysophospholipid receptors: signaling and biology. *Annu Rev Biochem*. **2004**, 73, 321-54.
70. **Graler, MH, Grosse R, Kusch A, Kremmer E, Gudermann T, Lipp M.** The sphingosine 1-phosphate receptor S1P4 regulates cell shape and motility via coupling to Gi and G12/13. *J Cell Biochem* **2003**, 89, 507-19.
71. **Kohno, T, Matsuyuki H, Inagaki Y, Igarashi Y.** Sphingosine 1-phosphate promotes cell migration through the activation of Cdc42 in Edg-6/S1P4-expressing cells. *Genes Cells*. **2003**, 8, 685-97.
72. **Graeler, M, Shankar G, Goetzl EJ.** Cutting edge: suppression of T cell chemotaxis by sphingosine 1-phosphate. *J Immunol* **2002**, 169, 4084-7.

73. **Wang, W, Graeler MH, Goetzl EJ.** Type 4 sphingosine 1-phosphate G protein-coupled receptor (S1P4) transduces S1P effects on T cell proliferation and cytokine secretion without signaling migration. *Faseb J* **2005**, 19, 1731-3.
74. **Glickman, M, Malek RL, Kwitek-Black AE, Jacob HJ, Lee NH.** Molecular cloning, tissue-specific expression, and chromosomal localization of a novel nerve growth factor-regulated G-protein-coupled receptor, nrg-1. *Mol Cell Neurosci.* **1999**, 14, 141-52.
75. **Anliker, B, Chun J.** Lysophospholipid G protein-coupled receptors. *J Biol Chem.* **2004**, 279, 20555-8.
76. **Malek, RL, Toman RE, Edsall LC, Wong S, Chiu J, Letterle CA, Van Brocklyn JR, Milstien S, Spiegel S, Lee NH.** Nrg-1 belongs to the endothelial differentiation gene family of G protein-coupled sphingosine-1-phosphate receptors. *J Biol Chem.* **2001**, 276, 5692-9.
77. **Yu, N, Lariosa-Willingham KD, Lin FF, Webb M, Rao TS.** Characterization of lysophosphatidic acid and sphingosine-1-phosphate-mediated signal transduction in rat cortical oligodendrocytes. *Glia.* **2004**, 45, 17-27.
78. **Jaillard, C, Harrison S, Stankoff B, Aigrot MS, Calver AR, Duddy G, Walsh FS, Pangalos MN, Arimura N, Kaibuchi K, Zalc B, Lubetzki C.** Edg8/S1P5: an oligodendroglial receptor with dual function on process retraction and cell survival. *J Neurosci.* **2005**, 25, 1459-69.
79. **Contos, JJ, Chun J.** Complete cDNA sequence, genomic structure, and chromosomal localization of the LPA receptor gene, lpA1/vzg-1/Gpcr26. *Genomics.* **1998**, 51, 364-78.
80. **Meyer zu Heringdorf, D, Jakobs KH.** Lysophospholipid receptors: signalling, pharmacology and regulation by lysophospholipid metabolism. *Biochim Biophys Acta.* **2007**, 1768, 923-40.
81. **Contos, JJ, Ishii I, Chun J.** Lysophosphatidic acid receptors. *Mol Pharmacol.* **2000**, 58, 1188-96.
82. **Contos, JJ, Ishii I, Fukushima N, Kingsbury MA, Ye X, Kawamura S, Brown JH, Chun J.** Characterization of lpa(2) (Edg4) and lpa(1)/lpa(2) (Edg2/Edg4) lysophosphatidic acid receptor knockout mice: signaling deficits without obvious phenotypic abnormality attributable to lpa(2). *Mol Cell Biol.* **2002**, 22, 6921-9.
83. **Yang, AH, Ishii I, Chun J.** In vivo roles of lysophospholipid receptors revealed by gene targeting studies in mice. *Biochim Biophys Acta.* **2002**, 1582, 197-203.
84. **Ishii, I, Contos JJ, Fukushima N, Chun J.** Functional comparisons of the lysophosphatidic acid receptors, LP(A1)/VZG-1/EDG-2, LP(A2)/EDG-4, and

- LP(A3)/EDG-7 in neuronal cell lines using a retrovirus expression system. *Mol Pharmacol.* **2000**, 58, 895-902.
85. **Bandoh, K, Aoki J, Hosono H, Kobayashi S, Kobayashi T, Murakami-Murofushi K, Tsujimoto M, Arai H, Inoue K.** Molecular cloning and characterization of a novel human G-protein-coupled receptor, EDG7, for lysophosphatidic acid. *J Biol Chem.* **1999**, 274, 27776-85.
86. **Im, DS, Heise CE, Harding MA, George SR, O'Dowd BF, Theodorescu D, Lynch KR.** Molecular cloning and characterization of a lysophosphatidic acid receptor, Edg-7, expressed in prostate. *Mol Pharmacol.* **2000**, 57, 753-9.
87. **Noguchi, K, Ishii S, Shimizu T.** Identification of p2y9/GPR23 as a novel G protein-coupled receptor for lysophosphatidic acid, structurally distant from the Edg family. *J Biol Chem.* **2003**, 278, 25600-6.
88. **Lee, CW, Rivera R, Gardell S, Dubin AE, Chun J.** GPR92 as a new G12/13- and Gq-coupled lysophosphatidic acid receptor that increases cAMP, LPA5. *J Biol Chem.* **2006**, 281, 23589-97.
89. **Kostenis, E.** Novel clusters of receptors for sphingosine-1-phosphate, sphingosylphosphorylcholine, and (lyso)-phosphatidic acid: new receptors for "old" ligands. *J Cell Biochem* **2004**, 92, 923-36.
90. **Ignatov, A, Lintzel J, Hermans-Borgmeyer I, Kreienkamp HJ, Joost P, Thomsen S, Methner A, Schaller HC.** Role of the G-protein-coupled receptor GPR12 as high-affinity receptor for sphingosylphosphorylcholine and its expression and function in brain development. *J Neurosci.* **2003**, 23, 907-14.
91. **Hinckley, M, Vaccari S, Horner K, Chen R, Conti M.** The G-protein-coupled receptors GPR3 and GPR12 are involved in cAMP signaling and maintenance of meiotic arrest in rodent oocytes. *Dev Biol.* **2005**, 287, 249-61.
92. **Mehlmann, LM, Saeki Y, Tanaka S, Brennan TJ, Evsikov AV, Pendola FL, Knowles BB, Eppig JJ, Jaffe LA.** The Gs-linked receptor GPR3 maintains meiotic arrest in mammalian oocytes. *Science.* **2004**, 306, 1947-50.
93. **Cuvillier, O, Pirianov G, Kleuser B, Vanek PG, Coso OA, Gutkind S, Spiegel S.** Suppression of ceramide-mediated programmed cell death by sphingosine-1-phosphate. *Nature.* **1996**, 381, 800-3.
94. **Kihara, A, Mitsutake S, Mizutani Y, Igarashi Y.** Metabolism and biological functions of two phosphorylated sphingolipids, sphingosine 1-phosphate and ceramide 1-phosphate. *Prog Lipid Res* **2007**, 150, 470-9.

95. **Liu, H, Sugiura M, Nava VE, Edsall LC, Kono K, Poulton S, Milstien S, Kohama T, Spiegel S.** Molecular cloning and functional characterization of a novel mammalian sphingosine kinase type 2 isoform. *J Biol Chem.* **2000**, 275, 19513-20.
96. **Igarashi, N, Okada T, Hayashi S, Fujita T, Jahangeer S, Nakamura S.** Sphingosine kinase 2 is a nuclear protein and inhibits DNA synthesis. *J Biol Chem.* **2003**, 278, 46832-9.
97. **Yoshimoto, T, Furuhata M, Kamiya S, Hisada M, Miyaji H, Magami Y, Yamamoto K, Fujiwara H, Mizuguchi J.** Positive modulation of IL-12 signaling by sphingosine kinase 2 associating with the IL-12 receptor beta 1 cytoplasmic region. *J Immunol.* **2003**, 171, 1352-9.
98. **Nava, VE, Lacana E, Poulton S, Liu H, Sugiura M, Kono K, Milstien S, Kohama T, Spiegel S.** Functional characterization of human sphingosine kinase-1. *FEBS Lett.* **2000**, 473, 81-4.
99. **Zemann, B, Kinzel B, Muller M, Reuschel R, Mechtcheriakova D, Urtz N, Bornancin F, Baumruker T, Billich A.** Sphingosine kinase type 2 is essential for lymphodepletion induced by the immunomodulatory drug FTY720. *Blood* **2005**, 107, 1454-8.
100. **Le Stunff, H, Milstien S, Spiegel S.** Generation and metabolism of bioactive sphingosine-1-phosphate. *J Cell Biochem.* **2004**, 92, 882-99.
101. **Mandala, S, Hajdu R, Bergstrom J, Quackenbush E, Xie J, Milligan J, Thornton R, Shei GJ, Card D, Keohane C, Rosenbach M, Hale J, Lynch CL, Rupprecht K, Parsons W, Rosen H.** Alteration of lymphocyte trafficking by sphingosine-1-phosphate receptor agonists. *Science.* **2002**, 296, 346-9.
102. **Ogawa, C, Kihara A, Gokoh M, Igarashi Y.** Identification and characterization of a novel human sphingosine-1-phosphate phosphohydrolase, hSPP2. *J Biol Chem.* **2003**, 278, 1268-72.
103. **Zhou, J, Saba JD.** Identification of the first mammalian sphingosine phosphate lyase gene and its functional expression in yeast. *Biochem Biophys Res Commun.* **1998**, 242, 502-7.
104. **van Veldhoven, PP, Mannaerts GP.** Sphingosine-phosphate lyase. *Adv Lipid Res.* **1993**, 26, 69-98.
105. **Reiss, U, Oskouian B, Zhou J, Gupta V, Sooriyakumaran P, Kelly S, Wang E, Merrill AH, Jr., Saba JD.** Sphingosine-phosphate lyase enhances stress-induced ceramide generation and apoptosis. *J Biol Chem.* **2004**, 279, 1281-90.

106. **Zhang, H, Desai NN, Olivera A, Seki T, Brooker G, Spiegel S.** Sphingosine-1-phosphate, a novel lipid, involved in cellular proliferation. *J Cell Biol.* **1991**, 114, 155-67.
107. **Ghosh, TK, Bian J, Gill DL.** Sphingosine 1-phosphate generated in the endoplasmic reticulum membrane activates release of stored calcium. *J Biol Chem.* **1994**, 269, 22628-35.
108. **Olivera, A, Kohama T, Edsall L, Nava V, Cuvillier O, Poulton S, Spiegel S.** Sphingosine kinase expression increases intracellular sphingosine-1-phosphate and promotes cell growth and survival. *J Cell Biol.* **1999**, 147, 545-58.
109. **Meyer zu Heringdorf, D, Lass H, Kuchar I, Lipinski M, Alemany R, Rumenapp U, Jakobs KH.** Stimulation of intracellular sphingosine-1-phosphate production by G-protein-coupled sphingosine-1-phosphate receptors. *Eur J Pharmacol.* **2001**, 414, 145-54.
110. **Hobson, JP, Rosenfeldt HM, Barak LS, Olivera A, Poulton S, Caron MG, Milstien S, Spiegel S.** Role of the sphingosine-1-phosphate receptor EDG-1 in PDGF-induced cell motility. *Science.* **2001**, 291, 1800-3.
111. **Pyne, S, Pyne NJ.** Sphingosine 1-phosphate signalling and termination at lipid phosphate receptors. *Biochim Biophys Acta.* **2002**, 1582, 121-31.
112. **Prieschl, EE, Csonga R, Novotny V, Kikuchi GE, Baumruker T.** The balance between sphingosine and sphingosine-1-phosphate is decisive for mast cell activation after Fc epsilon receptor I triggering. *J Exp Med.* **1999**, 190, 1-8.
113. **Ito, K, Anada Y, Tani M, Ikeda M, Sano T, Kihara A, Igarashi Y.** Lack of sphingosine 1-phosphate-degrading enzymes in erythrocytes. *Biochem Biophys Res Commun.* **2007**, 357, 212-7.
114. **Hanel, P, Andreani P, Graler MH.** Erythrocytes store and release sphingosine 1-phosphate in blood. *Faseb J* **2007**, 21, 1202-7.
115. **Pappu, R, Schwab SR, Cornelissen I, Pereira JP, Regard JB, Xu Y, Camerer E, Zheng YW, Huang Y, Cyster JG, Coughlin SR.** Promotion of lymphocyte egress into blood and lymph by distinct sources of sphingosine-1-phosphate. *Science.* **2007**, 316, 295-8.
116. **Aoki, J.** Mechanisms of lysophosphatidic acid production. *Semin Cell Dev Biol.* **2004**, 15, 477-89.

117. **Hooks, SB, Santos WL, Im DS, Heise CE, Macdonald TL, Lynch KR.** Lysophosphatidic acid-induced mitogenesis is regulated by lipid phosphate phosphatases and is Edg-receptor independent. *J Biol Chem.* **2001**, 276, 4611-21.
118. **McIntyre, TM, Pontsler AV, Silva AR, St Hilaire A, Xu Y, Hinshaw JC, Zimmerman GA, Hama K, Aoki J, Arai H, Prestwich GD.** Identification of an intracellular receptor for lysophosphatidic acid (LPA): LPA is a transcellular PPARgamma agonist. *Proc Natl Acad Sci U S A.* **2003**, 100, 131-6.
119. **Fujita, T, Inoue K, Yamamoto S, Ikumoto T, Sasaki S, Toyama R, Chiba K, Hoshino Y, Okumoto T.** Fungal metabolites. Part 11. A potent immunosuppressive activity found in *Isaria sinclairii* metabolite. *J Antibiot (Tokyo).* **1994**, 47, 208-15.
120. **Fujita, T, Hirose R, Yoneta M, Sasaki S, Inoue K, Kiuchi M, Hirase S, Chiba K, Sakamoto H, Arita M.** Potent immunosuppressants, 2-alkyl-2-aminopropane-1,3-diols. *J Med Chem.* **1996**, 39, 4451-9.
121. **Chiba, K, Hoshino Y, Suzuki C, Masubuchi Y, Yanagawa Y, Ohtsuki M, Sasaki S, Fujita T.** FTY720, a novel immunosuppressant possessing unique mechanisms. I. Prolongation of skin allograft survival and synergistic effect in combination with cyclosporine in rats. *Transplant Proc.* **1996**, 28, 1056-9.
122. **Hoshino, Y, Suzuki C, Ohtsuki M, Masubuchi Y, Amano Y, Chiba K.** FTY720, a novel immunosuppressant possessing unique mechanisms. II. Long-term graft survival induction in rat heterotopic cardiac allografts and synergistic effect in combination with cyclosporine A. *Transplant Proc.* **1996**, 28, 1060-1.
123. **Masubuchi, Y, Kawaguchi T, Ohtsuki M, Suzuki C, Amano Y, Hoshino Y, Chiba K.** FTY720, a novel immunosuppressant, possessing unique mechanisms. IV. Prevention of graft versus host reactions in rats. *Transplant Proc.* **1996**, 28, 1064-5.
124. **Pinschewer, DD, Ochsenbein AF, Odermatt B, Brinkmann V, Hengartner H, Zinkernagel RM.** FTY720 immunosuppression impairs effector T cell peripheral homing without affecting induction, expansion, and memory. *J Immunol.* **2000**, 164, 5761-70.
125. **Suzuki, S, Enosawa S, Kakefuda T, Shinomiya T, Amari M, Naoe S, Hoshino Y, Chiba K.** A novel immunosuppressant, FTY720, with a unique mechanism of action, induces long-term graft acceptance in rat and dog allotransplantation. *Transplantation.* **1996**, 61, 200-5.

126. **Suzuki, S, Li XK, Enosawa S, Shinomiya T.** A new immunosuppressant, FTY720, induces bcl-2-associated apoptotic cell death in human lymphocytes. *Immunology*. **1996**, 89, 518-23.
127. **Nikolova, Z, Hof A, Baumlin Y, Hof RP.** Combined FTY720/cyclosporine treatment promotes graft survival and lowers the peripheral lymphocyte count in a murine cardiac allotransplantation model. *Transplantation*. **2001**, 72, 168-71.
128. **Chiba, K, Yanagawa Y, Masubuchi Y, Kataoka H, Kawaguchi T, Ohtsuki M, Hoshino Y.** FTY720, a novel immunosuppressant, induces sequestration of circulating mature lymphocytes by acceleration of lymphocyte homing in rats. I. FTY720 selectively decreases the number of circulating mature lymphocytes by acceleration of lymphocyte homing. *J Immunol*. **1998**, 160, 5037-44.
129. **Brinkmann, V, Davis MD, Heise CE, Albert R, Cottens S, Hof R, Bruns C, Prieschl E, Baumruker T, Hiestand P, Foster CA, Zollinger M, Lynch KR.** The immune modulator FTY720 targets sphingosine 1-phosphate receptors. *J Biol Chem*. **2002**, 277, 21453-7.
130. **Yatomi, Y, Igarashi Y, Yang L, Hisano N, Qi R, Asazuma N, Satoh K, Ozaki Y, Kume S.** Sphingosine 1-phosphate, a bioactive sphingolipid abundantly stored in platelets, is a normal constituent of human plasma and serum. *J Biochem (Tokyo)*. **1997**, 121, 969-73.
131. **Graler, MH, Goetzl EJ.** The immunosuppressant FTY720 down-regulates sphingosine 1-phosphate G-protein-coupled receptors. *Faseb J* **2004**, 18, 551-3.
132. **Sanna, MG, Liao J, Jo E, Alfonso C, Ahn MY, Peterson MS, Webb B, Lefebvre S, Chun J, Gray N, Rosen H.** Sphingosine 1-phosphate (S1P) receptor subtypes S1P1 and S1P3, respectively, regulate lymphocyte recirculation and heart rate. *J Biol Chem*. **2004**, 279, 13839-48.
133. **Davis, MD, Clemens JJ, Macdonald TL, Lynch KR.** Sphingosine 1-phosphate analogs as receptor antagonists. *J Biol Chem*. **2005**, 280, 9833-41.
134. **Graeler, M, Goetzl J.** Activation-regulated expression and chemotactic function of shingosine 1-phosphate receptors in mouse splenic T cells. *FASEB Journal* **2002**, 16, 1874-1878.
135. **Jin, Y, Knudsen E, Wang L, Bryceson Y, Damaj B, Gessani S, Maghazachi AA.** Sphingosine 1-phosphate is a novel inhibitor of T-cell proliferation. *Blood*. **2003**, 101, 4909-15.

136. **Maeda, Y, Matsuyuki H, Shimano K, Kataoka H, Sugahara K, Chiba K.** Migration of CD4 T Cells and Dendritic Cells toward Sphingosine 1-Phosphate (S1P) Is Mediated by Different Receptor Subtypes: S1P Regulates the Functions of Murine Mature Dendritic Cells via S1P Receptor Type 3. *J Immunol.* **2007**, 178, 3437-46.
137. **Watterson, KR, Johnston E, Chalmers C, Pronin A, Cook SJ, Benovic JL, Palmer TM.** Dual regulation of EDG1/S1P(1) receptor phosphorylation and internalization by protein kinase C and G-protein-coupled receptor kinase 2. *J Biol Chem.* **2002**, 277, 5767-77.
138. **Lo, CG, Xu Y, Proia RL, Cyster JG.** Cyclical modulation of sphingosine-1-phosphate receptor 1 surface expression during lymphocyte recirculation and relationship to lymphoid organ transit. *J Exp Med* **2005**, 201, 291-301.
139. **Dorsam, G, Graeler MH, Seroogy C, Kong Y, Voice JK, Goetzl EJ.** Transduction of multiple effects of sphingosine 1-phosphate (S1P) on T cell functions by the S1P1 G protein-coupled receptor. *J Immunol* **2003**, 171, 3500-7.
140. **Huang, MC, Watson SR, Liao JJ, Goetzl EJ.** Th17 augmentation in OTII TCR plus T cell-selective type 1 sphingosine 1-phosphate receptor double transgenic mice. *J Immunol.* **2007**, 178, 6806-13.
141. **Goetzl, EJ, Kong Y, Voice JK.** Cutting edge: differential constitutive expression of functional receptors for lysophosphatidic acid by human blood lymphocytes. *J Immunol* **2000**, 164, 4996-9.
142. **Zheng, Y, Voice JK, Kong Y, Goetzl EJ.** Altered expression and functional profile of lysophosphatidic acid receptors in mitogen-activated human blood T lymphocytes. *Faseb J.* **2000**, 14, 2387-9.
143. **Goetzl, EJ, Graeler MH.** Sphingosine 1-phosphate and its type 1 G protein-coupled receptor: trophic support and functional regulation of T lymphocytes. *J Leukoc Biol.* **2004**, 76, 30-5.
144. **Goetzl, EJ, Zheng Y, Kong Y, Voice JK.** Lysophosphatidic acid (LPA) and sphingosine 1-phosphate (S1P) stimulation of Jurkat T cell migration through a Matrigel (MG) model basement membrane (abstract). *FASEB Journal* **2000**, 14, A1144.
145. **Kunisawa, J, Kurashima Y, Gohda M, Higuchi M, Ishikawa I, Miura F, Ogahara I, Kiyono H.** Sphingosine 1-phosphate regulates peritoneal B-cell trafficking for subsequent intestinal IgA production. *Blood.* **2007**, 109, 3749-56.

146. **Roskopf, D, Daelman W, Busch S, Schurks M, Hartung K, Kribben A, Michel MC, Siffert W.** Growth factor-like action of lysophosphatidic acid on human B lymphoblasts. *Am J Physiol.* **1998**, 274, C1573-82.
147. **Kveberg, L, Bryceson Y, Inngjerdingen M, Rolstad B, Maghazachi AA.** Sphingosine 1 phosphate induces the chemotaxis of human natural killer cells. Role for heterotrimeric G proteins and phosphoinositide 3 kinases. *Eur J Immunol.* **2002**, 32, 1856-64.
148. **Jin, Y, Knudsen E, Wang L, Maghazachi AA.** Lysophosphatidic acid induces human natural killer cell chemotaxis and intracellular calcium mobilization. *Eur J Immunol.* **2003**, 33, 2083-9.
149. **Maghazachi, AA.** G protein-coupled receptors in natural killer cells. *J Leukoc Biol.* **2003**, 74, 16-24.
150. **Shortman, K, Liu YJ.** Mouse and human dendritic cell subtypes. *Nat Rev Immunol* **2002**, 2, 151-61.
151. **Hart, DN.** Dendritic cells: unique leukocyte populations which control the primary immune response. *Blood* **1997**, 90, 3245-87.
152. **Idzko, M, Panther E, Corinti S, Morelli A, Ferrari D, Herouy Y, Dichmann S, Mockenhaupt M, Gebicke-Haerter P, Di Virgilio F, Girolomoni G, Norgauer J.** Sphingosine 1-phosphate induces chemotaxis of immature and modulates cytokine-release in mature human dendritic cells for emergence of Th2 immune responses. *Faseb J* **2002**, 16, 625-7.
153. **Oz-Arslan, D, Ruscher W, Myrtek D, Ziemer M, Jin Y, Damaj BB, Sorichter S, Idzko M, Norgauer J, Maghazachi AA.** IL-6 and IL-8 release is mediated via multiple signaling pathways after stimulating dendritic cells with lysophospholipids. *J Leukoc Biol* **2006**, 80, 287-97.
154. **Czeloth, N, Bernhardt G, Hofmann F, Genth H, Forster R.** Sphingosine-1-phosphate mediates migration of mature dendritic cells. *J Immunol.* **2005**, 175, 2960-7.
155. **Muller, H, Hofer S, Kaneider N, Neuwirt H, Mosheimer B, Mayer G, Konwalinka G, Heufler C, Tiefenthaler M.** The immunomodulator FTY720 interferes with effector functions of human monocyte-derived dendritic cells. *Eur J Immunol.* **2005**, 35, 533-45.
156. **Martino, A, Volpe E, Auricchio G, Izzi V, Poccia F, Mariani F, Colizzi V, Baldini PM.** Sphingosine 1-Phosphate Interferes on the Differentiation of Human Monocytes into Competent Dendritic Cells. *Scand J Immunol.* **2007**, 65, 84-91.
157. **Panther, E, Idzko M, Corinti S, Ferrari D, Herouy Y, Mockenhaupt M, Dichmann S, Gebicke-Haerter P, Di Virgilio F, Girolomoni G, Norgauer J.** The influence of

- lysophosphatidic acid on the functions of human dendritic cells. *J Immunol* **2002**, 169, 4129-35.
158. **Hume, DA, Ross IL, Himes SR, Sasmono RT, Wells CA, Ravasi T.** The mononuclear phagocyte system revisited. *J Leukoc Biol.* **2002**, 72, 621-7.
159. **Lee, H, Liao JJ, Graeler M, Huang MC, Goetzl EJ.** Lysophospholipid regulation of mononuclear phagocytes. *Biochim Biophys Acta.* **2002**, 1582, 175-7.
160. **Fueller, M, Wang DA, Tigyi G, Siess W.** Activation of human monocytic cells by lysophosphatidic acid and sphingosine-1-phosphate. *Cell Signal.* **2003**, 15, 367-75.
161. **Hornuss, C, Hammermann R, Fuhrmann M, Juergens UR, Racke K.** Human and rat alveolar macrophages express multiple EDG receptors. *Eur J Pharmacol.* **2001**, 429, 303-8.
162. **Girkontaite, I, Sakk V, Wagner M, Borggreffe T, Tedford K, Chun J, Fischer KD.** The sphingosine-1-phosphate (S1P) lysophospholipid receptor S1P3 regulates MAdCAM-1+ endothelial cells in splenic marginal sinus organization. *J Exp Med.* **2004**, 200, 1491-501.
163. **Nathan, C.** Neutrophils and immunity: challenges and opportunities. *Nat Rev Immunol.* **2006**, 6, 173-82.
164. **Rahaman, M, Costello RW, Belmonte KE, Gendy SS, Walsh MT.** Neutrophil sphingosine 1-phosphate and lysophosphatidic acid receptors in pneumonia. *Am J Respir Cell Mol Biol.* **2006**, 34, 233-41.
165. **Chihab, R, Porn-Ares MI, Alvarado-Kristensson M, Andersson T.** Sphingosine 1-phosphate antagonizes human neutrophil apoptosis via p38 mitogen-activated protein kinase. *Cell Mol Life Sci.* **2003**, 60, 776-85.
166. **Itagaki, K, Hauser CJ.** Sphingosine 1-phosphate, a diffusible calcium influx factor mediating store-operated calcium entry. *J Biol Chem.* **2003**, 278, 27540-7.
167. **Lee, C, Xu DZ, Feketeova E, Kannan KB, Yun JK, Deitch EA, Fekete Z, Livingston DH, Hauser CJ.** Attenuation of shock-induced acute lung injury by sphingosine kinase inhibition. *J Trauma.* **2004**, 57, 955-60.
168. **Chettibi, S, Lawrence AJ, Stevenson RD, Young JD.** Effect of lysophosphatidic acid on motility, polarisation and metabolic burst of human neutrophils. *FEMS Immunol Med Microbiol.* **1994**, 8, 271-81.
169. **Itagaki, K, Kannan KB, Hauser CJ.** Lysophosphatidic acid triggers calcium entry through a non-store-operated pathway in human neutrophils. *J Leukoc Biol.* **2005**, 77, 181-9.

170. **Hashimoto, T, Yamashita M, Ohata H, Momose K.** Lysophosphatidic acid enhances in vivo infiltration and activation of guinea pig eosinophils and neutrophils via a Rho/Rho-associated protein kinase-mediated pathway. *J Pharmacol Sci.* **2003**, 91, 8-14.
171. **Muller, J, Petkovic M, Schiller J, Arnold K, Reichl S, Arnhold J.** Effects of lysophospholipids on the generation of reactive oxygen species by fMLP- and PMA-stimulated human neutrophils. *Luminescence.* **2002**, 17, 141-9.
172. **Tou, JS, Gill JS.** Lysophosphatidic acid increases phosphatidic acid formation, phospholipase D activity and degranulation by human neutrophils. *Cell Signal.* **2005**, 17, 77-82.
173. **Roviezzo, F, Del Galdo F, Abbate G, Bucci M, D'Agostino B, Antunes E, De Dominicis G, Parente L, Rossi F, Cirino G, De Palma R.** Human eosinophil chemotaxis and selective in vivo recruitment by sphingosine 1-phosphate. *Proc Natl Acad Sci U S A.* **2004**, 101, 11170-5.
174. **Idzko, M, Laut M, Panther E, Sorichter S, Durk T, Fluhr JW, Herouy Y, Mockenhaupt M, Myrtek D, Elsner P, Norgauer J.** Lysophosphatidic acid induces chemotaxis, oxygen radical production, CD11b up-regulation, Ca²⁺ mobilization, and actin reorganization in human eosinophils via pertussis toxin-sensitive G proteins. *J Immunol.* **2004**, 172, 4480-5.
175. **Wedemeyer, J, Tsai M, Galli SJ.** Roles of mast cells and basophils in innate and acquired immunity. *Curr Opin Immunol.* **2000**, 12, 624-31.
176. **Lantz, CS, Boesiger J, Song CH, Mach N, Kobayashi T, Mulligan RC, Nawa Y, Dranoff G, Galli SJ.** Role for interleukin-3 in mast-cell and basophil development and in immunity to parasites. *Nature.* **1998**, 392, 90-3.
177. **Prodeus, AP, Zhou X, Maurer M, Galli SJ, Carroll MC.** Impaired mast cell-dependent natural immunity in complement C3-deficient mice. *Nature.* **1997**, 390, 172-5.
178. **Malaviya, R, Gao Z, Thankavel K, van der Merwe PA, Abraham SN.** The mast cell tumor necrosis factor alpha response to FimH-expressing *Escherichia coli* is mediated by the glycosylphosphatidylinositol-anchored molecule CD48. *Proc Natl Acad Sci U S A.* **1999**, 96, 8110-5.
179. **Jolly, PS, Bektas M, Olivera A, Gonzalez-Espinosa C, Proia RL, Rivera J, Milstien S, Spiegel S.** Transactivation of sphingosine-1-phosphate receptors by FcεpsilonRI triggering is required for normal mast cell degranulation and chemotaxis. *J Exp Med.* **2004**, 199, 959-70.

180. **Choi, OH, Kim JH, Kinet JP.** Calcium mobilization via sphingosine kinase in signalling by the Fc epsilon RI antigen receptor. *Nature*. **1996**, 380, 634-6.
181. **Lin, DA, Boyce JA.** IL-4 regulates MEK expression required for lysophosphatidic acid-mediated chemokine generation by human mast cells. *J Immunol*. **2005**, 175, 5430-8.
182. **Bagga, S, Price KS, Lin DA, Friend DS, Austen KF, Boyce JA.** Lysophosphatidic acid accelerates the development of human mast cells. *Blood*. **2004**, 104, 4080-7.
183. **Akbar, AN, Vukmanovic-Stejic M, Taams LS, Macallan DC.** The dynamic co-evolution of memory and regulatory CD4+ T cells in the periphery. *Nat Rev Immunol*. **2007**, 7, 231-7.
184. **Wang, W, Graeler MH, Goetzl EJ.** Physiological sphingosine 1-phosphate requirement for optimal activity of mouse CD4+ regulatory T Cells. *Faseb J* **2004**, 18, 1043-5.
185. **Sawicka, E, Dubois G, Jarai G, Edwards M, Thomas M, Nicholls A, Albert R, Newson C, Brinkmann V, Walker C.** The Sphingosine 1-Phosphate Receptor Agonist FTY720 Differentially Affects the Sequestration of CD4+/CD25+ T-Regulatory Cells and Enhances Their Functional Activity. *J Immunol* **2005**, 175, 7973-7980.
186. **Daniel, C, Sartory N, Zahn N, Geisslinger G, Radeke HH, Stein JM.** FTY720 ameliorates Th1-mediated colitis in mice by directly affecting the functional activity of CD4+CD25+ regulatory T cells. *J Immunol*. **2007**, 178, 2458-68.
187. **Halin, C, Scimone ML, Bonasio R, Gauguet JM, Mempel TR, Quackenbush E, Proia RL, Mandala S, von Andrian UH.** The S1P-analog FTY720 differentially modulates T-cell homing via HEV: T-cell-expressed S1P1 amplifies integrin activation in peripheral lymph nodes but not in Peyer patches. *Blood* **2005**, 106, 1314-22.
188. **Chi, H, Flavell RA.** Cutting edge: regulation of T cell trafficking and primary immune responses by sphingosine 1-phosphate receptor 1. *J Immunol* **2005**, 174, 2485-8.
189. **Kunisawa, J, Kurashima Y, Higuchi M, Gohda M, Ishikawa I, Ogahara I, Kim N, Shimizu M, Kiyono H.** Sphingosine 1-phosphate dependence in the regulation of lymphocyte trafficking to the gut epithelium. *J Exp Med* **2007**, 204, 2335-48.
190. **Kweon, MN, Yamamoto M, Kajiki M, Takahashi I, Kiyono H.** Systemically derived large intestinal CD4(+) Th2 cells play a central role in STAT6-mediated allergic diarrhea. *J Clin Invest*. **2000**, 106, 199-206.
191. **Kurashima, Y, Kunisawa J, Higuchi M, Gohda M, Ishikawa I, Takayama N, Shimizu M, Kiyono H.** Sphingosine 1-phosphate-mediated trafficking of pathogenic th2 and mast cells for the control of food allergy. *J Immunol*. **2007**, 179, 1577-85.

192. **Han, S, Zhang X, Wang G, Guan H, Garcia G, Li P, Feng L, Zheng B.** FTY720 suppresses humoral immunity by inhibiting germinal center reaction. *Blood* **2004**, 104, 4129-33.
193. **Vora, KA, Nichols E, Porter G, Cui Y, Keohane CA, Hajdu R, Hale J, Neway W, Zaller D, Mandala S.** Sphingosine 1-phosphate receptor agonist FTY720-phosphate causes marginal zone B cell displacement. *J Leukoc Biol.* **2005**, 78, 471-80.
194. **Yu, JY, DeRuiter SL, Turner DL.** RNA interference by expression of short-interfering RNAs and hairpin RNAs in mammalian cells. *Proc Natl Acad Sci U S A.* **2002**, 99, 6047-52.
195. **Ohno, H, Ushiyama C, Taniguchi M, Germain RN, Saito T.** CD2 can mediate TCR/CD3-independent T cell activation. *J Immunol.* **1991**, 146, 3742-6.
196. **Brummelkamp, TR, Bernards R, Agami R.** A system for stable expression of short interfering RNAs in mammalian cells. *Science* **2002**, 296, 550-3.
197. **Schwab, SR, Pereira JP, Matloubian M, Xu Y, Huang Y, Cyster JG.** Lymphocyte sequestration through S1P lyase inhibition and disruption of S1P gradients. *Science* **2005**, 309, 1735-9.
198. **Tsunemi, Y, Saeki H, Nakamura K, Nagakubo D, Nakayama T, Yoshie O, Kagami S, Shimazu K, Kadono T, Sugaya M, Komine M, Matsushima K, Tamaki K.** CCL17 transgenic mice show an enhanced Th2-type response to both allergic and non-allergic stimuli. *Eur J Immunol.* **2006**, 36, 2116-27.
199. **Kay, AB.** Eosinophils and asthma. *N Engl J Med.* **1991**, 324, 1514-5.
200. **Djukanovic, R, Lai CK, Wilson JW, Britten KM, Wilson SJ, Roche WR, Howarth PH, Holgate ST.** Bronchial mucosal manifestations of atopy: a comparison of markers of inflammation between atopic asthmatics, atopic nonasthmatics and healthy controls. *Eur Respir J.* **1992**, 5, 538-44.
201. **Graler, MH, Huang MC, Watson S, Goetzl EJ.** Immunological effects of transgenic constitutive expression of the type 1 sphingosine 1-phosphate receptor by mouse lymphocytes. *J Immunol.* **2005**, 174, 1997-2003.
202. **Zhang, K.** Accessibility control and machinery of immunoglobulin class switch recombination. *J Leukoc Biol.* **2003**, 73, 323-32.
203. **Sonoda, E, Hitoshi Y, Yamaguchi N, Ishii T, Tominaga A, Araki S, Takatsu K.** Differential regulation of IgA production by TGF-beta and IL-5: TGF-beta induces surface IgA-positive cells bearing IL-5 receptor, whereas IL-5 promotes their survival and maturation into IgA-secreting cells. *Cell Immunol.* **1992**, 140, 158-72.

204. **Manz, RA, Hauser AE, Hiepe F, Radbruch A.** Maintenance of serum antibody levels. *Annu Rev Immunol.* **2005**, 23, 367-86.
205. **Fujihashi, K, McGhee JR, Kweon MN, Cooper MD, Tonegawa S, Takahashi I, Hiroi T, Mestecky J, Kiyono H.** gamma/delta T cell-deficient mice have impaired mucosal immunoglobulin A responses. *J Exp Med.* **1996**, 183, 1929-35.
206. **Nagasawa, T.** Microenvironmental niches in the bone marrow required for B-cell development. *Nat Rev Immunol.* **2006**, 6, 107-16.
207. **Egawa, T, Kawabata K, Kawamoto H, Amada K, Okamoto R, Fujii N, Kishimoto T, Katsura Y, Nagasawa T.** The earliest stages of B cell development require a chemokine stromal cell-derived factor/pre-B cell growth-stimulating factor. *Immunity.* **2001**, 15, 323-34.
208. **Nie, Y, Waite J, Brewer F, Sunshine MJ, Littman DR, Zou YR.** The role of CXCR4 in maintaining peripheral B cell compartments and humoral immunity. *J Exp Med.* **2004**, 200, 1145-56.
209. **Yopp, AC, Ochando JC, Mao M, Ledgerwood L, Ding Y, Bromberg JS.** Sphingosine 1-phosphate receptors regulate chemokine-driven transendothelial migration of lymph node but not splenic T cells. *J Immunol.* **2005**, 175, 2913-24.
210. **Allman, D, Srivastava B, Lindsley RC.** Alternative routes to maturity: branch points and pathways for generating follicular and marginal zone B cells. *Immunol Rev.* **2004**, 197, 147-60.
211. **Allman, DM, Ferguson SE, Lentz VM, Cancro MP.** Peripheral B cell maturation. II. Heat-stable antigen(hi) splenic B cells are an immature developmental intermediate in the production of long-lived marrow-derived B cells. *J Immunol.* **1993**, 151, 4431-44.
212. **Schitteck, B, Rajewsky K, Forster I.** Dividing cells in bone marrow and spleen incorporate bromodeoxyuridine with high efficiency. *Eur J Immunol.* **1991**, 21, 235-8.
213. **Martin, F, Kearney JF.** Marginal-zone B cells. *Nat Rev Immunol.* **2002**, 2, 323-35.
214. **Pillai, S, Cariappa A, Moran ST.** Marginal zone B cells. *Annu Rev Immunol.* **2005**, 23, 161-96.
215. **Kaminski, DA, Stavnezer J.** Enhanced IgA class switching in marginal zone and B1 B cells relative to follicular/B2 B cells. *J Immunol.* **2006**, 177, 6025-9.
216. **Martin, F, Oliver AM, Kearney JF.** Marginal zone and B1 B cells unite in the early response against T-independent blood-borne particulate antigens. *Immunity.* **2001**, 14, 617-29.

217. **Baumgarth, N, Herman OC, Jager GC, Brown L, Herzenberg LA.** Innate and acquired humoral immunities to influenza virus are mediated by distinct arms of the immune system. *Proc Natl Acad Sci U S A.* **1999**, 96, 2250-5.
218. **Hayakawa, K, Hardy RR.** Development and function of B-1 cells. *Curr Opin Immunol.* **2000**, 12, 346-53.
219. **Macpherson, AJ, Gatto D, Sainsbury E, Harriman GR, Hengartner H, Zinkernagel RM.** A primitive T cell-independent mechanism of intestinal mucosal IgA responses to commensal bacteria. *Science.* **2000**, 288, 2222-6.
220. **Kroese, FG, Butcher EC, Stall AM, Lalor PA, Adams S, Herzenberg LA.** Many of the IgA producing plasma cells in murine gut are derived from self-replenishing precursors in the peritoneal cavity. *Int Immunol.* **1989**, 1, 75-84.
221. **Nguyen, KB, Watford WT, Salomon R, Hofmann SR, Pien GC, Morinobu A, Gadina M, O'Shea JJ, Biron CA.** Critical role for STAT4 activation by type 1 interferons in the interferon-gamma response to viral infection. *Science.* **2002**, 297, 2063-6.
222. **Trinchieri, G, Pflanz S, Kastelein RA.** The IL-12 family of heterodimeric cytokines: new players in the regulation of T cell responses. *Immunity.* **2003**, 19, 641-4.
223. **O'Garra, A.** Cytokines induce the development of functionally heterogeneous T helper cell subsets. *Immunity.* **1998**, 8, 275-83.
224. **Nakamura, T, Lee RK, Nam SY, Podack ER, Bottomly K, Flavell RA.** Roles of IL-4 and IFN-gamma in stabilizing the T helper cell type 1 and 2 phenotype. *J Immunol.* **1997**, 158, 2648-53.
225. **Minami, K, Yanagawa Y, Iwabuchi K, Shinohara N, Harabayashi T, Nonomura K, Onoe K.** Negative feedback regulation of T helper type 1 (Th1)/Th2 cytokine balance via dendritic cell and natural killer T cell interactions. *Blood.* **2005**, 106, 1685-93.
226. **Corthay, A.** A three-cell model for activation of naive T helper cells. *Scand J Immunol.* **2006**, 64, 93-6.
227. **Tang, A, Judge TA, Nickoloff BJ, Turka LA.** Suppression of murine allergic contact dermatitis by CTLA4Ig. Tolerance induction of Th2 responses requires additional blockade of CD40-ligand. *J Immunol.* **1996**, 157, 117-25.
228. **Watanabe, H, Unger M, Tuvel B, Wang B, Sauder DN.** Contact hypersensitivity: the mechanism of immune responses and T cell balance. *J Interferon Cytokine Res.* **2002**, 22, 407-12.

-
229. **Grabbe, S, Schwarz T.** Immunoregulatory mechanisms involved in elicitation of allergic contact hypersensitivity. *Immunol Today*. **1998**, 19, 37-44.
230. **Bradley, BL, Azzawi M, Jacobson M, Assoufi B, Collins JV, Irani AM, Schwartz LB, Durham SR, Jeffery PK, Kay AB.** Eosinophils, T-lymphocytes, mast cells, neutrophils, and macrophages in bronchial biopsy specimens from atopic subjects with asthma: comparison with biopsy specimens from atopic subjects without asthma and normal control subjects and relationship to bronchial hyperresponsiveness. *J Allergy Clin Immunol*. **1991**, 88, 661-74.
231. **Cohn, L, Tepper JS, Bottomly K.** IL-4-independent induction of airway hyperresponsiveness by Th2, but not Th1, cells. *J Immunol*. **1998**, 161, 3813-6.
232. **Kay, AB.** Allergy and allergic diseases. First of two parts. *N Engl J Med*. **2001**, 344, 30-7.
233. **Hamelmann, E, Gelfand EW.** Role of IL-5 in the development of allergen-induced airway hyperresponsiveness. *Int Arch Allergy Immunol*. **1999**, 120, 8-16.
234. **Idzko, M, Hammad H, van Nimwegen M, Kool M, Muller T, Soullie T, Willart MA, Hijdra D, Hoogsteden HC, Lambrecht BN.** Local application of FTY720 to the lung abrogates experimental asthma by altering dendritic cell function. *J Clin Invest*. **2006**, 116, 2935-44.
235. **Olivera, A, Urtz N, Mizugishi K, Yamashita Y, Gilfillan AM, Furumoto Y, Gu H, Proia RL, Baumruker T, Rivera J.** IgE-dependent activation of sphingosine kinases 1 and 2 and secretion of sphingosine 1-phosphate requires Fyn kinase and contributes to mast cell responses. *J Biol Chem*. **2006**, 281, 2515-25.
236. **Ammit, AJ, Hastie AT, Edsall LC, Hoffman RK, Amrani Y, Krymskaya VP, Kane SA, Peters SP, Penn RB, Spiegel S, Panettieri RA, Jr.** Sphingosine 1-phosphate modulates human airway smooth muscle cell functions that promote inflammation and airway remodeling in asthma. *Faseb J*. **2001**, 15, 1212-4.